DYNAMICS ON SCALE-INVARIANT STRUCTURES

Alexis Christou

Department of Theoretical Physics

University Of Oxford

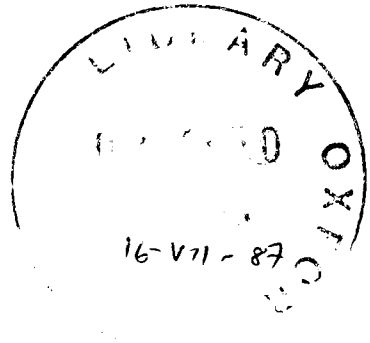

A Thesis submitted for the degree of

Doctor of Philosophy

at the University of Oxford

Trinity College

February 1987

To my family

There is plenty of time to win this game,

*and to thrash the *****ards too.*

Sir Francis Drake

So, Nat'ralists observe, a Flea

Hath smaller Fleas that on him prey,

And these have smaller Fleas to bit 'em,

And so proceed ad infinitum.

Jonathan Swift

Acknowledgments

It is a pleasure to thank my supervisor, Dr. R.B. Stinchcombe, for many stimulating conversations, continual help and encouragement throughout the past two and a half years.

It is also with pleasure that I thank Professor A.B. Harris with whom the work presented in chapters five and six was done.

I am especially grateful to many colleagues for their warmth and camaraderie, in particular to Kathy Armitstead, Steve Bell, Harald Borner, Hasnita Hashim, Prasenjit Saha and Mark Whittall.

Finally, I thank my wife Pipa, not only for her constant love and support, but also for those thousands of miles of commuting to and from London.

Support from SERC is acknowledged.

DYNAMICS ON SCALE-INVARIANT STRUCTURES

Alexis Christou

Trinity College, Oxford

A thesis submitted for the degree of Doctor of Philosophy

Hilary Term 1987

Abstract.

We investigate dynamical processes on random and regular fractals.

The (static) problem of percolation in the semi-infinite plane introduces many pertinent ideas including real space renormalisation group (RSRG) fugacity transformations and scaling forms. We study the percolation probability to determine the surface critical behaviour and to establish exponent relations. The fugacity approach is generalised to study random walks on diffusion-limited aggregates (DLA). Using regular and random models, we calculate the walk dimensionality and demonstrate that it is consistent with a conjecture by Aharony and Stauffer. It is shown that the kinetically grown DLA is in a distinct dynamic universality class to lattice animals. Similarly, the speculation of Helman-Coniglio-Tsallis regarding diffusion on self-avoiding walks (SAWs) is shown to be incorrect. The results are corroborated by an exact enumeration analysis of the internal structure of SAWs.

A 'spin' and field theoretic Hamiltonian formulation for the conformational and resistance properties of random walks is presented. We consider Gaussian random walks, SAWs, spiral SAWs and valence walks. We express resistive susceptibilities as correlation functions and hence ϵ-expansions are calculated for the resistance exponents. For SAWs, the local crosslinks are shown to be irrelevant and we calculate corrections to scaling.

A scaling description is introduced into an equation-of-motion method in order to study spin wave damping in d-dimensional isotropic Heisenberg ferro-, antiferro- and ferri- magnets near p_c. Dynamic scaling is shown to be obeyed by the Lorentzian spin wave response function and lifetime. The ensemble of finite clusters and multicritical behaviour is also treated. In contrast, the relaxational dynamics of the dilute Anisotropic Heisenberg model is shown to violate conventional dynamic scaling near the percolation bicritical point but satisfies instead a singular scaling behaviour arising from activation of Bloch walls over percolation cluster energy barriers.

CONTENTS

Chapter 1

Introduction: Dynamics on Scale-Invariant Structures.

To build a physical theory one generally firsts isolates a small range of lengths (or times, masses etc.) in which the relevant phenomena occur. This simplifies the problem. For example, one does not normally consider planetary motions when studying the evolution of a galaxy. Similarly, it is not necessary to treat the individual fluid molecules in order to understand streamline hydrodynamics. Thus, most phenomena in nature are scale-dependent.

However, there do exist important problems in physics which have no such characteristic governing length scale. Many body interacting systems near a continuous phase transition provide the archetypal example (Stanley 1971). Other examples include the Kondo problem (a magnetic impurity in a metal) (Wilson 1975) and indeed all of relativistic quantum field theory (see Wilson and Kogut 1974). Such scale-invariant problems have the property that the physical system appears qualitatively the same on all length scales.

Another circumstance involving scale-invariance arises when the structure itself, upon which the physical process takes place, is geometrically self-similar, such as is realised in certain random systems.

The notion of scale-invariance, apart from being of substantial esoteric interest, does in itself provide the key to an understanding of critical phenomena and disorder in much the same way as does *translational* invariance in crystalline solid state physics or *rotational* invariance in atomic physics.

Much research activity has been spent on many-body static processes on scale-invariant structures. Dynamical phenomena are much less well understood and potentially much richer. The divergence of characteristic lengths (eg the correlation length in percolation or RMS end-to-end distance for walk problems) induces critical behaviour into the dynamics. Firstly, mode softening occurs (for example

renormalisation of the diffusion constant or of spin wave stiffness) and eventually there is a crossover to anomalous dynamics controlled by new dynamical critical exponents.

This thesis reports a series of studies of dynamical many-body problems on scale-invariant structures.

A brief outline of this introductory chapter is as follows: We begin with a discussion of regular and stochastic fractals and introduce the concept of *fractal* (or Hausdorff) dimensionality. We then define the types of statistical mechanical models that we intend to study in this thesis. We proceed with a survey of the kinds of dynamical processes that we shall be looking at and discuss the general features of anomalous dynamics on scale-invariant structures. Before a rather formal section on the renormalisation group method we summarise its ancestry in the theory of phase transitions and critical phenomena. Finally, we give a plan of the thesis.

1. Regular and Random Fractals.

Consider firstly the mass M of a (conventional) d-dimensional homogeneous object, say a ball of radius R and volume V with uniform mass density c:

$$M = \int_V c\, d^d r = c \int_0^R \hat{\gamma}(d) r^{d-1} dr = c\gamma(d) R^d \propto R^d \qquad (1.1.1a)$$

where $\gamma(d)=\hat{\gamma}(d)/d=(\Gamma(\frac{1}{2}))^d/\Gamma(1+ d/2)$. The important observation of course is that the mass M *scales* with the length R and this scaling is governed by an exponent d which we call the dimensionality of the ball. Thus in two dimensions the mass is proportional to R^2 and in three to R^3 etc. The dimensionality of conventional objects (continua) is an integer. However this is not true for general sets. There exist sets for which a sensibly defined dimensionality is fractional: Mandelbrot (1977, 1982) has called these sets *fractals*. Rigourous definitions of the *fractal dimension* d_f may be found in the textbooks (see eg Mandelbrot 1982, or Falconer 1986). For our purposes, it suffices to define d_f as governing the length scaling of the mass (or *measure*) of the object,

$$M(R) \sim R^{d_f}. \qquad (1.1.1b)$$

For a conventional object $d_f=d$, where d is the dimension of the space in which it is embedded, while for fractals $d_f<d$ usually.

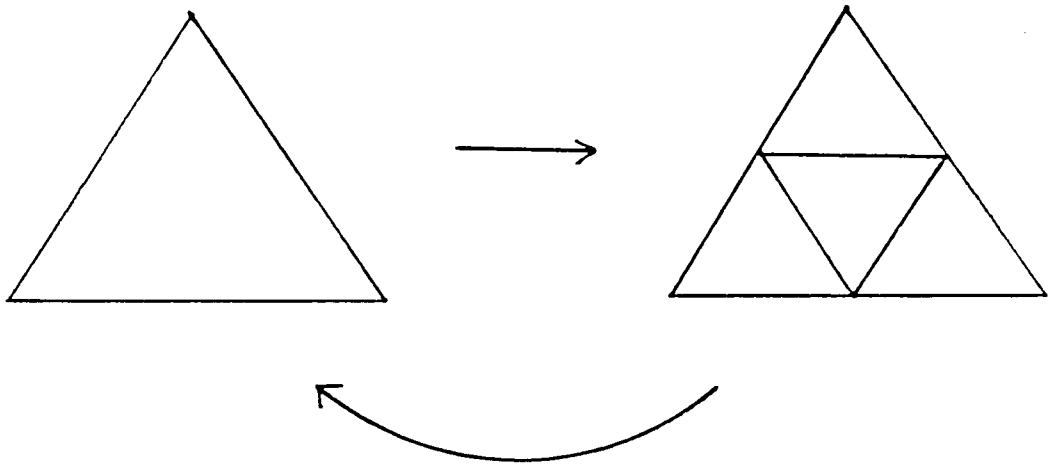

Fig.1.1.: Repeating this iterative procedure gives the Sierpinski gasket regular fractal. It is evidently invariant under length scale transformations by a factor $b=2^n$ and has fractal dimension log3/log2.

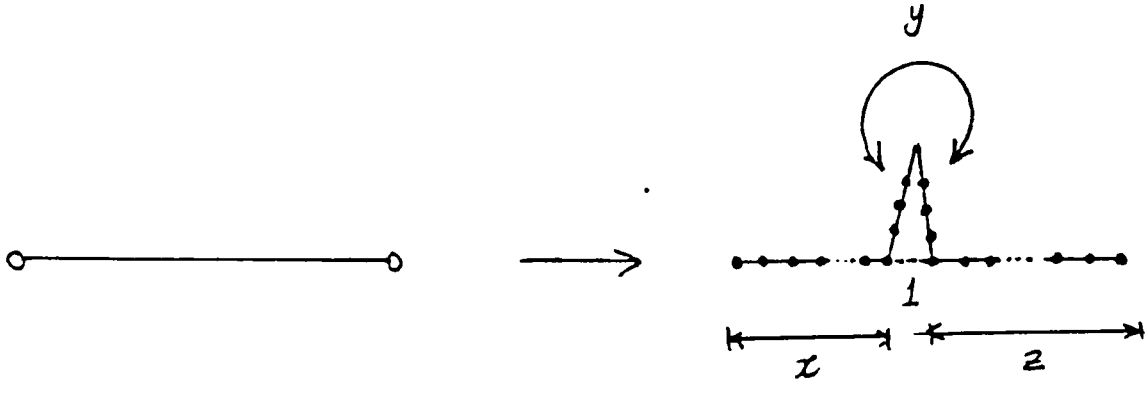

Fig.1.2.: Iterative construction of a regular model for a linked polymer.

Now consider the limit object created by iterating the procedure shown in fig.1.1: the *Sierpinski gasket*, which is embedded in a two-dimensional Euclidean space. After an infinite number of such iterations the gasket is evidently unchanged by length scale transformations by a length scale factor $b=2^n$, n integer. A little thought quickly gives the following relation for the *mass* M (or measure) as a function of size R:

$$M(2R) = 3M(R) \qquad (1.1.4)$$

Now, using (1.1.1b), we obtain

$$d_f = \frac{\log 3}{\log 2} \approx 1.585. \qquad (1.1.5)$$

Thus it is clear that the dimensionality of the gasket is not integral. Indeed for a gasket embedded in d-dimensions

$$d_f = \frac{\log (d+1)}{\log 2} < d. \qquad (1.1.6)$$

It is apparent that a variety of such iterative procedures may be defined to generate fractals with particular desired features. The Sierpinski gasket consists of loops within loops and voids on all length scales and has thus been considered (Gefen *et al* 1983) to be a reasonable, if incomplete (there are no singly connected {*red*} bonds), regular model of the percolation backbone at p_c.

Similarly, the process illustrated in fig.1.2 generates what appears to be an acceptable (though non-random) model for a linked protein (see Stinchcombe 1985) (see chapters 4,5,6). Associating zero mass with the H-bond (crosslink), it follows that

$$d_f = \frac{\log (x+y+z)}{\log (x+z+1)}. \qquad (1.1.7)$$

More relevant to real physical systems are random, stochastic or statistical fractals. In this thesis we study the following examples:

i) Percolation Clusters.

Site and bond percolation, although originally introduced purely as a graph theoretical problem (Broadbent and Hammersley 1957), is now a well established model for substitutional disorder in solid state physics. There are many excellent reviews of

percolation theory (see eg Essam 1980, Stauffer 1979) and we will only discuss the barest of essentials here.

Consider a lattice of sites (bonds) such that each site (bond) is independently present or absent with probablility p, 1−p respectively. p=1 represents the pure lattice with absence of disorder. As p decreases, larger clusters of absent sites (bonds) appear and the infinite cluster (connected cluster spanning the entire lattice) becomes increasingly ramified. Below a critical value of the density, $p=p_c$, the infinite percolation cluster breaks into a system of finite clusters (see fig.1.3.). This *percolation transition* is related to those of conventional thermal critical phenomena (see below). In fact a *geometrical* correlation length is defined as the RMS distance between connected sites (taken only over finite clusters). This clearly diverges on either side of the percolation transition and the singular part may be written as

$$\xi(p) \sim |p-p_c|^{-\nu_p}. \qquad (1.1.8a)$$

Enclosing portions of the cluster network within "hyperballs" of radius L, we define a configurationally averaged L dependent mass M(L), scaling as follows:

$$M(L) \sim L^{d_f}. \qquad (1.1.9)$$

It is a straightforward matter (Stinchcombe 1985) to show that d_f is in fact related to the embedding dimensionality d and to the percolation exponents β, ν as

$$d_f = d - \beta/\nu \quad < d. \qquad (1.1.10)$$

In d=2, $d_f \approx 1.89$ (for all type of lattices). The infinite percolation cluster at p_c (and indeed for all length scales L satisfying $L \ll \xi(p)$) is thus a fractal.

The divergence of the correlation length induces critical properties in other percolative quantities. The order parameter, for instance, is the *percolation probability* P(p), defined as the probability that a site is in the infinite cluster. Evidently this is non-zero only above p_c (the "ordered" phase) and vanishes below as required. In the vicinity of the percolation threshold, P(p) has a singularity governed by the exponent β:

$$P(p) \sim (p-p_c)^{\beta}. \qquad (1.1.8b)$$

The critical exponents for percolation are summarised in Table 1.2.

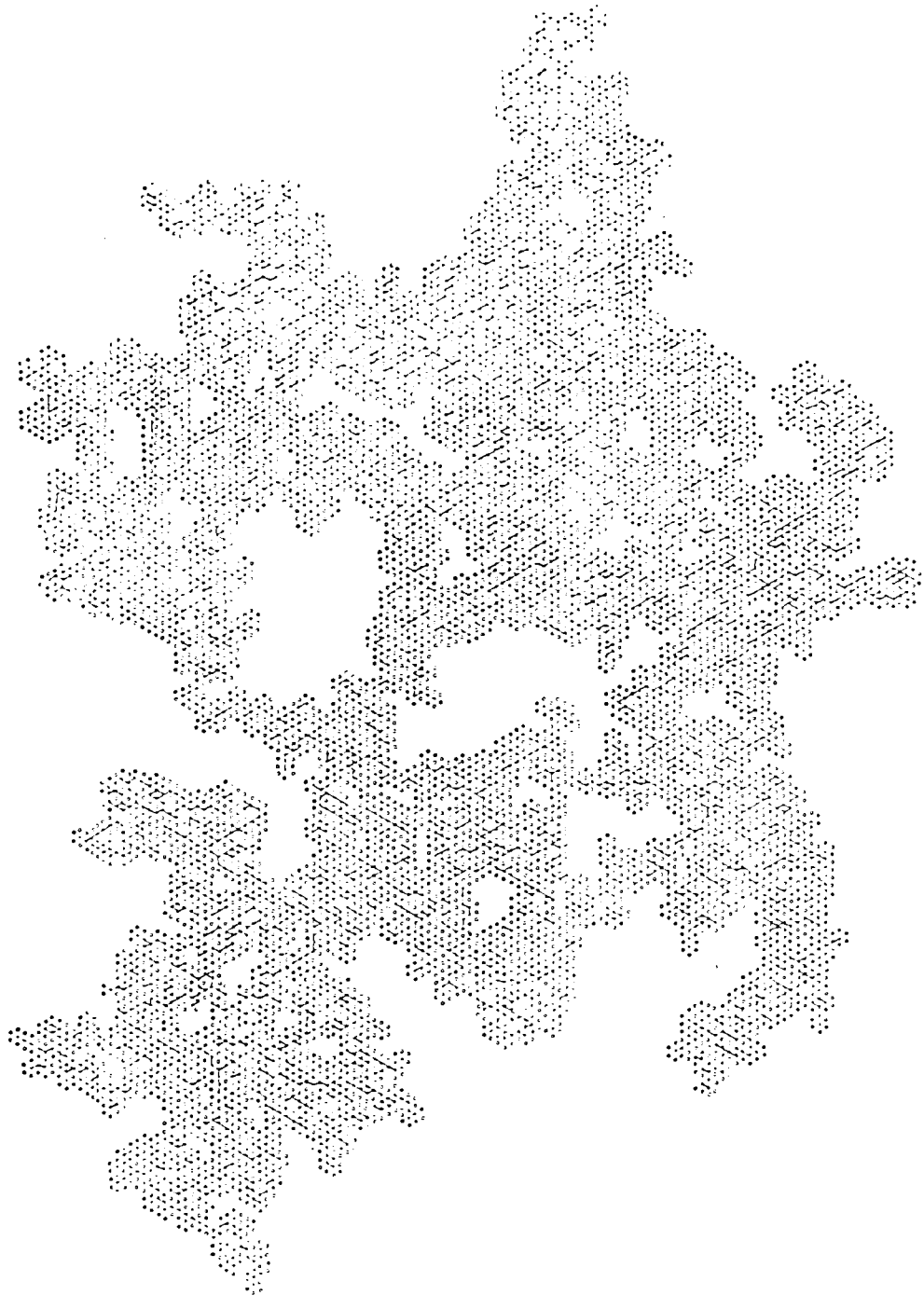

Fig.1.3.: A large percolation cluster just below p_c (from Stauffer 1979).

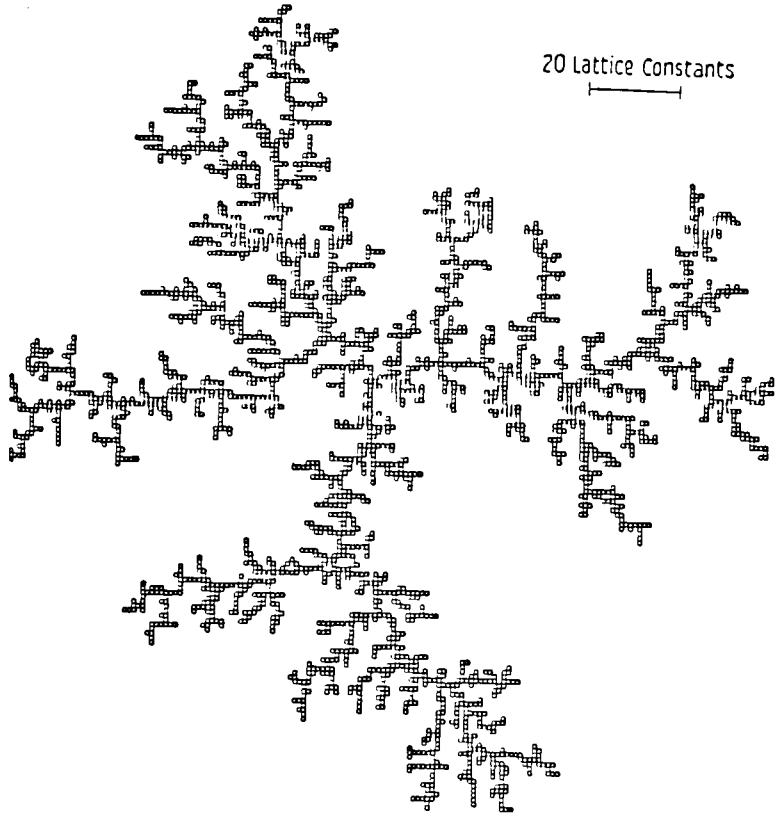

Fig.1.4.: A diffusion-limited aggregate (from Witten and Sander 1981).

ii) Diffusion-Limited Aggregates.

This is a popular model for particle-cluster aggregation (Witten and Sander 1981) of the sort that occurs in, eg, the coagulation of smoke particles (Forrest and Witten 1979). A description of the growth process resulting in clusters of the form shown in fig.1.4 is given in chapter 3. Numerically (Meakin 1983,4), it seems that these aggregates are inhomogeneous ramified fractals. Further their fractal dimensions appear to satisfy the crude relation $d_f \approx 5d/6$ for $d \leqslant 6$. Clearly this result cannot even be a reasonable approximation for $d \geqslant 12$, since, by addition of codimensions (Mandelbrot 1982), the cluster will be transparent with respect to the incoming diffusing particles.

iii) Random Walk Trails.

We will discuss diffusion as a dynamical process later. For now we treat the path of a (Markovian, Gaussian) random walk on a Euclidean lattice as a fractal substrate by associating a unit mass with each step of the walk. It is a simple problem to find the fractal dimension: Consider the random walk to start at the origin O at t=0. At each unit time interval the random walk progresses one further step in the (randomly) chosen direction. For a given walk realisation (see fig.1.5), let $\underline{R}_n$ be the position vector relative to the origin after n steps (ie at time t=n). Then

$$\underline{R}_{n+1} = \underline{R}_n + \underline{a} \qquad (1.1.11)$$

where $\underline{a}$ is a lattice vector. ie,

$$R_{n+1}^2 = (\underline{R}_n + \underline{a})^2 = R_n^2 + 2\underline{R}_n.\underline{a} + a^2 \qquad (1.1.12)$$

Then take a configurational average over all possible configurations of walks (denoted by $<\ldots>$). Since the walk is Markovian, it follows that $<\underline{R}_n.\underline{a}> \equiv R_n a<\cos\theta> = 0$ for large n. Thus

$$<R_{n+1}^2> = <R_n^2> + a^2. \qquad (1.1.13)$$

However, $<R_0>=0$ and so $<R_{n+1}^2> = na^2$, $n\to\infty$. Thus we see that the number of steps contained (on average) within a ball of radius R, ie M(R), scales as

$$M(R) \sim R^2. \qquad (1.1.14)$$

and so the fractal dimension of a Gaussian random walk is $d_f=2$ in *all* embedding dimensions. The conformation of Gaussian random walks (GRWs) is in fact a trivial

problem as the complete probability distribution $P_n(R)$ (in the limit $n\to\infty$, $R\to\infty$, $n/R\to\infty$) for end-to-end distances is straightforwardly obtained (McKenzie 1976):

$$P_n(R) = \frac{1}{(2\pi na^2/d)^{(d/2)}} \exp(-dR^2/2na^2). \qquad (1.1.15)$$

iv) Self-Avoiding Walks and Self-Avoiding Walks with Crosslinks.

Self-avoiding walks (SAWs) are similar to GRWs above except that no self-intersections are allowed at all. This destroys the Markovian nature of the walks and makes this model highly non-trivial and few exact results are known. A typical configuration is illustrated in fig.1.6. Flory (1953) developed a (mean-field) theory for the configurationally average end-to-end length. His original formulation has subsequently been modified by Fisher (1969) in a manner emphasising the dependence on embedding dimensionality. Owing to the significance of the result, we briefly recall Fisher's elegant argument. Write the partition function Z(R) for a walk of N steps with fixed end-to-end (Euclidean) distance R as

$$Z(R) = C_d R^{d-1}\exp(-dR^2/2n)\langle\exp(-\beta U_n)\rangle_R \qquad (1.1.16)$$

where C_d is a constant; $\beta=1/k_BT$. The Gaussian term $R^{d-1}\exp(-dR^2/2n)$ takes account of the connectivity of the chain and the term in U_n, the total interaction between step segments, and is averaged over all configurations such that $|\underline{R}_n-\underline{R}_0|=R$. Then write the free energy as the sum of two terms

$$F = \beta\log Z(R) = U_0 + U_1 \qquad (1.1.17)$$

where U_0 represents diffusive terms and U_1 the interactive terms. Flory theory assumes that $U_1=\frac{1}{2}B(T)n(n/A_dR^d)$, where B(T) is the effective strength of each interaction and (n/A_dR^d) is the probability that a step will interact with another. This is the mean-field approximation. Now, as in conventional mean-field theory one maximizes F with respect to R obtaining

$$\frac{R^2}{n} = \frac{d-1}{d} - \frac{1}{2}\frac{B}{A_d}\frac{n^2}{R^d}. \qquad (1.1.18)$$

For $d>4$, the constant term on the RHS of (1.1.18) dominates and one obtains

$$R \propto n^{\frac{1}{2}} \qquad (n\to\infty,\ d>4). \qquad (1.1.19a)$$

For $d<4$ it is assumed that the interaction term dominates:

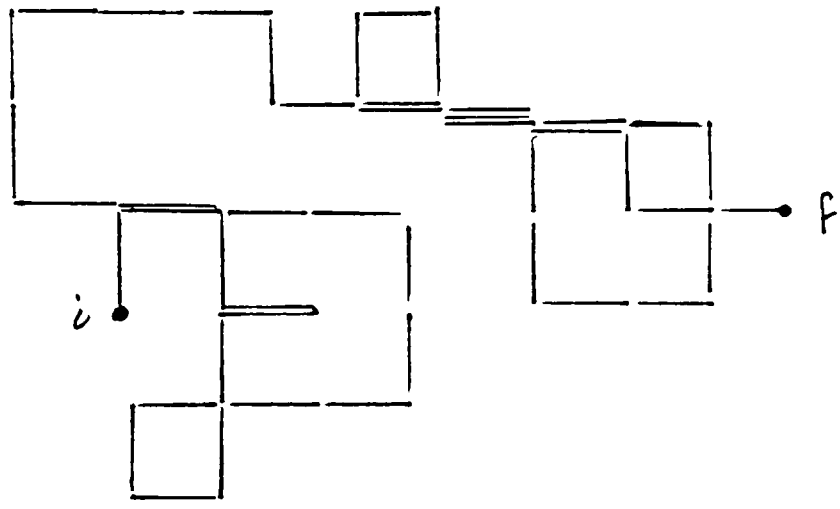

Fig.1.5: Gaussian random walk realisation. The RMS end-to-end distance scales as $<R_n> \sim n^{\frac{1}{2}}$.

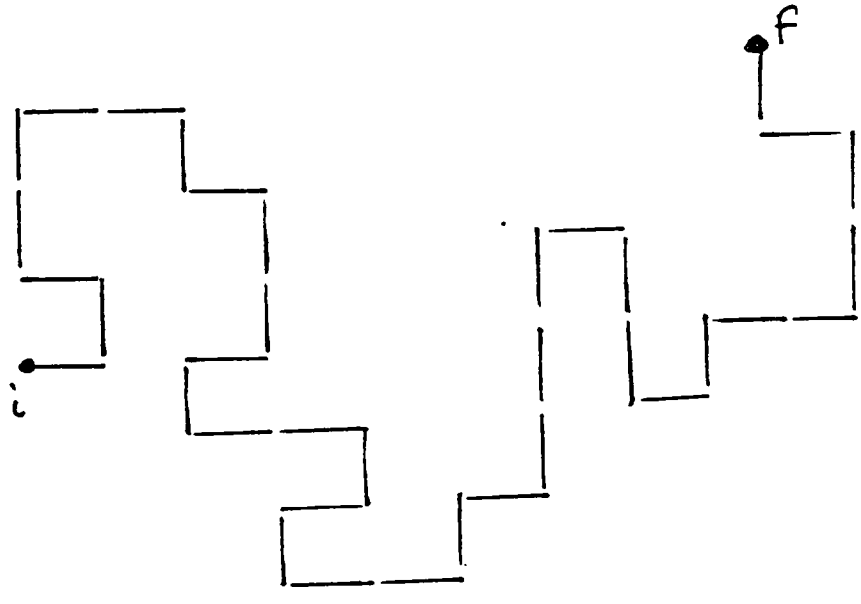

Fig.1.6.: Typical self-avoiding walk configuration.

$$R \propto n^{\nu} \qquad (n\to\infty,\ d<4). \qquad (1.1.19b)$$

Where $\nu = (1/d_f) = 3/(d+2)$. d=4 is identified as an upper critical dimensionality at which dimension the excluded problem becomes trivial since one recovers the critical exponents for the Gaussian random walk.

The SAW is important in statistical mechanics not only because it is a simple yet sensible model of linear polymers but also because of its close relation to magnetic models. de Gennes (1972) observed that a renormalisation group Feynman graph expansion for the n-component model (φ^4 model) (see below) generated diagrams which gave SAWs in the limit n=0. Subsequently Emery (1975) proved this isomorphism non-perturbatively and showed that, taking the *analytic* limit n→0 within the partition function for the continuous spin n-component model yielded the generating function for SAWs. In chapter 5, we rederive this result in a couple of lines.

The static configurations of proteins —— linear polymers with crosslinking disulphide and hydrogen bonds —— may be modelled by SAWs (Helman *et al* 1984). However for dynamical problems, eg electrical conductivity (see chps. 5,6), the H-bonds are expected to play a significant rôle and need to be incorporated into the model. This is achieved by including massless nearest neighbour segments joining sites not connected *a priori* by the walk backbone (fig.1.7)

2. Statistical Mechanical Models.

We introduce the models of importance to this thesis.

i) Ising model.

Consider a Bravais lattice in d-dimensions with a (localised) spin operator S_i^z associated with each site i. Define the Ising Hamiltonian as follows:

$$H = -\sum_{<i,j>} J_{ij}\, S_i^z S_j^z \;-\; \sum_i h_i^z S_i^z \qquad (1.2.1)$$

where h_i^z is a longitudinal magnetic field at site i and J_{ij} (>0 for ferromagnetism, <0 for antiferromagnetism) measures the coupling strength between spins at i and j.

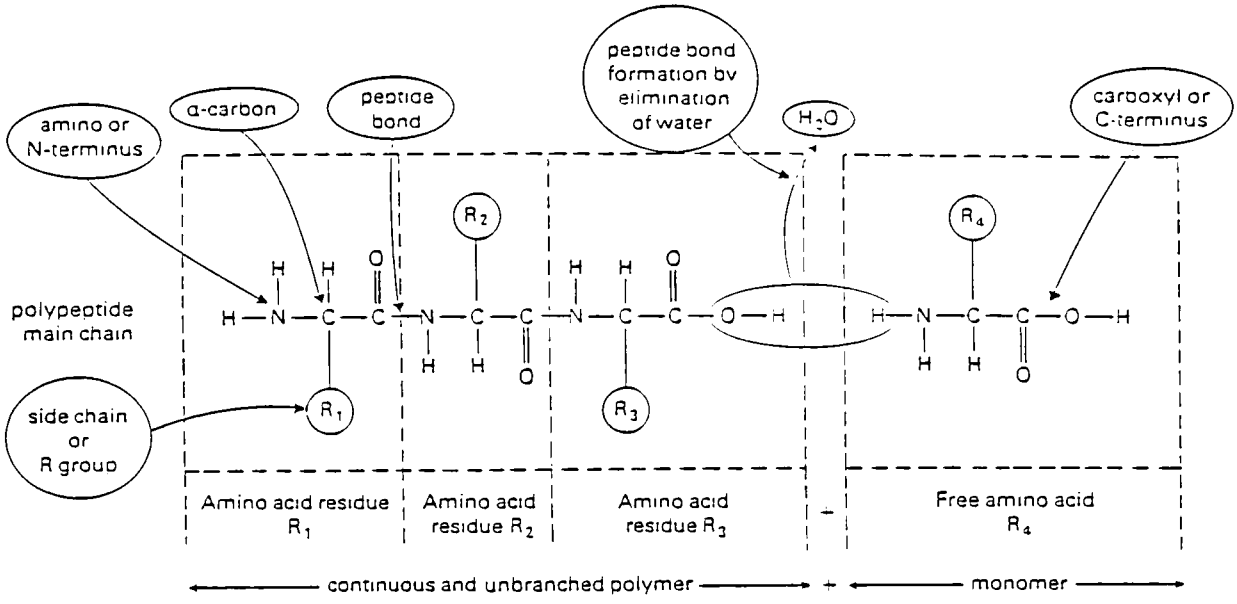

(a)

Fig.1.7.:

a) Chemical structure of a polypeptide chain.

b) Influence of crosslink Hydrogen and disulphide bonds on linear configuration.

c) SAW model for protein. The crosslink bonds may be viewed as springs (for the virational problem), resistances (for the resistor network problem), non-zero hopping terms (for diffusion) or non-zero spin couplings (for the spin wave problem)

a) and b) from Dickerson and Geis (1983).

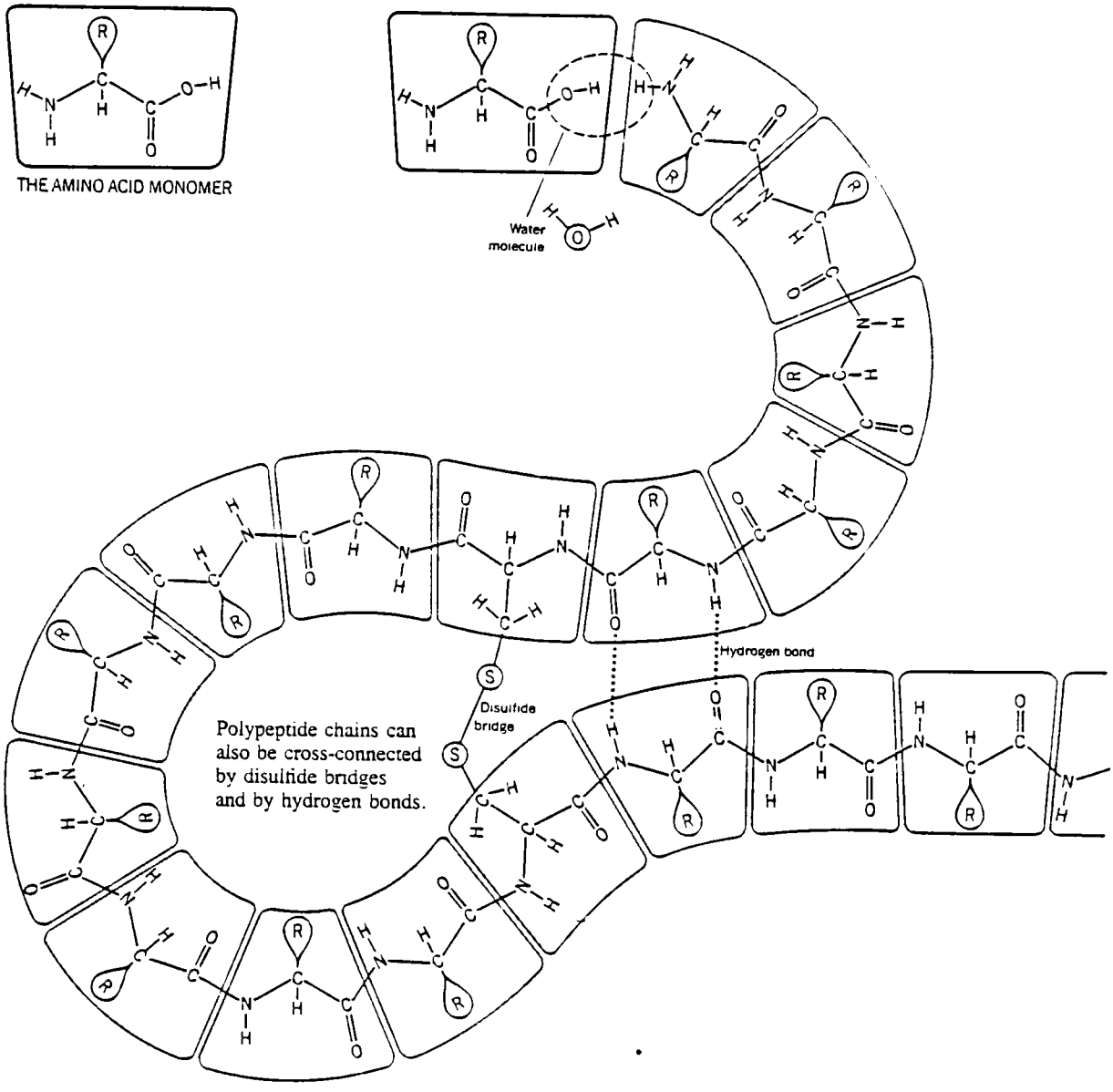
THE AMINO ACID MONOMER
Water molecule
Hydrogen bond
Disulfide bridge
Polypeptide chains can also be cross-connected by disulfide bridges and by hydrogen bonds.

(b)

(c)

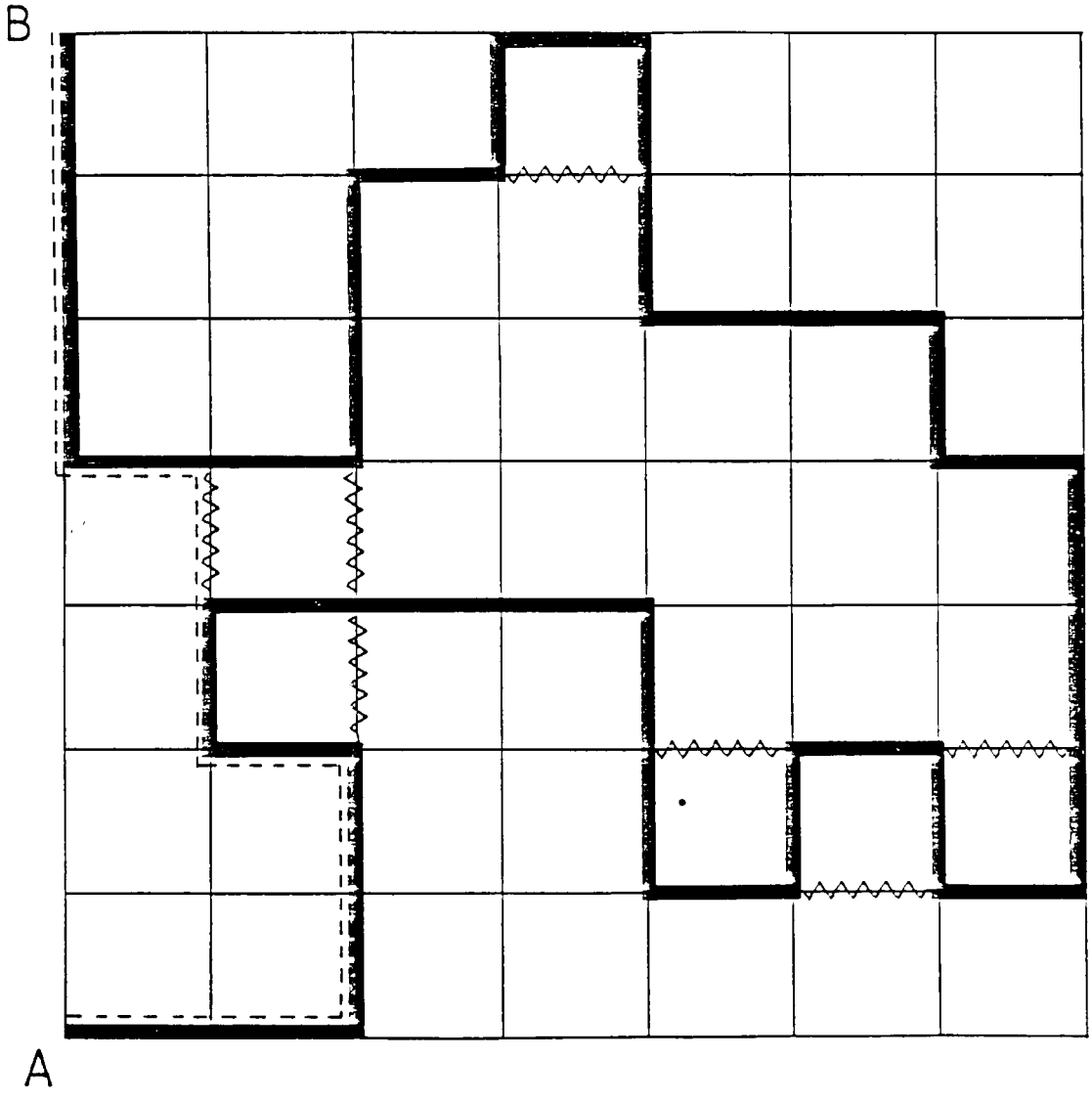

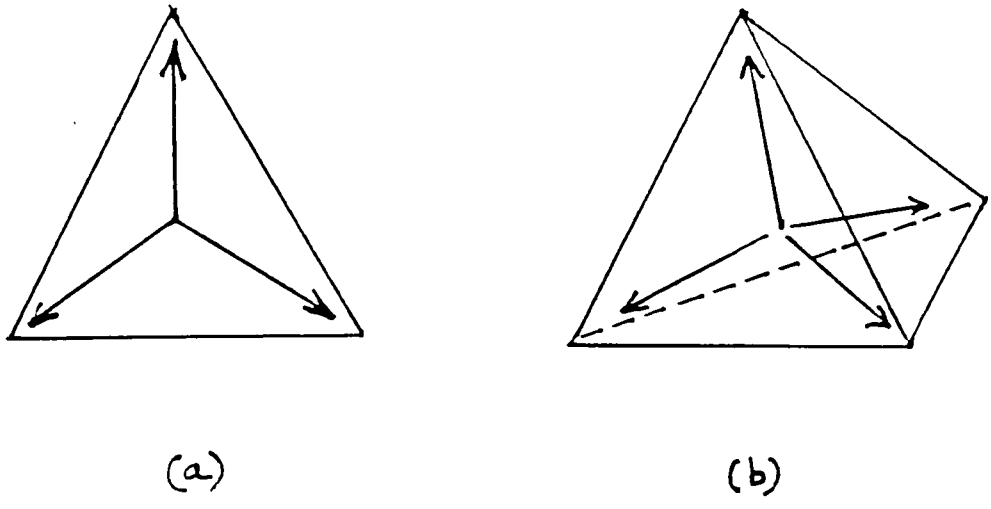

Fig.1.8.: The Potts model states. The q discrete states point from the centre to the corners of a (q-1)-dimensional simplex. a) q=3, b) q=4.

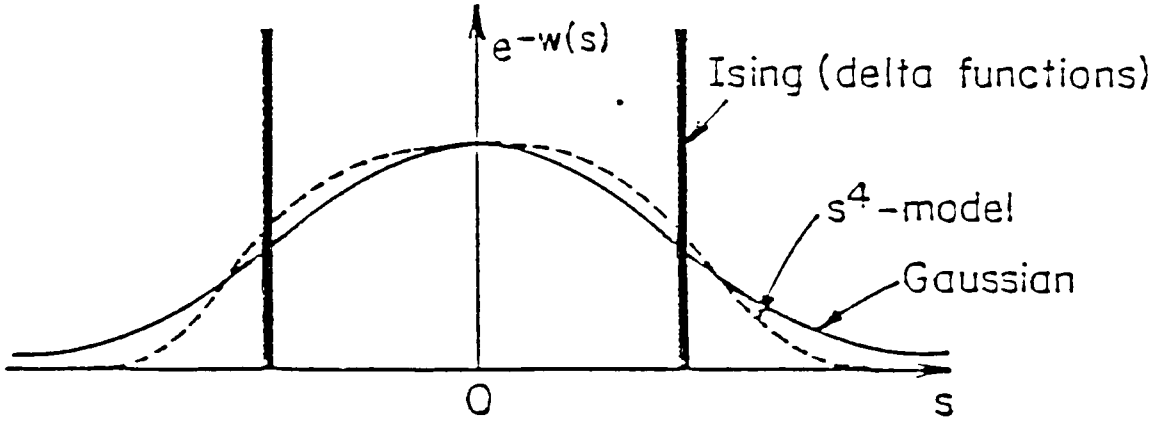

Fig.1.9.: Schematic comparison of the spin weighting functions exp[-w(s)] for the Ising, Gaussian and S^4 (or φ^4) models (from Fisher 1982).

Commonly J_{ij} is set to zero when i and j are not nearest neighbours. The spins are single component spins —— and may be considered to be classical vectors since the magnetic field is longitudinal. Thus in the $S=\frac{1}{2}$ Ising model the S_i^z may each be in either the "up" state $S_i^z=\frac{1}{2}$ or in the "down" state $S_i^z=-\frac{1}{2}$, and so the interaction term can take two values for each pair of sites depending on whether they are in the same or in different states. The elementary excitations of this model are spin flips.

The Ising model is much the simplest possible interacting system and yet exact solutions are few. The one-dimensional Ising model was solved in his thesis (Ising 1925). The two-dimensional model in zero field was solved in the celebrated paper of Onsager (1944). No exact solutions exist for either the 3d model or for the 2d model in a field.

ii) Heisenberg (n-component) and Anisotropic Heisenberg Models.

The n-component Heisenberg model is a generalisation of the Ising model to n-component spins (n>1) —— and thus to an n-component order parameter. The natural way to define the Hamiltonian is thus:

$$H = - \sum_{<i,j>} J_{ij}\, \underline{S}_i \cdot \underline{S}_j \quad - \quad \sum_i \underline{h}_i \cdot \underline{S}_i \qquad (1.2.2)$$

n=1 gives the Ising model, n=2 gives the XY model and n=3 gives the usual isotropic Heisenberg model. Stanley (1968) has demonstrated the equivalence of the $n\to\infty$ Heisenberg model with the exactly soluble *spherical model* (Berlin and Kac 1952). As mentioned earlier, n=0 is the self-avoiding walk (SAW) (de Gennes 1972). Finally, taking n=-2 gives the Gaussian model (see below).

The non-commutation of the spins is now relevant and introduces intrinsic dynamics, namely spin waves, which we discuss below. These elementary excitations are bosons and since the Heisenberg model obeys the Goldstone theorem they are gapless. The Goldstone symmetry is broken by either non-zero field $\underline{h}_i$ or anisotropy terms as follows:

$$H = - \sum_{<i,j>} J_{ij}\, (\alpha \underline{S}_i \cdot \underline{S}_j + (1-\alpha) S_i^z S_j^z) \quad - \quad \sum_i \underline{h}_i \cdot \underline{S}_i \qquad (1.2.3)$$

where α=1 gives the isotropic Heisenberg model and α=0 gives the Ising model; further

$\alpha \to \infty$ gives the XY model.

iii) Potts Model.

This magnetic model is a generalisation of the two-state Ising model to q discrete states. The Hamiltonian may be written as follows:

$$H = -(q-1) \sum_{<i,j>} J_{ij}\, \underline{v}_i \cdot \underline{v}_j - \sum_i \underline{h}_i \cdot \underline{v}_i \qquad (1.2.4)$$

where $\underline{v}_i$ are the (normalised) vectors pointing from the centre to the corners of a (q-1)-dimensional simplex. This is indicated schematically in fig.1.8. A little elementary trigonometry yields the result that

$$\underline{v}_i \cdot \underline{v}_j = 1 \qquad \text{if } \underline{v}_i = \underline{v}_j$$
$$= -\frac{1}{q-1} \qquad \text{otherwise.} \qquad (1.2.5)$$

q=2 is thus identically the Ising model. The Potts model has two further useful properties. Firstly, taking the analytic limit $q \to 1$ within the partition function gives the generating function for percolation clusters. Secondly, taking the analogous limit $q \to 0$ gives the resistor network problem (Kasteleyn and Fortuin 1969). That is, by taking the appropriate q limit, the Potts model generates a Hamiltonian formulation for these problems. This can be very useful for calculating critical exponents as we discuss below. The result for $q \to 0$ is discussed further in chp.5 and used to study the resistance of random walks.

iv) Continuous Spin Models.

It is possible —— and indeed in certain circumstances, highly desirable —— to express the discrete magnetic models (eg Ising) as continuous field theories. There are several ways in which this may be accomplished. One method is to use the *Hubbard-Stratanovich* transformation (see Chp.6). An alternative viewpoint is to set up a partition function such as

$$Z = \int_{-\infty}^{\infty} \prod_m dS_m \, e^{-w(S_m)} \exp\left\{ K \sum_{<i,j>} S_i S_j \right\} \qquad (1.2.6)$$

such that each spin is subject to a distribution (or *weight*) function $\exp(-w(S_i))$. For example,

$$e^{-w(S_i)} = 2\delta(S_i{}^2-1) \quad \Rightarrow \text{ Ising Model.} \qquad (1.2.7a)$$

$$= e^{-\frac{1}{2} b|S|^2} \quad \Rightarrow \text{ Gaussian model.} \qquad (1.2.7b)$$

$$= e^{-\frac{1}{2} b|S|^2 - u|S|^4} \quad \Rightarrow S^4 \text{ (or } \varphi^4\text{) model.} \qquad (1.2.7c)$$

Fig(1.9) summarises this information. Powerful field theoretic techniques may now be brought to bear no these models to, eg, calculate critical indices. It is generally believed that the exponents of the S^4 (or φ^4) model are identical to those of the Ising model. The reason why the higher order terms do not affect the critical properties is elucidated by the renormalisation group (RG) theory. Before a discussion of RG we should first say some words about the dynamical processes we will be investigating.

3. Dynamical Phenomena in Many Body Systems.

The bulk of this thesis concerns *linear* dynamical phenomena (excepting chp.2 which deals with a static problem and chp.8 which deals with a non-linear dynamical problem). We here introduce the kinds of dynamics that are considered.

a) Spin Waves

Consider the isotropic Heisenberg Hamiltonian given in (1.2.2), then defining $S_j^+ \equiv S_j^x + iS_j^y$ and using the usual method one obtains the following *linearised* equation of motion (Anderson 1952):

$$-i\frac{dS_i^+}{dt} = \sum_{<i,j>} J_{ij}(S_j^+ - S_i^+) + h_i^+. \qquad (1.3.1)$$

on taking the spin magnitude to be unity and $S^z \approx S \equiv 1$. Fourier transforming with respect to time yields the following linear difference equation:

$$\omega S_i^+(\omega) = \sum_{<i,j>} J_{ij}(S_j^+ - S_i^+) + h_i^+ \qquad (1.3.2)$$

This latter result is only slightly modified for the case of a two-sublattice Heisenberg antiferromagnet (see appendix P):

$$(-1)^{\alpha_i}\omega S_i^+(\omega) = \sum_{<i,j>} J_{ij}(S_j^+ + S_i^+) - h_i^+ \qquad (1.3.3)$$

where α_i=1,0 on the "up" and "down" sublattice respectively.

Fourier transformation of (1.3.2) with respect to spatial variables (for the trivial, non-random case ,J_{ij}=J, in zero field, h_i=0) yields the dispersion relation

$$\begin{aligned}\omega &= 4a^2(J(\underline{0})-J(\underline{k})) \\ &\approx Dk^2 \qquad ka \ll 1. \end{aligned} \qquad (1.3.4)$$

where $J(\underline{k})$ is the Fourier transform of J_{ij} and D (=2Ja^{2}d, for a hypercubic lattice) is the spin wave stiffness.

One effect of substitutional (ie percolative) disorder is to renormalise the spin wave stiffness $D \to D(p) \sim (p-p_c)^{t-\beta}$ — so D(p) vanishes as the percolation threshold is approached. This is an example of the effect known as *critical slowing down*. This is discussed more fully, together with disorder induced critical damping effects, in Chp.7 and Appendix P for antiferromagnets. A crossover argument (see introduction to Chp.7) yields the following *anomalous* dispersion relation in the critical regime (where $k\xi \gg 1$, $ka \ll 1, \xi/a \gg 1$):

$$\omega \sim k^z \qquad (1.3.5)$$

where z, the dynamic critical exponent is greater than two and is generally related to the static percolation critical exponents (see Chp.7) as follows:

$$z = 2 + (t-\beta)/\nu. \qquad (1.3.6)$$

Further, it may be shown that in this regime (Alexander and Orbach 1983, Lewis and Stinchcombe 1984) the density of states also scales with ω in an anomalous fashion:

$$\rho(\omega) \sim \omega^{d_s/2 - 1} \qquad (1.3.7)$$

where d_s is the *spectral* or *fracton* dimension; d_f is the percolation cluster fractal dimension and z the dynamic exponent introduced above. (1.3.7) of course compares

with the corresponding result $\rho(\omega)\sim\omega^{d/2-1}$ for spin waves in homogeneous space. These anomalous power law behaviours are induced by the divergence of the *geometrical* correlation length ξ_p. Alexander and Orbach (1983) have shown that the spectral dimension d_s is related to the dynamic exponent z and the substrate fractal dimension d_f:

$$d_s = 2d_f / z \qquad (1.3.8)$$

and have made the celebrated conjecture $d_s=4/3$ for all *homogeneous* fractals in *all* dimensions.

b) Vibrations (Phonons)

Considering Hooke's law forces such that the spring stiffness between sites i and j is J_{ij}, the resulting equation of motion for the particles is

$$\frac{d^2}{dt^2} u_i(t) = \sum_{<i,j>} J_{ij}(u_j - u_i) \qquad (1.3.9)$$

or Fourier time transformed

$$-\omega^2 u_i(\omega) = \sum_{<i,j>} J_{ij}(u_j - u_i) \qquad (1.3.10)$$

which is clearly isomorphic to (1.3.2) for spin waves. Fourier transformation with respect to space yields the usual low frequency dispersion relation $\omega=ck$. However, following the remarks concerning disorder induced critical slowing down we expect that the modified dispersion relation in the critical regime ($k\xi \gg 1$) to be as follows:

$$\omega \sim k^{z/2} \qquad (1.3.11)$$

where z is a dynamic critical exponent appropriate for phonons. In fact, owing to the isomorphism between (1.3.2) and (1.3.10) we see that the two dynamic critical exponents will be identical. In this case the density of vibrational states is expected to scale as follows:

$$\rho(\omega) \sim \omega^{d_s-1}$$

where $d_s=2d_f/z$, as before.

c) Diffusion (Random Walks)

Here the governing equation is the *master equation*:

$$-\frac{d}{dt} P_n(t) = \sum_{<m,n>} \{ w_{n,m} P_n(t) - w_{m,n} P_m(t) \} \qquad (1.3.12)$$

where $P_n(t)$ is the probability that the diffusing particle is at site n at time t. $w_{a,b}$ is the transition probability from site a to site b. That is, they are the elements of the Markov process transition matrix. Laplace transformation of (1.3.12) with respect to time yields

$$-s \tilde{P}_n(s) = \sum_{<m,n>} \{ w_{n,m} \tilde{P}_n(s) - w_{m,n} \tilde{P}_m(s) \} - P_n(t=0). \qquad (1.3.13)$$

This equation is of course isomorphic to the Fourier transformed equivalent equation for spin waves (1.3.2) discussed above. We return to this point below.

In analogy to the anomalous spin wave dispersion relation for spin wave on percolation clusters (or indeed *any* scale-invariant structure such that an appropriate geometrical correlation length diverges) the RMS end-to-end distance $<R_n>$ scales with n in a non-trivial way —— recall $<R_n> \sim n^{\nu}$, where $\nu = \frac{1}{2}$ for Euclidean spaces. On a general scale-invariant space $<R_n>$ will scale as follows:

$$<R_n> \sim n^{\nu} \qquad (1.3.14)$$

where, by analogy with our discussion of fractal spaces, we define the *dimensionality of the walk* as

$$d_w = \nu^{-1}. \qquad (1.3.15)$$

The analogue of the density of states for a diffusing particle is the probability of return to the origin after n steps $P_o(n)$. On a Euclidean lattice, it is easy to show (see Toulouse and Pfeuty 1975) that

$$P_o(n) \sim R^{-d} \sim n^{-d/2} \qquad (1.3.16)$$

In anology with spin waves above (1.3.7) the generalisation of (1.3.16) is

$$P_o(n) \sim R_n^{-d_f} \sim n^{-d_s/2} \qquad (1.3.17)$$

where d_s, the spectral dimension, is equal to $2d_f/d_w$. Alternatively, considering the number S_n of distinct sites visited during an n-step random walk, Rammal and Toulouse (1983) have argued that this too scales according to the spectral dimension, and claim that

$$S_n \sim n^{d_s/2} \qquad d_s<2 \qquad (1.3.18a)$$

$$\sim n \qquad d_s>2 \qquad (1.3.18b)$$

For Euclidean lattices $d_s \equiv d$, and (1.3.18) is consistent with asymptotic results on lattices (see eg Montroll and West 1979).

d) Electrical Conductivity.

Finally, although not strictly a dynamical problem, owing to its relation to the processes a,b,c above we also shall consider electrical conductivity on scale-invariant networks , in particular on walks (Chp.3,5,6). The governing equation of motion is now given by Kirchoff's laws (1847)

$$I(x_n) = \sum_{<m,n>} g_{m,n}[\, V(x_m) - V(x_n) \,] \qquad (1.3.19)$$

where $g_{m,n}$ is the electrical conductivity of the resistor connecting sites m and n. $I(x_n)$ is the current injected into site x_n. In a typical resistor network problem I might be set to $I(x)= \delta_{x,x_i} - \delta_{x,x_f}$. Setting $I(x) \propto \partial V(x,t)/\partial t$ then makes the resistor network problem isomorphic to a,b,c above (see also Last (1972) and Kirkpatrick 1979).

In summary, it is evident that using the generic set of dynamical variables $\{u_i\}$, the above four problems may be expressed in terms of the following set of linear equations:

$$\Omega u_i = \sum_{<i,j>} M_{ij} u_j \qquad (1.3.20)$$

where M_{ij} is a real symmetric dynamical matrix. Other related dynamical models which are isomorphic to (1.3.20) include Ising Glauber dynamics — in which the time depedence of the spin configuration is governed by a master equation — and electron tight binding models. "Goldstone" systems (eg spin waves, phonons, diffusion, Glauber dynamics), satisfying $\sum_j M_{ij} = M_{ii}$, have the consequence that $\sum_j u_j$ is a constant of the

motion and also have gapless excitation spectra. The tight binding models do not satisfy this relation.

4. Phase Transitions, Critical Phenomena and Scaling.

In the vicinity of a continuous (or second order) phase transition, the thermodynamic properties of the system become singular and these singularities are governed by a set of critical exponents.

The sort of systems we might be thinking of are, for example, a fluid (near the critical point), a superconductor in zero field, the λ-transition in liquid ^{4}He and order-disorder transitions in binary alloys. For the purposes of this section we will use that king of phase transition theory, namely the ferro-to-paramagnetic transition for a magnet in zero field, as our illustration. For the magnetic systems the set of critical exponents is defined in Table 1.1. Analogous definitions exist for fluids (Stanley 1971). Percolation is a model which shows so-called *geometrical critical behaviour*. Geometric quantities display singular properties near the percolation threshold in much the same way as do the thermal quantities in Table 1.1; we summarise the results in Table 1.2.

The observed critical exponents display two striking features. Firstly, they are independent of the detailed nature of the interactions —— strength and range of interactions, anisotropy strength, spin magnitude or lattice type. Rather, they seem only to depend on the dimensionality d of the space and the number of components n of the order parameter (see fig.1.10). Thus, for example, the 2d magnetic systems corresponding to the XY model share the same set of critical exponents as liquid He films (both have d=2, n=2). Secondly, for a given system, the critical exponents obey certain empirical relations indicating that they are not all independent. This latter observation was first put on a theoretical basis by Widom (1965) and Griffiths (1965) using the celebrated *homogeneity hypothesis* for the singular part of the Gibbs free energy. In the simple case of a two parameter problem (temperature $t=|(T-T_c)/T_c|$; field h) this takes the form:

$$G(t,h) = b^{-d}G(b^{\lambda_t}t, b^{\lambda_h}h) \qquad (1.4.1)$$

where b is arbitrary and d is the space dimension. The scaling function (1.4.1) is

Table 1.1.

Definitions of critical exponents for a typical magnetic system. The thermal variable t is usually $(T-T_c)/T_c$ {but see eg Chp.8}. The homogeneity hypothesis (and subsequently RG) shows that the exponents on either side of the transition are in fact identical.

Variable	Critical Exponent	
Specific Heat in a constant magnetic field	$C_H \sim (-t)^{-\alpha'}$	$t<0$
	$C_H \sim (t)^{-\alpha}$	$t>0$
Zero field Magnetisation	$M \sim (-t)^{\beta}$	$t<0$
Zero field isothermal susceptibility	$\chi_T \sim (-t)^{-\gamma'}$	$t<0$
	$\chi_T \sim (t)^{-\gamma}$	$t>0$
Critical isotherm (t=0)	$H \sim \lvert M \rvert^{\delta} \mathrm{sign}(M)$	
Correlation length	$\xi \sim (-t)^{-\nu'}$	$t<0$
	$\xi \sim (t)^{-\nu}$	$t>0$
Pair correlation function at criticality (t=0)	$\Gamma(r) \sim \lvert r \rvert^{-(d-2+\eta)}$	

Table 1.2.

Definition of critical exponents for the singular behaviour of geometrical percolation functions near p_c. $n_s(p)$ is the number of clusters comprising s connected sites per site. It is understood that we take the singular parts of the functions discussed

Geometric Function	Critical Exponent
Number of clusters $\sum_s n_s(p)$	$(p-p_c)^{2-\alpha}$
1st Moment $\sum_s s\, n_s(p)$	$\lvert p-p_c \rvert^{\beta}$
2nd Moment $\sum_s s^2 n_s(p)$	$\lvert p-p_c \rvert^{-\gamma}$
Critical generating function $\sum_s s\, n_s(p_c)\, e^{-hs}$	$h^{1/\delta}$
Mean distance between connected points (*Correlation length*) $\xi(p)$	$\cdot \lvert p-p_c \rvert^{-\nu}$

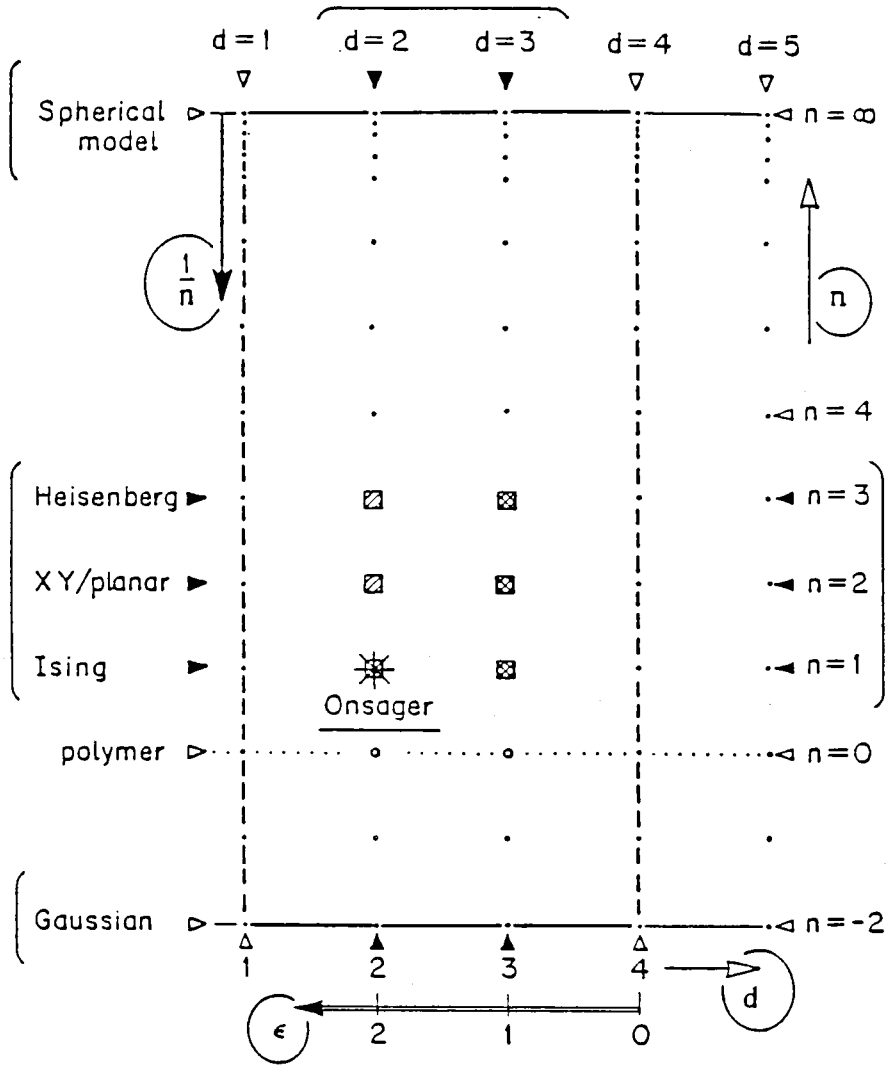

Fig.1.10.: Diagram of the (d,n) plane showing the expansion variables $\epsilon=4-d$ and $1/n$ (see below), the boundaries at $n=\infty$ and -2, and at $d=1$ and 4 and various physically relevant cases (From Fisher 1974).

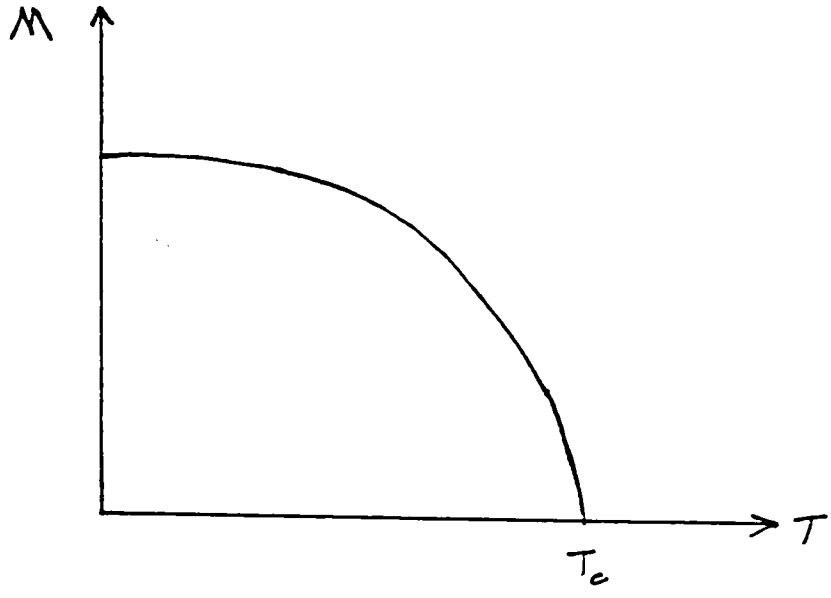

(a)

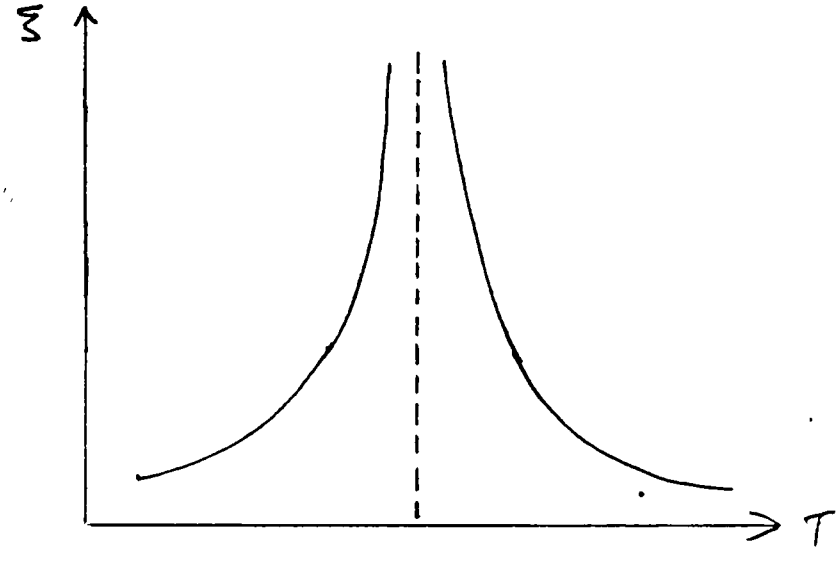

(b)

Fig.1.11.: Variation of a) Magnetisation with temperature for a ferromagnetic system; b) The correlation length with temperature in the vicinity of a second order phase treansition.

expected to take different forms below and above the transition. λ_t and λ_h are constants, and are related to the critical exponents. For example, differentiating (1.4.1) with respect to h yields

$$M(t,h) = b^{\lambda_h - d} M(b^{\lambda_t} t, b^{\lambda_h} h). \qquad (1.4.2)$$

To consider the exponent β, which defines the zero field magnetisation as one approaches the critical point t=0, we set h=0 and $b=(t)^{-1/\lambda_t}$, such that $T<T_c$. Then

$$M(t,h) = (-t)^{(d-\lambda_h)/\lambda_t} M(-1,0) \qquad (1.4.3)$$

and since $M(t,h=0) \propto (-t)^{\beta}$ we obtain $\beta=(d-\lambda_h)/\lambda_t$. Similar arguments (Stanley 1971, Chp.11) give the following further relations:

$$\alpha=\alpha'=2- d/\lambda_t \qquad (1.4.4a)$$

$$\gamma=\gamma'=(2\lambda_h-d)/\lambda_t \qquad (1.4.4b)$$

$$\delta=\lambda_h/(d-\lambda_h) \qquad (1.4.4c)$$

Thus one obtains (Widom 1965) the scaling laws

$$\alpha+2\beta+\gamma=2 \qquad (1.4.5a)$$

$$\gamma=\beta(\delta-1). \qquad (1.4.5b)$$

In order to derive the so-called *hyperscaling relations* involving η and ν, the following homogeneity assumption was used for the correlation function:

$$\Gamma(r,t) = b^{2(\lambda_h - d)} \Gamma(b^{-1} r, b^{\lambda_t} t). \qquad (1.4.6)$$

At the critical point (t=0) we know that $\Gamma(r,t)$ decays algebraically,

$$\Gamma(r,t=0) \sim \frac{1}{r^{(d-2+\eta)}}. \qquad (1.4.7)$$

Thus, putting t=0 and b=r into (1.4.6) gives $-(d-2+\eta)=2(\lambda_h-d)$; a similar argument yields $\nu=\lambda_t^{-1}$. Hence we obtain the relations

$$\gamma=\nu(2-\eta) \qquad (1.4.5c)$$

$$d\nu=(2-\alpha). \qquad (1.4.5d)$$

In fact, the assumption (1.4.6) is more fundamental than (1.4.1), which can be derived from the former. The crucial point in hyperscaling is that the value of "d" is indeed the embedding spatial dimension and not any anomalous one. The exponent relations

(1.4.5) seem to be satisfied in most situations (Stanley 1971) though (1.4.5d) is only satisfied at d=4 within Landau theory.

Scaling forms analogous to (1.4.1) have also been put forward for dynamic correlations (Ferrell *et al* 1967, Halperin and Hohenberg 1967, 1969). Denote the pair correlation function $C(r,t,\xi)=\langle S_r(t)S_0(0)\rangle$ and its Fourier transform $\chi(k,\omega,\xi)$. Here ξ is the correlation length —— this can have contributions from both thermal and geometrical (eg percolative) effects. The dynamic scaling hypothesis states that χ is a homogeneous function of only two arguments, ie

$$\chi(k,\omega,\xi) = k^{-(2-\eta+z)}F(k\xi,\omega k^{-z}). \qquad (1.4.8)$$

z is the dynamic critical exponent, giving the scaling of the characteristic frequency or width at the critical point ($\xi\to\infty$). Two asymptotic regimes with distinct dynamic behaviour are identified: The *hydrodynamic* regime ($k\xi\ll 1$) and the *critical* regime ($k\xi\gg 1$) (see fig.1.12). It is not clear that the dynamic scaling hypothesis is valid for all systems. For example, it has recently been shown to be violated by the kinetic Ising model on a percolating lattice using analytic (Henley 1986, Harris and Stinchcombe 1986) and numerical (Jain 1987, Chowdhury and Stauffer 1987) methods. These methods have been generalised to apply to the Potts model (see Lage 1987) which also appears to violate the dynamic scaling hypothesis. In this thesis (Chp.8) we demonstrate explicitly the dynamical crossover from the conventional dynamic scaling form (Hohenberg and Halperin 1977) to a singular dynamic scaling form for the anisotropic Heisenberg model.

In summary, any adequate theory of critical phenomena must explain two phenomena: homogeneity and universality.

Much progress towards understanding these processes was made in the late 60s. The key paper was that of Kadanoff (1966) which contained an intuitive and appealing discussion of the idea of thinning out degrees of freedom. He assumed, quite without any justification, that one could treat *superspin* blocks of ferromagnetic spins as if they were effectively single spins with effective nearest neighbour superspin interactions. He provided no algorithm for calculating the effective interaction from the original one. Kadanoff, however, did demonstrate that such assumptions yielded the set of scaling relations anticipated by the homogeneity hypothesis of Widom (1965). Kadanoff's paper

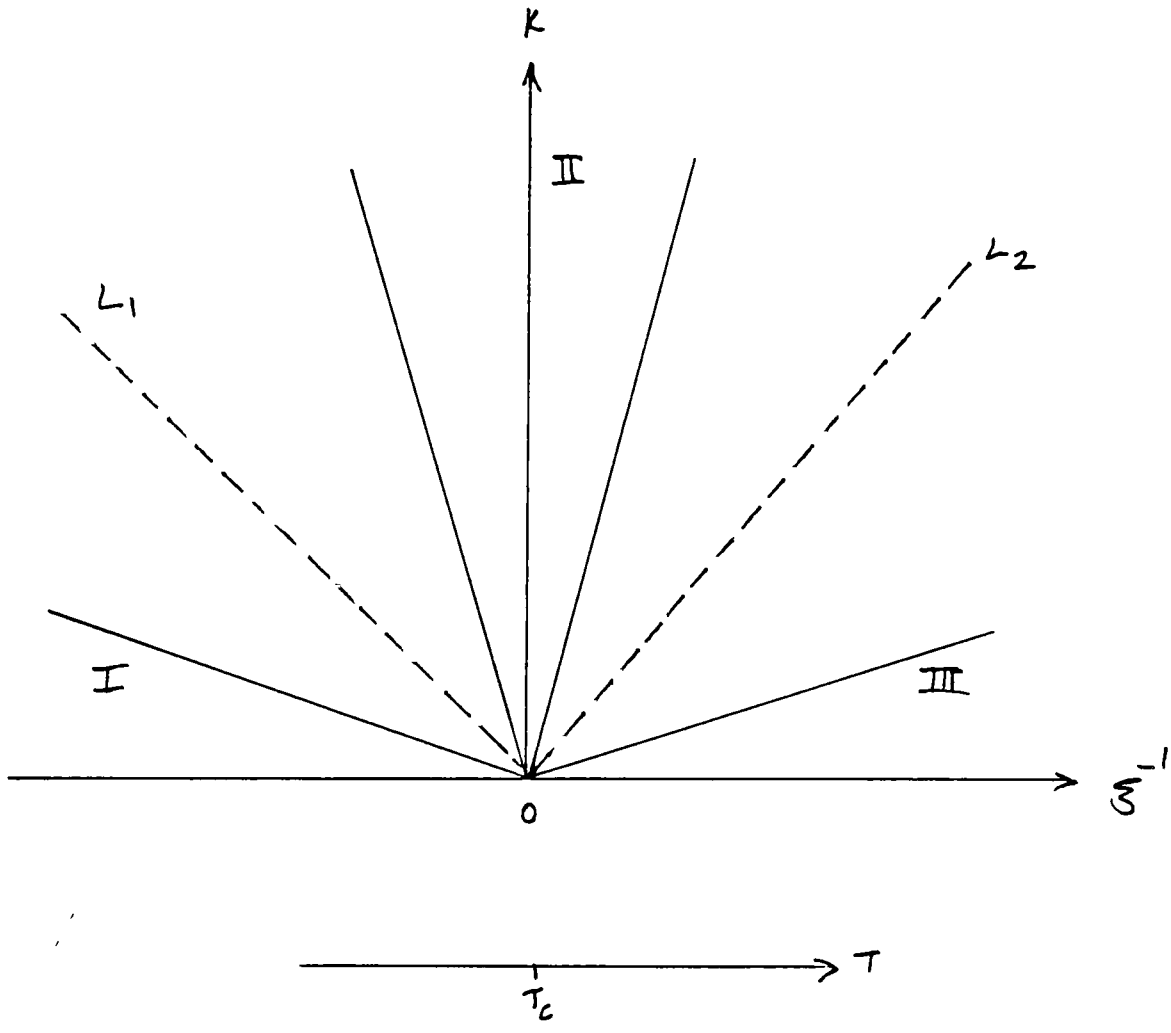

Fig. 1.12.: Schematic plot of the wave number k vs. the inverse correlation length ξ^{-1}. ξ diverges at $T = T_c$. The three asymptotic regions of distinct dynamical behaviour are (I) the hydrodynamic region below T_c ($\xi^{-1}<0$, $k|\xi| \ll 1$), (III) the hydrodynamic region above T_c ($\xi^{-1}>0$, $k\xi \ll 1$) and (II) the critical region near T_c ($k|\xi| \gg 1$). In all regions $ka \ll 1$, $|\xi/a| \gg 1$. The asymptotic forms in I and II are assumed to merge at L_1 ($k\xi = -1$), and similarly II and III on line L_2 ($k\xi=1$). (from Halperin and Hohenberg (1967))

is now recognised as the grandfather of modern RG methods and it provided a key idea for the development of renormalisation group theory (Wilson 1971, Wilson and Fisher 1971).

5. The Renormalisation Group.

The correlation length diverges as a system approaches its critical point. The many ($\sim 10^{23}$) degrees of freedom of the many body system (eg spin system) are behaving cooperatively and correlations on all length scales are equally important in driving the transition. The renormalisation group (RG) approach (Wilson 1971, Wilson and Fisher 1971) presents a rigorous formulation of the qualitative ideas of Kadanoff (1966). The original microscopic degrees of freedom are replaced in a stepwise manner: Thus short range degrees of freedom are succesively eliminated. In each step a prescription is given to construct an effective (course grained) degree of freedom. This elimination is achieved by, for example, a partial trace over a partition function.

We here summarise, for reference, the important ideas (for a full discussion of these and many more aspects of RG see Wilson and Kogut 1974). One stipulates that the partition function (and hence absolute ξ) is conserved. Thus the correlation length ξ/a (in units of lattice spacing) transforms as

$$(\xi/a)' = (1/b)(\xi/a). \qquad (1.5.1)$$

If $\underline{\mu}$ denotes the m parameters (temperture, field, interaction constants etc.) the resulting transformation of these parameters may be written as

$$\underline{\mu} \rightarrow \underline{\mu}' = R_b(\underline{\mu}) \qquad (1.5.2)$$

This is the RG recursion relation and R_b (a semi-group operator) is the operator giving the transformation of parameters resulting from the dilatation of length scale by a factor b.

At the physical critical point the correlation length is infinite and the system is scale-invariant: it will not notice the dilatation. This can arise at the fixed point $\underline{\mu}^*$,

$$\underline{\mu}^* = R_b(\underline{\mu}^*). \qquad (1.5.3)$$

Alternatively, at a critical point, $\underline{\mu}$ may be on a *critical surface* of points such that repeated applications of R_b to any point on the surface takes it into the fixed point.

This concept of flow through parameter space is illustrated in fig.1.13.

The properties of the operator R_b in the vicinity of the fixed point determine the critical exponents. Here write

$$\underline{\mu} = \underline{\mu}^* + \underline{\delta\mu} \qquad \underline{\mu}' = \underline{\mu}^* + (\underline{\delta\mu})' \qquad (1.5.4)$$

and hence, to terms linear in $(\delta\mu)$,

$$(\underline{\delta\mu})' = R_b{}^L(\underline{\delta\mu}). \qquad (1.5.5)$$

where $R_b{}^L$ is a linear (matrix) operator and $|\underline{\delta\mu}| \ll 1$. The eigenvalues $\lambda_1 \geq \lambda_2 \geq \ldots \geq \lambda_m$ and corresponding eigenvectors $\underline{e}_i$ of $R_b{}^L$ satisfy

$$R_b{}^L \underline{e}_i = \lambda_i(b)\underline{e}_i \qquad (1.5.6)$$

But since (semi-group property),

$$R_b R_{b'} = R_{bb'} \qquad (1.5.7)$$

we identify $\lambda_i(b)=b^{y_i}$, $y_1 \geq y_2 \geq \ldots \geq y_m$. Now, expand $\underline{\delta\mu}$ in the basis of eigenvectors $\underline{e}_i$,

$$\underline{\mu} = \underline{\mu}^* + t_1\underline{e}_1 + \ldots + t_2\underline{e}_m. \qquad (1.5.8)$$

Thus, operating R_b on $\underline{\mu}$ in the vicinity of the fixed point gives

$$\underline{\mu}' = R_b\underline{\mu} = \underline{\mu}^* + R_b{}^L\underline{\delta\mu} = \underline{\mu}^* + \sum_i t_i\, b^{y_i}\, \underline{e}_i. \qquad (1.5.9)$$

Now suppose that $y_1 > y_2 > 0 > y_3 > \ldots$. Then the terms with $i \geq 3$ will disappear after successive rescalings. The variables t_i $(i \geq 3)$ that will scale away are called *irrelevant* variables. The variables for which $y_i > 0$ are called *relevant*. Finally those for which $y_i = 0$ are *marginal* and can be dangerous in RG calculations, inducing unexpected crossovers. The existence of irrelevant variables provides an explanation of universality: disparate systems with critical points on a common critical surface (ie whose differences may be characterised by variables which emerge to be irrelevant) will flow to the same critical point and share the same set of critical exponents.

(1.5.9) also contains the essential ingredient for homogeneity as discussed earlier. To see this, consider the scaling behaviour of the singular part of Free energy:

$$G(\underline{\mu}) = b^{-d}G(\underline{\mu}') \qquad (1.5.10)$$

and so from (1.5.9) in the vicinity of a fixed point this equation may be written as

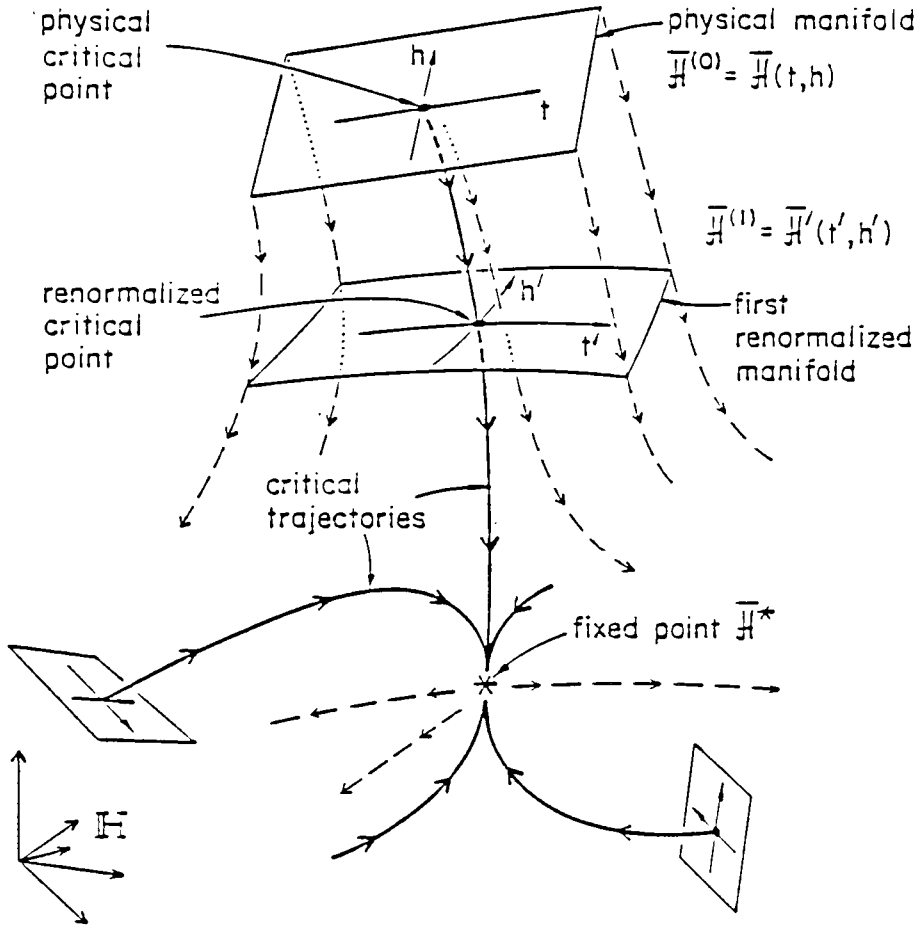

Fig.1.13.: Representation of the Hamiltonian (or *parameter*) space, showing initial or physical manifolds and subsequent renormalisation group flows. Critical trajectories are shown in bold: they terminate on the fixed point H^*. (from Fisher 1982)

$$G(\mu_1, \mu_2, \ldots, \mu_p) = b^{-d} G(b^{y_1}\mu_1, b^{y_2}\mu_2, \ldots, b^{y_p}\mu_p) \quad . \qquad (1.5.11)$$

But this is precisely the homogeneity assumption of Widom (1965) and others. Similar arguments may be applied to yield the corresponding result for the pair correlation function. Although hyperscaling has been assumed in stating (1.5.10), this can be checked within RG (Wilson and Kogut 1974).

Crossover phenomena can occur when a new relevant perturbation is introduced which drives the system to a new fixed point in parameter space (eg anisotropic terms in the Heisenberg magnet induce Ising-like critical behaviour sufficiently near T_c). The presence of percolative disorder, for instance, may or may not represent a relevant perturbation from pure critical behaviour. Essam and Garelick (1967) and Fisher (1968) showed that in a system with *annealed* disorder (impurity degrees of freedom in equilibrium with the other d.o.f.) the critical indices β,γ,ν are renormalised by a factor $(1-\alpha)^{-1}$, α by a factor $-(1-\alpha)^{-1}$, and η,δ are unchanged, where α is the pure system specific heat exponent, provided $\alpha>0$. When $\alpha<0$ the disordered system exponents are identical to the the pure ones. For the more realistic *quenched* systems, Harris (1974) argued that the pure fixed point is stable with respect to disorder for $\alpha<0$. For $\alpha>0$, a new distinct and stable *random* fixed point appears with corresponding random system critical exponents. This viewpoint has been confirmed by Harris and Lubensky (1974) who first applied RG to disordered systems.

Implementations of RG may be divided into two very different categories: *real space RG* and *momentum (or Hamiltonian) space RG*.

The main real space methods include:

i) Cluster decimation (Barber 1975, Kadanoff and Houghton 1975, Young and Stinchcombe 1975).

ii) Migdal-Kadanoff bond-moving (Migdal 1976, Kadanoff 1976).

iii) Block spin methods (Niemeyer and van Leeuwen 1974).

iv) Monte Carlo Renormalisation (see eg Swendsen 1982).

v) Phenomenological and other finite size scaling methods (Nightingale 1976, Sneddon 1978).

The real space methods usually have no expansion parameter for a controlled

development. They tend to obscure universality as they tend to be set up in different ways for different lattices etc. Their main advantages, however, are that they are intuitive and can provide very high accuracy in physically sensible dimensionalities. We will use blocking methods in many parts of this thesis (in parts of Chps.2,3,4,8) and a particularly simple illustration is presented in the next chapter.

The momentum space implementations use field theoretic and functional integral techniques (as originally developed by Wilson (1971) and Wilson and Fisher (1971)). The main momentum space techniques are:

i) ϵ-expansions from the upper critical dimension {ucd} (at which mean-field behaviour is correct) {eg ϵ=4-d for n-vector models, ϵ=6-d for percolation} (see below).

ii) ϵ-expansions from the lower critical dimension (at which T_c=0) {eg ϵ=d-2 for n-vector models, n>1} (Brézin *et al* 1976)

iii) 1/n expansions from spherical model behaviour (see Ma 1983).

In the ucd ϵ-expansions the process of transforming the length scale dilatation involves three steps:

i) Tracing over short wavelength degrees of freedom (ie $q_\Lambda/b \leqslant q \leqslant q_\Lambda$, where q_Λ is at the Brillouin zone edge).

ii) Rescaling the wavevectors by $q \to bq$.

iii) Scaling the spin magnitude by $S \to \zeta_b S$. This is done to maintain the form of the decay of correlations in the correlation function at criticality.

Symbolically (see also fig.1.14.), these three steps may be written

$$e^{H'\{S_q\}} = \left\{ \operatorname*{Tr}_{S_q^>} e^{H\{S_q^>, S_q^<\}} \right\}_{S_q^< \to \zeta_b S_{bq}} \qquad (1.5.12)$$

where $S_q^<$ and $S_q^>$ represent spin vectors with q-labels satisfying $0<q\leqslant q_\Lambda/b$ and $q_\Lambda/b<q\leqslant q_\Lambda$ respectively and q_Λ is the Brillouin zone edge.

This philosophy may be very easily illustrated (Fisher 1982) using the (trivial) Gausian model defined above. Here the partition function may be written as

$$Z = \int \prod_{\underline{q}} dS_{\underline{q}} \; e^{-\frac{1}{2} \int (r+eq^2) |S_{\underline{q}}|^2} \; . \qquad (1.5.13)$$

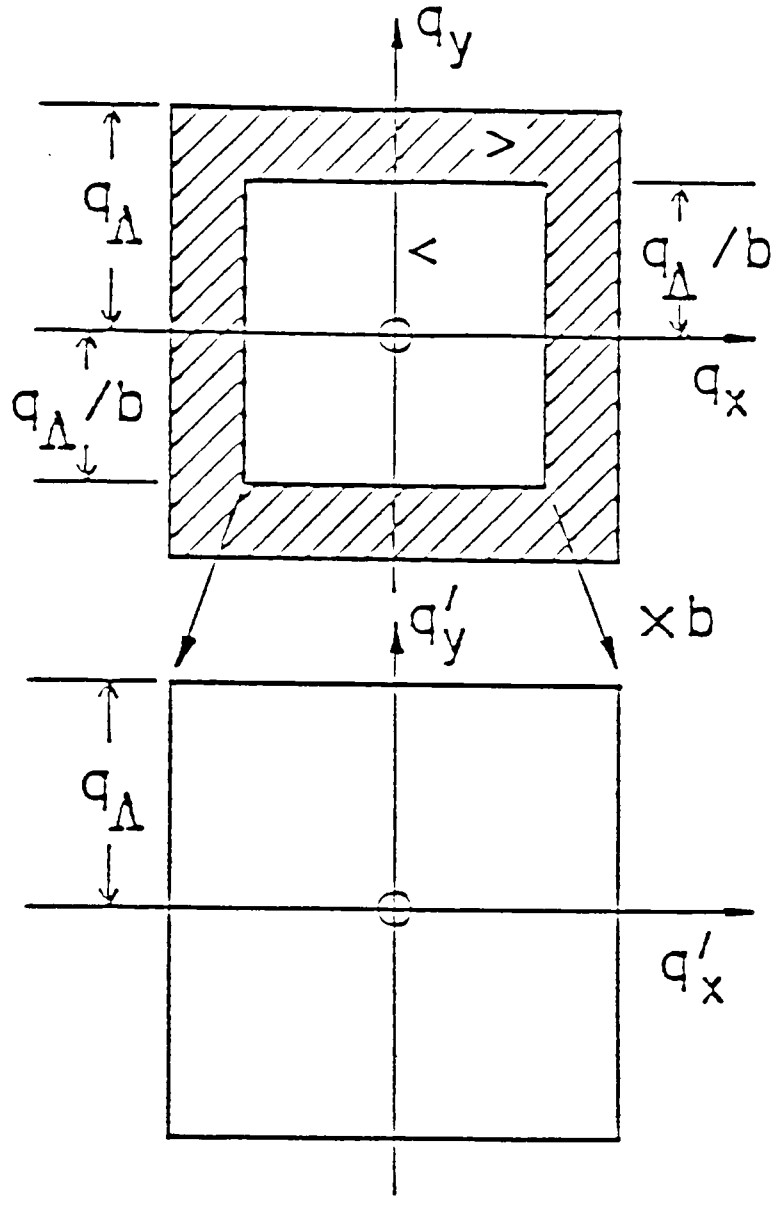

Fig.1.14.: Brillouin zone for the square lattice illustrating the construction of an inner zone, marked <, and an outer zone or *shell* marked >. After integrating over spin variables with momenta in the shell, the inner zone is expanded by a factor b to form the new, renormalised Brillouin zone (from Fisher 1982).

Integration over ther external regime is easily accomplished as the integrand factorises, and thus simply introduces a multiplicative constant. Hence

$$H'\{S_{\underline{q}<}\} = \tfrac{1}{2} \int_{\underline{q}} (r+eq^2)\ |S_{\underline{q}<}|^2 \qquad (1.5.14)$$

Then rescaling $q \to bq$ and $S_{q<} \to \zeta_b S_{bq}$ gives

$$H'\{S_{\underline{q}}\} = \tfrac{1}{2}\ \zeta_b^{\,2}\ b^{-d} \int_{\underline{q}} (r+e(q/b)^2)\,|S_{\underline{q}}|^2 \qquad (1.5.15)$$

and so we have the recursion relations

$$r' = \zeta_b^{\,2}\ b^{-d}\ r \qquad (1.5.16a)$$

$$e' = \zeta_b^{\,2} b^{-d-2}\ e. \qquad (1.5.16b)$$

The actual choice for ζ_b is, in principle arbitrary. However $\zeta_b = b^{(d+2-\eta)/2}$ is required in general to maintain the coefficient of the q^2 term to be unity. The reason for this choice is that the q^2 term is the one that sets the physical length scales. We explain this remark: the Fourier transform of the pair correlation function is expected to take the form (in a translationally invariant system),

$$\langle S_{\underline{q}} S_{\underline{p}} \rangle = G(\underline{q})\ \delta(\underline{p}+\underline{q}). \qquad (1.5.17)$$

At T_c, the power law decay of $G(\underline{q}) \propto |\underline{q}|^{-2+\eta}$ defines η. However, under RG rescaling we obtain, using $S_{q/b} \to \zeta_b S_q$,

$$\zeta_b^{\,2}\ \langle S_{\underline{q}} S_{\underline{p}} \rangle = b^{(d+2-\eta)}\ G(\underline{q})\ \delta(\underline{q}+\underline{p}). \qquad (1.5.18)$$

Since at T_c the correlations should be invariant with respect to the length scale ζ_b must be as given above.

More general RG are performed along similar lines. However, perturbation theory techniques (using the small parameter $\epsilon = d_u - d$) need to be used to evaluate the effects of higher order (eg φ^4) terms. It is possible to see that, in an approximate sense, u (the coefficient of φ^4) will renormalise as follows:

$$\begin{aligned} u' &= \zeta_b^{\,4}\ b^{-3d}\ u \\ &= b^{4-d-2\eta}\ u \\ &= b^{\epsilon-2\eta}\ u \end{aligned} \qquad (1.5.19)$$

ignoring contributions from higher order terms. Evidently u is *irrelevant* in the RG sense (scales to zero under successive iterations) for $d>4$. Thus $d=4$ is the upper critical dimension for the n-vector models, and for $d>4$ their critical properties are identical to those for the trivial Gaussian model. Further, this is the reason why the Ising model is expected to be in the same universality class as the φ^4 model —— the differences (ie φ^6 terms etc.) are irrelevant for d less than but close to four. Similarly φ^3 terms (in eg percolation) are irrelevant for $d>6$ and so the upper critical dimension for percolation is six. At $d\geq 6$ percolation on lattices has identical exponents to percolation on the Cayley tree (Toulouse 1974).

We have discussed these methods using formulations appropriate to static properties. This has been for the sake of simplicity and brevity. In chapter 6 we use these methods to study a dynamical problem, namely the resistance of random walk networks.

6. Plan of Thesis.

A *very* brief plan is as follows:

i) In Chapter 2, we consider percolation in the semi-infinite plane using simple Niemeyer-van Leeuwen (1974) blocking ideas and we investigate the crossover in the percolation probability function on approaching the surface. We also examine the relation of the fractal dimension of the surface clusters to critical exponents.

ii) Random walks on regular and random models for DLA are investigated in Chp.3 using RSRG. The applicability of the conflicting conjectures of Alexander and Orbach (1983) and Aharony and Stauffer (1984) is examined.

iii) A similar method is applied to SAWs and $\dot{S}AW$ models for proteins. A brief discussion of recent exact enumerations is also given.

iv) In Chp.5 we discuss a method for formulating spin-Potts Hamiltonian for conformational and resistance properties of walks. We use the Potts model in the limit $q\to 0$ together with specially constructed trace rules.

v) Using the results of Chp.5, we develop corresponding field theories and perform a momentum space RG calculation to determine the asymptotic end-to-end resistance scaling for GRWs, SAWs (trivial) and SAWs with crosslinks. These results are related to

those in Chp.3.

vi) In Chp.7, we study spin-wave damping in isotropic Heisenberg magnets near the percolation threshold. The transverse response function is determined in the hydrodynamic limit and we show that it does indeed satisfy the dynamic scaling hypothesis of Halperin and Hohenberg (1967). The analysis treats finite cluster response and relates critical exponents for the infinite cluster to those for the full system.

vii) In contrast, in Chp.8 we consider the relaxational dynamics of the *anisotropic* Heisenberg ferromagnet. Here, in an appropriately chosen regime the dynamics is dominated by domain (Bloch) wall diffusion. It appears that dynamic scaling is violated. Instead, a new *singular* dynamic scaling form governs the divergence of the characteristic relaxation time for all non-vanishing anisotropies provided the temperature is low enough. The crossover from conventional to singular dynamic scaling is demonstrated.

Fig.1.15.: Flow diagram showing development of and interrelationships in thesis.

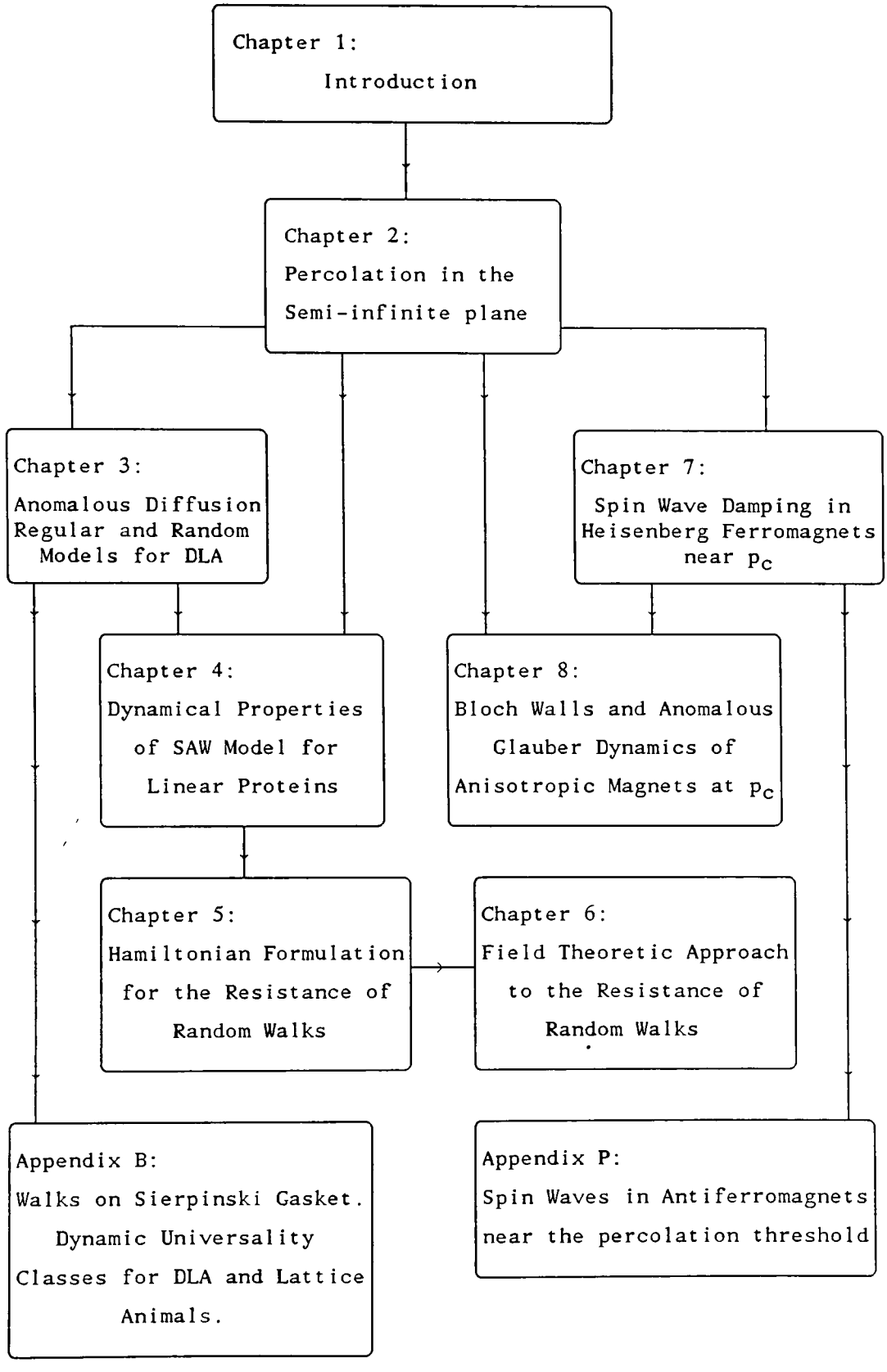

Chapter 2

Crossover and Critical Exponents for Percolation in the Semi-Infinite Plane.

The percolation problem in the semi-infinite plane is discussed in terms of the two competing length scales $\xi(p)$, the correlation length, and d, the distance from the surface. We propose a crossover hypothesis for the percolation probability $P(d,\xi(p))$ and identify two limiting regimes. For $\xi(p) \ll d$ the critical behaviour is governed by the usual exponent β while for $\xi(p) \gg d$ a new critical exponent, β_s , is required. Using simple RSRG procedures we obtain a sequence of approximations to β_s/β and these are seen to show good agreement with a recent Monte Carlo simulation of the system. Finally we indicate how the techniques are applied to the semi-infinite three dimensional case. This work has been published in J.Phys. A (Christou and Stinchcombe 1986a).

1. Introduction.

The problem of site percolation may be treated using Real-Space Renormalisation Group techniques (Reynolds *et al* 1977).Analogous methods exist for bond percolation (Young and Stinchcombe 1975). The original lattice, with site occupation probability p, is mapped onto one isomorphic to it, with an accompanying dilatation of length scale by a factor b.The renormalised probability of occupation is given by

$$p' = R_b(p) \qquad (2.1.1)$$

For systems with dimensionality greater than one this recursion relation has a non-trivial unstable fixed point in $0<p<1$ which represents the critical density of sites at which an infinite cluster of connected sites appears. At this critical density one observes singular behaviour in such quantities as mean (finite) cluster size , root-mean-square distance between connected sites ('correlation length'), mean number of finite clusters per site etc. (Essam 1980). Each singularity is characterised by its respective *critical exponent*. Furthermore linearising the transformation $p' = R_b(p)$ about

the critical point yields the *thermal* (rather than *magnetic*) eigenvalue λ, from which, for example, the 'correlation length' critical exponent ν may be derived in the usual way.

If however, in two dimensions, the occupation probability for sites in the $z>0$ upper half-plane is set to zero we are left with the problem of percolation in the semi-infinite plane. One may allow the occupation probability for percolation, or analogously, the coupling constant between sites in the Ising model to be different at the surface to that in the bulk. Indeed by doing so, workers have investigated the possibility of surface transitions in both semi-infinite percolation (DeBell 1979) and semi-infinite Ising systems (Dunfield and Noolandi 1980) in two and three dimensions.

In this chapter we study site percolation in the semi-infinite plane, setting a uniform occupation probability p in $z\leq 0$ and we apply Niemeyer-van Leeuwen type RSRG techniques (Niemeyer and van Leeuwen 1974) to the system in the two limiting regimes $\xi(p)\gg d$ and $\xi(p)\ll d$. In particular we postulate that the *percolation probability* P obeys a scaling form and exhibits crossover behaviour between power law forms governed by the usual exponent β for sites deep in the bulk ($\xi(p)\ll d$) and a new exponent, β_s, as one approaches the surface ($\xi(p)\gg d$). We develop a sequence of approximations leading to improved estimates of the quantity β_s/β. Our results are consistent with this hypothesis and give good qualitative agreement with recent Monte Carlo simulations (Watson 1985).

2. Scaling form and Surface-Bulk Crossover.

Consider a two dimensional lattice of sites with site occupation probability p,0 in $z\leq 0$ and $z>0$ respectively. Define the bulk *correlation length* ξ as the root-mean-square distance between connected sites far from the surface, where the mean is taken only over sites in finite clusters. For a site near the surface, two competing characteristic length scales enter: its distance d from the surface is one, and $\xi(p)$ is the other. In such a case, we define the *percolation probability* P as the probability that a site A at $z=-d$ is occupied and that it is connected to an infinite number of other sites. In the terminology of phase transition theory this is the *order parameter* and it is non-zero only for $p>p_c$. Denote this probability as $P(d,\xi(p))$. This is the usual, exact definition

for $P(d,\xi(p))$, however, as we show below, it needs to be modified to make itself amenable to the scaling formalism.

From the above considerations we expect the percolation probability to satisfy the following scaling form in the neighbourhood of the critical point,

$$P(d,\xi(p)) = C(p-pc)^{\beta}F(\xi(p)/d) \qquad p>p_c \qquad (2.2.1)$$

$$0 \qquad p\leq p_c$$

where $F(x)$ is a universal scaling function with the following limiting behaviour,

$$F(x)\rightarrow 1 \qquad \text{as } x\rightarrow 0 \qquad (2.2.2)$$

$$F(x)\rightarrow Bx^{-\alpha} \qquad \text{as } x\rightarrow\infty$$

and p_c satisfies $p_c = R_b(p_c)$.

Since $\xi(p)=D(p-p_c)^{-\nu}$ we observe that for $\xi(p)\gg d$

$$P(d,\xi(p)) = (BCD^{-\alpha}/d^{-\alpha})\cdot(p-pc)^{\beta+\nu\alpha} \qquad (2.2.3)$$

This expression defines the *surface critical exponent*,

$$\beta_s = \beta+\nu\alpha. \qquad (2.2.4)$$

If one imagines the semi-infinite system to have arisen from an infinite one from which a line of parallel bonds has been removed it is clear then that the scaling function $F(\xi(p)/d)$ may be interpreted as the following conditional probability that an arbitrarily selected site at $z=-d$ is on infinite cluster in the semi-infinite plane given that the site is on the infinite cluster in infinite plane. In particular then $F(x)\leq 1$, for all x, with equality only for $x\rightarrow 0$.

Note that our β_s is more commonly referred to as β_1 in the literature (see e.g. Bray and Moore 1977). Further, α, the crossover exponent is not to be confused with the specific heat exponent. See also the note added in the conclusions (p.147).

3. Real Space Renormalisation Group Approach for Bulk and Surface Exponents.

As mentioned above the definition of the percolation probability must be expressed in a manner accessible to the RSRG procedure. One may regard $P(d,\xi(p))$ as the sum of probabilities of certain 'classes of configurations' ('events') of the sites on the lattice such that the site A is on the infinite cluster in region $z\leq 0$. An approximate definition for $P(d,\xi(p))$ is obtained therefore by incorporating only a subset of these events into P.

It follows that considering a large number of events will yield a more reliable $P(d,\xi(p))$ and therefore more reliable critical exponents will be derived from that definition. Such a generalised approach is given in section 4. In the present section we consider the crudest model with only one event as follows,

Definition 1 :

Site A is in infinite cluster if:

i) it is occupied

ii) it is in a cell which transforms to an occupied renormalised site

iii) the renormalised site is in the infinite cluster of the renormalised lattice given that it is occupied.

This defines $P(d,\xi(p))$.

The infinite class of lattice configurations satisfying the above definition constitute an event. Notice also that Definition 1 is inductive.

Denote $P_b(p)= P(d,\xi(p))$ and $P_s(p)= P(d,\xi(p))$ for $\xi(p) \ll d$ and $\xi(p) \gg d$ respectively.

(i) Scaling Within Bulk, $\xi(p) \ll d$.

The definition 1 was introduced by Thouless (1978) to deal with the bulk exponent β. We first discuss this case, i.e. the treatment of sites very deep in the bulk, $\xi(p) \ll d$. We use a blocking transformation and the rule R_o to determine whether a renormalised site is occupied.The lattice of sites is partitioned into identical groups or *cells* of sites . A cell of sites in the original lattice is transformed into a site of the renormalised lattice. According to the rule R_o, a cell is transformed into an occupied renormalised site if and only if there is a cluster in the cell which spans the cell either horizontally or vertically.

As shown by Thouless, blocking on the triangular lattice with length scale dilatation factor $b= \sqrt{3}$ (figure 2.1(a)) yields,

$$p' = p^3+3p^2(1-p) \qquad (2.3.1)$$

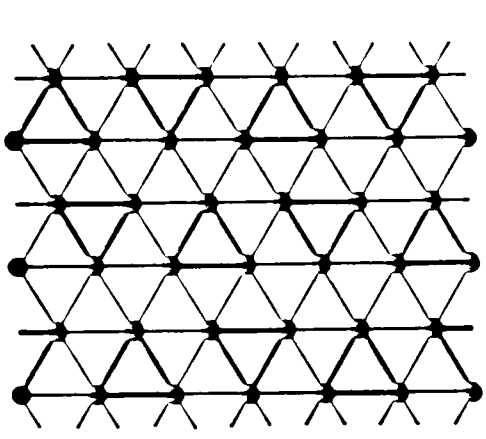

(a)

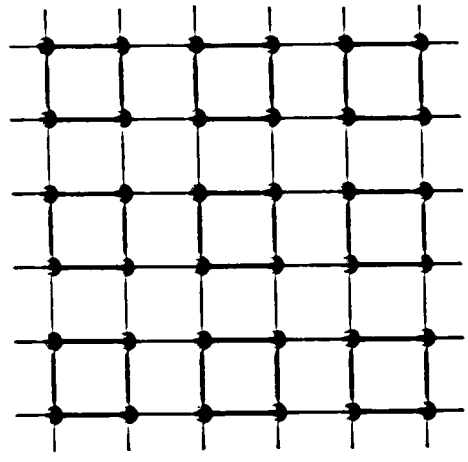

(b)

Fig.2.1.: Blocks used for the real space renormalisation of the site percolation problem in the bulk ($\xi(p) \ll d$) for a). the triangular lattice with $b=\sqrt{3}$ and b). the square lattice with b=2.

this has a non-trivial fixed point at the exact value $p_c = 1/2$ at which the percolation eigenvalue is $\lambda \equiv (dp'/dp)p_c = 3/2$. Definition 1 above then implies,

$$P_b(p) = p(2p(1-p)+p^2)P_b(p')/p' \qquad (2.3.2)$$

Linearising this result near the percolation threshold, $\xi(p) \gg 1$, yields,

$$P'/P \simeq 4/3 \qquad (2.3.3)$$

However in the bulk $P_b(p)=C(p-pc)^{\beta}$ $p>p_c$. From this we obtain $\lambda^{\beta}=4/3$. This then gives for the bulk exponent β,

$$\beta \simeq (\log 4/3)/(\log 3/2) \simeq 0.710 \qquad (2.3.4)$$

The same procedure may be used on the square lattice when b=2 (figure 2.1(b)). Here one obtains

$$P_b(p) = p(p^3+3p^2(1-p)+2p(1-p)^2)P_b(p')/p' \qquad (2.3.5)$$

and

$$p' = p^4+4p^3(1-p)+4p^2(1-p)^2 \qquad (2.3.6)$$

which yield $p_c=0.382$, $\lambda=1.53$ and so $\beta=1.131$.

Comparing these values for β with the corresponding series result $\beta = 0.139 \pm 0.003$ (Blease *et al* 1978) highlights a two-fold inadequacy in the above procedure. Firstly, considering only one event gives a severe underestimate for the numerical value of λ and hence overestimates β. This problem is a result of the crudeness of defn.1. However it leads to a corresponding overestimate in β_s, the surface exponent, as we demonstrate below. This problem is to a certain extent eliminated if we are interested in the ratio of β and β_s. Indeed encouraging results are observed below for β_s/β. Secondly, the choice of such small cells in the blocking introduces an uncontrolled approximation due to cell interfacing problems. These interfacing problems become less significant if one uses larger blocking cells, i.e larger b as demonstrated by Reynolds *et al* (1980). One therefore expects defn.1 to yield improved results if one chooses larger cells in the blocking procedure.

We wish to determine whether a particular site is present in the infinite cluster. When dealing with larger cells an ambiguity arises in the positioning of the cell relative to our site of interest. An average over cell positions must be taken. It is convenient to introduce the *conditional RG transformation* defined as the probability that a renormalised site is occupied given that one of its constituent 'original' sites is occupied. Denote this by $C_{b,s}(p)$ for bulk and surface sites respectively. Notice that an average over original sites must be taken. Defn.1 then becomes,

$$P_{b,s}(p)/p = C_{b,s}(p)P_{b,s}(p')/p' \qquad (2.3.7)$$

Now consider the b=3 blocking on the square lattice for sites with $\xi(p)/d \ll 1$. Here we have,

$$p' = p^9+9p^8(1-p)+36p^7(1-p)^2+82p^6(1-p)^3+93p^5(1-p)^4 +44p^4(1-p)^5+6p^3(1-p)^6 \qquad (2.3.8)$$

$$C_b(p) = p^8+8p^7(1-p)+28p^6(1-p)^2+(164/3)p^5(1-p)^3 +(155/3)p^4(1-p)^4+(176/9)p^3(1-p)^5+ 2p^2(1-p)^6 \qquad (2.3.9)$$

Using (2.3.7) above we obtain β=0.7169.

In a bxb cell on the square lattice there are 2^{bxb} possible distinct configurations of original sites, a subset of which configurations are 'percolating'. To obtain the RG and Conditional RG transformations one must determine the percolating configurations and weight each one appropriately. For b=4 blocking, a Fortran program utilising the cluster multiple labelling algorithm of Hoshen and Kopelman (1976) was used to do this on a VAX 11/780 machine. Here an average over the sixteen possible cell positions is taken for $C_b(s)$. The results are summarized in Table 2.1.

(ii) Scaling at Surface ($\xi(p) \gg d$).

We now treat sites on the surface, representing the limit of the regime $\xi(p) \gg d$. The probabilistic interpretation above for the scaling function $F(\xi(p)/d) < 1$ implies $\beta_s > \beta$. The geometrical origin of this difference lies in the fact that if a site on the surface of the

semi-infinite plane is to be connected to the infinite cluster it is constrained to do so via sites that are *not* above it. This constraint is relieved for sites deep in the bulk. Thus $P_b > P_s$ and so $\beta_s > \beta$. We now proceed to evaluate β_s.

The surface constraint is incorporated naturally into the blocking procedure if one defines $C_s(p)$, the surface conditional RG transformation, as the probability that a *surface* cell is occupied given that one of its constituent surface sites is occupied. As when calculating $C_b(p)$, an average must be taken over possible positions of surface cell relative to the surface site, but notice though that here certain surface cells contain sites that lie in $z>0$ and that these sites are occupied with probability zero. This idea is illustrated in figure 2.2(a) for $b=\sqrt{3}$ surface blocking in the triangular lattice. In this case we obtain,

$$C_s(p) = (1/6)(2p+3(2p-p^2)+0) \qquad (2.3.10)$$

where the zero corresponds to the one block with only one site in $z \leqslant 0$. Using $P_s(p)=pC_s(p)P_s(p')/p'$ for the percolation probability in $\xi(p) \gg d$ it follows that $\beta_s \simeq 1.51$ which, using the corresponding result for β, gives $\beta_s/\beta \simeq 2.13$

We perform the analogous procedure for a site on the surface of a square lattice. With b=2 blocking we find,

$$C_s(p)=(1/4)(2p+2(p^3+3p^2(1-p)+2p(1-p)^2)) \qquad (2.3.11)$$

which yields $\beta_s \simeq 1.630$ and $\beta_s/\beta \simeq 1.441$.

Both the above results are poor when compared to that obtained in a Monte Carlo investigation (Watson 1985) of the same system $\beta_s/\beta \simeq 0.41/0.14 \simeq 2.9$. This is so for two reasons. Firstly, the spurious errors in both β_s and β arising from the small cell blocking and from the limitations of defn.1 for $P(d,\xi(p))$ compound each other. Secondly, we note that the renormalised surface site 'senses' the surface only as a result of some of its constituent sites having probability zero of being occupied. It is this property of the surface cells that embodies the essential physics of the semi-infinite system. However in, for example, the b=2 surface blocking on the square lattice two of the four distinct surface blocks do not then sense the surface at all and so contribute to

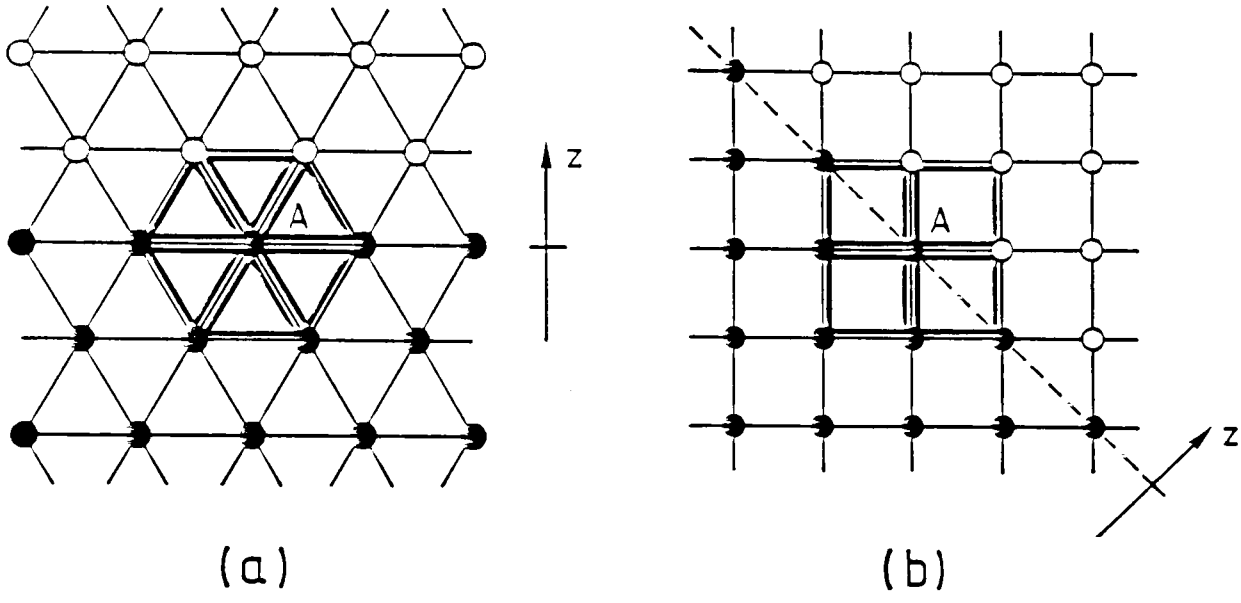

Fig.2.2.: Surface blocking for RS renormalisation of the semi-infinite percolation problem for a). the triangular lattice with $b=\sqrt{3}$ and b). the square lattice (diagonal surface cut) with b=2. The surface site A has Z (the coordination number) possible surface cells over which an average is to be taken. Sites in $z<0$ and $z>0$ are denoted by and are occupied with probability p,0 respectively.

keeping $C_S(p)$ artificially high and hence β_S low. This problem is inherent in small cell blocking and disappears when one uses larger cells. However if one considers a semi-infinite square lattice with a surface along the diagonal (so that nearest neighbours on the surface are next nearest neighbours of the lattice) we then expect (see figure 2.2(b)) the effect of the surface to be taken into account somewhat more faithfully. Universality arguments ensure that the physical value of β_S is left unchanged by this ploy.

We therefore treat b=2 blocking on the square lattice with a diagonally cut surface. In the bulk β is unaffected while on the surface we have,

$$C_S(p)=(1/4)(2(p^2+p(1-p))+(p^3+3p^2(1-p)+2p(1-p)^2)+0) \qquad (2.3.12)$$

Thus, using $P_S(p)=pC_S(p)P(p')/p'$ yields the result $\beta_S\simeq 2.50$ and $\beta_S/\beta\simeq 2.210$.

As mentioned above, it is possible to extract improved values of β_S/β if one uses larger cells. Scaling on the surface, when using larger cells, is analogous to that in the bulk with the additional requirement that sites present in the surface cells but in $z>0$ are taken to have occupation probability zero. As an illustration we consider surface scaling in the b=3 blocking of the square lattice with a diagonal cut. The surface conditional RG transformation is in this case given by,

$$\begin{aligned}C_S(p)=\ &(1/9)\{(p^8+8p^7(1-p)+28p^6(1-p)^2+55p^5(1-p)^3+51p^4(1-p)^4\\ &+18p^3(1-p)^5+2p^2(1-p)^6)+2(p^7+7p^6(1-p)+20p^5(1-p)^2+24p^4(1-p)^3\\ &+11p^3(1-p)4+p^2(1-p)^5)+(p^5+5p^4(1-p)+4p^3(1-p)^2)\\ &+\ 2(p^5+5p^4(1-p)+5p^3(1-p)^2)+3(\ 0\ )\}\end{aligned} \qquad (2.3.13)$$

and we obtain, $\beta_S\simeq 1.800$ and so $\beta_S/\beta\simeq 2.511$. The process is analogous for a straight cut. As anticipated, the b=4 blocking on the square lattice gives results which which are in even closer agreement with those obtained in the Monte Carlo simulation.

4. Extension of the Renormalisation Group Approach. The 'Two Event' Definition.

As one moves from small to larger cells it is apparent that β_s/β is approaching a limiting value. As explained above the square lattice with a diagonal cut captures the surface properties well and so gives good results for β_s/β given the level of sophistication of the 'one event' recursive definition of $P_s(p)$ and $P_b(p)$. The absolute values of β and βs converge less quickly onto the expected limits. This convergence may be accelerated by including further events into the definition of P_b and P_s.

Definition 2.

Site A is in the infinite cluster if,

Either i) it is occupied

ii) it is in a cell which transforms to an occupied renormalised site

iii) the renormalised site is in the infinite cluster of the renormalised lattice given that it is occupied;

or i) it is occupied

ii) it is in a cell which transforms to an unoccupied renormalised site

iii) the (absent) renormalised site is part of a cell which transforms into a twice renormalised site that is occupied and present in the infinite cluster of the twice renormalised lattice.

This redefines $P(d,\xi(p))$. Defn.2 is a two-event second order recursive definition. The above two events are mutually exclusive and so one may add their respective probabilities. In principle one may extend this process to obtain more accurate definitions of $P(d,\xi(p))$.

In this case, we have, for bulk and surface sites respectively,

$$P_{b,s}(p)/p = C_{b,s}(p)P_{b,s}(p')/p' + (1-C_{b,s}(p))D_{b,s}(p,p')P_{b,s}(p'')/p'' \qquad (2.4.1)$$

where $p''= R(p')= R^2(p)$ and $D(p,p')$ is the probability that a twice renormalised site is occupied given that one of its (once) renormalised sites is unoccupied.

We apply this result to the $b=\sqrt{3}$ blocking on the triangular lattice. In the bulk we have,

$$P_b(p)/p = (2p-p^2)P_b(p')/p'+(1-(2p-p^2))p'^2P_b(p'')/p'' \qquad (2.4.2)$$

Which on linearising yields $\beta\simeq 0.472$.

For sites at the surface we have,

$$P_s(p)/p = 1/6.(2p+3(2p-p^2)+0)P_s(p')/p' + (1-(1/6.(2p+3(2p-p^2)+0))1/6. \{2p'^2 + (2/3)p^2p'\}P_s(p'')/p'' \qquad (2.4.3)$$

From this it follows that $\beta_s\simeq 1.207$ and $\beta_s/\beta\simeq 2.557$.

Similar calculations are seen to give improved results when applied to b=2 blocking on the triangular lattice and to blocking on the square lattice (see Table 2.1).

5. Application to the Semi-Infinite Slab.

The above ideas may in principle be applied to semi- infinite lattices in three dimensions. Unfortunately the computations, even using the relatively straightforward defn.1 for the percolation probability are prohibitively involved for large cells. However, for completeness, we here present a b=2 blocking calculation for the three dimensional simple cubic lattice.

For sites in the bulk we obtain using defn.1,

$$P_b(p)/p = C_b(p)P_b(p')/p' \qquad (2.5.1)$$

$$p'= p^8 + 8p^7(1-p) + 28p^6(1-p)^2 + 56p^5(1-p)^3 + 68p^4(1-p)^4 + 48p^3(1-p)^5 + 12p^2(1-p)^6 \qquad (2.5.2)$$

and $$C_b(p) = p^7 + 7p^6(1-p) + 21p^5(1-p)^2 + 35p^4(1-p)^3 + 34p^3(1-p)^4 + 18p^2(1-p)^5 + 3p(1-p)^6 \qquad (2.5.3)$$

While on the surface with a 1:1:1 cut, for example, one obtains for the surface conditional probability $C_s(p)$,

$$C_s(p) = 1/8.(C_b(p) + 3(p^3+2p^2(1-p)+p(1-p)^2) + 3(p^6+6p^5(1-p)+15p^4(1-p)^2+19p^3(1-p)^3+12p^2(1-p)^4+p(1-p)^5)) \quad (2.5.4)$$

where $P_s(p)/p = C_s(p)P_s(p')/p'$

The results of these and other calculations are summarized in Table 2.1.

6. Discussion.

Our approach to site percolation in semi-infinite systems is based on identifying $\xi(p)/d$ as a crossover variable in a scaling expression and thence determining the asymptotic ('bulk' and 'surface') behaviour of the system. In particular we have constructed RS Scaling methods to yield the bulk and surface exponents, β and β_s respectively, for the percolation probability. The results, given in Table 2.1., give convergence of the ratio β_s/β to a value in agreement with unpublished Monte Carlo data ($\beta_s/\beta \simeq 2.95$) obtained by B.Watson (1985) for d=2. By elaborating the definition of the percolation probability we were able to obtain improved results for each value of cell size b.

In section 5 we demonstrated that the ideas are extended trivially to semi-infinite systems in three dimensions and results indicate that β_s/β is closer to 1 than in two dimensions. Although no numerical work is available to confirm this observation it is consistent with the idea that the surface is less important in higher dimensions: the 'surface constraint' on sites at z=0, that they must be connected to the infinite cluster via sites below them, becomes less stringent as the Euclidean dimensionality of the system is increased.

We now consider the relationship of β,β_s and the crossover exponent α to the structure of the infinite cluster in the semi infinite system. If we enclose a portion of the infinite cluster within a hypercube of side L then the mass M of sites scales as

$$M \propto L^{d_f} \quad (2.6.1)$$

where d_f defines the fractal dimensionality (Mandelbrot 1982) of the infinite cluster. A

Table 2.1.

Results of successive approximations to β, β_s and β_s/β using RSRG blocking on various semi-infinite systems.

Lattice type	Defn. of P	b	β	β_s	β/β_s
Triangular	1	$\sqrt{3}$	0.710	1.512	2.130
Triangular	2	$\sqrt{3}$	0.472	1.207	2.557
Triangular	1	2	0.924	2.129	2.304
Triangular	2	2	0.525	1.352	2.575
Square	1	2	1.131	1.630	1.441
Square	1	3	0.717	1.305	1.820
Square	1	4	0.568	1.197	2.106
Square (diagonal cut)	1	2	1.131	2.499	2.210
Square (diagonal cut)	1	3	0.717	1.800	2.511
Square (diagonal cut)	1	4	0.568	1.600	2.817
Square	2	2	0.709	1.271	1.793
Square (diagonal cut)	2	2	0.709	1.650	2.327
Simple Cubic	1	2	2.099	2.431	1.157
Simple Cubic (1:1:1 cut)	1	2	2.099	3.482	1.659

i) Defn.1: $P(d,\xi(p))/p = P(d/b,\xi(p'))C(p)/p'$

ii) Defn.2: $P(d,\xi(p))/p = P(d/b,\xi(p'))C(p)/p' + P(d/b^2,\xi(p")).(1-C(p)).D(p,p')/p"$

iii) In 2d, Monte Carlo result for $\beta_s \simeq 0.41$; $\beta_s/\beta \simeq 2.95$ ($\beta \simeq 0.139$)

simple scaling argument (e.g.Stauffer 1979) yields

$$d_f = d-\beta/\nu \qquad (2.6.2)$$

here d is the Euclidean (or *embedding*) dimensionality.

It is useful to define $\tilde{\xi}(p)$, the RMS distance between sites on the surface connected via sites in $z\leq 0$ and the associated exponent $\tilde{\nu}_s$ given by

$$\tilde{\xi}(p)\sim(p-p_c)^{-\tilde{\nu}_s} \qquad \text{near } p_c \qquad (2.6.3)$$

If D_f is the fractal dimensionality of the set of sites on the infinite cluster at z=0, an argument analogous to that for the bulk yields

$$D_f = (d-1) - \beta_s/\tilde{\nu}_s \qquad (2.6.4)$$

In fact it may be shown using a finite size scaling argument (Appendix A) that $\tilde{\nu}_s=\nu$ and so using the definition of the crossover exponent $\alpha = (\beta_s-\beta)/\nu$ we obtain

$$\alpha = (d_f-1) - D_f \qquad (2.6.5)$$

Further, addition of codimensions (Mandelbrot 1982) yields the result that the fractal dimension of the set of sites in the intersection of the infinite cluster with a hyperplane is d_f-1. We have therefore shown that α is the difference in dimension of the above set of sites and a subset of that set comprising those sites which are joined to an infinite number of sites on one particular side of the hyperplane.

Finally a study of the homogeneity properties of appropriately defined generating functions indicates that the usual scaling relations between the percolation exponents describing the critical behaviour apply to surface as well as bulk exponents. Further work therefore needs to be done to determine the one remaining independent surface critical exponent.

Chapter 3

Anomalous Diffusion on Regular and Random Models for Diffusion-Limited Aggregation.

Families of regular fractal models for Witten-Sander (DLA) clusters in d dimensions are proposed resembling the computer generated aggregates. We evaluate random walk dimensionalities exactly using resistance scaling ideas. The applicability of the conflicting conjectures of Alexander-Orbach (AO), $d_w=3d_f/2$, and Aharony-Stauffer (AS), $d_w=d_f+1$, to DLA is then examined. We find that the dendritic nature of the fractals presented ensures that AS is satisfied exactly in all dimensions. An RSRG fugacity transformation method is applied to the simplest of the regular fractals in d=2. The result for d_w is compared to the exact resistance scaling result to obtain an estimate of the error introduced by the RSRG. The RG method is then generalised to treat the random DLA problem. The resulting estimate for d_w is in fortuitously good agreement with AS, the corresponding Monte Carlo data and the results above for the regular fractal models. This work has been published in J.Phys. A (Christou and Stinchcombe 1986b).

1. Introduction.

The problem of random walks on percolation clusters at the percolation threshold (Rammal and Toulouse 1983, Gefen *et al* 1983) lattice animals (Family 1983, Gould and Kohin 1984) and other such 'fractal' systems e.g. hierarchical lattices (Given and Mandelbrot 1983) has received much attention since first introduced by de Gennes (1976) in the context of the 'ant in the labyrinth'.

Whereas such random fractals as percolation clusters or lattice animals are equilibrium clusters, DLA clusters (Witten and Sander 1981,1983) are formed kinetically and it is found that their static 'critical' behaviour lies in a new universality class (Gould *et al* 1983). Much less is known about random walks on DLA (Meakin and Stanley 1983) and in particular (Guyer 1984) whether spectral and walk dimensions of DLA satisfy conjectured relationships to the fractal dimension. This topic is studied in

the present chapter.

The growth process of a DLA cluster, as described by Witten and Sander (1981), is as follows. At t=1 a seed particle is placed at the centre of a large hypersphere. At t=2 a second particle is released at a random point on the hypersphere and allowed to perform a random walk until it reaches a perimeter site, where it sticks. At t=3 a third particle is released and so on until a large aggregate is built. The DLA aggregate so formed has an anomalous scale invariance. For instance, the density-density correlation function $<\rho(r'+r)\rho(r')>$ has the following asymptotic behaviour,

$$<\rho(r'+r)\rho(r')> \sim r^{-A}. \qquad (3.1.1)$$

The exponent A is related to the fractal (or *Hausdorff*) dimension (Mandelbrot 1982) d_f of the aggregate, which is defined by the following relationship between linear dimension ξ_f and number of particles N_f (both large) of the cluster:

$$N_f \sim (\xi_f)^{d_f}. \qquad (3.1.2)$$

A volume integration of (3.1.1) leads to the relation

$$d_f=d-A \qquad (3.1.3)$$

where d is the space dimension.

The statistical scale invariance underlying (3.1.1),(3.1.2) makes the theory of DLA expressible in the language of critical phenomena.

As a consequence of the specific growth process involved, DLA aggregates are distinctly different fractals (having different values of d_f) from either percolation clusters or random lattice animals (Gould *et al* 1983). It then becomes also necessary to understand the relevance of the specific growth type to dynamic processes such as diffusion on the DLA.

Apart from intrinsic interest in DLA as an example of a fractal in a new universality class it has application to a variety of systems. DLA has been used as a model for growth of tumours (Williams and Bjerknes 1972), coagulation of smoke particles (Forrest and Witten 1979), growth of crystals from an undercooled melt or a supersaturated solution (Langer 1980), turbulence (Hentschel and Procaccia 1982), dielectric breakdown (Niemeyer *et al* 1984) and viscous fingering (Nittmann *et al* 1985).

Now, in classical diffusion in Euclidean space only a single length scale exists. This length is the rms displacement ξ_w of the random walker from the origin. The number of steps N_w of the walk is related to ξ_w in the limit $N_w \gg 1$ by a power law form from which one defines the *dimensionality of the walk* d_w,

$$N_w \sim (\xi_w)^{d_w}. \qquad (3.1.4)$$

Diffusion processes on such Euclidean spaces, are characterised by the Flory result $d_w=1/\nu=2$ valid for all d.

When the 'ant' is on a fractal a second, competing length occurs. In the case of DLA this length is the *radius of gyration* ξ_f, introduced above as a measure of the linear dimension of the fractal cluster.

For diffusion on such fractal systems ($d_f<d$) we expect a crossover between the asymptotic behaviours of two limiting regimes. In the first one $\xi_w \gg \xi_f$ and $d_w=2$. We are interested in the 'self-similar' regime where $1 \ll \xi_w \ll \xi_f$. In this limit d_w depends on the particular system and the diffusion is said to be anomalous.

Further, Alexander and Orbach (1983) observed that the anomalous scaling of the density of states on a percolation cluster was governed by an exponent, the spectral or fracton dimension d_s, which appeared superuniversal in that it was independent of d. Alexander and Orbach showed that $d_s=2d_f/d_w$ and conjectured that

$$d_s \ (= 2d_f/d_w) = 4/3 \qquad (3.1.5)$$

independently of d. The AO conjecture has been extended to apply to homogeneous fractals (see Leyvraz and Stanley 1983) of which DLA clusters are an example.

However, recent arguments against the AO conjecture have emerged (see Family and Coniglio 1984) and accurate numerical work (Zabolitzky 1984) seems to indicate that AO fails in d=2. Aharony and Stauffer (1984) have presented an argument that applies to fractals with $d_f<2$ and they conclude that

$$d_w=d_f+1 \qquad (3.1.4)$$

implying a breakdown of the AO rule $d_w=3d_f/2$. Specifically, the AS conjecture should apply to DLA in two dimensions.

In this chapter we test the AO and AS conjectures for simple and generalised regular fractal models of DLA. We then proceed to apply RSRG ideas to the random

system. Our results favour the latter conjecture.

A plan of the chapter is as follows. In section 2 our initial investigation of the simplest of regular models for DLA, originally proposed by Vicsek (1983), is similar to the work of Guyer (1984) who treated walks on the fractal using RG on a diffusion equation. We map the system trivially onto an equivalent resistor network and use the method of resistance scaling (Stinchcombe and Watson 1976) to derive the analogue of the percolation conductivity exponent t and hence the dimensionality of walks on the regular fractal. We extend the method to the corresponding fractal family in d dimensions. We repeat the method for another, possibly more authentic, regular fractal family in d dimensions. Finally we investigate the effect of introducing loops on the spectral dimensionality.

In section 3 we limit ourselves to d=2 and apply Real Space Renormalisation Group fugacity transformation methods to the simpler of the fractals mentioned above. Results for d_w are obtained and compared to the exact results from section 2. This serves as a check for the RSRG method and indicates whether one is likely to obtain reasonable results when one applies it to the random case.

In section 4 we treat DLA proper (the random case) using RSRG and compare our results to those of the corresponding Monte Carlo simulation (Meakin and Stanley 1983).

2. Resistance Scaling for Regular Models of Diffusion Limited Aggregates.

When proposing suitable regular models for DLA aggregates, one must preserve the essential physical attributes of the random structures as suggested by Monte Carlo pictures (see Meakin 1983). For instance, the models should have some form of rotational symmetry and have suitable fractal dimensionality. They must also be dendritic (ie have no loops) as this seems to be a characteristic feature of the aggregates.

In dealing with DLA we are ipso facto dealing with site structures. In order to introduce a resistor network, it is however necessary to express the problem in terms of resistors or 'bonds'. We therefore need a non-random model of a DLA cluster which builds the cluster hierarchically but is comprised of both sites and bonds. In fig.3.1 we show three successive stages in the iterative construction of the simplest of such models

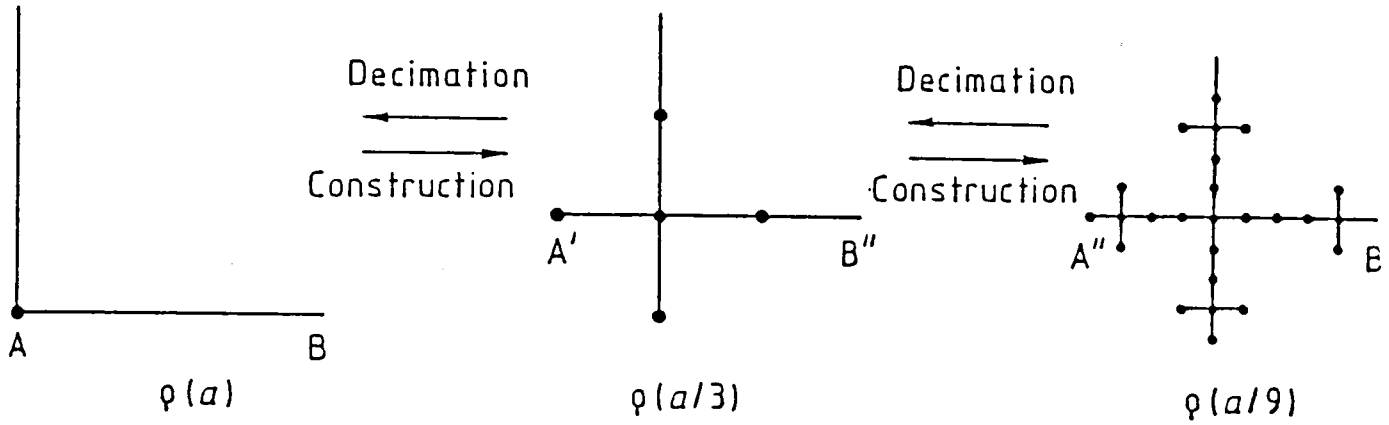

Fig.3.1.: Recursive construction of regular fractal resistor network for DLA comprised of sites and bonds.

(Vicsek 1983) . At each iteration the lattice spacing a is reduced to, say, a/b and more detail of the fractal is generated. This process is repeated such that $a \to a/b \to a/b^2 \to \ldots \to a/b^n$. In the limit $n \to \infty$ we obtain the regular fractal shape.

This construction may be reversed by decimation. Here short range degrees of freedom are eliminated followed by a length scale dilatation $a \to ba$. However, if we now assign a resistance $\rho(a)$ to each bond and, in the decimation-dilatation process, conserve the potential difference between two sites separated by a fixed length ξ, we then have the following scaling ansatz for the resistance,

$$\rho(ba) = b^{d_r}\, \rho(a). \qquad (3.2.1)$$

b is here the length scale dilatation factor and d_r is the fractal dimension of the effective one-dimensional resistance length of the aggregate. We then use the relation

$$d_w = d_f + d_r \qquad (3.2.2)$$

due to Alexander and Orbach (1982), Stanley and Coniglio (1984), to determine the random walk dimensionality d_w.

We illustrate the method for a b=3 dilatation and perform the decimation indicated in fig.3.2(a). Let V_{AB} be the potential difference between A and B when current I flows from A subject to $V_{AB} = V_{AC} = V_{AD}$. By trivial application of Ohm's and Kirchoff's laws one finds that

$$\begin{aligned} V_{AB}(a) &= (3/2)\, I\rho(a) \\ V_{A'B'}(ba) &= (1/2)\, I\rho(ba). \end{aligned} \qquad (3.2.3)$$

It then follows using the scaling ansatz that

$$d_r = \frac{\log 3}{\log 3} = 1 \qquad (3.2.4)$$

so using $d_w = d_f + d_r$ we obtain

$$d_w = \frac{\log 15}{\log 3} \approx 2.47. \qquad (3.2.5)$$

Repeating the process for a b=9 dilatation (fig.3.2(b)) one obtains,

$$d_r = \frac{\log(144/13)}{\log 9} \qquad (3.2.6)$$

and so

$$d_w = \frac{\log(3600/13)}{\log 9} \approx 2.56 \quad . \qquad (3.2.7)$$

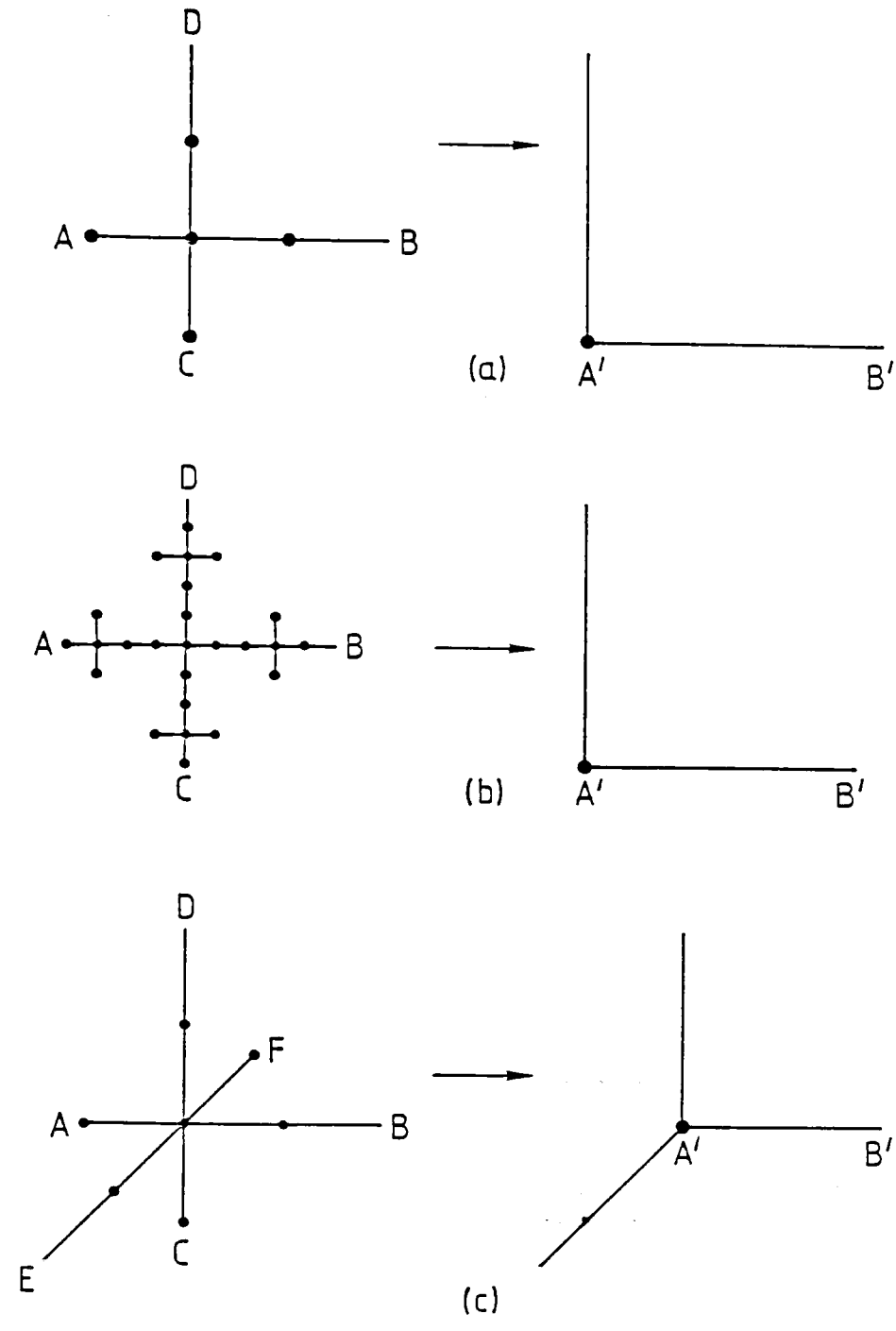

Fig.3.2.: Decimation for simple fractal model with length scale dilatation factor a). b=3 and b). b=9.

c). Decimation for simple model in three dimensions with scale factor b=3.

In fact the calculation is easily done for general $b=3^N$ and yields,

$$d_r = \frac{\log\{ (b-1) + (b^2-1)/(3b-1) \}}{\log b} \quad . \qquad (3.2.8)$$

In the limit of $b\to\infty$ we recover

$$d_r = 1. \qquad (3.2.9)$$

This result agrees exactly with the AS conjecture. It implies that the path followed by a particle, in traversing a region of the fractal of linear extent of order ξ_f, is essentially one-dimensional, albeit highly decorated. We therefore obtain for the random walk dimensionality d_w,

$$d_w = \frac{\log 15}{\log 3} \approx 2.47 \qquad (3.2.10)$$

and for the spectral dimensionality d_s,

$$d_s = \frac{2d_f}{d_w} = \frac{\log 25}{\log 15} \approx 1.19 \quad . \qquad (3.2.11)$$

The result above for d_s is over 10% lower than the AO prediction but in exact agreement with the AS conjecture. It is also consistent with the work by Guyer (1984) on the same model who used decimation on a discrete diffusion equation and obtained $d_r=1$. The result also agrees well with the Monte Carlo simulation of Meakin and Stanley (1983) on the random system which gave $d_s = 1.20$ $(+0.10,-0.05)$.

It is straightforward to generalise the above to apply for arbitrary embedding dimension d. We construct a family of fractals such that the 'unit cell' is now a d-dimensional cross with 2d arms (the case d=3 is shown in Fig.3.2(c)). From this one obtains,

$$d_f = \frac{\log(2d+1)}{\log 3} \quad . \qquad (3.2.12)$$

The resistance rescaling calculation in general d again yields the AS result $dr\to 1$ as $b\to\infty$. One therefore has,

$$d_w = \frac{\log 3(2d+1)}{\log 3} \quad \text{and} \quad d_s = \frac{2\log(2d+1)}{\log 3(2d+1)} \quad . \qquad (3.2.13)$$

In particular then for d=3, we have $d_s \approx 1.28$ which again compares favourably with the corresponding Monte Carlo result (Meakin and Stanley 1983) for the random system

$d_s = 1.30 \pm 0.06$.

From (3.2.12) it evident that for $d>4$ we have $d-d_f>2$. This however makes the cluster transparent to incoming random walkers whose path has dimensionality $d_w=2$. The incoming particles would therefore enter into the central regions of the aggregate and alter its structure, increasing its fractal dimension d_f. It would appear then that the family of fractals presented here are poor models for DLA aggregates for $d>4$. However the above problem is inherent in all such families of regular fractal representations of DLA clusters and arises here from the logarithmic dependence of d_f and d.

The above is repeated for the fractal shown in fig.3.3. This shape is more realistic than the previous one, particularly in d=2 since its fractal dimension $d_f(d=2)$ is $(\log 73/\log 13) \approx 1.673$ in very good agreement with the corresponding Monte Carlo result $d_f=1.678\pm0.047$ (Meakin 1983). In general d the $b\to\infty$ resistance rescaling results for this family are

$$d_f = \frac{\log(1+4d+8d^3)}{\log 13}$$

$$d_w = \frac{\log 13(1+4d+8d^3)}{\log 13}$$

$$d_s = \frac{2\log(1+4d+8d^3)}{\log 13(1+4d+8d^3)} \quad . \qquad (3.2.14)$$

The AO conjecture once again is violated whereas AS holds exactly. Notice that this family encounters the same problems as the former one for $d>4$.

Although we have limited our attention above to models with a C_4 symmetry the result $d_r=1$ follows for dendritic fractals with general C_n symmetry.

Finally, we introduce loops into our model and note their impact on diffusion on the cluster. We perform a b=5 rescaling on the model of fig.3.4. Solving the resulting set of eleven simultaneous equations yields $d_r=1.032$ and so $d_s=1.214$ while the analogous b=5 calculation on the same model without the loops gives $d_r=\log(40/7)/\log 5 \approx 1.083$ and so $d_s=1.115$. This 10% fall in the spectral dimensionality d_s on elimination of the loops in models in d=2 is typical and itself accounts for the deviation from the AO

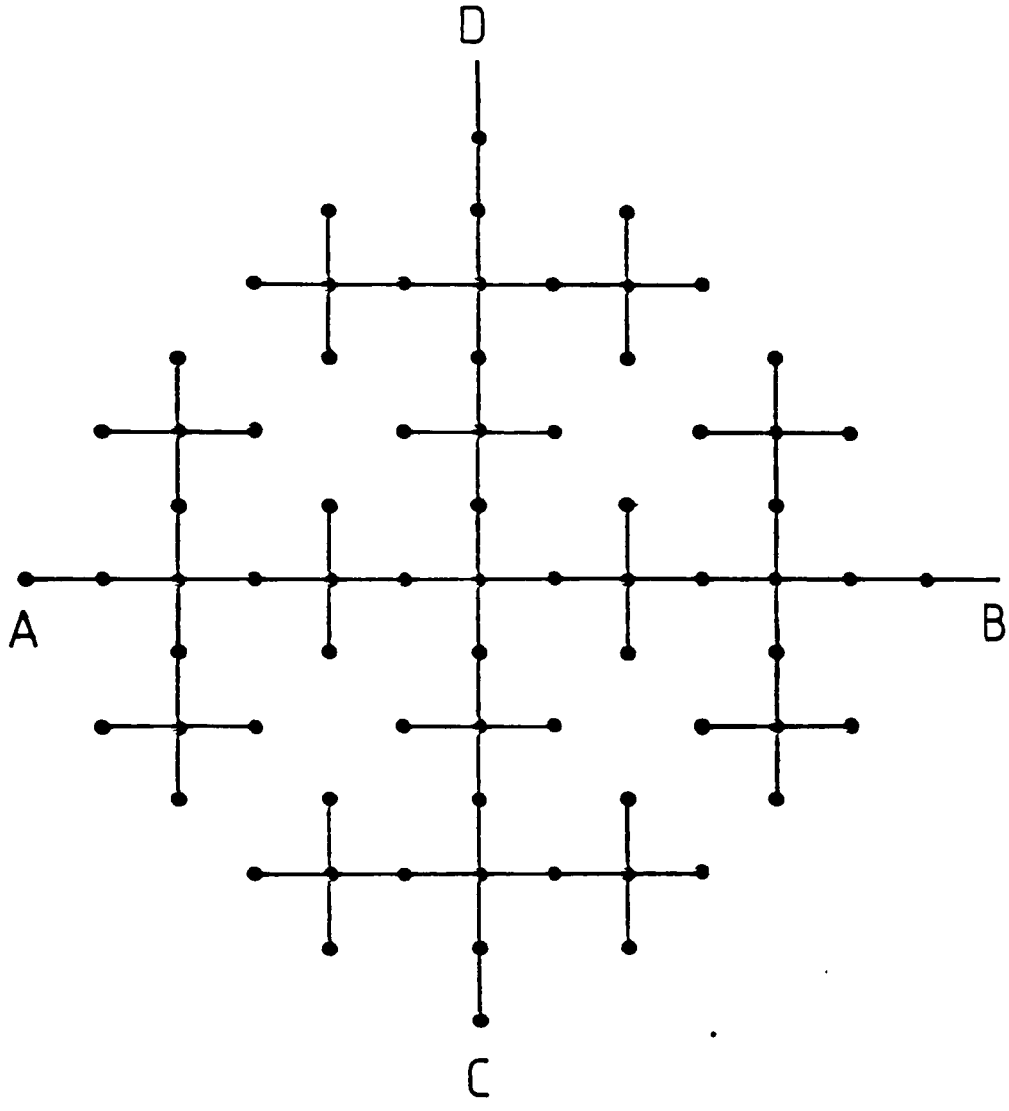

Fig.3.3.: Alternative model for DLA. In two dimensions this model has $d_f = \log 73/\log 13 \approx 1.673$ in very good agreement with numerical estimates for the random case. The dendritic structure of Monte Carlo generated pictures has been preserved.

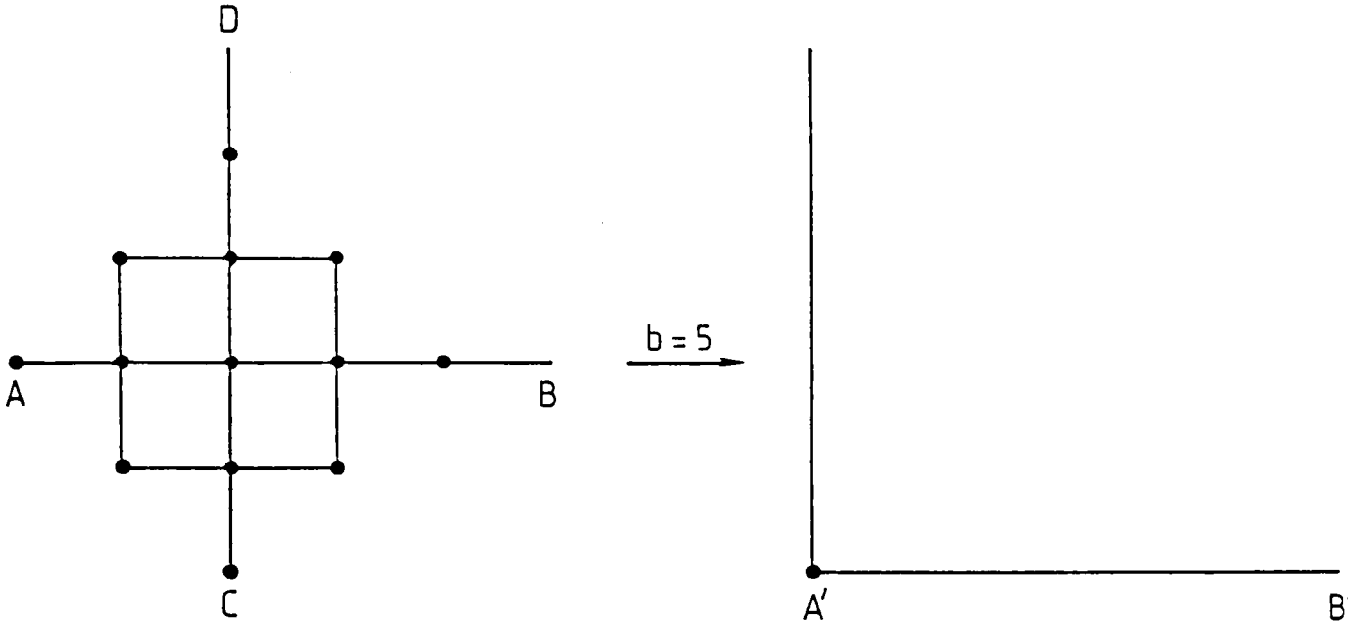

Fig.3.4.: Decimation for regular fractal, having loops on all length scales, by a factor b=5.

conjecture observed above in the $b\to\infty$ limit.

In the following section we use the regular models for DLA introduced above as fractal lattices upon which to apply fugacity transformation methods (Stanley *et al* 1982). This procedure then gives an error bound for the RSRG which would otherwise contain an uncontrolled approximation. We anticipate that the error introduced by the RSRG on the random system is similar to that introduced on the regular model.

3. RSRG Approach to Random Walks on Regular Models of Diffusion Limited Aggregates.

In forming the recursion relations below, we use the kinetic interpretation (Nakanishi and Family 1984) for the random walks as the local coordination number varies from site to site.

In evaluating each transformation our 'ant' begins his walk at A and finishes at B. For a walk of length n we assign a weight $W^n\{(1/Z_0)(1/Z_1)\ldots(1/Z_{n-1})\}$ where Z_i is the local coordination number of the site that the ant reached after i steps. Finally we sum over all possible walks to form the generating function G(W). We associate the renormalised fugacity W' with this generating function through

$$(1/2)W' = \sum_{\text{walks}} W^n\{(1/Z_0)(1/Z_1)\ldots(1/Z_{n-1})\} \quad . \qquad (3.3.1)$$

This recursion relation has a critical unstable fixed point at $0<W^*<\infty$ and if we define $\lambda_w = (\partial W'/\partial W)_{W^*}$ we obtain,

$$d_w = \frac{\log \lambda_w}{\log b} \quad . \qquad (3.3.2)$$

For computational reasons the infinite series G(W) must be truncated at N^{th} order in W. This has the effect of ignoring walks with number of steps n greater than N. One problem is to decide when to truncate.

The diffusion is on a fractal space with $d_f<d$ and as mentioned in the introduction two length scales ξ_w, ξ_f exist. We are interested in the self-similar limit and so we require that the maximum number of steps in a walk be restricted to $\xi_w \ll \xi_f$. At the critical fugacity W^* only random walks of length $\xi_w \sim N^{(1/d_w)}$ are important. We therefore ignore walks with $N>\xi_w{}^y$, with $y=d_w$. However, we have no a priori

knowledge about d_w except that $d_s>1$ and $d_w>d_f$ and these imply that

$$d_f < d_w < 2d_f. \qquad (3.3.3)$$

We therefore (c.f. Sahimi and Jerauld 1984) only treat walks whose number of steps N satisfy

$$N \leq (\xi_w)^{3d_f/2} \qquad (3.3.4)$$

eg for the model of fig.3.1 we choose $y\approx 2.197$. ξ_w being the end-to-end length of the random walk, which in the models we investigate equals the dilatation factor b. The legitimacy of the procedure was checked by using shorter or longer walks and little change in the results for d_w was observed; eg Inserting $y\epsilon[2.0,2.4]$ changes the extrapolated results by at most 4%.

The explicit summation over all possible random walks was carried out using a method described in Family and Gould (1984).

The results obtained (for the model of figure 3.1) were: $d_w=1.73$ from a b=3 renormalisation; $d_w=1.89$ (for b=9);
$d_w= 1.97$ (for b=27). We now assume (Reynolds *et al* 1980) that $d_w(b)$ is a quadratic in $(\log b)^{-1}$,

$$d_w(b) = d_w + C_1/(\log b) + C_2/(\log b)^2 . \qquad (3.3.5)$$

On extrapolating we find that in the $b\to\infty$ limit, $d_w=2.14$ which yields for the spectral dimension $d_s=1.37$. This result is in qualitative agreement with the Monte Carlo result, for the random case, of Meakin and Stanley ($d_s= 1.20$ (+0.10,−0.05) and the resistance rescaling technique for the same model ($d_s= 1.19$).

In the light of these results we proceed below with a related RSRG for the random DLA system.

4. An RSRG for Random Walks on DLA.

We now present a single cell RSRG for deriving d_w for random DLA in two dimensions. This involves three fugacity parameters. A fugacity K is associated with each occupied site of the cell, another fugacity W is associated with each step of the incoming particles and a third fugacity V is associated with each step of the random walker on the cluster. The calculation is in two stages. Firstly one constructs all possible

spanning clusters an a finite bxb cell. Universality arguments ensure that no generality is lost by limiting the treatment to a square lattice. One begins with a seed site in the lower left hand corner of the cell and introduces a random walker from the North or East. The random walker then diffuses through the cell and having landed on a site adjacent to the seed site it remains there and a new random walker is introduced and the process repeats itself. One then evaluates the number, C_{st}, of ways of growing a spanning cluster of s sites generated by random walks with total number of steps t. To preserve the symmetry we define a cluster to be spanning if it can be traversed both vertically and horizontally. The RSRG transformation for K is then given by (Gould et al 1983):

$$K' = \sum_{s,t} C_{st} K^s W^t \quad . \qquad (3.4.1)$$

This is analogous to the RSRG for lattice animals (Family 1983) and Self Avoiding Walks (de Queiroz and Chaves 1980).

To derive the recursion relation for W one renormalises all the possible walks on a bxb cell to a single step on the renormalised lattice as indicated in fig.3.5(a). As the incoming particles are diffusing on a pure lattice we may use the static interpretation for the random walks (see Nakanishi and Family 1984). One then obtains

$$W' = \sum_{n} C_n W^n \quad . \qquad (3.4.2)$$

C_n being the number of random walks of n steps spanning the cell in one direction. This transformation has two stable fixed points at W=0, W=∞ and an unstable fixed point in $0<W^*<\infty$. One then proceeds to find the doubly unstable fixed point (W^*,K^*) of the pair of transformations and then d_f follows in the usual way from the eigenvalue of the linearised transformation (3.4.1) at this fixed point. Gould et al (1983) find $d_f=1.71$ for b=2 and $d_f=1.67$ for b=3.

The next stage is to consider random walks on the DLA aggregate. As in section 3 we use the kinetic interpretation for the walks on the aggregate. We generate all possible spanning clusters in all possible ways as above and for each one we evaluate all the random walks on the cluster that start from the lower-left corner and traverse the cell vertically. Associating the generating function so derived with the corresponding

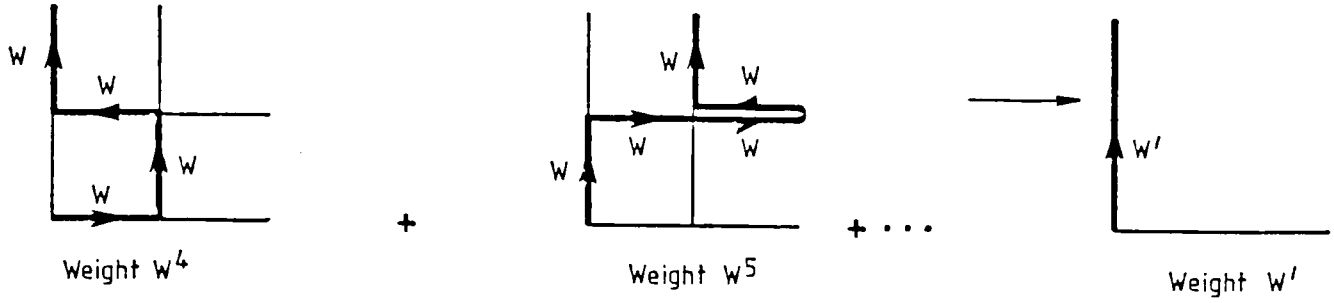

(a)

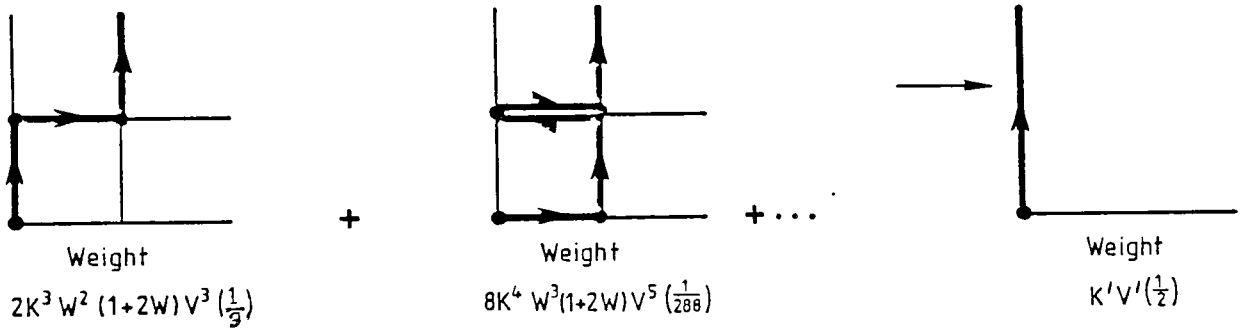

(b)

Fig.3.5.: a). b=2 static renormalisation for random walks on a pure lattice. Each step has weight W. All walks, originating from lower-left corner, traversing the bxb cell vertically with number of steps $N \leq b^{1/d_w}$ are weighted, summed and renormalised to W', the single step fugacity on the renormalised lattice. b). b=2 kinetic renormalisation for random walks on DLA. Each step of the random walk has weight V/Z_a for local coordination number Z_a. All spanning random walks on all spanning cluster configurations are weighted appropriately, summed and renormalised to $\frac{1}{2}K'V'$.

quantity on the renormalised lattice, one obtains:

$$(1/2)K'V' = \sum_{s,n} B_{sn}\Big(\sum_{t} C_{st}K^{s}W^{t}\Big)V^{n} \quad . \qquad (3.4.3)$$

where B_{sn} is the number of walks of n steps spanning in one direction in a cluster of s sites (together with a factor associated with the kinetic interpretation of the random walk on the cluster).

One then evaluates the critical fixed point $0<V^{*}<\infty$ and the associated eigenvalue $\lambda_V = (\partial V'/\partial V)_{K^*,W^*,V^*}$ from which one derives $d_w = \log\lambda_V/\log b$. We perform the procedure explicitly for a b=2 cell. As shown by Gould et al (1983), the recursion relations for K and W are

$$K' = 6K^3W^2(1+2W)+8K^4W^3(1+2W)$$

$$\text{and} \quad W' = W^2+2W^3+5W^4 14W^5 \qquad (3.4.4)$$

and we obtain for V' ,

$$(1/2)K'V' = ((7/12)\alpha+(1/6)\beta)V^2 + ((2/9)\alpha+(1/12)\beta)V^3 + ((55/108)\alpha+(5/36)\beta)V^4 + ((26/81)\alpha+(1/9)\beta)V^5 \qquad (3.4.5)$$

with $\alpha = 2W^2(1+2W)K^3$ and $\beta=8W^3(1+2W)K^4$.

The critical fixed point is

$$\begin{bmatrix} K^* \\ W^* \\ V^* \end{bmatrix} = \begin{bmatrix} 0.766 \\ 0.347 \\ 0.984 \end{bmatrix} \qquad (3.4.6)$$

and the eigenvalues here yield, d_f=1.71 and dw=1.74. The spectral dimensionality is then d_s=1.97.

For the b=3 cell we used a Fortran program on a VAX 11/780 machine to evaluate the transformations for K,W and V and hence the dimensionalities:

$$d_f=1.67 \text{ and } d_w=1.98. \qquad (3.4.7)$$

The closed form calculations for larger cells were unfeasible owing to the enormous amount of computer time needed. We cannot therefore exploit the usual extrapolation scheme (3.3.5) but as a first approximation to the $b\to\infty$ limit of d_w we perform linear extrapolation in $(\log b)^{-1}$ ie we assume that d_w takes the form $d_w(b)=d_w+C(\log b)^{-1}$.

This yields d_w=2.39 and d_s=1.39. The error associated with the RSRG on the regular system only affects d_w. Similarly, for the random system d_f is in excellent agreement with the numerical data. It is therefore reasonable to expect that the errors in the RG treatment of the regular and random DLA models may be related; we assume the relationship (which is supported, Appendix B, by a test on percolation infinite cluster models):

$$\frac{d_s(\text{exact},\text{random})}{d_s(\text{RG},\text{random})} \approx \frac{d_s(\text{exact},\text{regular})}{d_s(\text{RG},\text{regular})} \qquad (3.4.8)$$

Inserting our results into (3.4.8) yields d_s(exact,random) $\approx$ (1.19/1.37).1.39 $\approx$ 1.21 which is fortuitously close to that observed in the Monte Carlo work of Meakin and Stanley (1983) $d_s(d=2) = 1.20\ (+0.10,-0.05)$.

5. Discussion.

The aims of this chapter have been to establish which structural features of DLA aggregates are relevant to diffusion processes and to evaluate the spectral dimensionality d_s as a possible test of the conflicting conjectures of Alexander–Orbach and Aharony–Stauffer for these systems.

We have proposed regular fractal models on which calculations could be carried out exactly. Models were chosen suggestive of the Monte Carlo generated random aggregates. We note that the models used are neither homogeneous nor random and therefore violate the hypotheses of the AO and AS conjectures respectively. However, their structural similarity to their random counterparts indicates that results obtained for these regular models are indeed relevant to DLA. This seems to be borne out by the results of section 4 and the existing Monte Carlo data.

We find that the most important characteristic of the models as far as diffusion is concerned, is that they are *dendritic*. This fact is sufficient to account for the discrepancy between the value of d_s from the numerical work of Meakin and Stanley (1983) and the AO estimate of 4/3 in two dimensions. Other considerations such as nature of rotational symmetry of the aggregates or actual fractal dimension seem secondary. This would suggest, for example, that as one decreases the sticking

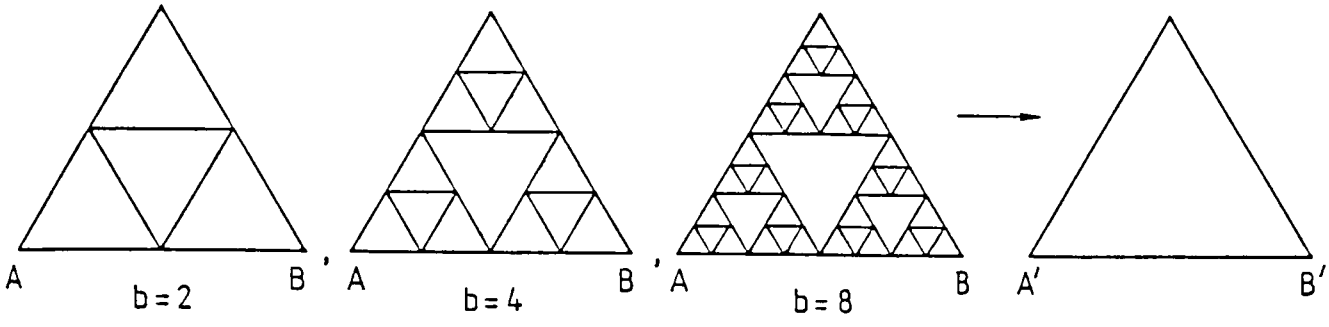

Fig.3.6.: b=2,4,8 decimation for the Sierpinsky gasket model of the percolation IIC. During the resistance rescaling $V_{AB}=V_{A'B'}$. For the RG process, random walks spanning from A to B are weighted and renormalised to $\frac{1}{2}V'$, the weight of the renormalised step from A' to B'. (Appendix B)

probability p in the generation of the aggregate, since d_f appears to be unchanged (Meakin 1983), ie p seems to be an irrelevant variable, and the structure remains dendritic, then the spectral dimension d_s will also remain essentially unchanged. Furthermore, consider the aggregate to be constructed from particles whose motion is characterised not by random walks but having instead Levy flight trajectories such that

$$P(x>U) = U^{-f}$$
$$P(x<1) = 0 \qquad (3.5.1)$$

where P(x>U) is the probability that the length of the step will be greater than or equal to U. The numerical work of Meakin (1984) indicates that d_f *is* affected, ie f is a *relevant* variable, while the dendritic nature of the clusters is preserved. Our reasoning suggests therefore that the dynamic properties of these new aggregates are determined uniquely in terms of the modified static geometry, in particular $d_s=2d_f/(d_f+1)$. Monte Carlo work needs to be done to confirm this.

We have shown that the resistance scaling exponent d_r is equal to unity in our regular models for all values of the embedding dimension d; this is another consequence of their dendritic nature. Our results are in agreement with the related work of Guyer (1984) on the regular Vicsek model. The value $d_r=1$ obtained for the DLA fractal models is consistent with the AS conjecture for d=2, since there $d_f<2$. This feature persists in the real clusters and so, if it is the only relevant feature the AO conjecture will fail for DLA while the AS conjecture will hold exactly not only for d such that $d_f<2$ but in general embedding dimension.

Finally, in section 4, we obtained an estimate for d_s in the random system using RSRG and the results of section 3. The result obtained is in good agreement with the numerical data, supporting the conclusion that $d_s(d=2)$ falls well short of the AO prediction for DLA clusters.

Chapter 4

Dynamical Properties of a Self-Avoiding Walk Model for Proteins.

Diffusion on the model for proteins introduced by Helman, Coniglio and Tsallis (HCT) is discussed using Real Space Renormalisation Group ideas. We perform cell-to-cell transformations in two dimensions for both the HCT model and the Self Avoiding Walk. For the latter system we expect trivial diffusive behaviour given by $d_w=2d_f=8/3$. For the HCT model, however, the impact of jumps across nearest neighbour (hydrogen bond) 'bridges' on diffusion is less clear. Our results are not consistent with the predictions that $d_w=2$ for the HCT model. Rather they would seem to support the assertion that $d_w^{HCT}>d_w^{SAW}$. This work has been published in J.Phys. A (Christou and Stinchcombe 1986c).

1. Introduction.

In this chapter we investigate a model for proteins introduced by Helman *et al* (1984). Firstly, we use a single cell Real Space Renormalisation Group method to determine the asymptotic time dependent behaviour of a de Gennes (1976) myopic ant on the non-trivial HCT model. We then summarise the results of an exact enumeration (series analysis) study for the structure of these models. A scaling theory is used to relate these two problems.

Interest in the problem arises in the context of spin-lattice relaxation rates of the Fe^{3+} ions in low spin haemoproteins and ferredoxin. The dominating two-phonon process leads to a rate $1/T_1$ related to the temperature T by the following scaling form,

$$1/T_1 \propto T^{3+2d_s} f(T/\theta, d_s) \qquad (4.1)$$

with θ, the Debye temperature and d_s, the spectral dimension (Alexander and Orbach 1982) for the proteins.

The experimental work of Stapleton *et al* (1980) and Allen *et al* (1982) finds the following low temperature behaviour for $1/T_1$,

$$1/T_1 \propto T^n \quad . \qquad (4.2)$$

This observation is consistent with (4.1) since in an appropriate low temperature regime the scaling function f takes a constant value and so the T dependence of $1/T_1$ is given simply by $1/T_1 \propto T^{2+3d_S}$.

These workers find $n \approx 6.3$ for haemoproteins and $n \approx 5.67$ for ferredoxin. In attempting to reconcile (4.2) with (4.1) Stapleton *et al* equated d_S in (4.1) with the fractal, or *Hausdorff*, dimension (Mandelbrot 1982) of the protein, d_f. This relates the radius of gyration of the protein $\langle R_f \rangle$ to the number of alpha-carbons by the power law

$$\langle R_f \rangle \sim N^{1/d_f} \quad . \qquad (4.3)$$

The numerical value for d_f for the proteins is accessible from the X-ray scattering data. Stapleton *et al* obtained $d_f=4/3$ for ferredoxin and $d_f=5/3$ for the haemoproteins. These results are consistent with the relaxation rate data for n and also with the Flory theory result for the excluded volume problem (Self Avoiding Walk) $d_f=(d+2)/3$ for d=2,3 respectively.

Now, information on the dynamic excitations on general fractal spaces may be obtained by considering diffusion on the network. The diffusing particle is represented by a 'myopic ant'. Such a random walker successfully takes a step at every time interval, as opposed to a blind ant which, if it discovers its chosen direction to be blocked, will remain stationary until the next time interval when it tries again.

When considering diffusion on fractals it is important to distinguish between two limiting regimes. If the RMS diplacement of the ant is $\langle R_w \rangle$ then in the regime $1 \ll \langle R_w \rangle \ll \langle R_f \rangle$ diffusion phenomena are self-similar and so are amenable to treatment using RSRG. In this regime $\langle R_w \rangle$ is given asymptotically by

$$\langle R_w \rangle \sim t^{1/d_w} \qquad (4.4)$$

for fixed though large N, where t is the time or equivalently, the number of steps of the ant. (4.4) defines the *dimensionality of the walk* d_w. On fractal space $d_w \neq 2$ in general but takes on some anomalous system dependent value. In the regime where the number of steps t of the ant is large compared to the number of bonds of the system N, $\langle R_w \rangle$ will saturate to

$$\langle R_w \rangle \sim N^{1/d_f} \quad . \qquad (4.5)$$

These regimes are bridged by a crossover region in which $\langle R_w \rangle$ is given by

$$\langle R_w \rangle \sim N^{1/d_f} \; g(N^{\theta}/t) \qquad (4.6)$$

where g is a universal scaling function and θ is the crossover exponent.

We confine our attention to the self-similar limit $1 \ll \langle R_w \rangle \ll \langle R_f \rangle$.

According to the Alexander-Orbach theory knowledge of d_w yields the scaling behaviour of the low frequency density of states $\rho(\omega) \propto \omega^{d_s-1}$ through the relation

$$d_s = 2d_f/d_w \qquad (4.7)$$

Consequently a simple SAW model for the proteins leads to a contradiction. A straightforward scaling argument (see footnote in Helman *et al* 1984) shows that for the quasi-linear SAW $d_w=2d_f$ and so from (4.7) one obtains $d_s=1$ in all dimensions. This result is inconsistent with the requirement above, $d_s=d_f$. In order to overcome this difficulty Helman *et al* introduced conducting but massless nearest neighbour crosslinks into the SAW model. They predicted that, provided the density of crosslinks or bridges was sufficiently high, the ant would 'see' the embedding Euclidean lattice and diffuse as if on Euclidean space. Their objective was therefore to create a protein model with SAW fractal dimension but with $d_w=2$, thereby restoring consistency with the experimental results. The 'massless bridges' were to be interpreted as hydrogen bonds.

Subsequent numerical work on the HCT model in two dimensions (Yang *et al* 1985 and Chowdhury and Chakrabarti 1985) however does not support the suggestions of Helman *et al*. Yang *et al* obtain $d_w=2.6$ and indicate that they would expect $d_w=2d_f=8/3$, as for the SAW, with more accurate calculations. Chowdhury and Chakrabarti however obtain an even higher result $d_w=2.78$. Furthermore the latter authors argue that $d_w>8/3$ strictly, this being a direct consequence of the ant's steps over the bridges which, in terms of chemical distance travelled measured along the chain, constitute Levy flights.

2. RSRG Analysis of Diffusion on SAW model for Proteins.

We consider the stochastic master equation governing the motion of the ant. Assigning a probability $P_n(t)$ that the ant is at site n of the HCT model at time t subject to $P_n(0) = \delta_{n,0}$ we obtain the time evolution from

$$\frac{dP_n(t)}{dt} = -VP_n(t) + \sum_m WP_m(t) \qquad (4.8)$$

where W is the transition rate for the ant to step from a site onto a *particular* nearest neighbour. The parameter V is simply the step rate given by WZ_n with Z_n the local coordination number. In the summation m runs over over Z_n occupied nearest neighbours.

During the renormalisation process, the embedding lattice is mapped onto one isomorphic to it together with an accompanied dilatation of space by a factor b and elimination of short range SAW degrees of freedom. The motion of the ant on the renormalised system is governed by an equation analogous to (4.5) but with a renormalised hopping rate V'. The asymptotic, scale-invariant, phenomena are observed at a critical rate $0 < V=V'=V^* < \infty$. Clearly we expect $V^*=1$ since our ant is myopic, not blind.

In deriving the explicit Real Space Renormalisation Group recursion relation for V, the step 'fugacity' (Stanley *et al* 1982) for the random walker, it becomes evident that one has to introduce a second fugacity K, associated with each step of the SAW. The parameter K, together with its RSRG transformation $K'= R_b(K)$ characterises the underlying fractal space. Similar approaches have been used in studying random walks on percolation clusters (Sahimi and Jerauld 1984), lattice animals (Family 1983) and Witten-Sander Aggregates (see chapter 3).

Firstly we derive the transformation for K following de Queiroz and Chaves (1980) and Redner and Reynolds (1981). One generates the set of SAWs starting in the lower-left corner of a bxb cell and finishing on one of the b sites at the top of the cell. Each traversing SAW configuration of n steps is weighted by a factor K^n. A grand canonical partition function $Z^b_{saw}(K)$ is defined for the cell thus

$$Z^b_{saw}(K) = \sum_n C_b(n)\, K^n \qquad (4.9)$$

where $C_b(n)$ is the number of spanning SAWs of n steps on a bxb cell. We set $R_b(K) = Z^b{}_{saw}(K)$. In general, the bxb cell is mapped onto a b'xb' cell via a 'cell-to-cell' transformation (Reynolds *et al* 1980), the renormalised partition function being given by

$$Z^{b'}{}_{saw}(K') = \sum_m C_{b'}(m)\ (K')^m \qquad (4.10)$$

In particular, for a cell-to-bond transformation, $Z^{b'=1}{}_{saw}(K') = K'$. If we stipulate that the partition function be conserved under renormalisation we have an implicit transformation $K \to K'$. This has a critical fixed point at $0<K^*<\infty$ where one evaluates the eigenvalue of the linearised transformation, $\lambda_k=(\partial K'/\partial K)_{K^*}$, from which follows the fractal dimension of the SAW, d_f, in the usual way.

The procedure is analogous to that outlined above when one introduces random walks on the HCT models. Here, we define a new partition function $Z^b{}_{rw}(K,V)$ given for a bxb cell by

$$Z^b{}_{rw}(K,V) = \sum_{n,t} C_b(n,t)K^nV^t((1/z_0)(1/z_1)\ldots(1/z_{t-1})) \qquad (4.11)$$

with $C_b(n,t)$ being the number of random walks of t steps spanning each HCT model configuration of n steps and z_i being the coordination number of the site visited by the ant after i steps. The factor $((1/z_0)(1/z_1)\ldots(1/z_{t-1}))$ arises from the fact that the weight associated with a particular ant step from a site a is V/z_a, where z_a is the local coordination number of a. Upon renormalisation the transformed partition function is

$$Z^{b'}{}_{rw}(K',V') = \sum_{m,r} C_{b'}(m,r)(K')^m(V')^r((1/z_0)(1/z_1)\ldots(1/z_{r-1})) \qquad (4.12)$$

For b'=1, we set $Z^{b'=1}{}_{rw}(K',V') = K'V'$.

Evidently, for a SAW without crosslinks, this 'kinetic' view (Nakanishi and Family 1984) of the random walk may be replaced by the more familiar 'static' interpretation $V/2 \to W$ as the local coordination number is constant.

A problem arises associated with the truncation of the infinite series (4.8) and (4.9). We note that at the critical fixed point (K^*,V^*) only random walks of length $t \leqslant \xi^{d_w}$ are important (see eg Sahimi and Jerauld), ξ being the end-to-end distance. However given that all we know of d_w is

$$d_f \leqslant d_w \leqslant 2d_f \qquad (4.13)$$

our choice of truncation point will necessarily be rather ad hoc. In our computations we firstly treat only walks satisfying $t \leqslant \xi^2$, this being the mid-point of the interval (4.10) since we know that $d_f=4/3$. We then repeat the process considering longer walks $t \leqslant \xi^{8/3}$. The results for d_w for the HCT model are affected significantly by choice of truncation point. However if we repeat the renormalisation for random walks on SAWs (with no cross-linking allowed) we observe that the value d_w^{HCT}/d_w^{saw} is much less affected by the truncation rule used.

We derive the recursion relations for the simplest of transformations b=2,b'=1 for the HCT model. Here, from de Queiroz and Chaves (1980),

$$K' = K^2 + 2K^3 + K^4 \qquad (4.14)$$

and enumerating all random walks such that $t \leqslant \xi^{8/3}$,

$$\begin{aligned} K'V' = \quad & K^2((1/2)V^2 + (1/2)V^4 + (1/2)V^6) \\ & + K^3((1/4)V^3 + (5/16)V^5 + (21/64)V^7) \\ & + K^3((1/4)V^3 + (5/16)V^5 + (21/64)V^7) \\ & + K^4((1/6)V^2 + (7/36)V^4 + (43/216)V^6). \end{aligned} \qquad (4.16a)$$

Define $\lambda_k=(\partial K'/\partial K)_{K^*}$ and $\lambda_v=(\partial V'/\partial V)_{V^*,K^*}$. One obtains

$$d_f = \frac{\log\lambda_k}{\log b}$$

and

$$d_w = \frac{\log\lambda_v}{\log b} \qquad (4.16b)$$

Hence for the b=2 cell-to-bond transformation (with $t \leqslant \xi^{8/3}$) for the HCT model one obtains $(K^*,V^*)=(0.4656,0.9613)$ and $d_f=1.398$ and $d_w=2.1000$.

The corresponding recursion relations for random walks on the SAW (in the static interpretation) are

$$\begin{aligned} K' &= K^2 + 2K^3 + K^4 \\ K'W' &= K^2(W^2+2W^4+4W^6) + K^3(W^3+3W^5+8W^7) \\ &\quad + K^3(W^3+3W^5+8W^7) + K^4(W^4+4W^6) \end{aligned} \qquad (4.17)$$

This system of equations yields $(K^*,W^*) = (0.4656,0.5773)$ and $d_f=1.398$ and $d_w=2.0280$.

Similarly, for a cell-to-cell transformation $1<b'<b$, one obtains for K,say, an implicit transformation (Reynolds *et al* 1978)

$$K'(b) = R_b(R_{b'}^{-1}(K'(b'))) \equiv R_{b/b'}(K'(b')) \qquad (4.18)$$

given in terms of the cell-to-bond transformation function $K'(b)=R_b(K)$. The value of K at which $K'(b)=K'(b')$ or equivalently $R_b(K)=R_{b'}(K)$ corresponds to K^*. It then follows that the fractal dimension, d_f, is obtained from the relation

$$d_f = \frac{\log(\lambda_k(b)/\lambda_k(b'))}{\log(b/b')} \qquad (4.19)$$

Here $\lambda_k(b)$ is the K-eigenvalue of the bxb cell-to-bond transformation, however it is evaluated at the fixed point (K^*,V^*) of the cell-to-cell transformation. Similarly for V',

$$V'(b) = G_b(G_{b'}^{-1}(V'(b')) \equiv G_{b/b'}(V'(b')) \qquad (4.20)$$

where G_b is the V RG cell-to-bond transformation function given by $V'=G_b(K;V)=Z^b_{saw}(K,V)/K'$, and the inverse is taken treating K only as a parameter. From (4.18) it follows that,

$$d_w = \frac{\log(\lambda_v(b)/\lambda_v(b'))}{\log(b/b')} \qquad (4.21)$$

where the eigenvalues λ_v are again evaluated at the cell-to-cell fixed point.

A, now familiar, problem with small cell RSRG is associated with cell interfacing. This phenomenon leads to errors both in the fixed points and in the eigenvalues. It is reasonable to expect however that such interfacing problems will vanish as $b\to\infty$ for a cell-to-bond transformation and $b\to\infty$ together with $b/b'\to 1$ for a cell-to-cell transformation (Reynolds *et al* 1978). In principle therefore, by evaluating tha RSRG recursion equations for larger b and also for $b/b'\to 1$ one will obtain improved estimates for the exponents. Assuming that the resulting sequences of exponents are monotonic in b it would then be possible to obtain reliable extrapolations to $b\to\infty$.

We proceed to do this therefore and the results are summarised in Tables 4.1-4.4. For the HCT model one must generate all spanning SAW configurations and for each

one enumerate exactly all random walks with $t \leqslant \xi^2$ and then repeat for $t \leqslant \xi^{8/3}$. For a b=4 cell for example with $t \leqslant \xi^{8/3}$ one must enumerate random walks of up to t=73 steps for each of the 649 spanning HCT SAWs. The corresponding calculation for a b=5 cell would involve counting and weighting the spanning random walks with number of steps t up to t=141 for 36368 spanning configurations. This required too much CPU time for our algorithm: an 180 minute run on a VAX 11/780 was insufficient. However, knowing the transfer matrix elements $T_i(K)$ (Redner and Reynolds 1981), where T_i is the weight associated with SAWs spanning a bxb cell from the origin to the i^{th} (i=1,...,b) site on the uppermost layer of the cell one is able to carry out the b=5 and b=6 transformations for SAWs without crosslinks for which diffusion is confined to the quasi-linear chains, ie not dependent on SAW conformation. This serves as a good check for the reliability of the lower b exponents for the SAW and hence for those of the HCT model.

The results for d_w^{HCT} and d_w^{SAW} obtained from the small cells considered are not sufficiently smooth to allow sensible extrapolations. In order to improve the accuracy of the exponents larger cells must be considered. This may be done using Monte Carlo renormalisation. As only relatively few spanning SAW configurations are sampled, longer random walks may then also be enumerated. We expect the dependence of the exponent d_w random walk length to vanish as t increases.

In Tables 4.5-4.6 we show $d_w^{HCT}(b/b')/d_w^{saw}(b/b')$ for various cell-to-cell transformations. The predictions of Helman *et al* would require d_w^{HCT}/d_w^{saw} =0.75. Our results our not consistent with this prediction. They are, however, in qualitative agreement with the Monte Carlo work of Yang *et al* who obtained d_w^{HCT}/d_w^{saw} = 0.97 and that of Chakrabarti and Chowdhury who obtained d_w^{Helman}/d_w^{saw} = 1.04. Despite the observed non-monotonic behaviour of the exponents,however our results would seem to favour the argument put forward by Chowdhury and Chakrabarti for $d_w^{HCT} > d_w^{saw}$.

In conclusion therefore we have developed and implemented a two-parameter small cell RSRG for random walks on SAWs, for which diffusion is trivial, and on the model of Helman *et al* for proteins. Our results are not consistent with the requirement that

Table 4.1.

Results of the cell-to-bond and cell-to-cell RSRG for random walks on the HCT model for proteins. We enumerate exactly all random walks on the HCT model of length t such that $t \leqslant \xi^2$.

b \ b'		1	2	3
2	K^*	0.466		
	V^*	1.128		
	d_f	1.398		
	d_w^{HCT}	1.815		
3	K^*	0.447	0.432	
	V^*	1.051	1.009	
	d_f	1.391	1.384	
	d_w^{HCT}	1.879	1.998	
4	K^*	0.435	0.423	0.416
	V^*	1.090	1.082	1.135
	d_f	1.386	1.377	1.369
	d_w^{HCT}	1.927	2.042	2.128

Table 4.2.

Results of the cell-to-bond and cell-to-cell RSRG for random walks on the HCT model for proteins. We enumerate exactly all random walks on the HCT model of length t such that $t \leqslant \xi^{8/3}$.

b \ b'		1	2	3
2	K^*	0.466		
	V^*	0.961		
	d_f	1.398		
	d_w^{HCT}	2.100		
3	K^*	0.447	0.432	
	V^*	0.947	0.941	
	d_f	1.391	1.384	
	d_w^{HCT}	2.237	2.458	
4	K^*	0.435	0.423	0.416
	V^*	1.013	1.021	1.060
	d_f	1.386	1.377	1.369
	d_w^{HCT}	2.368	2.680	3.153

Table 4.3.

Results of the cell-to-bond and cell-to-cell RSRG for random walks on SAW. We enumerate exactly all random walks on SAW of length t such that $t \leqslant \xi^2$.

b \ b'		1	2	3	4	5
2	K^*	0.466				
	W^*	0.650				
	d_f	1.398				
	d_wSAW	1.784				
3	K^*	0.447	0.432			
	W^*	0.581	0.538			
	d_f	1.391	1.384			
	d_wSAW	1.748	1.692			
4	K^*	0.435	0.423	0.416		
	W^*	0.553	0.531	0.526		
	d_f	1.386	1.377	1.369		
	d_wSAW	1.848	1.910	2.205		
5	K^*	0.426	0.417	0.411	0.407•	
	W^*	0.539	0.526	0.523	0.521	
	d_f	1.381	1.373	1.364	1.359	
	d_wSAW	1.916	2.022	2.277	2.379	
6	K^*	0.420	0.413	0.408	0.404	0.401
	W^*	0.530	0.522	0.519	0.518	0.515
	d_f	1.378	1.369	1.361	1.356	1.353
	d_wSAW	1.960	2.086	2.313	2.401	2.442

Table 4.4.

Results of the cell-to-bond and cell-to-cell RSRG for random walks on SAW. We enumerate exactly all random walks on SAW of length t such that $t \leqslant \xi^{8/3}$.

b \ b'		1	2	3	4	5
2	K^*	0.466				
	W^*	0.572				
	d_f	1.398				
	d_wSAW	2.038				
3	K^*	0.447	0.432			
	W^*	0.531	0.512			
	d_f	1.391	1.384			
	d_wSAW	2.117	2.136			
4	K^*	0.435	0.423	0.416		
	W^*	0.520	0.512	0.511		
	d_f	1.386	1.377	1.369		
	d_wSAW	2.247	2.361	2.663		
5	K^*	0.426	0.417	0.411	0.407	
	W^*	0.514	0.510	0.509	0.508	
	d_f	1.381	1.373	1.364	1.359	
	d_wSAW	2.357	2.521	2.813	3.001	
6	K^*	0.420	0.413	0.408	0.404	0.401
	W^*	0.510	0.508	0.507	0.506	0.505
	d_f	1.378	1.369	1.361	1.356	1.353
	d_wSAW	2.438	2.625	2.901	3.077	3.169

Table 4.5.

The results for $d_w^{HCT}(b/b')/d_w^{SAW}(b/b')$ for various cell-to-cell transformations. Monte Carlo work of Chowdhury and Chakrabarti indicates that $d_w^{HCT}/d_w^{SAW} \approx 1.04$. We evaluate all random walks such that $t \leqslant \xi^2$.

b \ b'	1	2	3
2	1.0173		
3	1.0747	1.1806	
4	1.0428	1.0688	0.9654

Table 4.6.

The results for $d_w^{HCT}(b/b')/d_w^{SAW}(b/b')$ for various cell-to-cell transformations. Monte Carlo work of Chowdhury and Chakrabarti indicates that $d_w^{HCT}/d_w^{SAW} \approx 1.04$. We evaluate all random walks such that $t \leqslant \xi^{8/3}$.

b \ b'	1	2	3
2	1.0306		
3	1.0563	1.1509	
4	1.0538	1.1348	1.1840

$d_w^{HCT}/d_w^{saw} = 0.75$ as speculated by Helman *et al.* However they do seem broadly in agreement with the available numerical data which suggest that $d_w^{HCT}/d_w^{saw} \approx 1$. On the other hand, they would appear to support the conclusions of Chowdhury and Chakrabarti that $d_w^{Helman} > d_w^{saw}$. One would expect d_w^{saw} to be affected by the presence of crosslinks only if these links were distributed along the SAW in some hierarchical fashion. This is in fact what seems to happen as loops created by crosslinks have smaller loops within them, and so on on all length scales, leading to the scale-invariance that we have exploited in our renormalisation scheme above.

Finally, we point out that saturation effects for the non-scale-invariant limit where the number of random walk steps t is much greater than SAW length N are not observable within this RG framework since it is implicit that the SAW or HCT model remains invariant under space dilatations.

After the work reported in this section was completed the work of Chowdhury (1985) was drawn to our attention. In his paper Chowdhury implements a b=2 cell-to-bond transformation for random walks on the HCT model. He treats walks satisfying $N \leqslant \xi^2$ on the b=2 cell using the 'static' interpretation, a procedure inconsistent with the governing diffusion equation. Our conclusions are in agreement.

3. Scaling Theory for Exponent Laws.

The result $d_w^{HCT} > d_w^{SAW}$ above implies that the Hydrogen bond crosslinks hinder diffusion (and therefore conduction) which goes rather against intuitive expectations. If the loops are distributed in a hierarchical fashion this is usually an indication that they (and therefore the crosslinks) are relevant and will therefore split the universality classes.

Given that we expect the crosslinks to accelerate diffusion —— as they are essentially Levy flights relative to paths along the length of the quasilinear SAW —— and, equivalently, lower the resistance we would expect in this picture that $d_w^{HCT} < d_w^{SAW}$. The position is thus thoroughly unclear and needs to be resolved.

Consider the diagram fig.1.7c. of a SAW of N steps. We first introduce some quantities of interest. Let R_N be the end-to-end distance between A and B. This is related to N in the usual way $R_N \sim N^{(1/d_f)}$, defining the fractal dimension. Recall the

Flory approximation, suprisingly accurate in two dimensions, $d_f=1/\nu=(d+2)/3$.

Let L_N be the shortest distance moving along the chain from A to B (indicated by the dotted line), then define t_L as

$$L_N \sim N^{t_L}. \tag{4.22}$$

Let f_N be the fraction of singly connected bonds (analogous to the red bonds of percolation theory) between A and B, then define t_f,

$$Nf_N \sim N^{t_f}. \tag{4.23}$$

Finally, let ρ_N be the resistance between A and B and then we introduce t_ρ as

$$\rho_N \sim N^{t_\rho}. \tag{4.24}$$

We note the physically clear inequalities:

$$Nf_N \leqslant \rho_N \leqslant L_N \leqslant N \tag{4.25}$$

with the consequences:

$$t_f \leqslant t_\rho \leqslant t_L \leqslant 1. \tag{4.26}$$

In fact $t_{f,\rho,L}\equiv 1$ above the upper critical dimension. We present two arguments relating d_w^{HCT} and d_w^{SAW} ($=2d_f\approx 8/3$, in 2d). Firstly we consider that random walks on the HCT model effectively diffuse through the backbone of the protein avoiding the longer journeys around the loops. This argument will surely lead to an under estimate and so a lower bound to d_w^{HCT}.

Consider now a spanning random walk of n steps having diffused on the backbone. Then

$$n \sim L_N^2 \sim N^{2t_L} \tag{4.27a}$$

however

$$n \sim R_N^{d_w} \sim N^{(d_w/d_f)} \tag{4.27b}$$

hence

$$d_w^{HCT} = 2d_f t_L = d_w^{SAW} t_L \tag{4.27c}$$

correcting the previous calculation of Chowdhury and Chakrabarti (1985). Recall that owing to the isomorphism between the master equation for diffusion and the linearised spin wave equation of motion: $d_w\equiv z$. Hence (4.27c) also applies to the Heisenberg spin wave dynamical exponent.

For our second argument, we need the Einstein relation between mobility and conductivity. For our purposes it is conveniently expressed as follows

$$d_w = d_f + d_r \qquad (4.28)$$

where d_r is the resistance scaling exponent governing the length scaling of the resistance (see Chp.3):

$$\rho(ba) \sim b^{d_r}\rho(a) \qquad (4.29a)$$

or in other words

$$\rho(R_N) \sim R_N{}^{d_r} \sim N^{(d_r/d_f)} \qquad (4.29b)$$

and so $$t_\rho = d_r/d_f \qquad (4.29c)$$

and hence $$d_w{}^{HCT} = d_f(1+t_\rho) \qquad (4.29d)$$

or $$d_w{}^{HCT} = d_w{}^{SAW}(1+t_\rho)/2. \qquad (4.29e)$$

This latter result is exact as long as the Einstein relation is valid for our system. It has, in fact, been shown to be valid for a regular fractal representation of these random chains (Stinchcombe 1985).

4. Exact Enumeration Approach for Protein Structure.

The problem of finding $d_w{}^{HCT}$ now reduces to an evaluation of the above "conductivity" exponents. There have been two previous attempts to evaluate $t_{f,\rho,L}$. Ball and Cates (1984) performed an ϵ-expansion (to first order in ϵ) using a renormalisation prescription developed by des Cloiseaux (1980,81) and concluded that $t_f=t_\rho=t_L=1$ in all dimensions. Bhattacharya and Chakrabarti (1984) performed an exact enumeration study for relatively short walks on the two dimensional simple square lattice (N=13) and on the two dimensional triangular lattice (N=10) and evaluated only t_L, their result being $t_L=0.977\pm0.008$ for d=2 which they claimed to definitely exclude $t_L=1$ in disagreement with the Ball and Cates value.

We report, very briefly, our related exact enumerations. This work is still in progress at the time of writing and the analysis of the data is very incomplete.

In two dimensions, we have enumerated Nf_N and L_N (lower and upper bounds respectively for the resistance) on the square lattice (N=19), triangular lattice (N=13) and the extrapolated results (obtained by the crude ratio method together with a least squares fit) give, in contrast to the suggestions of Bhattacharya and Chakrabarti (1984), $t_{L,\rho}=1.00\pm0.01$ which <u>is</u> consistent with the Ball and Cates result. This indicates that the

lengths of SAW considered by Bhattacharya and Chakrabarti were not sufficient to allow for corrections to scaling (curvature in the data).

The results in three dimensions are however, rather more intriguing. Plots for L_N and f_N are overleaf (figs.4.1 and 4.2) and a crude least squares analysis (not shown in figures) indicates that $t_{\rho,L} \approx 0.92 \pm 0.02$. Further, provided the correction to scaling terms are analytic then the value unity seems surely excluded.

Although the enumeration problem is one of exponential time complexity, it is hoped that with more powerful computers (eg ULCC Cray 1S, Rutherford Cray XMP48) further steps will be obtained in the near future. To obtain more reliable extrapolations (particularly in the presense of confluent singularities) Padé approximants and differential Padés will probably need to be used.

This work is very incomplete and only included in the thesis to demonstrate the problems involved. Although the exact enumerations have yielded reasonably accurate evaluations of the "conductivity" exponents, the theoretical reasons for our results are not yet fully understood and neither is the question of dynamic universality classes established.

In the following two chapters we present a resolution of these two points.

Table 4.7.

Number of walks c_N (not new results) and mean shortest path L_N for SAWs with N steps on the two dimensional quadratic lattice.

N	c_N	L_N
1	4	1
2	12	2
3	36	2.555555556
4	100	3.36
5	284	3.985915493
6	780	4.769230769
7	2172	5.379373849
8	5916	6.150101420
9	16268	6.764445537
10	44100	7.522721088
11	120292	8.142553121
12	324932	8.891214162
13	881500	9.516501418
14	2374444	10.25765695
15	6416596	10.88744686
16	17245332	11.62264200
17	46466676	12.25626838
18	124658732	12.98653187

Table 4.8.

Number of walks c_N, mean number of crosslinks H_N, mean shortest path L_N and number of singly connected (red) bonds Nf_N in SAWs with N steps on the three dimensional simple cubic lattice. The c_N are not new results.

N	c_N	H_N	L_N	Nf_N
1	6	0	1	1
2	30	0	2	2
3	150	0.16	2.68	2.52
4	726	0.2644628099	3.471074380	3.206611570
5	3534	0.4550084890	4.103565365	3.689303905
6	16926	0.6012052464	4.842963488	4.306983339
7	81390	0.7952819757	5.466642094	4.795503133
8	387966	0.9598366867	6.174850373	5.376842301
9	1853886	1.155501471	6.790595538	5.862318395
10	8809878	1.330299466	7.476799565	6.419646220
11	41934150	1.526808675	8.086521224	6.901466084
12	198842748	1.707896493	8.756422014	7.441805059
13	943975128	1.904943706	9.361561627	7.920329297

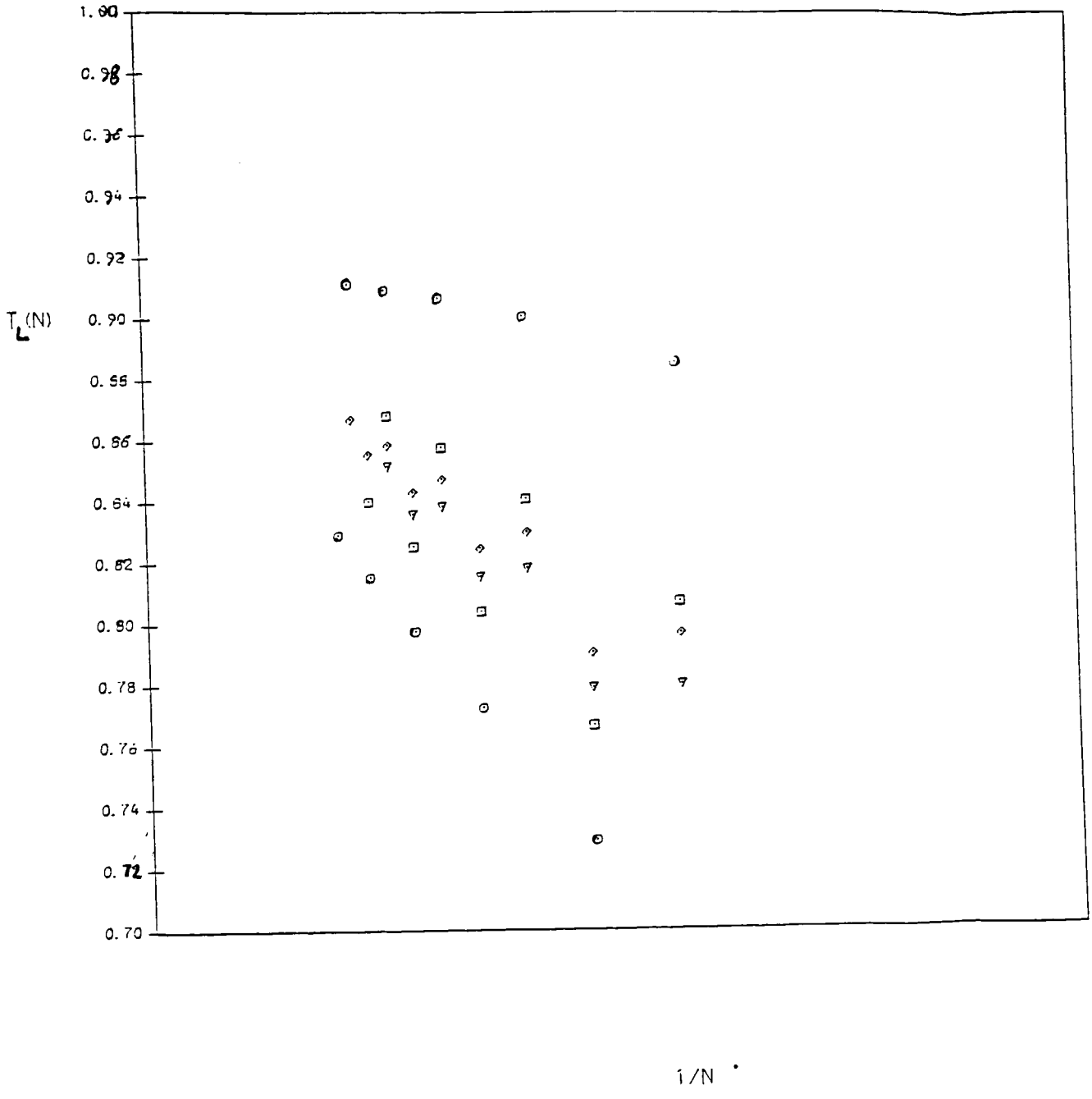

Fig.4.1.: Sequence of approximants to t_L, the exponent governing the divergence of the shortest path $L_N \sim N^{t_L}$. The plot is for SAWs on the 3d simple cubic lattice where steps up to N=13 were obtained. The sequence $t_L(N)$ has the property $t_L(N) \to t_L$ as $(1/N) \to 0$.

For the points ○ , ◇ , □ , ▽ , the ratio method generates the sequence $t_L(N) = (N/i)[\,(L_{N+i}/L_N) - 1\,]$ with i=1,2,3,4 respectively.

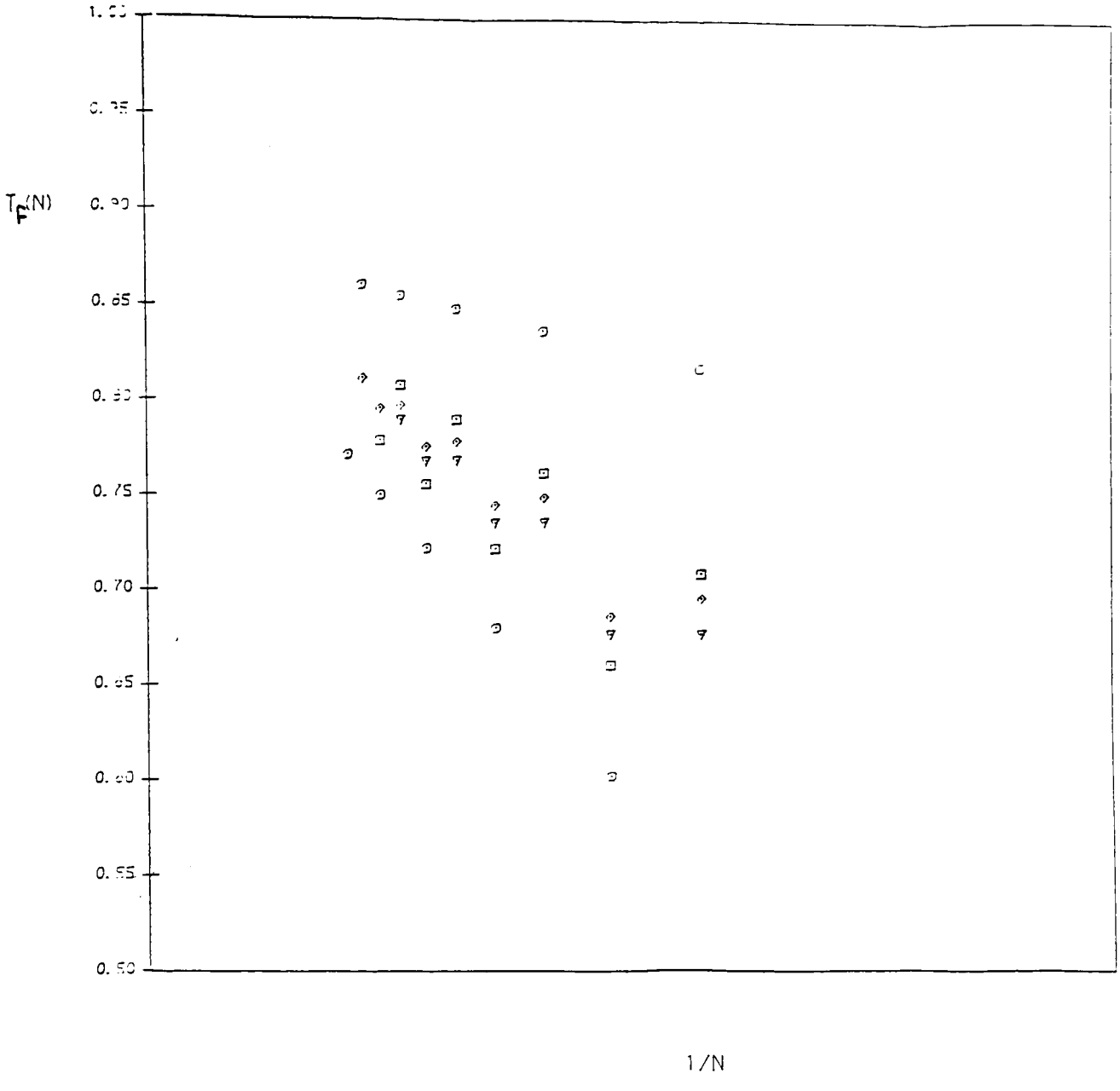

Fig.4.2.: Sequence of approximants to t_f, the exponent governing the divergence of the number of red bonds $Nf_N \sim N^{t_f}$. The plot is for SAWs on the 3d simple cubic lattice where steps up to N=13 were obtained. The sequence $t_f(N)$ has the property $t_f(N) \to t_L$ as $(1/N) \to 0$.

For the points ⊙ , ◈ , ⊡ , ▽ , the ratio method generates the sequence $t_f(N) = (N/i)[\,(f_{N+i}/f_N) - 1\,]$ with i=1,2,3,4 respectively.

Chapter 5

Hamiltonian Formulation for the Conformation and Resistance of Random Walks.

Hamiltonian formulations are developed for a variety of random walk models, including wholly or partially self-avoiding walks and chiral self-avoiding walks. The walks are generated by associating novel trace rules for the spin-like operators that appear in the Hamiltonians. We use these Hamiltonians to define canonical averages in terms of which the respective walk susceptibilities (generating functions) are expressed as appropriate spin-spin correlation functions. The well known relation between the q-state Potts model in the limit $q \to 0$ and the resistance of networks is then exploited in order to extend the above scheme to calculate resistive properties of such walks. For both Gaussian Random Walks (GRWs) and Self-Avoiding Walks (SAWs) we thereby express the resistive susceptibility as a correlation function involving both spin and Potts variables. We illustrate how this formulation can lead to the construction of the corresponding field theories. The detailed field theoretic treatment is given in the following chapter. This work has been submitted to J. Phys. A (Harris and Christou 1987a).

I. Introduction

In this chapter we present a technique for constructing Hamiltonian representations and hence field theories for the resistive and related properties of geometrical lattice-based objects. Our approach may be viewed as an extension of the idea of deGennes (1972, 1975) for self-avoiding walks. We construct a Hamiltonian bilinear in "spin" operators, which are defined to obey such trace rules as are necessary to reproduce the statistical properties desired. We illustrate the method for a range of lattice walk problems. In particular, we study Gaussian Random Walks (GRWs) and Self-Avoiding Walks (SAWs) (for a review of various random walk problems see Fisher 1984) in detail and we extend the discussion to treat interacting SAWs, including *chiral*

or *helical* SAWs (Privman 1983, Guttmann and Wormald 1984), and *valence* walks (VWs) (Domb and Joyce 1972) in which multiple visits to a given site are permissible up to some fixed integer index p; SAWs correspond to p=1 and GRWs to p=∞. An advantage of our formulation is that it makes the relationship between the above models explicit, especially when a field-theoretic representation is developed. Although the walk models that we treat are inherently interesting as problems in network theory, our conclusions also have ramifications for other topics of substantial current interest in the theory of critical phenomena for random systems. We outline the backround to these problems below. We stress however that the procedure is a general one and can in principle be applied to a variety of models.

Fluid flow in very low porosity media is a problem whose relation to ordinary percolation theory is unclear. The channels in which flow takes place occupy a small fraction of the system and yet these channels are sufficiently well correlated that the pore network forms an infinite cluster (Sen 1981). These correlations, the exact nature of which are not known, cause the percolation concentration, p_c, to appear to be much smaller than in ordinary uncorrelated percolation. In discussing the problem we will talk in terms of the analogue resistor network in which the random pore sizes are analogous to random conductances connecting adjacent sites on a cubic lattice in d spatial dimensions. A model which has been proposed (Banavar *et al* 1984) to treat such a system is one in which the pore network is regarded as a system of nodes connected by GRWs. In terms of the electrical network one can imagine nodes connected by random walks and the conductivity of a bond in the proposed model is taken to be pg_0, where p is the number of times the bond is traversed in the random walk and g_0 is the unit of conductance. The fluctuations in pg_0 mimic the variation of width of the channel in a porous medium.

Another problem of current interest concerns linear dynamical processes such as phonons, spin waves or electrical conductivity on certain linear proteins (Stapleton *et al.* 1980, Allen *et al* 1982, Helman *et al* 1984). These linear molecules can have hydrogen-bond crosslinks and these give rise to non-trivial static conformations. There has been substantial controversy (see, for example, chapter 4 of this thesis and

references therein) surrounding the theoretical interpretation of the experimentally observed spin–lattice relaxation rates in low–spin haemoproteins and ferredoxin.

These proteins are modelled by lattice–based SAWs such that all nearest neighbours occupied by the walk are connected. Some typical configurations of such SAWs with crosslinks are illustrated in fig.5.1. The vibrational problem may be re–expressed as a problem in resistor network theory and so we are led to study the resistance of SAWs with bridges. As we shall demonstrate, this problem is intrinsically related to the problem of the resistance of GRWs discussed above.

In these formulations a quantity of interest in *conformational* studies is $<\rho_N{}^2>$, the mean–square end–to–end distance of walks of length N steps while in the *resistor network* problem one would be interested in the end–to–end resistance, $<R_N>$, of walks of length N. With regard to this latter problem, simulation and series studies (Banavar *et al* 1984) have focussed their attention on both $P_N(R)$, the probability that a walk of N steps has an end–to–end resistance R, and on $<R_N>$, the value of R averaged over walks of N steps. We show how conformational and resistive properties may be expressed as suitable correlation functions with respect to *spin* Hamiltonians. As will become apparent, the technique we use is a very general one with possibly wide application. In the following chapter we will use the Hubbard–Stratanovich transformation to develop field theories from such spin Hamiltonians. In this way one can develop renormalisation group treatments from which the universality class of the various statistical problems considered can be determined.

Briefly, this chapter is organised as follows. In section II we describe the process of generating walks by defining trace rules for the spin–like operators that occur in a Hamiltonian representation. These trace rules have the effect of selecting and weighting appropriately the subset of all possible graphs that correspond to the problem of interest. We illustrate the method for a selection of models including GRWs, SAWs, SAWs with crosslinks, helical walks and valence walks. Furthermore, one is able to express the walk susceptibility as a spin–spin correlation function with canonical averages defined with respect to the appropriate density matrices. In section III we present a formulation similar to that used by Dasgupta *et al* (1978) for the resistance of walks in

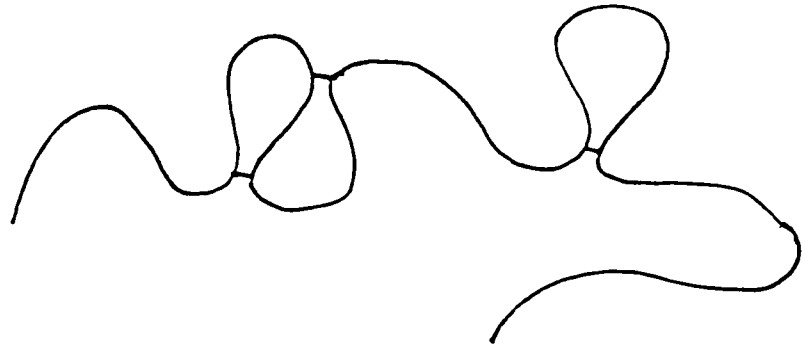

Fig.5.1.: A typical configuration for SAW with crosslinks. The presence of conducting crosslinks allows for non-trivial circuits to be formed.

terms of a replicated Potts model coupled in the case of GRWs to a replicated Gaussian variable and in the case of SAWs with crosslinks to a replicated n-component spin variable. Higher order resistive susceptibilities (Harris and Lubensky 1987) and the probability distribution $P_N(R)$ are in principle calculable from the higher order spin-Potts correlation functions using these Potts-decorated spin Hamiltonians. In section IV we give a brief discussion of the significance of our results. Some of the work on GRWs has previously been reported in Banavar *et al* (1984).

II. Use of Trace Laws to Generate Walks

In the first instance we consider a purely conformational problem. That is, we are interested in the ordinary generating function for walks χ_0 defined by

$$\chi_0(x,x';K) = \sum_N K^N \sum_{\gamma \subseteq \Gamma_N(x,x')} 1 = \sum_N K^N C_N(x,x') \qquad (5.1a)$$

where the sum over γ is over all walks γ in the ensemble $\Gamma_N(x,x')$ of N step walks of the type considered (SAW or GRW) which begin at x and end at x'. Also we set

$$\chi_0(x;K) = \sum_{x'} \chi_0(x,x';K) = \sum K^N C_N \quad . \qquad (5.1b)$$

Thus $C_N(x,x')$ is the number of walks from x to x' of length N and C_N is the total number of walks of length N starting from a fixed point.

Our aim is to formulate a Hamiltonian from which $\chi_0(x,x';K)$ can be calculated and thereby the asymptotic properties of long walks obtained. Typically, and depending on the type of walk being considered, the C_N have the following asymptotic ($N \gg 1$) form (for general reviews see McKenzie 1976 and de Gennes 1979):

$$C_N \sim \mu^N N^{\gamma-1} \quad , \qquad (5.2)$$

where γ is a universal critical exponent and μ ($\equiv 1/K_c$) is the so-called connectivity which is lattice dependent (McKenzie 1976, de Gennes 1979). Clearly for GRWs, $\mu=Z$ and $\gamma=1$, where Z (=2d , on a hypercubic lattice) is the lattice coordination number. From (5.2) one sees that for $K \to K_c$

$$\chi_0(x;K) \sim |K-K_c|^{-\gamma}, \qquad (5.3)$$

so that an asymptotic determination of χ_0 gives γ. We first desribe how to generate GRWs. As we shall see, the procedure for other types of walks is similar.

To develop a Hamiltonian for GRWs which yields $\chi_0^{grw}(x,x';K)$ we will use the well-known identity for the inverse of a matrix A:

$$[A^{-1}]_{ij} = \frac{\int u_i u_j e^{-\frac{1}{2}\sum_{k,l} u_k A_{kl} u_l} Du}{\int e^{-\frac{1}{2}\sum_{k,l} u_k A_{kl} u_l} Du}, \qquad (5.4)$$

where $Du=\prod_k du_k$ all the integrations run from $-\infty$ to $+\infty$. Now consider the matrix in site labels A(x,x') defined by

$$\begin{aligned} A(x,x';K) &= \delta_{x,x'} - K\gamma_{x,x'} \\ &\equiv \delta_{x,x'} + M_{x,x'} \end{aligned} \qquad (5.5)$$

where δ is the Kronecker delta and $\gamma_{x,x'}$ is unity if sites x and x' are nearest neighbours and zero otherwise. It is clear that when A^{-1} is expanded in powers of K, one generates the complete ensemble of random walks. More general walks can be obtained by a more general choice of M. Thus

$$\langle u(x)u(x')\rangle \equiv \chi_0(x,x';K) = \frac{\int Du\, e^{-\frac{1}{2}\sum_r u(r)^2} e^{-\sum_{y,y'} M_{y,y'}u(y)u(y')} u(x)u(x')}{\int Du\, e^{-\frac{1}{2}\sum_r u(r)^2} e^{-\sum_{y,y'} M_{y,y'}u(y)u(y')}}, \qquad (5.6)$$

where r,y,y' are dummy variables. Accordingly, we introduce the notation whereby

$$\underset{u}{Tr}\,\{\ldots\} = \int Du\, e^{-\frac{1}{2}\sum_r u(r)^2} \{\ldots\} \qquad (5.7)$$

in which case (5.6) becomes

$$\langle u(x)u(x')\rangle \equiv \frac{\underset{u}{Tr}\, u(x)u(x')e^{-H(u)}}{\underset{u}{Tr}\, e^{-H(u)}} = \chi_0(x,x';K), \qquad (5.8)$$

where

$$H(u) = \tfrac{1}{2} \sum_{x,x'} u(x)M(x,x';K)u(x') \ ,$$

$$= -\tfrac{1}{2} \sum_{x,x'} K\gamma_{x,x'}\, u(x)u(x') \qquad (5.9)$$

Note that Tr_u implies an average over u with a Gaussian weight as in (5.7).

In the above procedure random walk graphs are selected using the properties of Gaussian integrals. These properties define the so-called trace laws. In general, however we may define trace laws *a priori* for operators without regard to explicit representations. For SAWs, we introduce n-component spin variables s_α to reproduce the well known result (deGennes 1972, 1975) that SAWs are given by the $n\to 0$ limit of the Heisenberg model. Consider the average

$$\langle s_1(x)s_1(x')\rangle \equiv \frac{\operatorname{Tr}_s e^{-H(s)} s_1(x)s_1(x')}{\operatorname{Tr}_s e^{-H(s)}} \ , \qquad (5.10)$$

where H(s) is the Heisenberg Hamiltonian

$$H(s) = -\sum_{\alpha,\langle x,x'\rangle} K\, s_\alpha(x)s_\alpha(x') \ . \qquad (5.11)$$

In order that $\langle s_1(x)s_1(x')\rangle$ count SAWs connecting sites x and x' we define the following trace rules for the spin variables s_α,

$$\begin{aligned} \operatorname{Tr}(1) &= 1 \\ \operatorname{Tr}(s_\alpha) &= 0 \\ \operatorname{Tr}(s_\alpha s_\beta) &= \delta_{\alpha\beta} \\ \operatorname{Tr}(s_{\alpha_1} s_{\alpha_2} s_{\alpha_3} \cdots s_{\alpha_k}) &= 0 \qquad k>2 \end{aligned} \qquad (5.12)$$

Since $s_\alpha(x)$ always appears within a trace, it is fully specified by its trace rules and it is not necessary to construct explicitly a representation for which, for example, $\operatorname{Tr} s_\alpha{}^2 = 1$ but $\operatorname{Tr} s_\alpha{}^4 = 0$. Operators associated with different sites are taken to be independent so that traces over operators involving different sites factorise. We also require that the s_α commute within the traces. The self-avoidance constraint results from the fact that traces of $s_\alpha{}^p$ with $p>2$ vanish.

In order to see that Hamiltonian (5.11) does indeed generate SAWs for n→0, note that under trace operations the Boltzmann factor $e^{-H(s)}$ is effectively

$$e^{-H(s)} = \prod_{<x,x'>} (1+K \sum_{\alpha=1}^{n} s_\alpha(x)s_\alpha(x')) \qquad (5.13)$$

apart from contributions which vanish as n→0. In this limit the partition function is unity because any sum over replica indices is proportional to n→0. Also one sees that in $<s_1(x)s_1(x')>$ diagrams involving k loops lead to contributions of order $n^k \to 0$, so that indeed this correlation function is the generating function for SAWs:

$$<s_1(x)s_1(x')> = \chi_0(x,x';K) \quad . \qquad (5.14)$$

To illustrate the flexibility of this scheme we now consider the related problem of *valence* walks (VWs) (see Domb and Joyce 1972). In this problem the (lattice-based) walks are permitted to visit a site up to a maximum of p times. The additional fugacity associated with sites visited r times is denoted ℓ_r. Some short VWs are shown in Fig. 5.2a with their associated weights. SAWs correspond to setting $\ell_r=\delta_{r,1}$ (i.e. p=1) while GRWs correspond to the case $\ell_r=1$ for all r (i.e. p=∞). In particular, choosing $\ell_r=e^{-wr}$, w being a constant, reduces the general model to that of Domb and Joyce (1972). For the problem of valence walks we wish to obtain the generating function

$$\chi_0(x,x';K;\{\ell\}) = \sum_N K^N \sum_{\gamma \subseteq \Gamma_N^{grw}(x,x')} w(\gamma) \quad , \qquad (5.15)$$

where the valence fugacity is $w(\gamma)=\prod_y \ell_{n(y,\gamma)}$, where $n(y,\gamma)$ is the number of times the site y is visited by the walk γ and $\ell_0=1$.

To include the additional fugacities ℓ_r it seems natural to replace $K\gamma_{x,x'}$ in (5.9) by $K\gamma_{x,x'}s(x)s(x')$ and define the trace of $s(x)^{2r}$ to be ℓ_r. However, what we need is an average over s(x) of the *quotient* in (5.4) which indicates the need for a quenched average. Thus we are led to consider the replicated Hamiltonian

$$H(u,s) = -\tfrac{1}{2} \sum_{\alpha,x,x'} K\,\gamma_{x,x'}\{s_\alpha(x)\,s_\alpha(x')\}\,u_\alpha(x)\,u_\alpha(x') \quad , \qquad (5.16)$$

where α assumes the values 1, 2 ... n with n→0 and $s_\alpha(x)$ for each site x obeys the trace rules

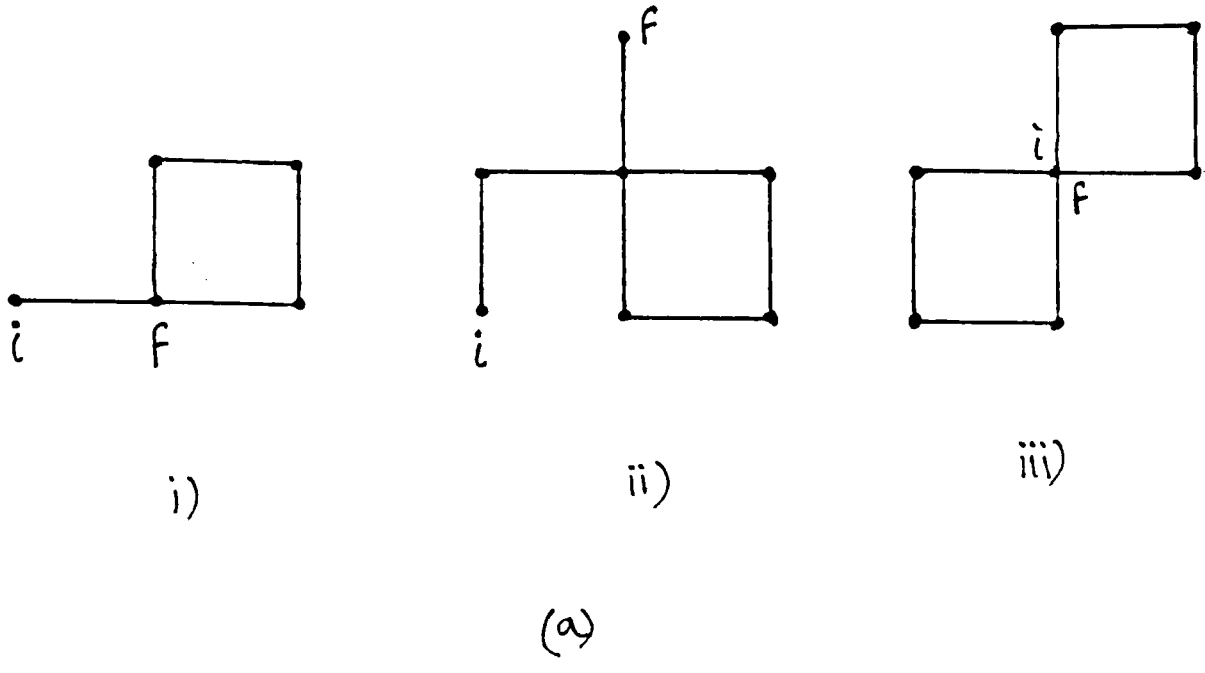

Fig.5.2a.: Examples of valence walks on the two dimensional square lattice. The walks start at the site i and end at f. The fugacity associated with sites visited r times is given by $K\ell_r$, and so the respective weights are i) $K^5\ell_1{}^4\ell_2$ ii) $K^7\ell_1{}^6\ell_2$ iii) $K^8\ell_1{}^6\ell_3{}^1$.

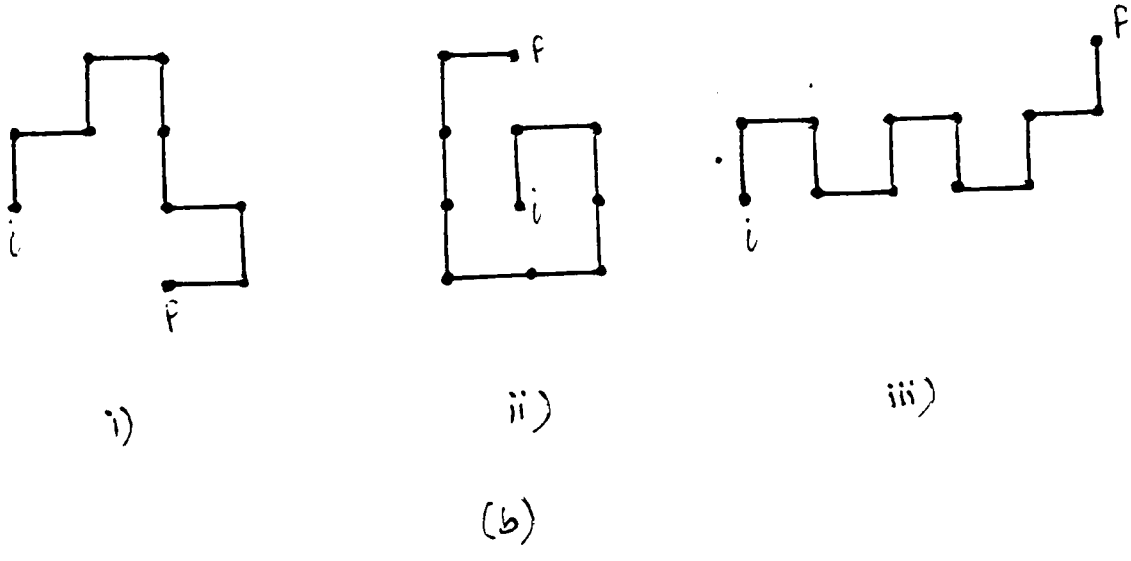

Fig.5.2b.: Examples of spiral SAWs on the two dimensional square lattice with associated weights: i) $K^9\ell_c{}^5\ell_a{}^2$ ii) $K^{10}\ell_c{}^5$ iii) $K^{11}\ell_c{}^5\ell_a{}^5$.

$$\mathrm{Tr}(1) = 1$$

$$\mathrm{Tr}(s_{\alpha 1}\, s_{\alpha 2} \ldots s_{\alpha j}) = 0, \qquad \text{if } j \text{ is odd}$$

$$= \ell_{j/2} \qquad \text{if } j \text{ is even and}$$

$$\alpha 1 = \alpha 2 = \ldots \alpha j. \qquad (5.17)$$

Consider now the $n \to 0$ limit of

$$C_{x,x'} \equiv \langle u_1(x) s_1(x) u_1(x') s_1(x') \rangle$$

$$= \frac{\mathrm{Tr}_{u,s}\, u_1(x) s_1(x) u_1(x') s_1(x') \exp[-H(u,s)]}{\mathrm{Tr}_{u,s} \exp[-H(u,s)]} . \qquad (5.18)$$

where the trace over u is again as in (5.7). Since replica summations vanish as $n \to 0$, one sees that the denominator above is unity, and if we first take the trace over the u variables, we get

$$C_{x,x'} = \mathrm{Tr}_s\, s_1(x) s_1(x')\ \ \mathrm{Tr}_u\, u_1(x) u_1(x') \exp[-h(u,s)]$$

$$\times\ \{\ \mathrm{Tr}_u\ \exp[-h(u,s)]\ \}^{n-1} , \qquad (5.19)$$

where h(u,s) is H(u,s) for n=1. For $n \to 0$ we obtain the desired quenched average:

$$C_{x,x'} = \mathrm{Tr}_s \sum K^N \sum_{\gamma \subseteq \Gamma_N^{grw}(x,x')} \prod_y s_1(y)^{2n(y,\gamma)} , \qquad (5.20)$$

where $n(y,\gamma)$ is as above. Now the trace rules ensure that each site carries its proper fugacity factor so that

$$\langle u_1(x) s_1(x) u_1(x') s_1(x') \rangle = \chi_0(x,x';K;\{\ell\}) . \qquad (5.21)$$

By introducing appropriate conjugate fields using the Hubbard-Stratanovich transformation one can obtain a field theory for this model in which the dependence on the ℓ_k's is made explicit. This procedure is illustrated in Appendix E. In this way one can establish that a finite number p of permissible multiple visits represents a relevant perturbation from GRW to SAW critical conformational behaviour (Lax *et al* 1978).

Finally, we apply the technique to another problem which has received much recent interest, namely that of spiral SAWs (Privman 1983, Guttmann and Wormald 1984,

Fisher *et al* 1984). We now consider SAWs in d dimensions with a, say, two dimensional embedded plane chosen within which the walks show an affinity to spiral. For each pair of successive steps in this chosen plane we associate "chiral" fugacities ℓ_c, ℓ_s, and ℓ_a, respectively, for the cases when the walk turns clockwise, goes straight, or turns anticlockwise with, say, $\ell_c > \ell_s = 1 > \ell_a$ (see fig.5.2b for examples of such walks and associated weights). Setting $\ell_a = 0$, $\ell_c \neq 0$, say, reduces to the 'hard' spiral walks introduced by Privman (1983). Now we consider the Hamiltonian

$$H(s,t) = -K \sum_{x,\alpha,\delta} s_\alpha(x,\delta)\, t_\alpha(x+\delta,-\delta) \ , \qquad (5.22)$$

where $\alpha = 1, 2 \ldots n$ with $n \to 0$ and δ is summed over the z nearest neighbour vectors. A factor $s_\alpha(x,\delta)t_\alpha(x+\delta,-\delta)$ will be interpreted as a step *from* x *to* $x+\delta$, or alternatively, at a given site x, $t_\alpha(x,-\delta)$ indicates that the *entering* step was traversed in the direction δ and $s_\alpha(x, \delta')$ that the *exiting* step was in the direction δ'. Thus we define the trace rules for operators at each site x so that the only non-zero traces are

$$\mathrm{Tr}\ 1 = 1$$

$$\mathrm{Tr}\ t_\alpha(x,-\delta)\, s_\alpha(x, \delta') = \ell(\delta, \delta') \ , \qquad (5.23)$$

where $\ell(\delta,\delta')$ is the chiral fugacity associated with the pair of successive steps in directions first δ then δ'. (For example, if the sequence of sites $x-\delta$, x, $x+\delta'$ forms a clockwise turn in the chosen plane, $\ell(\delta,\delta') = \ell_c$.) Because only 0 or 2 operators can appear at a given site, one has effectively,

$$\exp[-H(s,t)] = \prod_{x,\delta} [1 + K \sum_{\alpha} s_\alpha(x,\delta)\, t_\alpha(x+\delta,-\delta)\ ] \ . \qquad (5.24)$$

As before, since loops introduce multiplicative factors of n, one sees that $\langle t_\alpha(x_i,\delta)\, s_\alpha(x_f,\delta')\rangle$ counts walks which begin at x_i and end at x_f with appropriate chiral fugacity at all *internal* sites. At the sites x_i and x_f the chiral fugacity is that as if the walk had entered site x_i in the direction $-\delta$ and had left site x_f in the direction δ'. These end effects will not affect the asymptotics of the walks, but to avoid end effects one may consider

$$C_{x_i,x_f} = L^{-2} \sum_{\delta,\delta'} \langle t_\alpha(x_i,\delta)\, s_\alpha(x_f,\delta')\rangle \ , \qquad (5.25)$$

where $L=\sum_{\delta} \ell(\delta,\delta')$ is assumed to be independent of δ'. Then

$$C_{x_i,x_f} = \chi_0(x_i, x_f; K; \{\ell\}) \ . \qquad (5.26)$$

III. Formulation of Resistances in terms of a Potts Model

So far, we have been considering the problem of the conformational generating function χ_0 which relates to the problem of end-to-end distances. In principle, we are now in a position to investigate the resistive properties of all the models discussed above. In this section we report the results of work on GRWs (Banavar *et al,* 1984), SAWs and SAWs with crosslinks.

We study the following models for the end-to-end resistance of walks on a hypercubic lattice in d spatial dimensions. The walks we consider are such that each step of the walk connects nearest-neighbours on the hypercubic lattice. The resistance of a walk is defined by associating a conductance σ_0 with each step of the walk. Thus, if a bond is traversed ℓ times in a GRW, its conductance is taken to be $\ell\sigma_0$. For the SAWs we also associate a *bridge* conductance σ_b between nearest-neighbours on the walk if they are not directly connected *a priori.*

To calculate the end-to-end resistance $R(\gamma)$ of the walk γ between sites x_i and x_f we must solve Kirchoff's circuit equations for the voltages when a unit current is injected at site x_i and removed at site x_f. These equations are

$$\sum_n g_{m,n}[V(x_m)-V(x_n)] = I(x_m) \ , \qquad (5.27)$$

where $I(x)=\delta_{x,x_i}-\delta_{x,x_f}$, where $g_{m,n}$ is the conductance connecting sites x_m and x_n. Then $R(\gamma)=V(x_i)-V(x_f)$. Examples of such GRWs and SAWs with the associated value of $R(\gamma)$ are shown in Fig.5.3.

The distribution of walks γ in the ensemble $\Gamma_N(x,x')$ {for either GRWs or SAWs} induces a probability distribution for $R(\gamma)$. We may study the moments of this distribution, or equivalently, the following generating function:

$$F(x,x';K,\ell) = \sum_N K^N \sum_{\gamma\subseteq\Gamma_N(x,x')} e^{-\ell R(\gamma)} = F(x-x';K,\ell). \qquad (5.28)$$

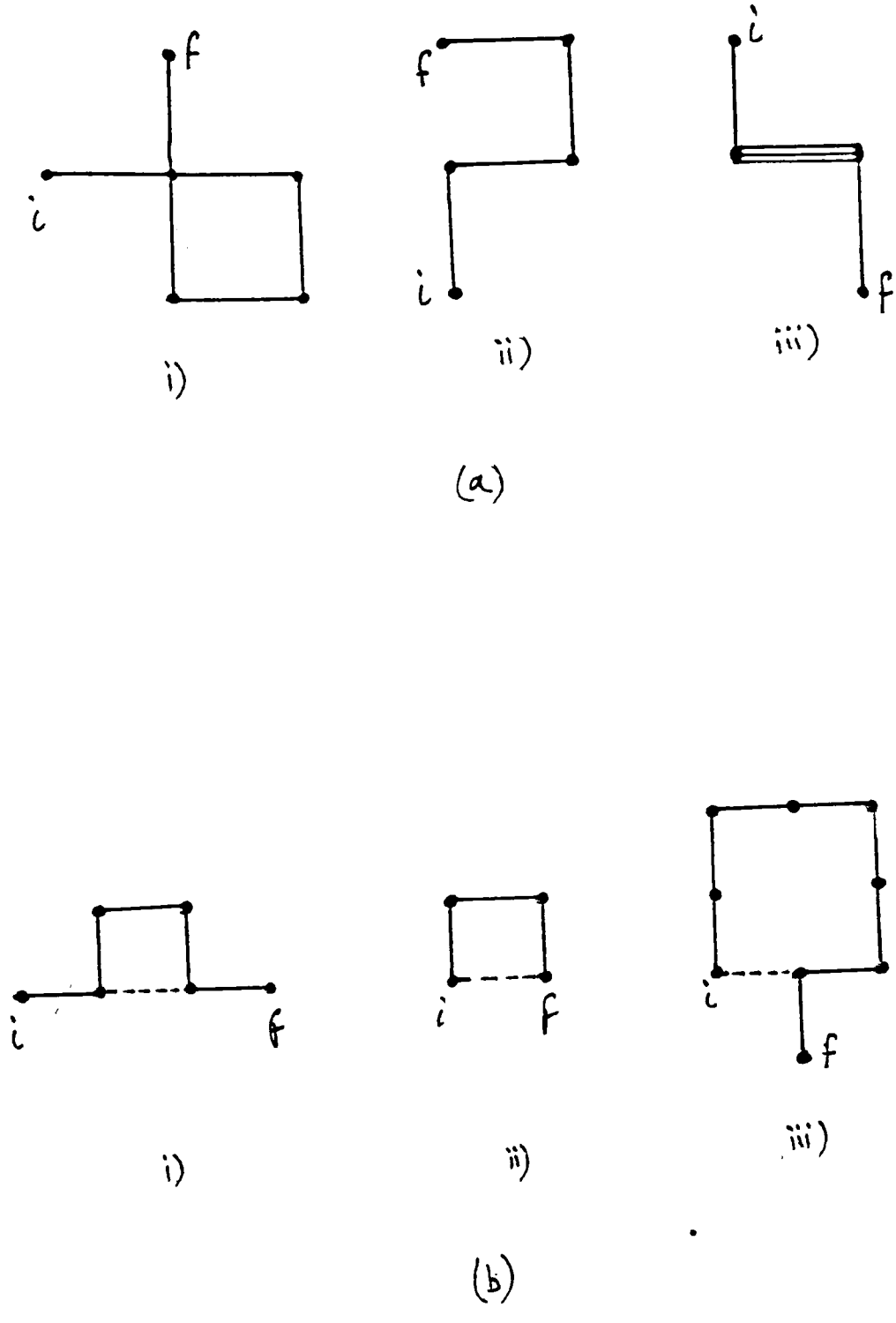

Fig.5.3.: Examples of GRWs (a) and SAWs with crosslinks (b). If each step has an associated unit resistance, the end-to-end resistance of the walks shown are respectively: (a) 2, 4, 7/3 and (b) 11/4, 3/4, 15/8.

Clearly, F(x,x';K,0) is the ordinary generating function for walks, introduced in the previous section

$$\chi_0(x,x';K) = F(x-x';K,0) = \sum_N K^N \sum_{\gamma\subseteq\Gamma_N(0,x-x')} 1 \equiv \chi_0(x-x';K) \tag{5.29}$$

We now define the *resistive susceptibility*, χ_1 by

$$\chi_1(x,x';K) = -\frac{\partial}{\partial \ell} F(x-x';K,\ell)\Big|_{\ell=0}$$

$$= \sum_N K^N \sum_{\gamma\subseteq\Gamma_N(0,x-x')} R(\gamma) \equiv \chi_1(x-x';K) \tag{5.30a}$$

and

$$\chi_1(x;K) = \sum_{x'} \chi_1(x,x';K) = \sum_N K^N C_N \langle R_N\rangle \tag{5.30b}$$

where $\langle R_N\rangle$ is the mean resistance of walks of length N. Thus χ_1 is the generating function for the average end-to-end resistance of walks. Higher moments of the distribution of resistances $R(\gamma)$ are obtained by further derivatives with respect to ℓ. We will present a formalism in which arbitrary moments of $R(\gamma)$ can in principle be obtained.

An evaluation of $\chi_1(x; K)$ leads to a determination of the scaling behaviour of $\langle R_N\rangle$. To see this define the exponent x by

$$\langle R_N\rangle \sim N^x \tag{5.31}$$

Then x is determined by the divergence of χ_1 near the critical point $|K-K_c| \ll 1$, where one has

$$\chi_1(x;K) \sim |K-K_c|^{-(x+\gamma)} , \tag{5.32}$$

where γ is the universal exponent introduced above.

We will develop Hamiltonians with respect to which $\chi_1(x; K)$ can be expressed as a suitable correlation function analogous to the procedure employed in section II for the conformational problem. In order to generate $R(\gamma)$, we use the q-state Potts model in the limit $q\to 0$. The original formulation of Kasteleyn and Fortuin (1969) and Fortuin and Kasteleyn (1972) is not convenient for this purpose. Instead we use the modification

introduced by Dasgupta *et al* (1978) in which the resistance R(x,x') between sites x and x' is related to a Potts model as follows. Let $\underline{v}(x)$ be a unit vector in q−1 dimensional space which can assume q values, which we denote $\underline{\epsilon}^{\sigma}$ with σ=1, 2, ... q. For q=2 these vectors are the usual "up" and "down" states of the Ising model. For general q they are unit vectors which point from the centre to the vertices of a q−1 dimension simplex, e. g. for q=3 an equilateral triangle and for q=4 a regular tetrahedron. For our calculations we need only the following properties of these vectors.

$$q^{-1} \sum_{\sigma} \epsilon^{\sigma}_{\mu} \epsilon^{\sigma}_{\nu} \equiv q^{-1} \operatorname*{Tr}_{v} v_{\mu} v_{\nu} = (q-1)^{-1} \delta_{\mu,\nu} , \qquad (5.33)$$

$$(q-1)\, \underline{v} \cdot \underline{v}' \equiv (q-1) \sum_{\mu} \epsilon^{\sigma}_{\mu} \epsilon^{\sigma'}_{\mu} = (q\, \delta_{\sigma,\sigma'} - 1) , \quad (5.34)$$

when $\underline{v}=\underline{\epsilon}^{\sigma}$ and $\underline{v}'=\underline{\epsilon}^{\sigma'}$ and $\epsilon^{\sigma}{}_{\mu}$ is the μ^{th} (μ=1,...,q−1) component of $\underline{\epsilon}^{\sigma}$ (as in Zia and Wallace 1975). To treat a resistor network one considers the following Potts Hamiltonian,

$$-H = J(q-1) \sum_{i<j} g_{ij}\, \underline{v}(x_i) \cdot \underline{v}(x_j) \qquad (5.35)$$

where g_{ij} is the conductance between sites i and j in the network. In the limit when the number of states q goes to zero one has (Dasgupta *et al* 1978, Harris and Lubensky 1987)

$$\lim_{J\to\infty} \langle \underline{v}(x) \cdot \underline{v}(x') \rangle = \nu(x,x') \left[1 - J^{-1} R(x,x') \right], \qquad (5.36)$$

where $\nu(x,x')$ is unity if the sites x and x' are connected by nonzero conductances and is zero otherwise. Here

$$\langle \underline{v}(x) \cdot \underline{v}(x') \rangle = \frac{\operatorname*{Tr}_{v} e^{-H(v)} \underline{v}(x) \cdot \underline{v}(x')}{\operatorname*{Tr}_{v} e^{-H(v)}} , \qquad (5.37)$$

where $\operatorname*{Tr}_{v}$ indicates a trace over all Potts variables.

It is important to take the limit q→0 before J→∞, in which limit we interpret the quantity qJ to be zero. In what follows it will be convenient to use the representation

$$e^{-H(v)} = \prod_{i<j} e^{-J_{ij}} \left[1 + \frac{e^{qJ_{ij}} - 1}{q} + \frac{(q-1)}{q}(e^{qJ_{ij}}-1)\underline{v}(x_i).\underline{v}(x_j) \right] \tag{5.38}$$

where $J_{ij}=Jg_{ij}$. The equivalence of (5.37) and (5.38) may be shown by comparing them for the two cases $\underline{v}(x_i).\underline{v}(x_j)=1$ and $\underline{v}(x_i).\underline{v}(x_j)=-(q-1)^{-1}$. We take the limit $qJ\to 0$ whence

$$e^{-H(v)} = e^{-E_0} \prod_{i<j} \left[1 + \frac{(q-1)}{1+J_{ij}^{-1}} \underline{v}(x_i).\underline{v}(x_j) \right] \tag{5.39}$$

where E_0 is a constant. To average over the distribution of conductances g_{ij} induced by the distribution of walks we will introduce replicas.

We firstly describe how to treat the resistances of GRWs. As we shall see, the formulation for SAWs is similar. It is necessary to marry the Potts formulation above for the resistance of networks with the ideas in section II for the generation of random walks. The present situation is similar to that of valence walks in that, to generate the necessary quenched average over conformations of GRWs we must use the replica trick. A detailed analysis given in Appendix D shows that the end-to-end resistance of GRWs can be obtained from the following replica Hamiltonian

$$H_{uv} = -\tfrac{1}{2} K \sum_{\alpha=1}^{n} \sum_{x,x'} u_\alpha(x)\gamma_{x,x'}u_\alpha(x') \prod_{\beta=1}^{m} [1+\frac{(q-1)}{(1+t)} \underline{v}_\beta(x).\underline{v}_\beta(x')]. \tag{5.40}$$

Here $u_\alpha(x)$ is an n-replicated Gaussian variable needed to generate GRWs, $\underline{v}_\beta(x)$ is an m-replicated q-state Potts variable, and we have used (5.39) with $t=1/J$. We will need to consider the limit when first m, then q, then n and finally t go to zero. In Appendix D we show that χ_0^{grw} and χ_1^{grw} are given in terms of correlation functions

$$\chi_0^{grw}(x,x';K) \equiv \chi_0^{grw}(x-x';K) = \langle u_1(x)\ u_1(x') \rangle \tag{5.41a}$$

$$\chi_1^{grw}(x,x';K) \equiv \chi_1^{grw}(x-x';K) = -\frac{\partial}{\partial t} \langle u_1(x)\underline{v}_1(x).\underline{v}_1(x')u_1(x') \rangle \tag{5.41b}$$

where χ_1^{grw} was defined in (5.30), $\langle \ldots \rangle$ indicates an average with respect to H_{uv}, $u_1(x)$ denotes the variable $u_\alpha(x)$ for $\alpha=1$, and $\underline{v}_1(x)$ the variable $\underline{v}_\beta(x)$ for $\beta=1$.

Similarly, using the formalism developed in the previous section, we also show in Appendix D that the resistance of SAWs is obtained by considering the following Hamiltonian:

$$H_{sv} = -\sum_{\alpha,<x,x'>} \Big[K\, s_\alpha(x) s_\alpha(x') \exp\Big\{ J(\sigma_0-\sigma_b)(q-1)\sum_\beta \underline{v}_\beta(x).\underline{v}_\beta(x') \Big\} + T(x)T(x')J\sigma_b(q-1)\sum_\beta \underline{v}_\beta(x).\underline{v}_\beta(x') \Big] \qquad (5.42)$$

and the corresponding density matrix $\rho=e^{-H_{sv}}$. As before α and β are replica indices with $\alpha=1,\ldots,n$ and $\beta=1,\ldots,m$; $m,n\to 0$. Also the operators s_α obey the trace rules in (5.12) and commute within the trace. For the crosslinking variables T(x) we define the following trace laws:

$$Tr(T^j s_{\alpha 1} s_{\alpha 2} s_{\alpha 3} \ldots s_{\alpha k}) = \delta_{k,2}\delta_{\alpha 1,\alpha 2}, \qquad (5.43)$$

which applies for all integer j. It is evident that setting $\sigma_b=0$ gives the more familiar SAWs without crosslinks whose resistive properties are of course completely trivial. Also, with the trace rule of (5.43) it is apparent that the term involving $\sigma_b T(x)T(x')$ is only effective when sites x and x' are sites on the SAW generated by the s_α, as discussed in Appendix D.

We also show in Appendix D that analogous expressions to those in (5.41) apply for χ_0^{saw} and χ_1^{saw} with u_α replaced by s_α and averages are taken with respect to H_{sv}. Once again we will consider the limit in which m, n, q and t go to zero in that order. For both models, higher order averages of $R(\gamma)$ can be generated by considering correlation functions which include products of Potts vectors for different replicas.

Finally, we stress that the usefulness of (5.41) is that it indicates that the resistive susceptibility (from which the scaling behaviour of the end-to-end resistance of walks can be obtained) can be calculated as the u_1v_1 (or s_1v_1 for SAWs) correlation function for the Hamiltonian H_{uv} (or H_{sv}). Elsewhere we will give the details of a renormalisation group analysis based on a field-theoretic representation of the above Hamiltonian. The result of such an analysis is a determination of the scaling behaviour of the resistance as characterised by the exponent x in (5.31).

Chapter 6

Field Theoretic Approach to the Resistance of Random Walks.

We address the problem of the asymptotic critical behaviour of the end-to-end resistance $<R_N> \sim N^x$ for Gaussian random walks (GRWs), self-avoiding walks (SAWs) and self-avoiding walks with crosslinks. Using the spin-Potts Hamiltonians developed in the previous chapter we derive the associated field theories, within which the resistive susceptibility is expressed in terms of a crossover anisotropy. In the absence of this crossover anisotropy all the two-point correlation functions for GRWs are Gaussian for all d, but for $d<4$ there is a non-vanishing fixed-point value of a quartic potential (which determines the resistive susceptibility). The solutions to the recursion relations for the various symmetry quartic potentials are shown to be consistent with the Gaussian two-point functions expected for a GRW. Athough the four-point functions connot be calculated exactly for dimensionality less than four, their form can be deduced by heuristic arguments. To second order in $\epsilon \equiv 4-d$, where d is the spatial dimension, the result $x=1-(\epsilon/4)-(\epsilon^2/16)$ is obtained. The logarithmic corrections expected at $d=4$ are evaluated. For SAWs, it is shown that the crosslinks introduce a hierarchy of novel symmetry but irrelevant quartic potentials leaving potentials with precisely the same symmetry as those found for GRW. The difference in the bare values of the potential coefficients is significant however and takes the model to the SAW (without crosslinks) fixed point. We show that the presence of crosslinks only introduces corrections to leading order scaling, which we evaluate. Finally, we analyse the fixed point structure of parameter space in a unifying manner. This work has been submitted to J. Phys. A (Harris and Christou 1987b).

I. Introduction

The resistance of random networks, especially that of percolation cluster networks (Kirkpatrick 1973), is a well established problem in statistical mechanics (see Harris and

Lubensky 1987 and references therein). Indeed much progress has been made in the (field theoretic) study of percolation cluster networks since the development of the renormalisation group (RG) theory (Dasgupta *et al* 1978). Rather less attention however has been focussed on the related and physically significant problem of the resistance of walks (Sen 1981). Indeed substantial controversy has developed over the interpretation of experimental studies of the dynamical properties of such fractal structures (see, for example, chapter four in particular).

In the present work, we will study the problem of the resistance of lattice based random walks using field theoretic RG. The models we propose to treat are: Gaussian random walks (GRWs), self-avoiding walks (SAWs) and self-avoiding walks with nearest-neighbour crosslinks (Fig. 6.1a,b,c).

We refer the reader to the previous chapter and to the work of Harris and Christou (1987) (henceforth referred to as I) for the details concerning backround to the models, the formulation of the resistor network problems and the construction of the appropriate spin Hamiltonians. Here we will only quote the results of that chapter. Namely, one can obtain the resistive properties of GRWs using the following Hamiltonian:

$$H_{uv} = -\tfrac{1}{2} K \sum_{\alpha=1}^{n} \sum_{x,x'} u_\alpha(x)\gamma_{x,x'}u_\alpha(x') \prod_{\beta=1}^{m} \left[1+\frac{(q-1)}{(1+t)}\, \underline{v}_\beta(x).\underline{v}_\beta(x')\right]. \tag{6.1}$$

where $u_\alpha(x)$ is an n-replicated Gaussian variable needed to generate GRWs, $\underline{v}_\beta(x)$ is an m-replicated q-state Potts variable, and t=1/J, the coupling constant in the equivalent Potts Hamiltonian. Averages <X> with respect to this Hamiltonian are defined by

$$\langle X \rangle = \frac{\mathrm{Tr}_u \mathrm{Tr}_{\underline{v}}\, X\, e^{-H_{uv}}}{\mathrm{Tr}_u \mathrm{Tr}_{\underline{v}}\, e^{-H_{uv}}} \tag{6.1a}$$

where Tr_u stands for:

$$\mathrm{Tr}_u \{\ldots\} \equiv \prod_{\alpha,x} \int_{-\infty}^{+\infty} du_\alpha(x)\, e^{-\frac{1}{2}u_\alpha(x)} \{\ldots\} \tag{6.1b}$$

and Tr_v denotes the usual trace over v's at all sites and in all replicas.

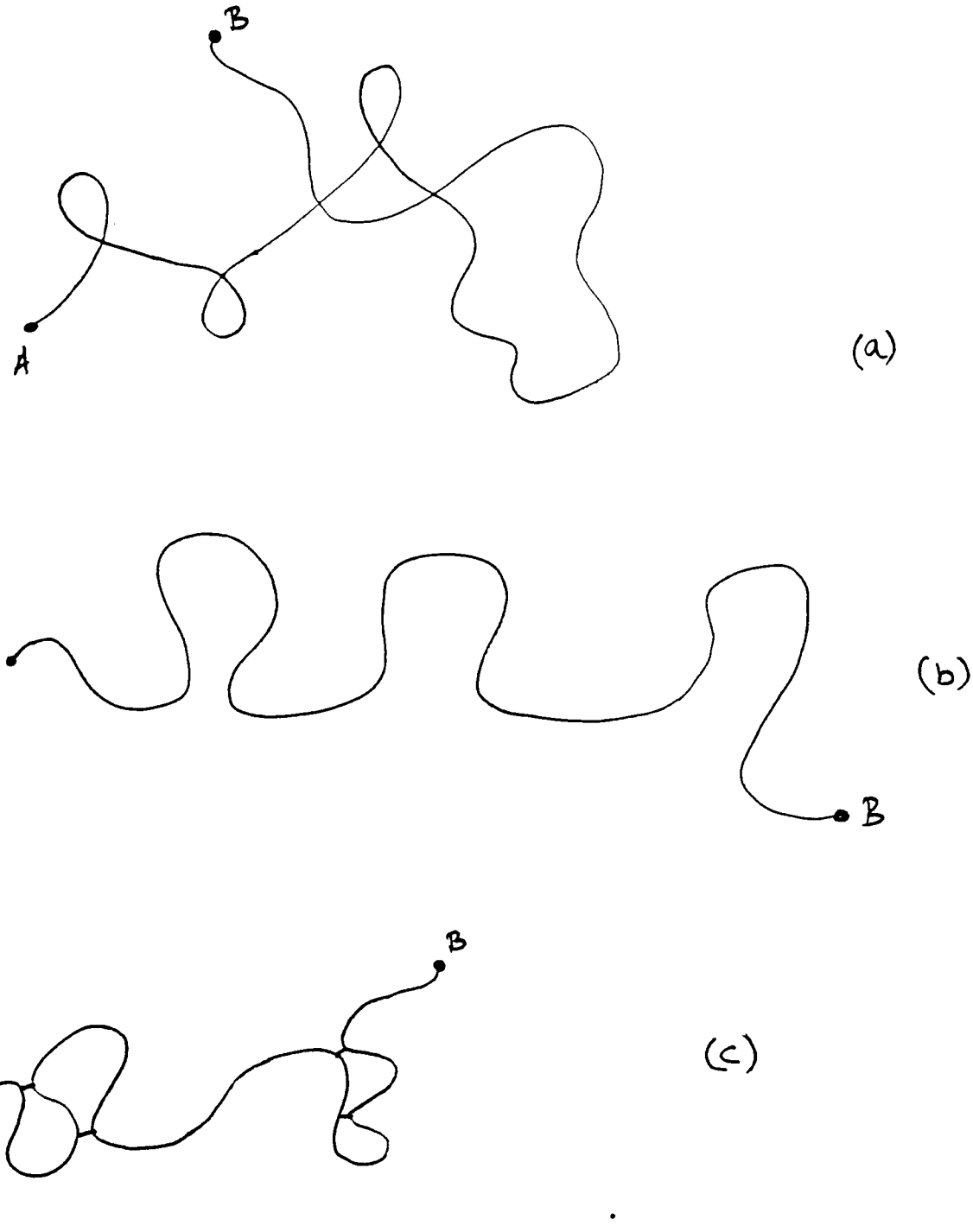

Fig.6.1.:

a) A typical GRW in two dimensions.

b) SAW in two dimesions for which (trivially) x=1.

c) SAW with crosslinks. The crosslinks short circuit the backbone and so we expect

$x<1$.

We will need to consider the limit when first m, then q, then n and finally t go to zero. H_{uv} generates GRWs such that each step has an associated unit conductance; if a bond is traversed ℓ times it has a conductance ℓ.

Similarly, it was shown in chapter five that the resistance of SAWs (with crosslinks) is obtained by considering the following Hamiltonian:

$$H_{sv} = -\sum_{\alpha,<x,x'>} \Big[K\, s_\alpha(x) s_\alpha(x')\, e^{J(\sigma_0-\sigma_b)(q-1)\sum_\beta \underline{v}_\beta(x).\underline{v}_\beta(x')} + T(x)T(x')J\sigma_b(q-1)\sum_\beta \underline{v}_\beta(x).\underline{v}_\beta(x') \Big] \tag{6.2}$$

and the corresponding density matrix $\rho = e^{-H_{sv}}$. Here, as before α and β are replica indices with $\alpha=1,\ldots,n$ and $\beta=1,\ldots,m$; $m,n\to 0$. Also, in order to generate SAWs, the operators s_α are defined to obey the following trace rules,

$$\mathrm{Tr}(1) = 1 \tag{a}$$

$$\mathrm{Tr}(s_\alpha) = 0 \tag{b}$$

$$\mathrm{Tr}(s_\alpha s_\beta) = \delta_{\alpha,\beta} \tag{c}$$

$$\mathrm{Tr}(s_{\alpha_1} s_{\alpha_2} \ldots s_{\alpha_k}) = \delta_{k,2}\delta_{\alpha_1,\alpha_2} \tag{d}$$

$$\mathrm{Tr}(T^j s_{\alpha_1} s_{\alpha_2} \ldots s_{\alpha_k}) = \delta_{k,2}\delta_{\alpha_1,\alpha_2}. \tag{e}$$

(6.3)

where the latter trace applies for all integer j. The operators also commute within the trace. H_{sv} generates SAWs so that each step has an associated conductance σ_0 and lattice nearest-neighbours not connected directly *a priori* are also given a conductance σ_b. Evidently setting $\sigma_b=0$ gives the more familiar SAWs without crosslinks whose resistive properties are of course completely trivial. Also, with the trace rule of (6.3e) it is apparent that the term involving $\sigma_b T(x)T(x')$ is only effective when sites x and x' are sites on the SAW generated by the s_α. Once again we will consider the limit in which m, n, q and t go to zero in that order. For both models, higher order averages of $R(\gamma)$ can be generated by considering correlation functions which include products of

Potts vectors for different replicas.

Specifically, we are interested in the critical behaviour of the susceptibility $\chi_0(x;K)\equiv\sum_{x'}\chi_0(x,x';K)$ and the *resistive* susceptibility $\chi_1(x;K)\equiv\sum_{x'}\chi_1(x,x';K)$ for the walks introduced above. These functions, together with higher order resistive susceptibilities may be defined in terms of the following moment generating function,

$$F(x,x';K,\ell) \equiv \sum_N K^N \sum_{\gamma\subseteq\Gamma_N(x,x')} e^{-\ell R(\gamma)} = F(x-x';K,\ell). \tag{6.4}$$

Here K is a fugacity, γ is a GRW (or SAW) of length N and $\Gamma_N(x,x')$ is the ensemble of GRWs (or SAWs) of length N with end-points at x and x'. Hence we define $\chi_0(x,x';K)=F(x-x';K,\ell=0)$ and $\chi_1(x,x';K) = -(\partial/\partial\ell)F(x-x';K,\ell)|_{\ell=0}$. Higher order resistive generating functions are defined similarly.

The susceptibilities $\chi_{0,1}$ diverge at the same critical value K_c of the fugacity and the leading order singularity is characterised as follows

$$\chi_0(x;K) \sim |K-K_c|^{-\gamma}$$

$$\chi_1(x;K) \sim |K-K_c|^{-(x+\gamma)}. \tag{6.5}$$

where the universal critical exponent γ governs the asymptotic N-dependence of C_N, the number of N-step walks from the origin, as follows (McKenzie 1976, de Gennes 1979):

$$C_N \sim \mu^N N^{\gamma-1} \tag{6.6}$$

where the connectivity μ is $1/K_c$. The critical exponent entering χ_1 is related to the large N dependence of the configurationally averaged end-to-end resistance $\langle R_N\rangle$ of N-step walks,

$$\langle R_N\rangle \equiv \frac{\sum_{x'} \sum_{\gamma\subseteq\Gamma_N(x,x')} R(\gamma)}{C_N} \sim N^x. \tag{6.7}$$

Clearly, x=1 for SAWs (without crosslinks).

We have shown already shown that the susceptibilities χ_0^{grw} and χ_1^{grw} are given in terms of correlation functions

$$\chi_0^{grw}(x,x';K) \equiv \chi_0^{grw}(x-x';K) = \langle u_1(x)u_1(x')\rangle$$

$$\chi_1^{grw}(x,x';K) \equiv \chi_1^{grw}(x-x';K) = -\frac{\partial}{\partial t}\langle u_1(x)\underline{v}_1(x).\underline{v}_1(x')u_1(x')\rangle. \tag{6.8}$$

$\langle\ldots\rangle$ indicates an average with respect to H_{uv}, $u_1(x)$ denotes the variable $u_\alpha(x)$ for $\alpha=1$, and $\underline{v}_1(x)$ the variable $\underline{v}_\beta(x)$ for $\beta=1$. The analogous results were shown to apply (I)for $\chi_0^{saw}(x,x';K)$ and $\chi_1^{saw}(x,x';K)$ with u_1 replaced by s_1 and the averages taken with respect to the density matrix defined by H_{sv}.

We will develop field theories from the above Hamiltonians and obtain ϵ-expansions for the exponent x for GRWs and SAWs with crosslinks.

A plan of this chapter is as follows: In section II we construct field theoretic Hamiltonians using the usual Hubbard-Stratanovich transformation. In section III we develop a unified perturbation treatment of GRWs and SAWs using renormalisation group techniques. The resistive properties of the walks are generated by application of an anisotropy field which leads to a description of the resistive susceptibility as a crossover phenomenon. The logarithmic corrections present at the upper critical dimension, d=4 are also given. In section IV the effect of crosslinks on the resistance of SAWs is treated. Finally, in section V we give some heuristic estimates for the exponent x for GRWs and discuss the significance of our results to related processes, eg diffusion.

II. Field Theoretic Formulation

In this section we develop field theoretic Hamiltonians from which the various correlation functions we seek can be obtained. To this end we first perform a Hubbard-Stratanovich transformation. We consider first the (simpler) case of GRWs. For the purpose of the Stratanovich transformation we write the Hamiltonian H_{uv} in the following bilinear form in single site operators

$$H_{uv} = -\tfrac{1}{2} K \sum_{\alpha,x,x'} \gamma_{x,x'} u_\alpha(x) u_\alpha(x')$$

$$-\tfrac{1}{2} K\left[\frac{(q-1)}{(1+t)}\right] \sum_{\substack{\alpha,x,x' \\ \beta_1,\mu_1}} \gamma_{x,x'} u_\alpha(x) v_{\beta_1}^{\mu_1}(x) u_\alpha(x') v_{\beta_1}^{\mu_1}(x')$$

$$-\tfrac{1}{2}K\left[\frac{(q-1)}{(1+t)}\right]^2 \sum_{\substack{\alpha,x,x' \\ 1\leqslant\beta_1<\beta_2\leqslant m \\ \mu_1,\mu_2}} \gamma_{x,x'} u_\alpha(x) v^{\mu_1}_{\beta_1}(x) v^{\mu_2}_{\beta_2}(x) u_\alpha(x') v^{\mu_1}_{\beta_1}(x') v^{\mu_2}_{\beta_2}(x')$$

$$+ \ldots \qquad (6.9)$$

The general term in H_{uv} of order $(q-1)^p$ is

$$-\tfrac{1}{2}K\left[\frac{(q-1)}{(1+t)}\right]^p \sum_{\substack{\alpha,x,x' \\ 1\leqslant\beta_1<\beta_2\ldots<\beta_p\leqslant m \\ \mu_1,\mu_2,\ldots,\mu_p}} \gamma_{x,x'} u_\alpha(x) u_\alpha(x') \prod_{k=1}^{p} v^{\mu_k}_{\beta_k}(x) v^{\mu_k}_{\beta_k}(x') \qquad (6.10)$$

Here the μ label the components and range over the values 1,2,...,q-1 and α is the replica variable for the Gaussian variables which we will refer to as scalar indices, and the β are the Potts replica indices, which we will refer to as tensor indices, α and β range over the values 1,2,..,n and 1,2,...,m respectively. We now introduce the full set of fields $\{\psi\}$ conjugate to these operators, such that

$$e^{-H_{uv}} = \int D\Psi \; e^{-L^{grw}(\psi,u,v)}, \qquad (6.11)$$

where $D\Psi$ indicates an integration over all the ψ. For this purpose we use the relation

$$\exp\left(\tfrac{1}{2}\sum_{i,j} y_i V^{-1}_{ij} y_j\right) = C\int \prod_k dx_k \exp\left(-\tfrac{1}{2}\sum_{i,j} x_i V_{ij} x_j + \sum_\ell y_\ell x_\ell\right) \qquad (6.12)$$

to construct L^{grw}, where V^{-1} is the matrix inverse of V and C is a constant which becomes unity in the limit of zero replicas and which we ignore.

The field $\psi^{\mu_1,\mu_2,\ldots,\mu_p}_{\alpha,\beta_1,\beta_2,\ldots,\beta_p}$ is conjugate to the variable

$u_\alpha v^{\mu_1}_{\beta_1} v^{\mu_2}_{\beta_2} \ldots v^{\mu_p}_{\beta_p}$ as in Stephen and Grest (1977) or Dasgupta *et al* (1978).

The Hamiltonian $L^{grw}(\psi,u,v)$ is:

$$L^{grw}(\psi,u,v) = \frac{1}{2K}\sum \psi_\alpha(x)\gamma^{-1}_{x,x'}\psi_\alpha(x')$$

$$+ \frac{1+t}{2K}\sum \psi_{\alpha,\beta_1}^{\mu_1}(x)\gamma^{-1}_{x,x'}\psi_{\alpha,\beta_1}^{\mu_1}(x') \quad +\ldots$$

$$+ \frac{(1+t)^p}{2K}\sum \psi_{\alpha,\beta_1,\beta_2,\ldots,\beta_p}^{\mu_1,\mu_2,\ldots,\mu_p}(x)\gamma^{-1}_{x,x'}\psi_{\alpha,\beta_1,\beta_2,\ldots,\beta_p}^{\mu_1,\mu_2,\ldots,\mu_p}(x') +\ldots$$

$$+ \sum \psi_\alpha(x)u_\alpha(x) + \sum \sqrt{(q-1)}\psi_{\alpha,\beta_1}^{\mu_1}(x)u_\alpha v_{\beta_1}^{\mu_1}(x) + \ldots$$

$$+ (q-1)^{p/2}\psi_{\alpha,\beta_1,\ldots,\beta_p}^{\mu_1,\ldots,\mu_p}(x)u_\alpha(x)\prod_{k=1}^{p} v_{\beta_1}^{\mu_1}(x) + \ldots, \qquad (6.13)$$

We can write this in the form,

$$L^{grw}(\psi,u,v) = L_0{}^{grw}(\psi)+V^{grw}(\psi,u,v) \qquad (6.14)$$

where

$$L_0{}^{grw}(\psi) = \frac{1}{2K}\sum \psi_\alpha(x)\gamma^{-1}_{x,x'}\psi_\alpha(x')$$

$$+ \frac{1+t}{2K}\sum \psi_{\alpha,\beta_1}^{\mu_1}(x)\gamma^{-1}_{x,x'}\psi_{\alpha,\beta_1}^{\mu_1}(x') \quad +\ldots$$

$$\ldots - \tfrac{1}{2}\sum\psi_\alpha(x)^2 - \tfrac{1}{2}\sum\psi_{\alpha,\beta_1}^{\mu_1}(x)^2 - \tfrac{1}{2}\sum \psi_{\alpha,\beta_1,\beta_2}^{\mu_1,\mu_2}(x)^2 - \ldots$$

(6.15)

Here and below, in expressions for the Hamiltonian all replica indices and component labels are summed over with the condition that $\beta_1<\beta_2<\ldots<\beta_p$ in order to reproduce correctly the product over β in (6.1). The terms involving $\gamma_{x,x'}{}^{-1}$ are summed over x and x' and the others over x. The general term of the type in line two of (6.15) is

$$\frac{(1+t)^p}{2K} \sum \psi_{\alpha,\beta_1,\beta_2,\ldots,\beta_p}^{\mu_1,\mu_2,\ldots,\mu_p}(x)\gamma^{-1}_{x,x'}\psi_{\alpha,\beta_1,\beta_2,\ldots,\beta_p}^{\mu_1,\mu_2,\ldots,\mu_p}(x') \tag{6.16}$$

and the general term of the type of the last line of (6.15) is

$$-\tfrac{1}{2}\sum \psi_{\alpha,\beta_1,\beta_2,\ldots,\beta_p}^{\mu_1,\mu_2,\ldots,\mu_p}(x)^2 \ . \tag{6.17}$$

In $V^{grw}(\psi,u,v)$ we include the terms

$$V^{grw}(\psi,u,v) = \tfrac{1}{2}\sum \psi_{\alpha,\beta_1,\beta_2,\ldots,\beta_p}^{\mu_1,\mu_2,\ldots,\mu_p}(x)^2$$

$$+ \sum \psi_\alpha(x)u_\alpha(x) + \sum \sqrt{(q-1)}\psi_{\alpha,\beta_1}^{\mu_1}(x)u_\alpha(x)v_{\beta_1}^{\mu_1}(x) + \ldots \tag{6.18}$$

where the general term with a ψ with p tensor indices is

$$(q-1)^{p/2}\psi_{\alpha,\beta_1,\ldots,\beta_p}^{\mu_1,\ldots,\mu_p}(x)u_\alpha(x)\prod_{k=1}^{p} v_{\beta_1}^{\mu_1}(x), \tag{6.19}$$

In writing L_0^{grw} and V^{grw} we have added and subtracted quadratic terms so that when the traces over the Gaussian variables are performed, V^{grw} will only contain higher-than-quadratic order terms in the ψ.

We now perform the traces over the original 'spin' variables u and v. We define

$$e^{-L^{grw}(\psi)} = \underset{u}{\mathrm{Tr}}\ \underset{v}{\mathrm{Tr}}\ e^{-L^{grw}(\psi,u,v)} = e^{-[L_0^{grw}(\psi)+V^{grw}(\psi)]} \tag{6.20}$$

where Tr_u is as in (6.1b) and Tr_v is the usual trace over Potts states (see I), so that

$$V^{grw}(\psi) = -\log\Big[\underset{u}{\mathrm{Tr}}\,\underset{v}{\mathrm{Tr}}\ e^{-V^{grw}(\psi,u,v)}\Big] \tag{6.21}$$

In order to perform the trace over u we note that V^{grw} is a linear function of the $u_\alpha(x)$ which we may write as follows

$$V^{grw}(\psi,u,v) = X + \textstyle\sum_\alpha u_\alpha(x)Y_\alpha \tag{6.22}$$

Thus

$$V^{grw}(\psi) = -\log \underset{u}{\mathrm{Tr}}\,\underset{v}{\mathrm{Tr}}\ e^{-X}\, e^{-\sum_\alpha Y_\alpha u_\alpha}$$

$$= -\log \operatorname{Tr}_{v} e^{\left[\frac{1}{2}\sum_{\alpha} Y_{\alpha}^{2} - X\right]}$$

$$= -\log \operatorname{Tr}_{v} \left[1 + \left\{\tfrac{1}{2}\sum_{\alpha} Y_{\alpha}^{2} - X\right\} + \tfrac{1}{2}\left\{\tfrac{1}{2}\sum_{\alpha} Y_{\alpha}^{2} - X\right\}^{2} + \ldots \right] \tag{6.23}$$

Using the Potts trace rules one can show that

$$X = \operatorname{Tr}_{v} \left[\tfrac{1}{2}\sum_{\alpha} Y_{\alpha}^{2} \right] \tag{6.24}$$

then v^{grw}, correct to fourth order in the $\{\psi\}$ becomes:

$$v^{grw} = -\tfrac{1}{8} \operatorname{Tr}_{v} \left[(\textstyle\sum_{\alpha} Y_{\alpha}^{2})^{2} \right] + \tfrac{1}{8} \left[\operatorname{Tr}_{v} \textstyle\sum_{\alpha} Y_{\alpha}^{2} \right]^{2} \tag{6.25}$$

We have omitted additive constant terms as they are of no importance. However, more significantly, we have also neglected higher order terms than the quartic in the ψ. In a renormalisation group calculation these higher order terms are irrelevant (Bruce *et al* 1974, Wilson and Kogut 1974)), and only provide less singular corrections to the leading order scaling of critical properties.

We therefore find $v^{grw}(\psi)$ to be given by

$$v^{grw}(\psi) = \sum_{x} v^{grw}(\psi(x)) \ , \tag{6.26}$$

where to order ψ^4 the local potential $v^{grw}(\psi)$ is given by

$$v^{grw}(\psi) = -\tfrac{1}{8} \sum \psi_{\alpha, \begin{Bmatrix}\mu_1\\ \beta_1\end{Bmatrix}} \psi_{\alpha, \begin{Bmatrix}\mu_2\\ \beta_2\end{Bmatrix}} \psi_{\alpha', \begin{Bmatrix}\mu_3\\ \beta_3\end{Bmatrix}} \psi_{\alpha', \begin{Bmatrix}\mu_4\\ \beta_4\end{Bmatrix}} .$$

$$\Bigg\{ q^{-m} \operatorname{Tr}_{v} \prod_{i} \sqrt{(q-1)}\, v^{\mu_1 i}_{\beta_1 i} \prod_{j} \sqrt{(q-1)}\, v^{\mu_2 j}_{\beta_2 j} \prod_{k} \sqrt{(q-1)}\, v^{\mu_3 k}_{\beta_3 k} \prod_{\ell} \sqrt{(q-1)}\, v^{\mu_4 \ell}_{\beta_4 \ell}$$

$$+ q^{-2m} \cdot \left[\operatorname{Tr}_{v} \prod_{i} \sqrt{(q-1)}\, v^{\mu_1 i}_{\beta_1 i} \prod_{j} \sqrt{(q-1)}\, v^{\mu_2 j}_{\beta_2 j} \right] \left[\operatorname{Tr}_{v} \prod_{k} \sqrt{(q-1)}\, v^{\mu_3 k}_{\beta_3 k} \prod_{\ell} \sqrt{(q-1)}\, v^{\mu_4 \ell}_{\beta_4 \ell} \right] \Bigg\}$$

(6.27)

Here and above, $\{\beta_1\}$ denotes the set of indices $\beta_{11},\beta_{12},\beta_{13},\ldots$ and similarly with the component indices $\{\mu_i\}$. At any site x the Potts variable v^{μ}_{β} may assume any one of (q−1) values. All the fields act at site x which is then summed over. In (6.27) the sum is also carried over all sets $\{\beta_1\},\{\beta_2\}$, etc. In each sum over $\{\beta\}$ there are 2^m terms corresponding to independently choosing each replica to either belong or not belong to the set.

The null set φ is an allowable term, since $\psi_{\alpha,\{\varphi\}}^{\{\varphi\}}$ is ψ_{α}.

For each β there is always a corresponding μ which ranges over q−1 possible values.

The interaction $v^{grw}(\psi)$ is therefore a sum of two sets of quartic potentials, each having its own symmetry type. We write $v^{grw}(\psi)=v_{2,2}(\psi)-v_4(\psi)$, where v_4 represents the single trace term in (6.27) and $v_{2,2}$ the two trace term. It may be useful to think of these terms as generalisations of the TrQ^4 and $(TrQ^2)^2$ terms in the formulation of Priest and Lubensky or alternatively as $(\sum u^2)^2$ and $(\sum u^4)$ terms in a Heisenberg Hamiltonian with cubic anisotropy (see Aharony 1976).

A few terms involving a small number of tensor indices in $v_4(\psi)$ are

$$
\begin{aligned}
v_4(\psi) = {} & \tfrac{1}{8}\,\psi_{\alpha}^{2}\,\psi_{\alpha'}^{2} \\
& + \tfrac{1}{2}\,\psi_{\alpha}\,\psi_{\alpha'}\,\psi_{\alpha,\beta}^{\mu}\,\psi_{\alpha',\beta}^{\mu} \\
& + \tfrac{1}{2}\,\psi_{\alpha,\beta_1}^{\mu_1}\,\psi_{\alpha',\beta_1}^{\mu_1}\,\psi_{\alpha,\beta_2}^{\mu_2}\,\psi_{\alpha',\beta_2}^{\mu_2} \\
& + \tfrac{1}{2}\,\psi_{\alpha}\,\psi_{\alpha,\beta}^{\mu_1}\,\psi_{\alpha',\beta}^{\mu_2}\,\psi_{\alpha',\beta}^{\mu_3}\,\lambda_{\mu_1,\mu_2,\mu_3} \\
& + \tfrac{1}{2}\,\psi_{\alpha,\beta}^{\mu_1}\,\psi_{\alpha,\beta}^{\mu_2}\,\psi_{\alpha',\beta}^{\mu_3}\,\psi_{\alpha',\beta}^{\mu_4}\,\lambda_{\mu_1,\mu_2,\mu_3,\mu_4}
\end{aligned}
\qquad (6.28)
$$

Here we introduced the form factors λ for the potentials defined by

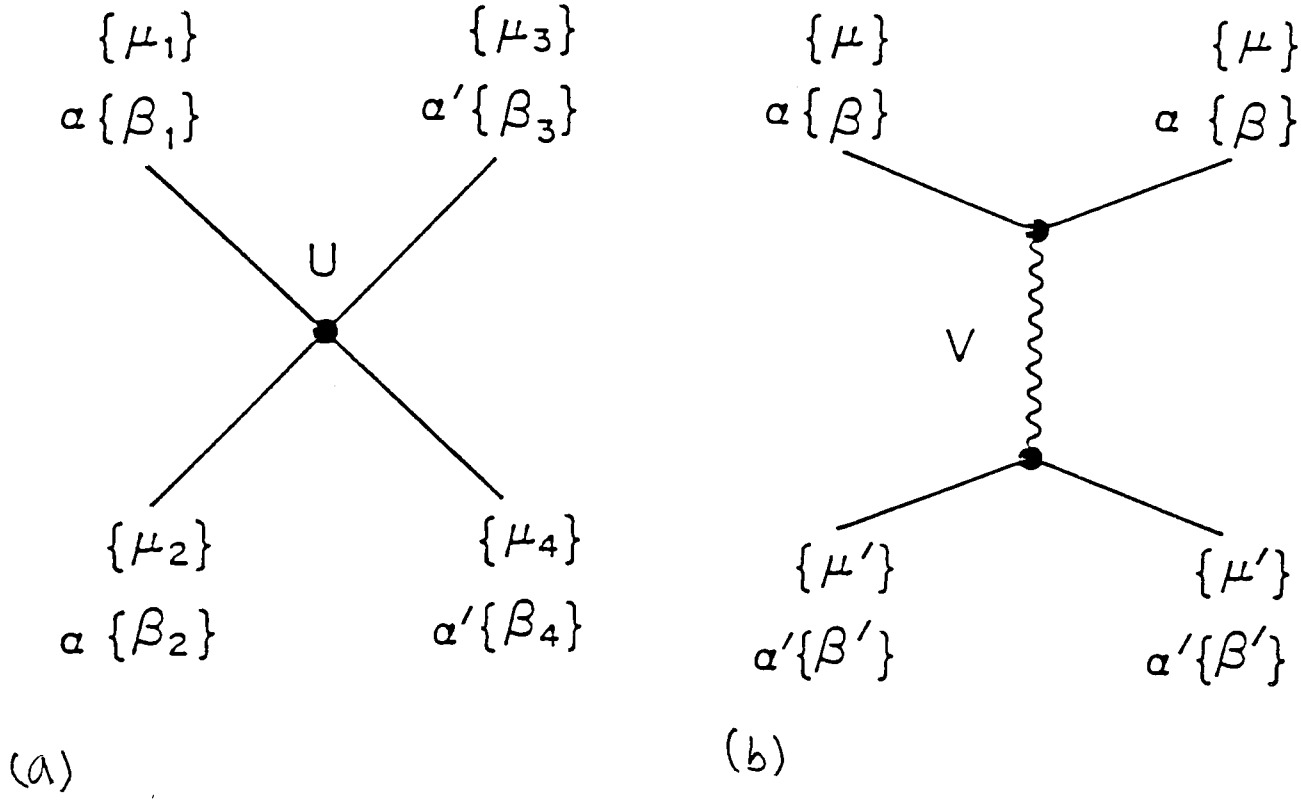

Fig.6.2.: Diagrammatic representation of a) uv_4 and b) $vv_{2,2}$. Here α and α' are scalar indices and $\{\beta\}$ denotes a set of replica indices with $1 \leq \beta_1 < \beta_2 \ldots < \beta_k \leq m$ and $\{\mu\}$ the corresponding set of component labels $\mu_1, \mu_2, \ldots, \mu_k$, where $1 \leq \mu_i \leq (q-1)$ and k can be 0,1, ... ,m.

$$\frac{1}{q}\,\mathrm{Tr}\;1 = 1$$

$$\lambda_{\mu} = \frac{1}{q}\sum_{\sigma}(q-1)^{\frac{1}{2}}\,\epsilon_{\sigma}^{\mu} = \frac{1}{q}(q-1)^{\frac{1}{2}}\,\mathrm{Tr}_{v}\,v^{\mu} = 0$$

$$\lambda_{\mu,\nu} = \frac{1}{q}\sum_{\sigma}(q-1)\,\epsilon_{\sigma}^{\mu}\epsilon_{\sigma}^{\nu} = \frac{1}{q}(q-1)\,\mathrm{Tr}_{v}\,v^{\mu}v^{\nu} = \delta_{\mu,\nu}$$

$$\lambda_{\mu,\nu,\rho} = \frac{1}{q}\sum_{\sigma}(q-1)^{3/2}\,\epsilon_{\sigma}^{\mu}\epsilon_{\sigma}^{\nu}\epsilon_{\sigma}^{\rho} = \frac{1}{q}(q-1)^{3/2}\mathrm{Tr}_{v}\,v^{\mu}v^{\nu}v^{\rho}$$

$$\lambda_{\mu,\nu,\rho,\tau} = \frac{1}{q}\sum_{\sigma}(q-1)^{2}\,\epsilon_{\sigma}^{\mu}\epsilon_{\sigma}^{\nu}\epsilon_{\sigma}^{\rho}\epsilon_{\sigma}^{\tau} = \frac{1}{q}(q-1)^{2}\mathrm{Tr}_{v}\,v^{\mu}v^{\nu}v^{\rho}v^{\tau}$$

$$\text{etc.} \qquad (6.29)$$

While some example terms from $v_{2,2}(\psi)$ are

$$v_{2,2}(\psi) = 1/8\;\psi_{\alpha}{}^{2}\psi_{\alpha'}{}^{2}$$

$$+\;1/8\;(\psi_{\alpha})^{2}(\psi_{\alpha',\beta}^{\mu})^{2}$$

$$+\;1/8\;(\psi_{\alpha,\beta}^{\mu})^{2}(\psi_{\alpha',\gamma}^{\nu})^{2}$$

$$+\;1/8\;(\psi_{\alpha,\beta_1,\beta_2}^{\mu_1,\mu_2})^{2}(\psi_{\alpha',\beta_3,\beta_4}^{\mu_3,\mu_4})^{2} \qquad (6.30)$$

It is clear that the potential comprising $v_{2,2}(\psi)$ form a subset of those in $v_4(\psi)$.

We recall that the $v_{2,2}(\psi)$ term has the same symmetry as the Heisenberg model for $n\to 0$ with nq^m components. Finally, we remark that there are no third order terms in the field theory because (as can be seen in (6.27)) the Gaussian variable u cannot occur an odd number of times

A similar analysis, given in detail in Appendix F, can be applied to the SAW Hamiltonian, (6.2). We have made the substitutions $\sigma_0\to(1+\lambda)$, $\sigma_b\to\lambda$. Once again, the

Hamiltonian may be expressed as a product of bilinear terms for which one may define appropriate conjugate fields and perform a Stratanovich transformation to derive a field theory. We denote the resulting classical, real fields by

$$\{ \varphi_{(\alpha,p),\beta_1,\beta_2,\ldots,\beta_p}^{\mu_1,\mu_2,\ldots,\mu_p} \} \quad \text{or symbolically} \quad \{ \varphi_{(\alpha,p),\{\beta\}}^{\{\mu\}} \},$$

and obtain the following Hamiltonian:

$$L^{saw}(\Phi) = L_0{}^{saw}(\Phi) + V^{saw}(\Phi) \tag{6.31}$$

where the quadratic part of the Hamiltonian $L_0(\Phi)$ is given by

$$L_0(\Phi)=\tfrac{1}{2} \sum_{\substack{x,x' \\ \ell}} \frac{(1+J^{-1})^{\ell}}{K} \sum_{\{\beta\},\{\mu\}} \varphi_{(\alpha,\ell),\{\beta\}}^{\{\mu\}}(x)\gamma^{-1}_{x,x'}\varphi_{(\alpha,\ell),\{\beta\}}^{\{\mu\}}(x')$$

$$- \tfrac{1}{2} \sum_{\substack{x,\alpha,\ell \\ \{\beta\},\{\mu\}}} \left[\varphi_{(\alpha,\ell),\{\beta\}}^{\{\mu\}}(x) \right]^2 \tag{6.32}$$

and

$$V^{saw}(\Phi) = \tfrac{1}{8} \sum_{S_1} \varphi_{(\alpha,\ell),\{\beta\}}^{\{\mu\}}(x)^2 \varphi_{(\alpha',\ell'),\{\beta'\}}^{\{\mu'\}}(x')^2$$

$$-\tfrac{1}{8} \sum_{S_2} \left[\varphi_{(\alpha,\ell),\{\beta_1\}}^{\{\mu_1\}} \varphi_{(\alpha,\ell),\{\beta_2\}}^{\{\mu_2\}} \varphi'^{\{\mu_3\}}_{(\alpha',\ell'),\{\beta_3\}} \varphi'^{\{\mu_4\}}_{(\alpha',\ell'),\{\beta_4\}} \right]$$

$$\cdot \operatorname{Tr}_{v,v'} \left\{ q^{-2m} \left\{ \prod_i \sqrt{(q-1)} v_{\beta_{1i}}^{\mu_{1i}} \prod_j \sqrt{(q-1)} v_{\beta_{2j}}^{\mu_{2j}} \prod_k \sqrt{(q-1)} v'_{\beta_{3k}}^{\mu_{3k}} \prod_\ell \sqrt{(q-1)} v'_{\beta_{4\ell}}^{\mu_{4\ell}} \right\} \right.$$

$$\left. \cdot \prod_{\tilde{\beta}=1}^{m} \left[1 + J\lambda q \cdot \delta_{\sigma_{\tilde{\beta}}(x),\sigma_{\tilde{\beta}}(x')} \right] \right\}. \tag{6.33}$$

With the notation as follows: S_1 is the set of suffices $\{<x,x'>,x=x',\alpha,\alpha',\ell,\ell',\{\beta\},\{\beta'\},\{\mu\},\{\mu'\}\}$ and similarly, $S_2=\{<x,x'>,x=x',\alpha,\alpha',\ell,\ell'\{\beta\},\{\beta'\},\{\mu\},\{\mu'\}\}$. φ denotes the field $\varphi(x)$, while φ' denotes $\varphi(x')$. $\delta_{\sigma,\sigma'}$ is unity if σ and σ' represent the same Potts state and vanishes otherwise.

As in the random walk case we have neglected additive constant terms and have also discarded terms of higher order than quartic as we anticipate that they will be irrelevant with regard to the asymptotic behaviour of the resistive susceptibilities in the limit of long walks. Bearing in mind that the anomalous term becomes unity for $\lambda\to 0$ we see from (6.33) that $V^{saw}(\Phi)$ becomes a *local* two-trace potential analogous to $v_{2,2}(\Psi)$ found for GRWs. This is as required for the $n\to 0$ n-component Heisenberg model.

We provide a brief discription of the symmetry potential types that are present in $V^{saw}(\Phi)$. Firstly consider the special case $\lambda=0$. This problem is of course the self-avoiding walk model without bridges whose resistive properties are completely trivial, but as we shall see this will provide a strong check on the calculations. For the general case, $\lambda\neq 0$ we expand $V^{saw}(\Phi)$ as follows:

$$V^{saw}(\Phi) = \tfrac{1}{8}\sum_{S_1} \varphi^{\{\mu\}}_{(\alpha,\ell),\{\beta\}}(x)^2 \varphi^{\{\mu'\}}_{(\alpha',\ell'),\{\beta'\}}(x')^2$$

$$-\tfrac{1}{8}\sum_{S_2}\left[\varphi^{\{\mu_1\}}_{(\alpha,\ell),\{\beta_1\}}\varphi^{\{\mu_2\}}_{(\alpha,\ell),\{\beta_2\}}\varphi'^{\{\mu_3\}}_{(\alpha',\ell'),\{\beta_3\}}\varphi'^{\{\mu_4\}}_{(\alpha',\ell'),\{\beta_4\}}\right]\sum_{i=0}^{m} w_i \qquad (6.34)$$

The notation is as in (6.33). The w_i are given by the following expression

$$w_i = \left[\frac{1}{J\lambda}\right]^i \operatorname*{Tr}_{\underline{v}(x),\underline{v}(x')} q^{-2m}\left[q^{m-i}\left(\prod v \ldots \prod v\right)\sum_{\substack{\{\tilde{\beta}\}\\ i}}\ \sum_{\subseteq\{\beta\}} \Delta(\{\tilde{\beta}\}_i,x,x')\right] \qquad (6.35)$$

where $\{\tilde{\beta}\}_i$ is a subset of the m Potts replicas and comprises i distinct replicas and the

summation is taken over all such partitions. For $\{\tilde{\beta}\} \equiv \{\beta_{1,i},\beta_{2,i},\ldots,\beta_{i,i}\}$, the function $\Delta(\{\tilde{\beta}\}_i,x,x')$ is given by the following product of Kronecker deltas,

$$\Delta(\{\tilde{\beta}\}_i,x,x') = \prod_{j=1}^{i} \left\{ \delta_{\sigma_{\beta_{j,i}}(x),\sigma_{\beta_{j,i}}(x')} \right\} \qquad (6.36)$$

Hence we see that the w_i represent a hierarchy of 'direct product' terms which *interpolate* from $v_{2,2}$ symmetry (i=0) to v_4 symmetry (i=m). For general i, the Potts replicas within a typical w_i term will partition themselves such that the i replicas in $\{\tilde{\beta}\}_i$ have v_4 symmetry and the others have $v_{2,2}$ symmetry. We may therefore represent this potential in the following symbolic manner,

$$w_i = v_4(1) \otimes v_4(2) \otimes \ldots \otimes v_4(i) \otimes v_{2,2}(i+1) \otimes v_{2,2}(i+2) \otimes \ldots \otimes v_{2,2}(m). \quad (6.37)$$

Replica symmetry is not broken as all possible partitions are summed over.

The advantage of using field theoretic expressions for these problems is that we are now in a position to use the existing powerful techniques of the Hamiltonian Renormalisation Group theory to calculate, in principle, arbitrary powers of the end-to-end resistance. However using RG one calculates averages of the $\psi-\psi$ correlation functions with respect to the field theoretic Hamiltonian and it is not clear *a priori* what their relation to the spin-Potts correlation functions actually is. So, although the resistive susceptibilities are given in terms of uu,uuvv,... etc. correlation functions, as given in the introduction, these may in fact be straightforwardly related to their field theoretic counterparts by partial integration (see Wilson and Kogut 1974) in the usual way. Thus for random walks,

$$<u_\alpha(x)u_\alpha(x')> = K^{-1}[\gamma^{-1}]_{xx'} + K^{-2}\sum_{yy'}[\gamma^{-1}]_{xy}[\gamma^{-1}]_{x'y'}<\psi_\alpha(y)\psi_\alpha(y')>_\psi \qquad (6.38)$$

where $<\ldots>_\psi$ denotes an average with respect to $e^{-L^{grw}(\psi)}$. Likewise

$$\langle u_\alpha(x) v_{\mu_1}^{\sigma_1}(x) v_{\mu_1}^{\sigma_1}(x') u_\alpha(x') \rangle = -\left[\frac{1+t}{K}\right][\gamma^{-1}]_{xx'}$$

$$+ \left[\frac{1+t}{K}\right]^2 \sum_{yy'} [\gamma^{-1}]_{xy}[\gamma^{-1}]_{x'y'} \langle \psi_{\alpha,\beta_1}^{\mu_1}(y) \psi_{\alpha,\beta_1}^{\mu_1}(y') \rangle_\psi \tag{6.39}$$

and so forth. The analogous results follow for SAWs, with u_α replaced by s_α. Since the critical properties only depend on the correlation function at large separation and since, near the critical point $K\gamma$ is of the order unity, we have

$$\langle u_\alpha(x) u_\alpha(x') \rangle \sim \langle \psi_\alpha(x) \psi_\alpha(x') \rangle_\psi \tag{6.40}$$

and similarly for higher order correlation functions and for SAWs.

Before proceeding with a renormalisation group analysis of L^{grw} and L^{saw} we study the effects of V^{grw} within perturbation theory. First of all, for t=1/J=0 the situation must be as follows. All correlation functions of the form $\langle \psi(x)\psi(x') \rangle_\psi$, where ψ is a single site operator with some array of tensor indices, must be Gaussian, ie given by the non-interacting random walk result. Thus if we write schematically,

$$L = \tfrac{1}{2} \sum_q (r+q^2)\ \psi(q)\psi(-q) + V(\psi(q)), \tag{6.41}$$

in terms of Fourier transformed variables, then we should find that V introduces no corrections to r and that the r for the various ψ with different tensor indices should remain exactly equal to their bare value, $(zK)^{-1}-1$. In fact, the q-dependent self energy for the two-point functions should vanish identically to all orders in V for all sets of tensor indices.

One can actually go further to make general arguments about some of the four-point irreducible interactions. For instance, consider

$$\langle u_\alpha(x_1) \underline{v}(x_1) . \underline{v}(x_2) u_\alpha(x_2) u_{\alpha'}(x_3) \underline{v}(x_3) . \underline{v}(x_4) u_{\alpha'}(x_4) \rangle \tag{6.42}$$

for $\alpha \neq \alpha'$. We will call this an unlinked term because the Potts variables do not link Gaussian variables of different scalar indices (α). Imagine evaluating (6.42) by first integrating over the u. Since $\alpha \neq \alpha'$, contributions only come from configurations representing two random walks, one from x_1 to x_2 and the other from x_3 to x_4. For such configurations, the Potts variables are redundant, in that they give unity at all times. Thus the correlation function obeys Wick's theorem in that it is given by the product of seperate correlation functions,

$$<u_\alpha(x_1)\underline{v}(x_1).\underline{v}(x_2)u_\alpha(x_2)>.<u_{\alpha'}(x_3)\underline{v}(x_3).\underline{v}(x_4)u_{\alpha'}(x_4)> \tag{6.43}$$

This argument indicates that for t=0 the corresponding four point vertex is identically zero (for $\alpha \neq \alpha'$). These arguments produce powerful checks on the proposed treatment of $L^{grw}(\psi)$. As will become clear, we only need to understand on detail the situation for t=0, because for small t the treatment of the crossover is trivial.

Indeed, for the case of Gaussian random walks, one may wonder how the four-point vertices can be non-zero at all, since in the pure random walk problem with no Potts variables all the n-point correlations are Gaussian in all dimensions. the point is that these higher correlation functions are not the usual n-point random walk correlation functions. Consider, for instance, for $\alpha \neq \alpha'$,

$$<u_\alpha(x_1)\underline{v}_\beta(x_1).\underline{v}_\beta(x_3)u_\alpha(x_2)u_{\alpha'}(x_3)\underline{v}_{\beta'}(x_1).\underline{v}_{b'}(x_4)u_{\alpha'}(\dot{x}_4)> \tag{6.44}$$

which we denote by φ. Basically φ measures the occurrence of two random walks connecting x_1 with x_2 and x_3 with x_4, but also, due to the Potts variables, depends on whether sites x_1 and x_3 are connected. Thus φ is no longer simply a product of correlations for two independent random walks. Since φ no longer obeys Wick's theorem, there must exist a corresponding non-zero four point interaction. This

interaction is expected to become relevant for spatial dimensionality, d, less than four, due to the presence of fourth order terms in $V^{grw}(\psi)$. Alternatively, one can argue that two random walks each of fractal dimension 2 will begin to interact when d becomes less than 4 (see Aizenmann 1982 for further discussion of related points). The interaction will not , of course, occur for

$$<u_\alpha(x_1)u_\alpha(x_2)u_{\alpha'}(x_3)u_{\alpha'}(x_4)> \qquad (6.45)$$

and the four-point interaction of this symmetry must vanish.

III. Renormalization Group Analysis

In this section we carry out the renormalization group (RG) analysis of the Hamiltonians $L^{grw}(\Psi)$ and $L^{saw}(\Phi)$. Using this approach we will show the following. For GRWs: 1) When t = 0 the r_ℓ's for different number, ℓ, of tensor indices remain simultaneously critical for zK = 1, as we expect for GRWs. In addition, for t = 0 the self energy, $\sum^{(2)}(q)$ is identically zero, indicating that for t = 0 all the two point correlations are Gaussian, as expected for a GRW. 2) Under RG iterations when t = 0 the potential remains proportional to $v_{2,2} - v_4$ and hence the RG flow can be described by a coupling constant renormalisation. 3) Those four point functions which are argued to be zero for t = 0 remain zero under RG iterations. Thus the calculation seems to be correct. We will calculate the exponent associated with the resistive susceptibility to order ϵ^2 and will display the logarithmic corrections expected when $\epsilon \ll \ln(1-zK)$, where $\epsilon = 4-d$. For SAWs: 1) When t=0 the potentials w_i do not appear as their coefficients vanish and so all we are left are the $v_{2,2}$ and v_4 potentials. However here u and v (respectively the coefficients of v_4 and $v_{2,2}$) do not satisfy the crucial relation u+v=0. Under scaling, the SAWs (with crosslinks) thus flow toward the n-component fixed point $u^*=0$, $v^*\neq 0$ as expected for conformational properties. 2) When we turn on the anisotropy t the potentials w_i for $1 \leqslant i < m$ are in fact turn out to be irrelevant and although initially non-zero, they all scale away. Thus SAWs and SAWs with crosslinks remain in the same universality class in the presence of the anisotropy t, the bridges only introduce correction terms to leading order scaling and we evaluate

these. 3) The exponent associated with the the anisotropy-induced crossover is checked near the SAWs fixed point and indeed found to be unity as required for SAWs.

We begin by writing the Hamiltonian, including all the potentials that we have introduced, in the following schematic form

$$H = \tfrac{1}{2}\int d^dq \sum_{\ell}(r_\ell + q^2)\mathrm{Tr}Q_\alpha^{(\ell)}(\underline{q})Q_\alpha^{(\ell)}(-\underline{q})$$

$$+\int_s \Pi d^d q_s \sum_{i,j,k,l} \delta\Big(\sum_{p=1}^{4}\underline{q}_p\Big)\Big[u\mathrm{Tr}\, Q_\alpha^{(i)}(\underline{q}_1)Q_\alpha^{(j)}(\underline{q}_2)Q_{\alpha'}^{(k)}(\underline{q}_3)Q_{\alpha'}^{(l)}(\underline{q}_4)$$

$$+w(i)\ \mathrm{Tr}_{\substack{\underline{v}(x)\\ \underline{v}(x')}}\left[\left\{Q_\alpha^{(a)}(\underline{q}_1)Q_\alpha^{(b)}(\underline{q}_2)\mathrm{Tr}\, Q_{\alpha'}^{(c)}(\underline{q}_3)Q_{\alpha'}^{(d)}(\underline{q}_4)\right\}\Delta(\{\beta\}_i)\right]$$

$$+ v\ \mathrm{Tr}\, Q_\alpha^{(i)}(\underline{q}_1)Q_\alpha^{(j)}(\underline{q}_2)\mathrm{Tr}\, Q_{\alpha'}^{(k)}(\underline{q}_3)Q_{\alpha'}^{(l)}(\underline{q}_4)\Big] \qquad (6.46)$$

Here the notation Tr indicates the average over all σ's of the appropriate form factors. Each line therefore carries a factor $(q-1)^{\frac{1}{2}}\epsilon$. The set of potentials w(i) are summed over i=1,...,m. For the case of GRWs the bare values of the potential coefficients are v = -u = $\frac{1}{8}$, w(i)=0 and $r_p=[(1+t)^p/zK]-1$. For SAWs (with crosslinks), the corresponding bare values are v=$\frac{1}{8}$+Z/8, u=-Z/8, $w(i)=(J\lambda)^{-i}$, and $r_p=[(1+t)^p/zK]-1$. Here Z is the coordination number of the lattice. For now, we set it to zero. Terms of order higher than ψ^4 are irrelevant near d = 4 (Wilson and Kogut 1974) and will not be considered further. In contrast to previous (conformational) formulations of these problems (de Gennes 1972,1975, Le Guillou and Zinn-Justin 1977) the trace rules enable us to determine the numerical values of the bare potentials.

$L^{grw}(\Psi)$ is therefore the special case of $L^{saw}(\Phi)$ when the w(i) are set to zero and, as will emerge in the analysis, u and v satisfy u+v=0. Accordingly, we will first treat the (simpler) case of GRWs and later generalise the discussion to include the effects of

$w(i)\neq 0$ and $u+v\neq 0$.

Initially we study the case $t = 0$ so that all r's are simultaneously critical, i.e. $r_m = r_0$. We remark that setting $t=0$ also sets $w(i)=0$ for $1\leqslant i\leqslant m$. We first construct the RG equation for r_k', via the momentum shell recursion relations. For this calculation we use the method of Bruce *et al* (1974) wherein one need only keep track of terms in the recursion relations involving powers of lnb, where b is the usual length rescaling factor. The terms of order u are given by the diagram of Fig. 6.3a. We will always analyse a diagram by studying which lines are labelled by a given replica. The matrix element for the entire diagram is then the sum, taken over all possible labellings, of the product of matrix elements within each replica. For the diagram of Fig. 6.3a, since we consider the recursion relation for r_k', we know that for k replicas there are two external legs. Out of these, we have ℓ replicas which also have internal lines, and $k-\ell$ which only appear on the external lines, where $\ell=0,1,2...k$. If the replica appears on all lines, we have the case shown in Fig. 6.3b, otherwise the situation is an in Fig. 6.3c. For the m-k replicas which do not appear on the external lines, j replicas appear on the internal lines and m-k-j appear nowhere. These two possible situations for a given replica are shown in Fig. 6.3d and 6.3e, respectively. Note that when the internal lines are covered, there occurs an additional factor (q-1) due to the internal sum over components. This is clear for Figs. 6.3d and 6.3e. For Fig. 6.3c the replica in question contributes a factor $\delta_{\mu,\nu}$. For Fig. 6.3b the replica contributes a factor

$$\sum_{\rho}\lambda_{\mu\nu\rho\rho} = \frac{(q-1)^2}{q}\sum_{\sigma\rho}(\epsilon_\mu^\sigma)\ (\epsilon_\nu^\sigma)\ (\epsilon_\rho^\sigma)^2=(q-1)\delta_{\mu,\nu}. \qquad (6.47)$$

Summing over $p=\ell+j$ we thereby find a contribution from this diagram of

$$r' \sim 8b^{2-\eta}\ u\sum_{p}\frac{m!}{m-p!p!}(q-1)^p\ A(r) = 8b^{2-\eta}uA(r). \qquad (6.48)$$

Since r_k' does not depend on k, we denote it by r'. Since random walks are Gaussian, η should be zero and we will verify this in a moment. Here and below we use the notation of Bruce *et al* for the integrals represented by the various diagrams. (The values of some of these integrals are listed in Table 6.1.) Note that there are only

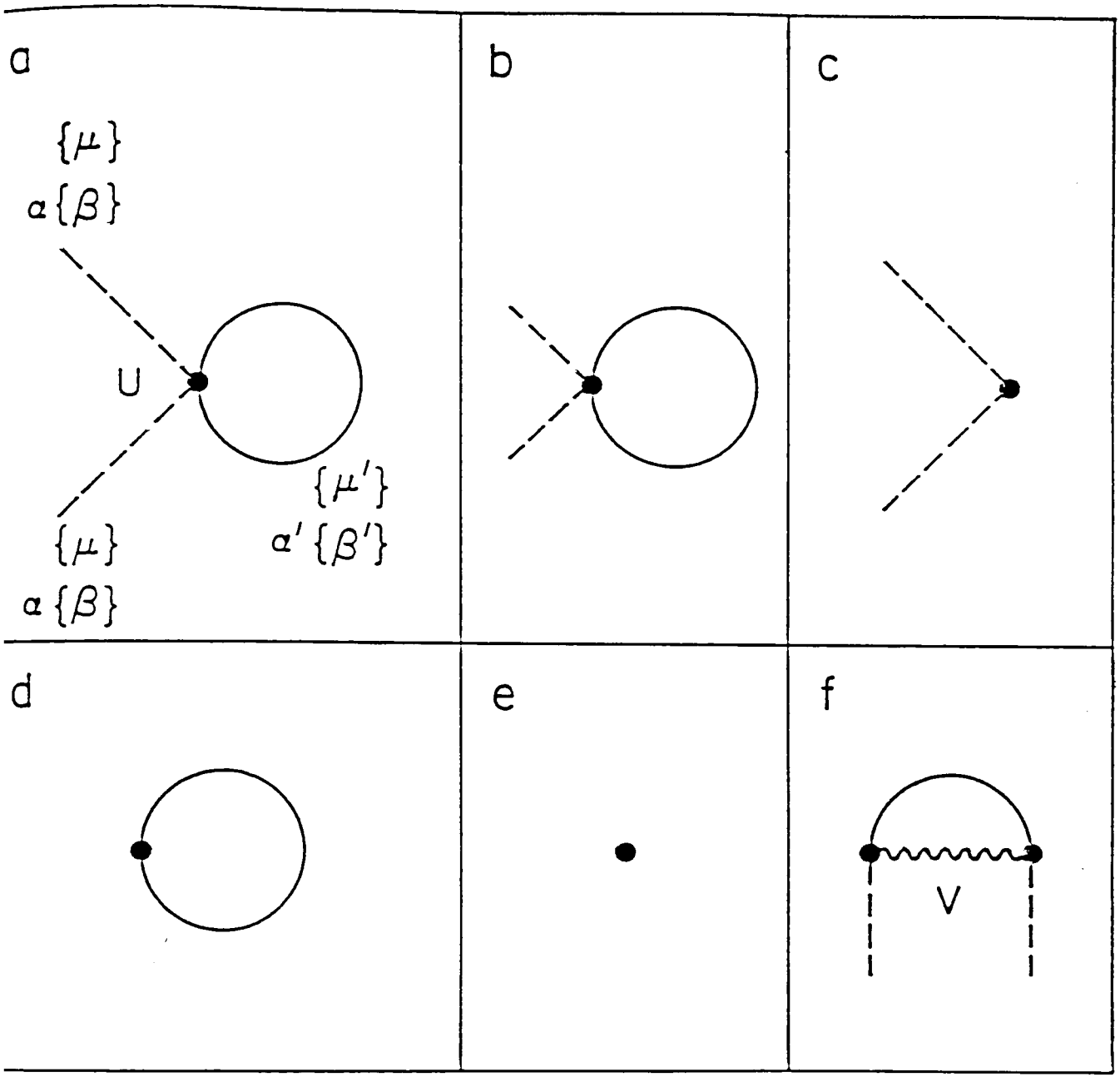

Fig.6.3.: Diagrammatic representation of terms for r_k' linear in: a) u or f) v. In this and succeeding diagrams, solid lines represent propagators of internal lines (whose momenta are integrated over), and dashed lines represent external momenta. For the term of order u the situation within a given replica is of the type shown in panels b or c if the replica is on the external line (ie is in the set $\{\beta\}$) or of the type of panels d or e otherwise. Types b and d have a form factor (q−1) due to an internal summation over a component index, whereas the form factor for types c and e in unity.

Table 6.1.

Values of various integrals (from Bruce *et al* 1974). Here we only include terms of order $(\log b)^k$.

Integral	Value
$-A'(r) = C(r)$	$K_d \log b \left[1 + \frac{\epsilon}{2} \log b\right]$
$-\frac{1}{3} B'(r) = D(r)$	$\frac{1}{2} K_d^2 \log b \left[1+\log b\right]$

four ways to contract this diagram, because connecting lines with the same scalar index leads to a sum over α giving a factor $n = 0$. For the diagrams in Fig. 6.3f the situation is simpler, since all lines have the same indices, so that

$$r' \sim 8b^{2-\eta} v A(r) \tag{6.49}$$

To order ϵ^2 we need to consider the graphs in Fig. 6.4. First consider the graphs of order u^2 as in Fig. 6.4a. For the k replicas which appear on the external line, the internal lines can be as in Fig. 6.5a, 6.5b, or 6.5c. We sum over the internal component indices and obtain the q-dependent form factors for the replica in question shown beside each graph. To illustrate the calculations, consider the diagram of Fig. 6.5c and call the form factor for the replica in question $F_{\mu\nu}$. Then we have

$$F_{\mu\nu} = \frac{1}{q^2} \sum_{\sigma\sigma'} \sum_{\rho\tau\eta} (q-1)^4 \, \epsilon_\rho^\sigma \, \epsilon_\rho^\sigma \, \epsilon_\tau^\sigma \, \epsilon_\eta^\sigma \, \epsilon_\rho^{\sigma'} \, \epsilon_\tau^{\sigma'} \, \epsilon_\eta^{\sigma'} \, \epsilon_\nu^{\sigma'} \tag{6.50a}$$

$$= \frac{1}{q^2} \sum_{\sigma\sigma'} (q-1) \, \epsilon_\mu^\sigma \, \epsilon_\nu^{\sigma'} \, (q\delta_{\sigma\sigma'} - 1)^3 \tag{6.50b}$$

$$= (q^2 - 3q + 3)\delta_{\mu,\nu} \tag{6.50c}$$

as written in Fig. 6.5c. In the graphs of Fig. 6.5a there is a factor of three since there are three ways to select the lines of Fig. 6.4a to be labelled. Adding all these possibilities gives a form factor of q^2 for each of the k replicas present on the external line. For the other m-k replicas the situation is as in Figs. 6.5d, 6.5e, or 6.5f. Adding these form factors we again find a factor of q^2. Thus with the diagram of Fig. 6.4a we associate a total matrix element of $q^{2m} = 1$. For the diagram of Fig. 6.4b a similar analysis using Figs. 6.5g–6.5j gives a form factor of q for each replica and therefore a total matix element for the entire diagram of $q^m = 1$. Similarly, the diagram of Fig. 6.4c has a total matrix element of unity. In all, to second order in u and v we have

$$r' = b^{2-\eta}[r + 8(u+v)A(r) - 64(u+v)^2 B(r) - 64(u+v)^2 A(r)C(r)] \tag{6.51}$$

The last term in (6.51) comes form the diagram of Fig. 6.6 whose evaluation is discussed in Appendix H. The equation for η can be obtained by generalizing the

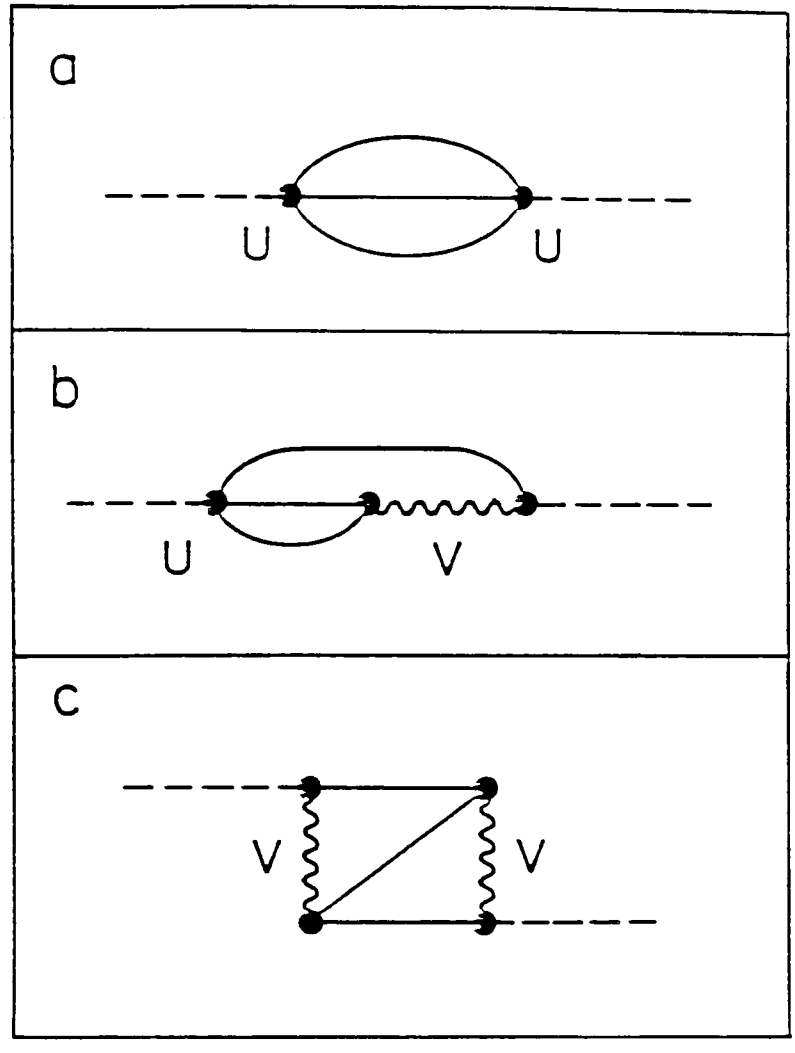

Fig.6.4.: Diagrams for r_k' of order a) u^2, b) uv, c)v^2. The scalar and tensor indices are not shown.

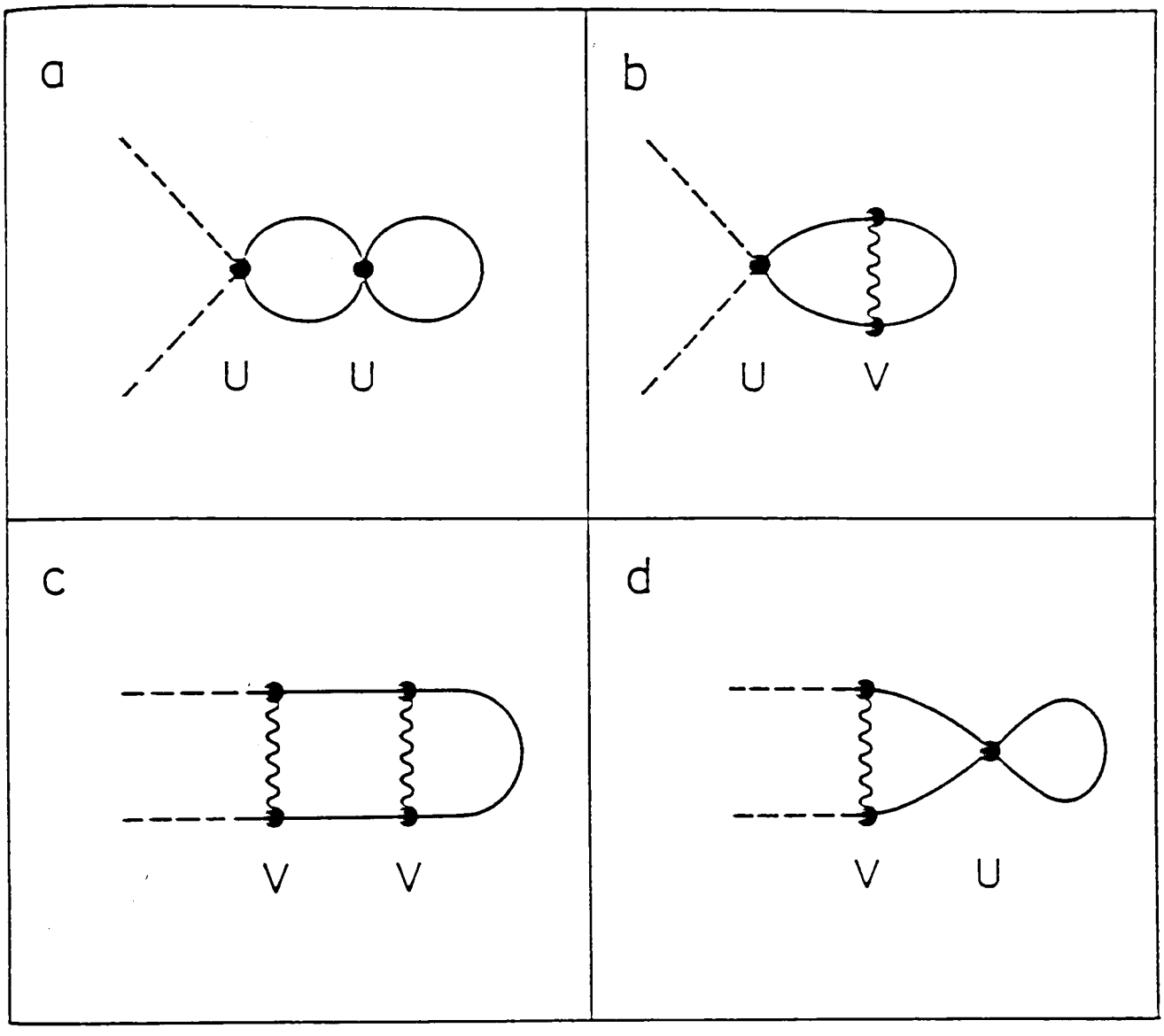

Fig.6.6.: Additional second order diagrams from r_k' with mass insertions.

result given by Bruce *et al* (1974),

$$\eta = 16K_d^2(u + v)^2 . \qquad (6.52)$$

There are several checks on these calculations. First of all, the terms on the right hand side of (6.51) and (6.52) involving only powers of u or only powers of v have the same coefficients as for the n-component Heisenberg model in the limit $n \to 0$. Also, for $u + v = 0$, r is Gaussian, and η vanishes corresponding to point 1 in the first paragraph in this section.

Next we turn to the equations for u' and v'. Consider first the u^2 terms, the topology of which is illustrated in Fig. 6.7a. We now have the following counting problem. We must sum over all possible ways that replica and component indices can be distributed over the internal lines keeping the indices of the external lines fixed to yield a renormalization of a given fourth order vertex. We must include the appropriate form factor, which is obtained as a product of the form factors of each replica. The various possible labellings of the diagram 7a within a given replica are shown in diagrams 8a-8k, and the associated form factor is given beside the diagram. To illustrate the calculations we evaluate the form factor for the case when the replica is labelled as in Fig. 6.8a. We denote this quantity by $F_{\mu\nu\rho\tau}$ and have

$$F_{\mu\nu\rho\tau} = \frac{(q-1)^4}{q^2} \sum_{\sigma\sigma'} \epsilon_m^\sigma \epsilon_\nu^\sigma \epsilon_\rho^{\sigma'} \epsilon_\tau^{\sigma'} \sum_{\xi\xi'} \epsilon_\xi^\xi \epsilon_\xi^{\xi'} \epsilon_\xi^\xi \epsilon_\xi^{\xi'} \qquad (6.53a)$$

$$= \frac{(q-1)^2}{q^2} \sum_{\sigma\sigma'} \epsilon_\mu^\sigma \epsilon_\nu^\sigma \epsilon_\rho^{\sigma'} \epsilon_\tau^{\sigma'} (q\delta_{\sigma\sigma'} - 1)^2 \qquad (6.53b)$$

$$= (q-2)\lambda_{\mu\nu\rho\tau} + \delta_{\mu\nu}\delta_{\rho\tau} . \qquad (6.53c)$$

The result in (6.53c) is potentially very dangerous in that it seems to indicate the possibility that under renormalization potentials may appear which have mixed symmetry, i.e. having "u"-like symmetry in some replicas and "v"-like symmetry in others. Fortunately, this does not happen, as one can see by combining the results of Figs. 6.8a, 6.8b, and 6.8c. If all diagrams in Fig. 6.8 having the same structure of external lines are combined, one obtains a factor q for the replica in question. Therefore, the form factor for diagram 7a is $q^m = 1$. The diagrams of order uv and v^2 are also shown in Fig. 6.7. The form factors for Figs. 6.7c, 6.7d, and 6.7e are unity because

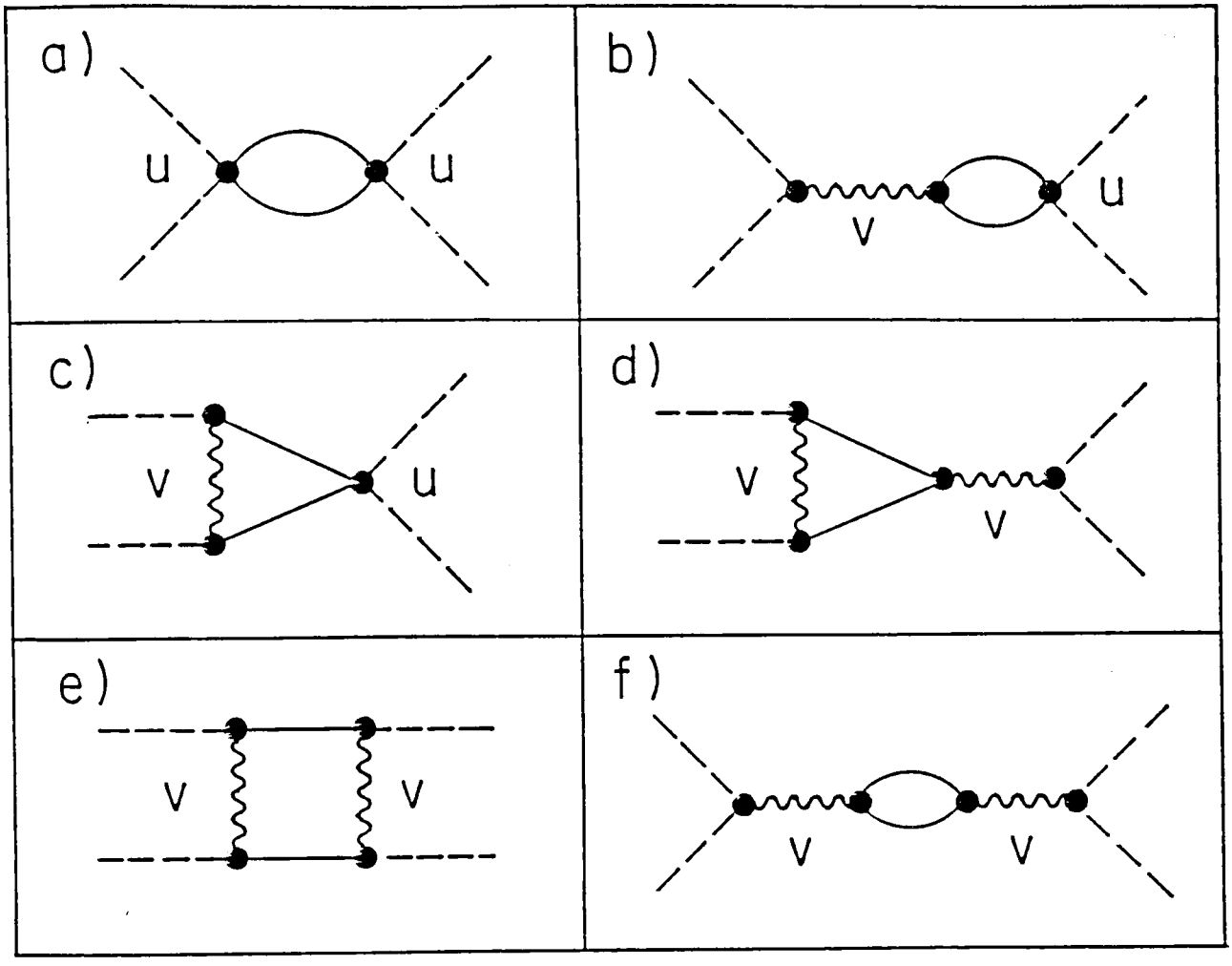

Fig.6.7.: Diagrams for u' of order a) u^2 and c) uv and for v' of order b) uv and d),e),f) v^2. The contributions from panel f) vanish.

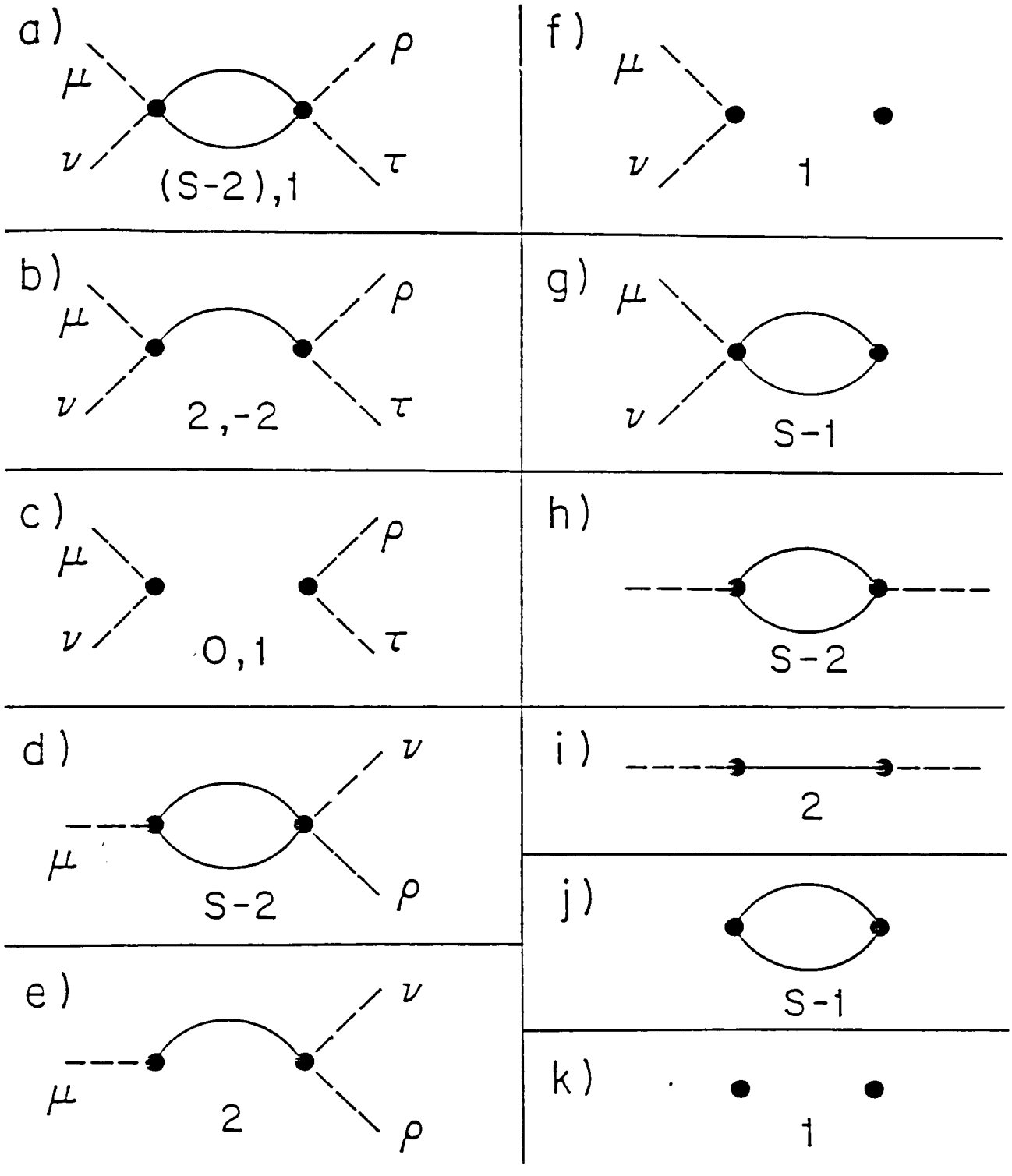

Fig.6.8.: The various possible configurations together with their q-dependent form factors within a given replica for the diagram of Fig. 6.7a. In Figs. 6.8a,b,c, the notation x,y indicates a matrix element $x\lambda_{\mu\nu\rho\tau} + y\delta_{\mu,\nu}\ \delta_{\rho,\tau}$. Note that when diagrams 8a,b,c are combined, the term in $\delta_{\mu,\nu}\ \delta_{\rho,\tau}$ vanishes, so that u' has the same tensor structure as u.

for each replica no independent internal indices are allowed by the v vertex. In Fig. 6.7b one obtains a factor q for each replica so that this diagram has form factor $q^m = 1$. The labelling of the scalar indices is again similar to that for the n-component Heisenberg model for $n \to 0$ and the diagram of Fig. 6.7f vanishes due to an internal sum over scalar indices. When the sum over scalar indices is performed, we find that

$$u' = b^{\epsilon-2\eta}[u-16C(r)(2u^2+3uv)] \qquad (6.54a)$$

$$v' = b^{\epsilon-2\eta}[v-16C(r)(uv+2v^2)]. \qquad (6.54b)$$

From the calculations so far we can evolve the contractions of two interaction vertices into a single renormalised interaction. For this purpose we classify the interactions as shown schematically in Fig. 6.9. The results are given as a "multiplication table" in Table 6.2. We will use these in the order-ϵ^2 calculation now. There are two topologies to be considered, as shown in Fig. 6.10. For both of these, the results for terms involving only u vertices or only v vertices are the same as for the Heisenberg model with $n \to 0$. For the u^2v and uv^2 contributions to Fig. 6.10a we contract the potentials as per Table 6.2. (This table only includes the way the tensor indices are contracted. The numerical coefficients in, say, (6.53) are obtained by performing the sums over the scalar indices.) In this scheme each vertex can have its scalar indices arranged in two ways: either like indices are on the same side of the ladder or they are not. These two possibilities for u and v are denoted by subscripts "a" and "b", respectively, in Fig. 6.9. The calculations are aided by the observation that ladder graphs with two or more "a" potential drop out, and also a graph can only contribute to v' if a v_a is present. From all the diagrams having topology of Fig. 6.10a we find

$$u' = b^{\epsilon-2\eta}[320u^3+768u^2v+576uv^2]C(r)^2 \qquad (6.55a)$$

$$v' = b^{\epsilon-2\eta}[192u^2v+384uv^2+320v^3]C(r)^2. \qquad (6.55b)$$

The calculations for the diagram in Fig. 6.10b are performed similarly. The simplest

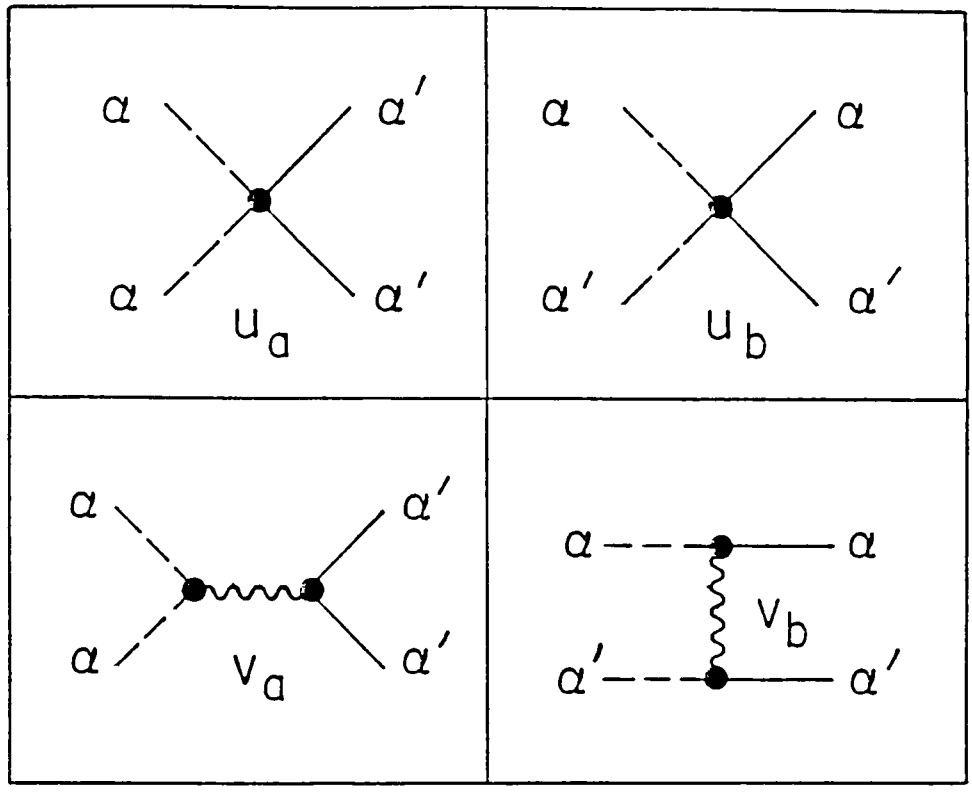

Fig.6.9.: Specification of vertices according to the placement of their scalar indices. the diagram of Fig. 6.7a represents $(u_a+u_b)^2$, whereas Fig. 6.7d,e,f represent $v_b v_a$, $v_b{}^2$ and $v_a{}^2$ respectively. The results of connecting the internal lines of pairs of these vertices are given in Table 6.2

Table 6.2.

Multiplication table for vertices shown in Fig.6.9.

	u_a	u_b	v_a	v_b
u_a	0	u_a	0	u_a
u_b	u_a	u_b	v_a	u_b
v_a	0	v_a	0	v_a
v_b	u_a	u_b	v_a	v_b

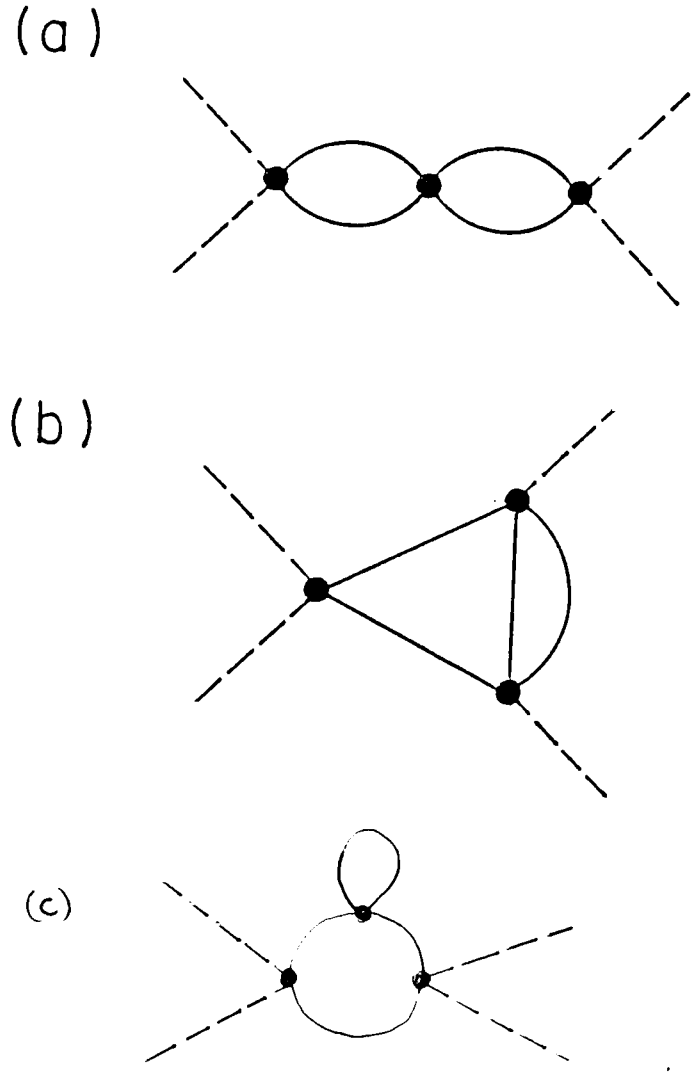

Fig.6.10.: Third order diagrams for u'. The topology of the diagrams for v' is similar.

way to proceed is to consider for each vertex the two inequivalent ways of assigning scalar indices to the lines. Thus each diagram has 8 conceivable scalar labellings, of which two vanish because of an internal sum over scalar indices. Each such labelling can be reduced by using the results of Table 6.2 to collapse the two potentials with one external line into a single potential with two external lines, after which the calculation proceeds as for Fig. 6.7. Similar statements apply for the diagram in Fig.6.10c which can be evaluated using Table 6.2. The form factor for all diagrams is unity, but it is necessary (and fortunately easy) to figure out which diagrams contribute to u'and which to v'. In this way we find the result to order ϵ^2:

$$u' = b^{\epsilon-2\eta}\,[u - 16C(r)(2u^2+3uv) +64C(r)^2(5u^3+12u^2v+9uv^2) +128D(r)(11u^3+30u^2v+21uv^2) +256A(r)E(r)(2u^3+5u^2v+3uv^2)\,]. \tag{6.56a}$$

$$v' = b^{\epsilon-2\eta}\,[v - 16C(r)(uv+2v^2) +64C(r)^2(3u^2v+6uv^2+5v^3) +128D(r)(3u^2v+12uv^2+11v^3) +256A(r)E(r)(2v^3+3uv^2+u^2v)\,]. \tag{6.56b}$$

We note several checks. If u = 0 or if v = 0, the recursion relation for the non-zero potential reduces to that of the n-component Heisenberg model with n→0; this is required since v has the same symmetry as the (conformational) potential for the Heisenberg model. That this applies for u non-zero as well is a consequence of (u+v)'=F(u+v;r,ϵ,b), where F(...) is the n→0 component Heisenberg recursion relation. In particular, if u+v = 0, then u'+v' = 0. Since this relation holds for the bare potentials, it also holds for the fixed point of interest. These observations lead to the conclusions 2 and 3 for GRWs stated in the first paragraph of this section. Using the data of Table 6.1 we find that the fixed point values of u and v which satisfy u+v = 0 are given by

$$v^* = -u^* = \frac{2\epsilon+\epsilon^2}{32K_d} + 0(\epsilon^3). \tag{6.57}$$

The location (to order ϵ) and stability of the various fixed points of (6.56) are shown in Fig. 6.11. The instability of the random walk fixed point of (6.57) away from the direction of u+v = 0 indicates that perturbations will be relevant. We identify the stable fixed point $u^*=0, v^*\neq 0$ as that corresponding to SAWs (n-component Heisenberg model, $n\to 0$) where one obtains from (6.56) the usual fixed point

$$v^* = \frac{\epsilon+(21/32)\epsilon^2}{32K_d} + 0(\epsilon^3). \qquad (6.58)$$

Such variations therefore correspond to a cross-over away from the GRW resistor problem to that corresponding to Heisenberg model and therefore SAWs (no links). We discuss this point further when we treat the SAW crosslinking potentials w(i).

Now we proceed to calculate the cross-over exponent for GRWs associated with turning on t, where t is the infinitesimal splitting parameter introduced in (6.1) above. For this purpose we need to generalize the above equations for the case when

$$r_p = \frac{(1+t)^p}{zK} - 1 \sim r_o + pt/zK \equiv r_o + p\omega, \qquad (6.59)$$

where ω is an anisotropy field. We write

$$(r_p+q^2)^{-1} = (r_0+q^2)^{-1} - p\omega(r_0+q^2)^{-2}, \qquad (6.60)$$

and recursion relations for ω are developed in the usual way. To first order in ϵ the calculation can easily be done using (6.48) and (6.49). On the right hand side of (6.48), for instance, it is clear that A(r) is actually $A(r_p)$, because we need the propagator for the case when p replicas are involved. Next consider how (6.49) should be modified to describe r_k'. Referring to Fig. 6.3f we see that the internal propagator has the same r as the external line. Thus in (6.49) we should replace r everywhere by r_k. Thus Eqs. (6.48) and (6.49) lead to

$$r_k' = b^2 [r_k + 8[uA(r_0)+vA(r_k)] + O(\epsilon^2)]. \qquad (6.61)$$

In the notation of (6.59) this relation becomes

$$\omega' = b^2\omega[1+8vA'(0)+O(\epsilon^2)] \qquad (6.62)$$

where $A' = dA/dr = -C(r)$. The ϵ^2 terms omitted in (6.62) are derived in Appendix

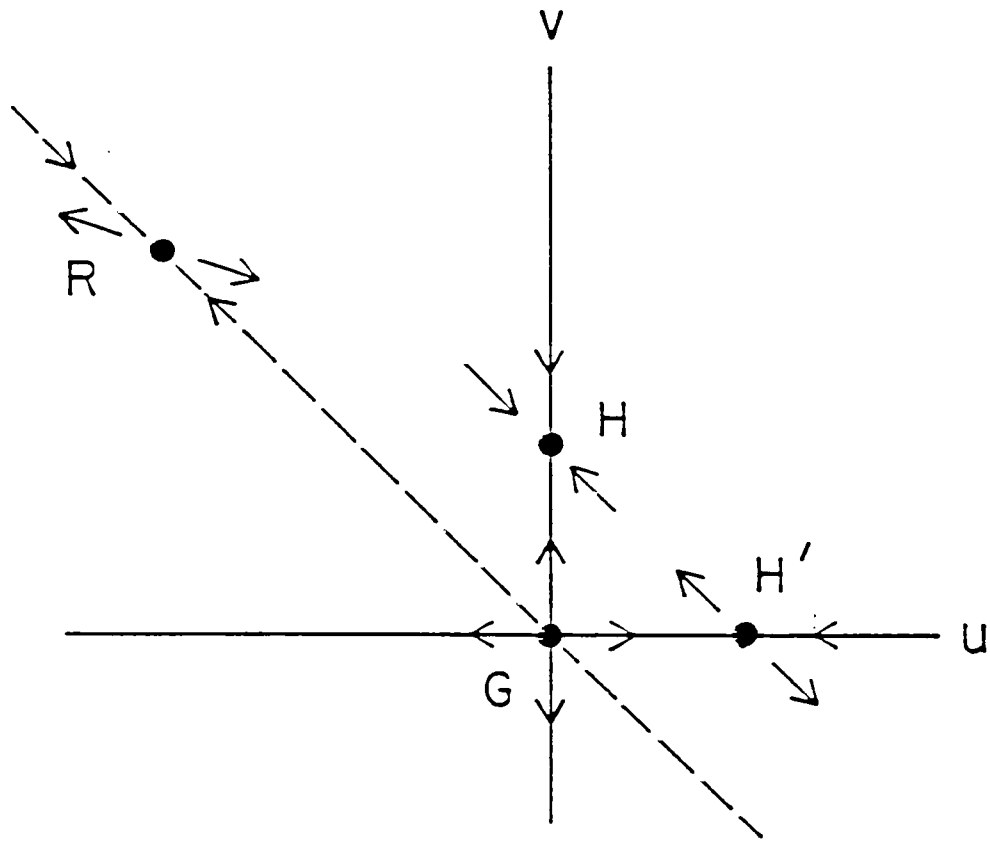

Fig.6.11.: The flow diagram for the recursion relations of (6.56). The Gaussian fixed point (G) is doubly unstable. The random walk fixed point (R) is singly unstable and lies on the ridge u+v=0. The Heisenberg fixed point (H) with v non-zero is stable and corresponds to the SAW fixed point. The other 'Heisenberg' fixed point (H'), with u non-zero, is unstable and represents a multicritical point. There is an unstable ridge line for u+v=0 (on which R and G lie) and a stable 'valley' for $u+v=\epsilon/(16K_d)$ {on which H and H' lie). Points above the ridge line to infinity. The diagram is very similar to that for SAW in a random medium (Kim 1983).

H and yield the result

$$r_k' = b^2[r_k+8[uA(r_0)+vA(r_k)] -64v^2B(r_k)-128uv(B(0)+(k/3)\omega B'(0))-64u^2B(r_0) -64v^2C(0)A(r_k)] \quad (6.63)$$

with the corresponding result for ω,

$$\omega' = b^2\omega[1+8vA(0)-64B'(0)(v^2+2/3uv)-64C(0)A'(0)v^2], \quad (6.64)$$

where $B' = -3D(r)$. To order ϵ^2 we may write this latter recursion relation as

$$\omega' = \omega b^{\varphi/\nu}. \quad (6.65)$$

For GRWs $\nu=\frac{1}{2}$ and so we find using (6.57),

$$\varphi = 1- \frac{\epsilon}{4} - \frac{\epsilon^2}{16} \cdot \quad (6.66)$$

Similarly, for SAWs we obtain, using (6.58) and (6.63) the usual result (Bruce *et al* 1974)

$$\nu = \tfrac{1}{2} + \frac{\epsilon}{16} + \frac{15\epsilon^2}{512} \quad (6.67)$$

whence using (6.64) we obtain to second order in ϵ, $\varphi=1$ for SAWs as, of course, required. This provides a powerful check that the method is behaving sensibly.

We now relate the exponent tabulated in the numerical simulation and enumeration studies (Banavar *et al* 1984) of φ, where one defines an exponent x by

$$\langle R_N\rangle \sim N^x, \quad (6.68)$$

where $\langle R_N\rangle$ indicates the average end-to-end resistance of all random walks of length N. Consider firstly the case of GRWs. Since the total number of walks of length N steps in z^N, we may write (6.5) as

$$\chi_1 \equiv \sum_x \chi_1(x;K) = \sum_N (zK)^N\langle R_N\rangle. \quad (6.69)$$

In terms of the dependence written in (6.67) we have

$$\chi_1 \sim (1-zK)^{-x-1} = r^{-x-1}. \quad (6.70)$$

On the other hand, if we set

$$G(r,t) \equiv \sum_x \langle u_1(x)\underline{v}_1(x).\underline{v}_1(x')u_1(x')\rangle, \qquad (6.71)$$

then the recursion relations allow us to write

$$G(r,t) = b^2 G(b^2 r, b^{2\varphi} t). \qquad (6.72)$$

We take $b^2 = r^{-1}$ and expand the right-hand side of (6.72) in powers of the infinitesimal, t:

$$G(r,t) = G(r,0) + \text{const}.\, t r^{-1-\varphi}. \qquad (6.73)$$

Then (6.8) gives

$$\chi_1 \sim r^{-1-\varphi}, \qquad (6.74)$$

so that $x = \varphi$.

For SAWs the number of walks of length N steps is given by $\mu^N N^{\gamma-1}$ (McKenzie 1976, de Gennes 1979) and thus

$$\chi_1 = \sum_N (\mu K)^N N^{\gamma-1} \langle R_N \rangle \qquad (6.75)$$

and so

$$\chi_1 \sim (1-\mu K)^{-(x+\gamma)}. \qquad (6.76)$$

Similarly $$G(r,t) = b^{2-\eta} G(b^{1/\nu} r, b^{\varphi/\nu} t). \qquad (6.77)$$

Putting $b^{1/\nu} = r^{-1}$ gives,

$$G(r,t) = G(r,0) + \text{const}.\, x\ t\ r^{-(2-\eta)\nu}\ r^{-\varphi}. \qquad (6.78)$$

Thence

$$\chi_1 \sim r^{\{-(2-\eta)\nu-\varphi\}} \sim r^{-(\gamma+\varphi)} \qquad (6.79)$$

since $\gamma=(2-\eta)\nu$. φ=x for SAWs then follows using (6.69).

It is also useful to connect the RG results for GRWs to the exact enumeration studies (Banavar *et al* 1984). For this purpose it is useful to describe the cross-over from power-law to logarithmic corrections which occurs in the limit d→4. We discuss this point in Appendix J where we obtain the result (correct to order ϵ)

$$\chi_1 = r^{-1-\varphi} H^{\theta}, \qquad (6.80)$$

where

$$H = r^{\epsilon/2} + \underset{\epsilon}{C}\,(1-r^{\epsilon/2}), \tag{6.81}$$

and $\theta = -1/2$. This exponent is negative because fluctuations cause x to be less than its mean-field value, whereas usually one sees the case where the susceptibility exponent is enhanced by fluctuations and $\theta = 2\partial\gamma/\partial\epsilon > 0$.

IV. Influence of the Crosslink Potentials, w(i) on the Recursion Relations.

We now focus on the SAWs and deal with the problem of turning on the crosslink conductance σ_b (or λ) and hence the *direct sum* potentials w(i). In Appendix J, we consider how the presence of non-zero w(i) modify the recursion relations. In fact because of the sums over Potts replicas involved in the w(i) potentials, the contribution from them to u' and v' vanishes when we take the limit $m \to 0$. Thus the recursion relations for u and v are given by (6.56a) and (6.56b) even in the presence of the crosslink potentials. Furthermore we have shown that, near the SAW fixed point (6.58) we have the following linearised recursion relations for the w(i)

$$w(i)' = b^{\epsilon-2\eta}\, w(i)\, [1-48C(r)v^*] \tag{6.82}$$

where $v^* = \epsilon(1+(21/32)\epsilon)/32K_d$. These equations follow upon observing that the v_b vertices are the 'identity elements' of the 'multiplication' Table 6.2. Using the known result for the momentum integral we find

$$w(i)' = b^{-\frac{1}{2}\epsilon}\, w(i) \tag{6.83}$$

At least to $O(\epsilon)$, the w(i) are therefore irrelevant variables. Finally there remains the question of the contribution to r_ℓ'. This calculation is outlined in Appendix J and we find to first order in ϵ the following extra terms appearing in the recursion relation for r_ℓ',

$$r_\ell' = \sum_{\substack{a=0,\ldots,\ell \\ b=0,\ldots,m-\ell \\ c=0,\ldots,a+b}} \begin{bmatrix} \ell \\ a \end{bmatrix} \begin{bmatrix} m-\ell \\ b \end{bmatrix} \begin{bmatrix} a+b \\ c \end{bmatrix} (A(r_{\ell-a+c}))\, (q-1)^c\, w(m-a-b) \tag{6.84}$$

In Appendix J we have developed a Nelson-Rudnick formulation (Rudnick and Nelson 1976) for the recursion relations for the r_ℓ including the contribution from the w(i)

above. From this we are able to calculate the correction to scaling terms introduced by the w(i) and our result is as follows,

$$\langle R_N \rangle \sim N(1+AN^{-\epsilon/4}) \qquad (6.85)$$

where $A<0$.

V. Discussion and Conclusion.

To begin, we give some heuristic estimates for the values of the exponent x for GRWs. Consider firstly the situation in one dimension. After N steps, the end of the random walk is of order $N^{\frac{1}{2}}$ lattice constants from its starting point. If we assume that all the N steps are uniformly spread over this interval, then it is clear that each step has a conductance of order $N/N^{\frac{1}{2}} = N^{\frac{1}{2}}$. The resistance of $N^{\frac{1}{2}}$ such conductors in series is of order unity. Thus, to the extent that we can ignore fluctuations, we expect x to be zero in one dimension. An exact calculation (Harris 1987) shows that fluctuations lead to logarithmic corrections to this result so that $\langle R_N \rangle \sim \ln N$.

Now consider the situation in higher dimension. For $d>1$, where our arguments are unfortunately more qualitative, a random walk will of course contain loops in which no current flows and also parallel paths. Since parallel paths are hard to take account of by a simple argument we will ignore them. As far as loops are concerned, if we delete all the loops from a random walk, as shown in Fig. 6.12, we then obtain a realization of a self-avoiding walk (SAW). The ensemble of walks we obtain in this way does not reproduce the usual ensemble of SAWs of course. For a random walk we know that the real-space separation, r_{if}, between its initial and final points is of order

$$r_{if} \sim N^{\frac{1}{2}}. \qquad (6.86)$$

For a SAW one has

$$r_{if} \sim (N_{SAW})^{\nu_{SAW}}, \qquad (6.87)$$

where N_{SAW} is the number of steps in the SAW. Thus

$$N_{SAW} \sim (r_{if})^{1/\nu_{SAW}} \sim N^{1/(2\nu_{SAW})}. \qquad (6.88)$$

For $d>2$, as we shall see, multiple traversals of a bond are unimportant, in which case the number of self-avoiding steps is the same as the end-to-end resistance, so that Eq.

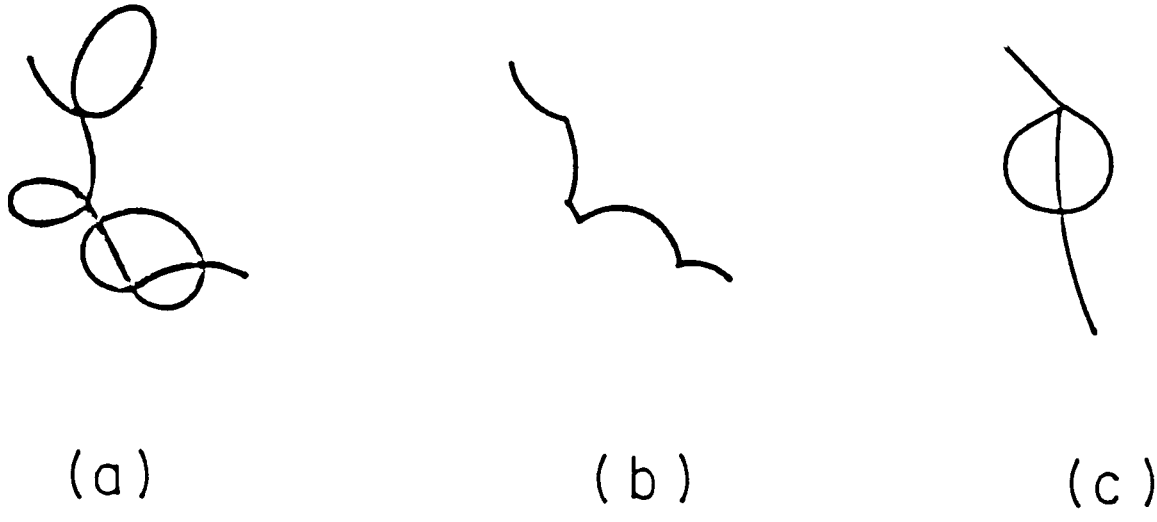

Fig.6.12.:

a) A random walk with various types of self-intersections.

b) The walk of panel a) with loops removed so that only a SAW remains.

c) A parallel circuit is improperly treated when loops are simply removed.

(81) gives the estimate

$$x = 1, \qquad d>4 \tag{6.89a}$$

$$= \frac{1}{2\nu_{SAW}} \approx \frac{d+2}{6}, \qquad 2<d<4, \tag{6.89b}$$

where we have used Flory's estimate (Flory 1953, de Gennes 1979) for ν_{SAW}. This argument gives larger values of x than are obtained form numerical methods (Banavar *et al* 1984) or the ϵ–expansion. The results of the various methods are listed in Table 6.3. The result in Eq. (6.89) overestimates x because ν for random walks with loops removed is larger than ν_{SAW}, which we inserted into Eq. (6.81). This is because removing loops leaves a straighter walk than one would typically find for a SAW. Therefore, in our argument we should replace ν_{SAW} by a larger quantity, which in turn would lead to a smaller (i.e. better) estimate for x. It is also true that by neglecting the possibility of covering a given bond several times we are also overestimating $<R_N>$. However, according to the data in Banavar *et al* (1984), whether or not repeated bond traversals are taken into account does not affect x, as long as $d \geq 2$.

In fact, we can see that the regime $d<2$ is qualitatively different from that for $d>2$ in that the average density of steps, ρ, inside the volume of size $N^{\frac{1}{2}}$ becomes large for $d>2$. For example, for $d = 1$ we see that Eq. (6.81) is correct with ν_{SAW}. What is wrong is to identify N_{SAW} as $<R_N>$. Since we know the average density to be

$$\rho \sim N/N^{d/2}, \tag{6.90}$$

we estimate the average resistance of a bond for $d<2$ to be of order ρ^{-1}. Therefore, for $d<2$ we have

$$<R_N> = N_{SAW}/\rho \tag{6.91a}$$

$$= N^{\frac{d+2}{6}(1-d/2)} \sim N^{2/3(d-1)} \tag{6.91b}$$

This argument correctly predicts that $x \to 0$ as $d \to 1$, in agreement with the exact

result (Harris 1987).

The resistance problem studied in this chapter may be related to other dynamical problems of interest in statistical mechanics, and in particular to diffusion. If we consider the scaling properties of the root-mean square distance travelled by a random walker $\langle \xi_w \rangle$ (de Gennes 1979) on the fractal substrate (itself a walk):

$$\langle \xi_w \rangle \sim N^{1/d_w}. \qquad (6.92)$$

This defines the dimensionality of the path of the 'ant'. Using what amounts to an Einstein relation (Kirkpatrick 1973) between conductivity and mobility, d_w may be determined from φ as follows

$$d_w = d_f\ (1+\varphi) \qquad (6.93)$$

In particular, for SAWs with crosslinks, φ=1 and so d_w=2d_f which is, of course, identical to the corresponding result for diffusion along a quasilinear chain. New, extended exact enumeration evidence corroborates this result (see chapter four).

In summary we may list our conclusions as follows.

1) We have developed a field theoretic formulation for the average end-to-end resistance $\langle R_N \rangle$ of Gaussian random walks, self-avoiding walks and self-avoiding walks with nearest neighbour crosslinks of length N steps. In principle, arbitrary powers of the resistance can be calculated by this method.

2) We have obtained an $\epsilon = 4 - d$ expansion for the exponent x for GRWs defined by

$$\langle R_N \rangle \sim N^x : \quad x = 1 - \frac{\epsilon}{4} - \frac{\epsilon^2}{16} + O(\epsilon^3). \qquad \text{for GRWs} \qquad (6.94a)$$

and similarly for SAWs (including corrections to scaling),

$$\langle R_N \rangle \sim N^x(1+AN^{-\Delta}) : \quad x=1 + O(\epsilon^3),\ \Delta = \epsilon/4 + O(\epsilon^2)$$

for SAWs with crosslinks.

(6.94b)

3) We have obtained the form of the logarithmic corrections to the power law behaviour for $\langle R_N \rangle$ for GRWs which are expected at d=4 with the results as given in Eqs. (6.80) and (6.81).

4) A qualitative argument is given which suggests that $d^*=2$ is a lower critical dimension at which multiple traversals of bonds become relevant. For $d>2$, the present model and that (Banavar *et al* 1984) in which bonds traversed q times have unit resistance for all $q \geq 1$ should differ, whereas for $d>2$, they are probably in the same universality class (Banavar *et al* 1984). At $d = 2$ one of these models may have logarithmic corrections to the power law $\langle R_N \rangle \sim N^x$.

Table 6.3.

Values of the exponent x for GRWs from various methods in spatial dimensions d=2,3,4.

Method	d=2	d=3	d=4
RG[a]		0.69	1.00[c]
Series[b]	0.54 ± 0.04	0.76	1.00[d]
Simulation[b]	0.46 ± 0.01	0.73	1.00[e]
Eqn.(6.89)	2/3	5/6	1

a. Using (6.66) for $d \geq 3$.

b. See Banavar *et al* (1984).

c. With logarithmic corrections as in (6.80).

d. The logarithmic corrections were adjusted by fitting the parameter C in (6.81), to yield x=1 at d=4.

e. At d=4 a fit was made to the form $\langle R_N \rangle \sim N/(\log N)^{\theta}$, where θ was found to be about 0.5.

Chapter 7

Spin Wave Damping in Heisenberg Ferromagnets near the Percolation Threshold.

The decay of zero temperature spin-wave excitations near the percolation threshold in bond diluted d-dimensional (d>1) Heisenberg ferromagnets is investigated using a Green function equation of motion method. The diagrammatic perturbation theory is convergent in the hydrodynamic limit ($k\xi \ll 1$) and the following expression is obtained there for the damping, or decay rate: $\Gamma_c(k,\xi) \propto (p-p_c)^{-\nu d+(t-\beta)} k^{d+2}$, ($k\xi \ll 1$). This form satisfies the requirements of the dynamic scaling principle, by which $\Gamma_c(k,\xi)=k^z g(k\xi)$ for general $k\xi$, and $z=2+(t-\beta)/\nu$. An explicit expression, applicable in the hydrodynamic regime and consistent with dynamic scaling, is also obtained for the infinite cluster transverse dynamic structure function. The approach is extended to incorporate the ensemble of finite clusters and to treat the case of non-zero temperature and also the experimentally more relevant situation of site dilution. This work has been published in J.Phys. C (Christou and Stinchcombe 1987e).

I. Introduction

In this chapter we study the critical spin dynamics of substitutionally disordered ferromagnetic Heisenberg systems (Korenblit and Shender 1978, Harris and Kirkpatrick 1977, Stinchcombe 1985). Static dilution-induced critical phenomena in these models have been studied intensively (for a review of this area, see Stinchcombe 1983) however much less is known about their dynamic critical properties, particularly their damping, near the percolation threshold.

In one dimension the equations of motion are readily solved (Stinchcombe and Harris 1983) to give the transverse contribution to the dynamic linear response of the bond-dilute classical ferromagnetic chain at zero temperature. This method has subsequently been extended to deal with the corresponding antiferromagnetic system (Maggs and Stinchcombe 1984) as it is antiferromagnets that occur rather more

commonly in nature.

For reasons that we discuss below, the dynamic critical behaviour in d=1 is fundamentally different to that in d>1 and so few insights into the d>1 properties are afforded by solutions to the one-dimensional problems.

In higher dimensions, pioneering work on non-critical dynamic effects in randomly dilute Heisenberg ferromagnets was done by Izyumov (1966), who solved exactly the problem of a single isolated magnetic impurity in an otherwise crystalline ferromagnet, and by Murray (1966), who treated the low-frequency, long-wavelength situation in the limit of low vacancy concentration using a variational approach. Murray's results were subsequently rederived by Kaneyoshi (1969) using a Green function perturbation theory, and by Edwards and Jones (1971) who also demonstrated the novel feature of an analytic interference series. Harris *et al* (1974) performed a CPA for ferromagnetic spin-waves at T=0 and evaluated response functions and density of states over a wide range of vacancy concentration. However CPA fails near the critical percolation threshold where fluctuations are dominant. Nickel (1974) calculated the first ten response function frequency moments for arbitrary wavevector and disorder and hence determined the response function itself numerically using a Pade approximant representation. In the critical region regular fractal models of these dilute systems have shown themselves amenable to exact analytic treatment (Harris and Stinchcombe 1983), and approximate scaling calculations have been performed for the real (random) system (see eg Stinchcombe 1985) from which approximations to the dynamical exponent for spin waves (see below) have been obtained.

In the present work we consider spin-waves in a ferromagnet near the critical concentration where a tenuous infinite cluster of connected magnetic sites exists. We use a continuum approach, valid in carefully defined low frequency regimes, to derive expressions for spin-wave life-time and transverse response functions.

Now, standard wavevector-space descriptions demonstrate that in pure, classical Heisenberg systems below the critical temperature, the low energy ferromagnetic excitations are propagating spin-waves (see eg Ashcroft and Mermin 1976). The dispersion relation for the excitation (or "characteristic") frequency ω_c at small

wavevector k is given in this case by

$$\omega_c = Dk^2 \qquad (7.1.1)$$

D is the normalised, lattice-dependent spin-wave stiffness coefficient and the result (7.1.1) holds in all dimensions.

When bond (or site) disorder is introduced, so that the system contains a fraction p of 'magnetic' bonds (or sites) and (1-p) non-magnetic ones, it has been established (Murray 1966) that spin-wave excitations persist above the percolation threshold. In such a system one may identify a *correlation length* ξ_p as, say, the root-mean-square size of the finite clusters (or, equivalently, of the voids) (Essam 1980) and it is evident that the nature of the dynamics will depend on the ratio

$$\frac{\xi_p}{\lambda} \propto k\xi_p \qquad (7.1.2)$$

Here λ is the spin-wave wavelength. One region of interest is the hydrodynamic, or effective medium, limit $k\xi_p \ll 1$. In this region slightly damped and therefore well defined spin-waves exist with dispersion relation (Brenig *et al* 1971)

$$\omega_c = D(p)k^2 \qquad (7.1.3)$$

D(p), the effective spin-wave stiffness, is a monotone increasing function of p and would appear to vanish at the percolation threshold p_c (mode softening). In fact, Kirkpatrick (1973) has demonstrated that D(p) is directly related to static properties of the percolating cluster by the equation

$$D(p) = \frac{\sigma(p)}{P(p)} \qquad (7.1.4)$$

where $\sigma(p)$ is the DC bulk conductivity of a dilute resistor network and P(p), the percolative order parameter, is the probability that a bond (site) is a member of the infinite cluster. Moreover, in the vicinity of the percolation threshold p_c, the singular behaviour of $\sigma(p)$ and P(p) is governed by certain universal critical exponents (Essam 1980) such that

$$\sigma(p) \propto (p-p_c)^t \qquad p \geq p_c$$

$$P(p) \propto (p-p_c)^{\beta} \qquad p \geq p_c \qquad (7.1.5)$$

where generally $t > \beta > 0$ and so one obtains

$$D(p) \propto (p-p_c)^{(t-\beta)} \qquad p \geq p_c \qquad (7.1.6)$$

The other regime of interest is the critical, or *fracton*, regime $k\xi_p \gg 1$. Here the divergence of the percolative correlation length ξ_p gives rise to anomalous dispersion making

$$\omega_c \propto k^z \qquad (7.1.7)$$

These two regimes are joined by a third, 'crossover', region $k\xi_p \sim 1$ in a manner described below and, assuming that the crossover is not discontinuous, 'matching' the extremal regimes across the crossover region leads to an exponent law relating z to static percolative exponents (Harris and Stinchcombe 1983; a similar argument has been given for the case of anomalous diffusion by Alexander and Orbach (1982), by Rammal and Toulouse (1982), and by Gefen *et al* (1983)).

However, as pointed out above, disorder not only renormalises the spin-wave dispersion law but also introduces damping and so the spin-waves develop a finite life-time. As the excitation spectrum is given by the complex poles of some appropriately defined Green function the characteristic frequency develops an imaginary part. We write by analogy with (7.1.3) and (7.1.7) the complex characteristic frequency $\Omega_c(k,\xi_p)$ as

$$\Omega_c(k,\xi_p) = \omega_c(k,\xi_p) + i\Gamma_c(k,\xi_p) \qquad (7.1.8)$$

where $\omega_c(k,\xi_p)$ takes its respective limiting forms (7.1.3),(7.1.7) for $k\xi_p \ll 1$ and $k\xi_p \gg 1$. $\Gamma_c(k,\xi_p)$ is the damping term and in this chapter we investigate the behaviour of this function and that of the rescaled damping Γ_c/ω_c, for $p \geq p_c$, by treating the hydrodynamic regime using a perturbation expansion, and extending into the critical regime by crossover arguments.

A plan of this chapter is as follows. For completeness, in section II we formally describe the model that we study. In section III we recall the consequences of the

dynamic scaling hypothesis (Halperin and Hohenberg 1969, Hohenberg and Halperin 1977) for the characteristic frequency ω_c and obtain a dynamic scaling form for the damping, or linewidth, Γ_c, in d>1. We proceed in section IV to determine the k and ξ_p dependence of the width in d>1 using a Green function approach applicable in the hydrodynamic regime. We also derive the form of the infinite cluster transverse dynamic structure function in this regime from which we extract the static and dynamic critical exponents η_t and z. An argument is presented in section V which relates the critical exponents arising from the response of the ensemble of finite clusters to those obtained for the infinite cluster response. In section VI we use a multicritical scaling ansatz for the correlation length to determine the behaviour of the spin-wave damping at non-zero temperature. Finally, in the discussion section, we first gather all our results together, to make them easily accessible for experimental comparisons. We then indicate the relation between bond and site dilution as far as spin-wave damping is concerned and make explicit the difference between d=1 and d>1.

II. The Model

We consider the spin dynamics of a d-dimensional (d>1) bond-diluted isotropic Heisenberg ferromagnet at zero temperature in the presence of a time- and site-dependent reduced transverse field $\underline{h}_i$. The Hamiltonian for this system is

$$H = - \sum_{<ij>} J_{ij}\, \underline{S}_i \cdot \underline{S}_j - \sum_i \underline{h}_i \cdot \underline{S}_i \quad . \qquad (7.2.1)$$

The spins $\underline{S}_i$ are taken to be classical spins (S large) normalised to unity. The exchange couplings J_{ij} act only between nearest neighbours and are independent random variables with the following binary probability distribution

$$P(J_{ij}) = (1-p)\, \delta(J_{ij}) + p\, \delta(J_{ij}-J) \qquad (7.2.2)$$

p is the bond occupation probability, and we set J>0 for ferromagnetic coupling.

Using the standard methods, the linearised equations of motion derived from (7.2.1) are

$$-i \frac{d}{dt} S_i^+(t) = h_i^+ + \sum_{<ij>} J_{ij}\, (S_j^+ - S_i^+) \qquad (7.2.3)$$

S^+_i is the usual combination ($S^+_i \equiv S^x_i + iS^y_i$) of the transverse spin components at site i and the summation in (7.2.3) is taken over the nearest neighbours of i. This is the equation governing transverse (spin-wave) dynamics, and it would be trivial without the randomness of the J_{ij}.

III. Consequences of Dynamic Scaling for the Decay Rate, Γ_c, of Spin-Waves near the Percolation Threshold p_c

We define the transverse dynamic structure function $\chi(k,\omega,\xi)$,

$$\chi(k,\omega,\xi) = \langle S^+_k S^-_{-k} \rangle \qquad (7.3.1)$$

where $\langle \ldots \rangle$ denotes averaging over *disorder* (rather than thermal) configuration. As we are interested in the zero temperature dynamics, the correlation length ξ is here the percolation-correlation length. The dynamic scaling hypothesis (Halperin and Hohenberg 1977) for a system in the vicinity of a continuous phase transition (ξ large) states that $\chi(k,\omega,\xi)$ may be written, for small k,ω, as a homogeneous function of two arguments

$$\chi(k,\omega,\xi) = k^{-(2-\eta_t+z)} F(k\xi, \omega k^{-z}) \qquad (k,\omega,1/\xi \to 0) \qquad (7.3.2)$$

where η_t is the exponent characterising the decay of instantaneous transverse correlations and z is the dynamic critical exponent. F(x,y) is some arbitrary homogeneous scaling function. Interest in the dynamic structure function arises primarily in the context of inelastic neutron scattering experiments: the measured inelastic differential scattering cross-section is proportional to $\chi(k,\omega,\xi)$.

The n^{th} moment $\langle \omega^n \rangle$ of χ is defined by

$$\langle \omega^n \rangle \equiv \frac{\int \chi(k,\omega,\xi)\ \omega^n\ d\omega}{\int \chi(k,\omega,\xi)\ d\omega} \qquad (7.3.3)$$

Then the dynamic scaling hypothesis implies that there exists a sequence of scaling functions $\{f_i\}$ such that

$$\langle \omega^n \rangle = k^{nz} f_n(k\xi) \qquad (7.3.4)$$

In particular one may define the characteristic frequency ω_c and width, or damping, Γ_c as follows,

$$\omega_c = \langle\omega\rangle$$

$$\Gamma_c = \{ \langle\omega^2\rangle - \langle\omega\rangle^2 \}^{\frac{1}{2}} \qquad (7.3.5)$$

So, using (7.3.4), we conclude that ω_c and Γ_c may be written in the following scaling forms,

$$\omega_c = k^z f_1(k\xi)$$

$$\Gamma_c = k^z g(k\xi) \qquad (7.3.6)$$

where $g(x)=\sqrt{(f_2(x)-f_1^2(x))}$. The forms (7.3.6) apply throughout the range of $k\xi$, provided only $k,1/\xi$ are both small; in particular the considerations in the introduction require $f_1(x)\to$constant as $x\to\infty$ and $f_1(x)\to x^{2-z}$ as $x\to 0$. Equating this form for ω_c in the hydrodynamic limit to expression (7.1.3) and using (7.1.6) leads to the exponent law (Alexander and Orbach 1982, Rammal and Toulouse 1982, Gefen *et al* 1983, Harris and Stinchcombe 1983)

$$z = 2 + (t-\beta)/\nu \qquad (7.3.7)$$

In deriving (7.3.7) it is tacitly assumed that no 'fracton' discontinuity exists in the density of spin-wave states thereby allowing the use of such crossover arguments. Should such a fracton edge exist (Entin-Wohlman *et al* 1984) then relations such as (7.3.7) will come under question.

Further, information on the asymptotic properties of g(x) will, through the ratio Γ_c/ω_c, reveal the nature of the attenuation of spin-waves in the hydrodynamic and critical regimes. We obtain this information for the hydrodynamic region in section IV.

Now, from the discussion in the introduction of this chapter we expect from (7.1.8) by analogy with (7.1.3) the following form for $\Gamma_c(k,\xi)$ in the hydrodynamic regime $k\xi \ll 1$:

$$\Gamma_c(k,\xi) = \gamma(p)k^a \propto (p-p_c)^{-\mu} k^a \propto k^{a-\mu/\nu}(k\xi)^{\mu/\nu} \qquad (7.3.8)$$

This implies, using (7.3.6) and (7.3.7), that

$$\mu = (a-2)\nu - (t-\beta) \qquad (7.3.9)$$

This is a constraint on the exponents a and μ imposed by the scaling form (7.3.6), ie only one of the exponents is independent. Although a and μ will be universal, we do

expect them to be dependent on embedding dimensionality.

In the following section we use a Green function formalism to determine a and μ.

IV. Green Function Calculation on Continuum Equations of Motion

We now focus our attention on the linearised spin-wave equation of motion (7.2.3). In the limit $ka \ll 1$ and $k\xi \ll 1$, where a is the lattice parameter, one may legitimately adopt a continuum viewpoint in which the difference equation (7.2.3) becomes, for a hypercubic lattice, the following partial differential equation,

$$-i\frac{\partial u(\underline{r},t)}{\partial t} = h(\underline{r},t) + D(\underline{r})\,\nabla^2 u(\underline{r},t) + \underline{\nabla} D(\underline{r}).\underline{\nabla} u(\underline{r},t) \tag{7.4.1}$$

where $S_i^+(t) \to u(\underline{r},t)$, $h_i^+(t) \to h(\underline{r},t)$ and $a^2 J_{ij} \to D(\underline{r})$. $D(\underline{r})$ is here the configuration dependent local spin-wave stiffness coefficient. This is seen to be the case by recalling that there exists an isomorphism between dilute linear dynamics and the resistor network problem (Last 1972). Within this isomorphism $a^2 J_{ij}$ is the analogue of σ_{ij}/C (σ_{ij}, the bond conductivity; C, the capacitance at each site) and P(p) is the analogue of C. Therefore, in the dynamical situation, it follows from (7.1.4) that $a^2 J_{ij}$ becomes $D(\underline{r})$ in the continuum limit as required. $D(\underline{r})$ fluctuates about its configurational average value $\langle D \rangle$ over a length scale determined by the correlation length ξ.

We may write (7.4.1) as

$$-i\frac{\partial u(\underline{r},t)}{\partial t} = h(\underline{r},t) + \underline{\nabla}.((D(\underline{r})-\langle D\rangle)\underline{\nabla} u(\underline{r},t)) + \langle D\rangle \nabla^2 u(\underline{r},t) \tag{7.4.2}$$

which yields the following Green function equation of motion,

$$(\omega - \langle D\rangle k^2)\, G(\underline{k},\underline{k}";\omega) = \int \{\Delta(\underline{k}-\underline{k}')\underline{k}.\underline{k}'\} G(\underline{k}',\underline{k}";\omega) \frac{d^d\underline{k}'}{(2\pi)^d} + \delta(\underline{k}-\underline{k}") \tag{7.4.3}$$

where $G(\underline{k},\underline{k}';\omega)$ is defined by

$$\varphi(\underline{k},\omega) = \int H(\underline{k}',\omega) G(\underline{k},\underline{k}';\omega)\, d^d\underline{k}' \tag{7.4.4}$$

and $\varphi(\underline{k},\omega)$ is the space and time Fourier transform of $u(\underline{r},t)$. The momentum space integrations are taken over the first Brillouin zone. $\Delta(q)$ is the space Fourier transform

of the fluctuation in spin-wave stiffness,

$$\Delta(\underline{q}) = \int e^{i\underline{q}.\underline{r}}(D(\underline{r})-\langle D\rangle)d^d\underline{r} \qquad (7.4.5)$$

$H(\underline{k},\omega)$ is the negative of the Fourier transform of $h(\underline{r},t)$.

In the manner described in Appendix K, (7.4.3) may be written formally as a self-consistent equation for $G(\underline{k},\underline{k}';\omega)$ by introducing the unperturbed Green function $G^0(\underline{k},\underline{k}';\omega)$ and the vertex interaction $V(\underline{k},\underline{k}')$ (both defined in the appendix K),

$$\underline{\underline{G}} = \underline{\underline{G}}^0 + \underline{\underline{G}}^0\underline{\underline{V}}\underline{\underline{G}} \qquad (7.4.6)$$

$G^0(\underline{k},\underline{k}';\omega)$ describes unattenuated spin-waves in a 'mean lattice' with renormalised spin-wave stiffness $\langle D\rangle=D(p)$ and so it constitutes a virtual crystal approximation to the problem. An integration (or summation in the corresponding discrete calculation) over internal wave vectors is understood in the G^0VG term.

Using $\langle\ldots\rangle$, as before, to denote configurational average we define the self energy $\Sigma(k,\omega,\xi)$ by

$$\langle G\rangle = G^0 + G^0\Sigma\langle G\rangle \qquad (7.4.7)$$

The configurational average restores translational invariance and so we denote $\langle G(\underline{k},\underline{k}';\omega)\rangle \equiv \delta(\underline{k}-\underline{k}')\langle G(\underline{k};\omega)\rangle$. Σ can be obtained, formally, by a diagrammatic method similar to that introduced by Edwards (1958). In principle a summation of terms to all orders is required. However, in the hydrodynamic regime $k\xi \ll 1$ it is possible (Appendix K) to identify the (power law) dependence of each diagram contribution on k,ξ and also the corresponding dependence on fluctuations in $D(\underline{r})$ in terms of a product of cumulants of the renormalised fluctuation variable $((D(\underline{r})/\langle D\rangle)-1)$. In this way it can be shown that for $k\xi \ll 1$ the dominant contribution to the self energy is provided by the term of second order in V, namely

$$\Sigma(\underline{k},\omega,\xi) = \int \frac{\langle |\Delta(\underline{k}-\underline{k}')|^2\rangle (\underline{k}.\underline{k}')^2}{(\omega-\langle D\rangle k'^2)} \frac{d^d\underline{k}'}{(2\pi)^d} \qquad (7.4.8)$$

As demonstrated in the appendix K we extract the spin wave decay rate from

$$\Gamma_c(\underline{k},\xi) = \lim_{\epsilon\to 0} (\mathrm{Im}\ \Sigma(\underline{k},\omega+i\epsilon,\xi)) \qquad (7.4.9)$$

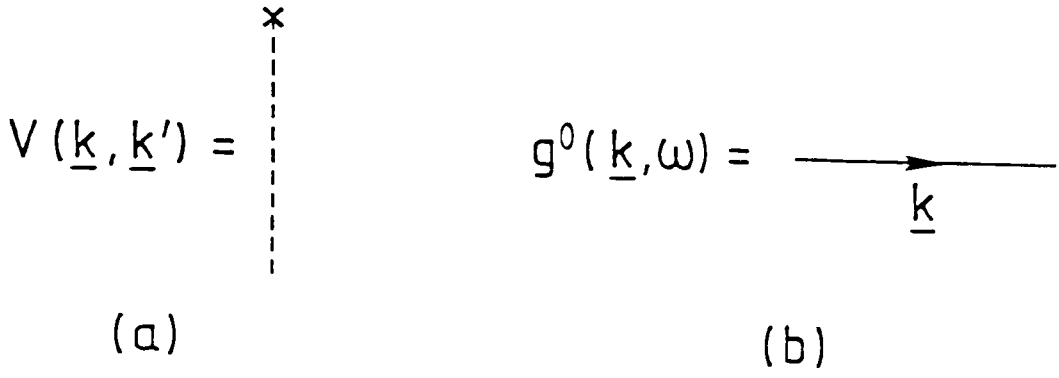

Fig.7.1.: Diagrammatic representations for a) the vertex interaction $V(\underline{k},\underline{k}')$ and b) the unperturbed propagator.

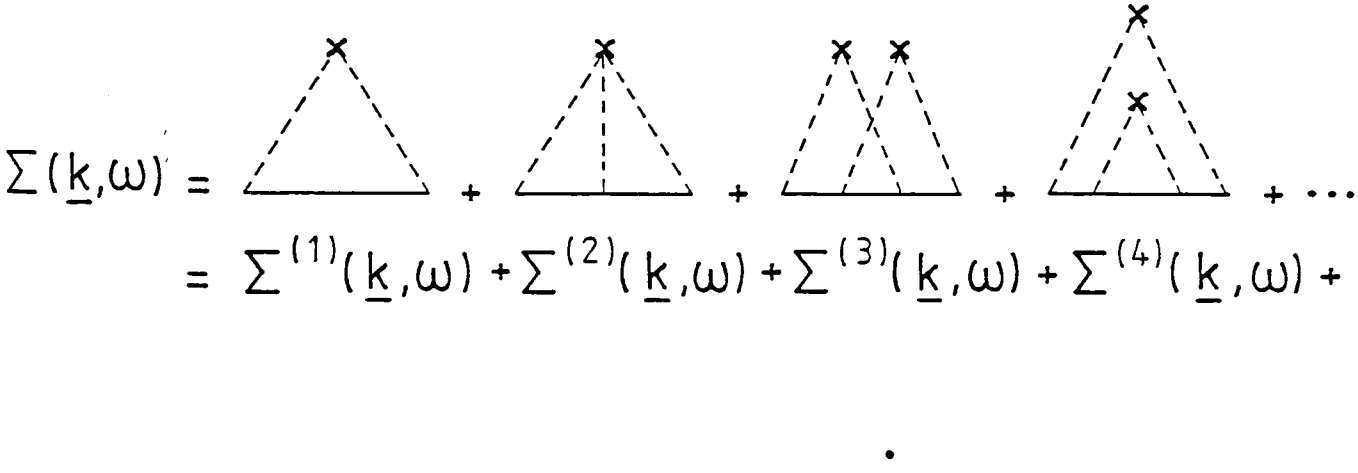

Fig.7.2.: The diagrammatic expansion for the self energy $\Sigma(\underline{k},\omega)$. The infinite series consists of all possible irreducible diagrams constructed from propagators and vertices defined in fig.7.1. We label the selection of diagrams shown by $\Sigma^1(\underline{k},\omega),\ldots, \Sigma^4(\underline{k},\omega)$ respectively.

and so we arrive at the following leading order form for Γ_c,

$$\Gamma_c(\underline{k},\xi) = \int <|\Delta(\underline{k}-\underline{k}')|^2>(\underline{k}.\underline{k}')^2\delta(\omega-<D>k'^2)\ \frac{d^d\underline{k}'}{(2\pi)^d}\ [1+O(k\xi)]$$

$$k\xi \ll 1 \qquad (7.4.10)$$

To obtain the $(p-p_c)$ dependence of Γ_c we use the following scaling ansatz for the n-point spin-wave stiffness correlation function,

$$< (D(\underline{r}_1)-<D>)(D(\underline{r}_2)-<D>)\ldots(D(\underline{r}_n)-<D>) >$$

$$= \xi^{-n(t-\beta)/\nu}\ L(\ (\underline{r}_1-\underline{r}_2)/\xi, (\underline{r}_2-\underline{r}_3)/\xi, \ldots, (\underline{r}_{n-1}-\underline{r}_n)/\xi) \qquad (7.4.11)$$

where $L(a_1,\ldots,a_{n-1})$ is some scaling function. (7.4.11) also expresses the fact that translational invariance is restored by the configurational averaging.

In the case of low vacancy concentration (cf Edwards and Jones 1971) the role of the spin-wave stiffness correlation functions $<\{\prod(D(\underline{r}_i)-<D>)\}>$ is replaced by $<\{\prod(J_{ij}-pJ)\}>$. The latter average depends only on whether some of the defect bonds coincide and vanishes if any particular bond occurs only once. In the present problem, correlations extend to a distance $\sim\xi$ and so, by analogy, the average product $<\{\prod(D(\underline{r}_i)-<D>)\}>$ depends only on whether the scattering centres $\underline{r}_i$ are within a distance ξ of one another and vanishes if any particular centre is greater than a distance ξ (the average size of the larger voids) from any other. One may therefore interpret the scattering involved in the diagram expansion to result from *clusters* with linear dimension ξ much smaller than the wavelength λ of the spin-wave ($k\xi \ll 1$). Therefore associated with the diagram $\Sigma^{(1)}(\underline{k},\omega)$, say, is the factor $<(D(\underline{r})-<D>)^2>/<D>$, whilst associated with $\Sigma^{(4)}(\underline{k},\omega)$ is a term $<(D(\underline{r})-<D>))^2>^2/<D>^3$, etc. In the continuum approximation, local averages are understood which, in effect, 'iron out' the fluctuations of $D(\underline{r})$, giving $|((D(\underline{r})/<D>)-1)| \ll 1$. We show below that it is this effect, together with $k\xi \ll 1$, that ensures the convergence of the perturbation theory.

Using (7.4.11), via (7.4.5), together with (7.1.6) and some changes of integration variable, to evaluate (7.4.10) we find that the dependence of the spin-wave damping Γ_c on k and $(p-p_c)$ (or ξ), and $(D(\underline{r})/<D>)-1$ is given (see Appendix K) in the

hydrodynamic limit by

$$\Gamma_c(\underline{k},\xi) \propto \frac{\langle (D(r)-\langle D\rangle)^2\rangle}{\langle D\rangle} (p-p_c)^{-\nu d} k^{d+2} \qquad k\xi \ll 1$$

$$\propto (p-p_c)^{-\nu d+(t-\beta)} k^{d+2} \qquad (7.4.12)$$

The result (7.4.12) is consistent with the relation (7.3.9), which of course is a necessary condition for the validity of dynamic scaling for the transverse dynamic structure function. Using the relation $\xi \sim (p-p_c)^{-\nu}$ and the scaling law (7.3.6) together with the relation (7.3.7), the result (7.4.12) corresponds to $g(x) \to x^{d-((t-\beta)/\nu)}$ for $x \to 0$.

Using (7.4.11) the diagram contributions of perturbation theory are , for general $k\xi$, consistent with $\Sigma(\omega_c)=k^z F(k\xi)$, with z given by (7.3.7), which shows how dynamic scaling arises with the use of the 'geometric' scaling (7.4.11).

We note that the perturbation theory is valid (see Appendix K) only for $k\xi \ll 1$ and so it cannot give the form of $g(k\xi)$ for large $k\xi$, which is required for full knowledge of the spin-wave damping in the critical regime $k\xi \gg 1$. However it is possible that g(x) becomes a power of x at large x, in which case the damping becomes, for $k\xi \gg 1$,

$$\Gamma_c(\underline{k},\xi) \propto k^z (k\xi)^{\alpha} \qquad (7.4.13)$$

Further work needs to be done to determine α. The properties of Γ_c/ω_c at p_c will indicate whether spin-waves at p_c are localised ($\alpha>0$), damped ($\alpha=0$) or propagating without attenuation ($\alpha<0$). In Appendix N we calculate Γ_c in the critical regime for the one-dimensional case and we find,

$$\Gamma_c(\underline{k},\xi) \propto k^z (k\xi)^{-1} \qquad (7.4.14)$$

and so we identify $\alpha=-1$. This is less than zero, as expected, since $k\xi \gg 1$ is the pure limit in one dimension.

The perturbation theory described in Appendix K also yields information concerning the response function itself in the hydrodynamic limit. An explicit expression for χ is obtained in the hydrodynamic regime (see Appendix L) and has the following form,

$$\chi(k,\omega,\xi) = \lim_{\epsilon \to 0} \left(\mathrm{Im} \langle G(\underline{k},\omega+i\epsilon)\rangle \right)$$

$$= k^{-(2-\eta_t+z)} F(k\xi, \omega k^{-z}) \qquad (7.4.15)$$

where $$F(x,y) = \frac{x^{2+d-z}}{(y-x^{2-z})^2 + (x^{2+d-z})^2} \qquad (7.4.16)$$

and we observe that $\eta_t=2$, and $z=2+(t-\beta)/\nu$ for the bond-diluted system.

Regarding $x=k\xi$ as a parameter, the response χ (7.4.15) in the hydrodynamic regime is therefore a Lorentzian centered about the characteristic frequency $\omega_c \propto k^z(k\xi)^{2-z}$ and with width $\Gamma_c \propto k^z(k\xi)^{2-z+d}$. Thus $(\Gamma_c/\omega_c)=(k\xi)^d \to 0$ as $k\xi \to 0$; the extreme limit $k\xi=0$ represents an effective medium situation in which the spin-wave response is a delta function and so the spin-waves are renormalised but are not attenuated.

The form (7.4.16) for the hydrodynamic response function indeed satisfies the dynamic scaling hypothesis (7.3.2). We remark however that the critical exponents derived above arise from the response of the infinite cluster alone to the applied transverse field. In the following section we consider the response due to the finite clusters in order to find the exponents η_t' and z' for the full system.

V. Critical Exponents for the Ensemble of Finite Clusters

Near the percolation threshold, p_c, the fraction of sites in the infinite cluster is vanishingly small ($\beta>0$). The response to external fields will be dominated by the large but finite clusters. Indeed the exponents observed in a typical experiment on a dilute ferromagnet near p_c will be those arising from the finite cluster response (except for obvious exceptions, like magnetisation, which depend entirely on the presence of the infinite cluster).

In this section we relate the critical exponents resulting from the response of the ensemble of finite clusters to those obtained above for the infinite cluster.

Consider a finite cluster containing s connected sites. The method that we use to determine the finite cluster response relies on the following premise: that on length scales much smaller than the linear dimensions of the cluster, it will have thermostatic and dynamical properties identical to those of the infinite cluster. As we demonstrate in Appendix M this leads to a relation between $\chi_f(k,\omega,\xi)$, the transverse response function

for the finite cluster ensemble and $\chi(k,\omega,\xi)$, the infinite cluster response, which is the function that we have been dealing with hitherto. Allowing for modes up to some arbitrary frequency ω_0, and considering finite clusters of size greater than the minimum required to support such low frequency modes, we obtain (Appendix M),

$$\int\int^{\omega_0} \chi_f(k,\omega,\xi)\, d^d\underline{k}d\omega \quad \propto \int\int^{\omega_0} \chi(k,\omega,\xi)\ \omega_0^{\,d_f/\delta d_w}\ d^d\underline{k}d\omega \qquad (7.5.1)$$

We next differentiate (7.5.1) with respect to ω_0 and assign the scaling form (7.3.2) to χ and a similar form to χ_f :

$$\chi_f(k,\omega,\xi) \;=\; k^{-(2-\eta_t'+z')}\, F(k\xi, \omega k^{-z'}) \qquad (7.5.2)$$

As we indicate in the Appendix M, from (7.5.1) and (7.5.2) it follows that

$$\eta_t' \;=\; \eta_t + \beta/\nu \;=\; 2 + \beta/\nu \qquad \text{and}$$

$$z' \;=\; z \;=\; 2 + (t-\beta)/\nu \qquad (7.5.3)$$

for a bond-dilute system, ie the infinite and finite clusters share the same dynamic exponent z but have different values of η_t. However $\beta/\nu = d - d_f$, the difference between embedding dimension d and the fractal dimension d_f (Mandelbrot 1982) of the infinite cluster, is small for two and three dimensional percolation clusters and so the difference between infinite and finite cluster critical effects will be correspondingly small.

VI. Spin-Wave Damping Near a Multicritical Point

It has been implicit in our discussion thus far that the dynamics has been at zero temperature. We now determine the temperature dependence of the spin-wave damping at p_c for a diluted Heisenberg ferromagnet in d>2 dimensions by considering $(p-p_c=0, T=0)$ to be a multicritical point in a two-dimensional parameter space $(p-p_c, T)$. Near this point one may write the correlation length (Stinchcombe 1983, Kumar 1984),

$$\xi \;\sim\; (p-p_c)^{-\nu}\, B\left[\frac{T}{(p-p_c)^{\varphi}}\right] \qquad (7.6.1)$$

B(x) being a scaling function with the following asymptotic properties,

$$B(x) \to B_0 \qquad x \to 0$$

$$\to B_\infty x^{-\nu/\varphi} \qquad x \to \infty \qquad (7.6.2)$$

In (7.6.1) ν is the percolation-correlation length exponent, as before; φ is the

percolation-thermal 'crossover index', and it is actually equal to the conductivity exponent t in (7.1.5) (Stinchcombe 1979, Coniglio 1981). In two dimensions a form analogous to (7.6.1) will apply in the limit of vanishing anisotropy (Stinchcombe 1983, Kumar 1984).

Provided standard dynamic scaling arguments still apply, in which the criticality is controlled by the ratio of a single correlation length to the wavelength, (7.3.6) still holds at non-zero temperature; however ξ is not now simply the percolation-correlation length ξ_p, but is given instead by (7.6.1). In this case,

$$\Gamma_c = k^z g(k\xi) \qquad (7.6.3)$$

while the scaling function g(x) has the following hydrodynamic limiting form,

$$g(x) \to g_0 x^{2+d-z} \qquad x \to 0 \qquad (7.6.4)$$

We identify two distinct hydrodynamic regimes of interest. Consider the long wavelength behaviour of the width in the following two limits:

$$0 < (p-p_c) \ll 1 \quad , \quad T=0 \qquad (7.6.5)$$

$$(p-p_c)=0 \quad , \quad 0 < T \ll 1 \qquad (7.6.6)$$

The limit (7.6.5) corresponds to the zero temperature situation considered earlier and using (7.6.1),(7.6.2),(7.6.3),(7.6.4) we recover the result

$$\Gamma_c \propto (p-p_c)^{-(d+2-z)\nu} k^{d+2} \qquad (7.6.7)$$

(which can be regarded as a justification for the use of the same power in (7.6.4) as that occurring in the hydrodynamic limit in the previous section of this chapter). The limit (7.6.6) gives (using (7.6.1)-(7.6.4)) the low-temperature behaviour for the width at $p=p_c$,

$$\Gamma_c \propto [T^{-(d+2-z)\nu/\varphi}] k^{d+2}. \qquad (7.6.8)$$

However in the same limit (7.6.6) the characteristic frequency ω_c takes the form $\omega_c \propto T^{-(2-z)\nu/\varphi} k^2$ and so $(\Gamma_c/\omega_c) = T^{-\nu d/\varphi} k^d \propto (k\xi)^d \to 0$ as $k\xi \to 0$ as before.

Finally, we remark that dynamic scaling for Γ_c appears to be violated (Henley 1985, Harris and Stinchcombe 1985, Stinchcombe 1985, Jain 1986) for Ising magnets in $d>1$ at the percolation threshold as $T \to 0$. The breakdown of the dynamic scaling principle in Ising systems, however, results from the suppression of domain boundary diffusion at percolation cluster branchings owing to activation difficulty. The mechanism for this rate

suppression clearly does not exist in the (isotropic Heisenberg) systems studied here and so we expect that the assumption used to introduce (7.6.3) is here valid, together with the consequences, particularly (7.6.8), just discussed. The generalisation to the anisotropic Heisenberg model is discussed in Chapter 8, and here dynamic scaling will be seen to break down for the same basic reasons as in the Ising case.

VII. Summary and Discussion

We conclude this chapter with a short summary followed by a discussion of some of the issues raised by the text.

This work has addressed the problem of the decay of spin-wave excitations in a substitutionally disordered d-dimensional (isotropic) Heisenberg ferromagnet near the percolation threshold where the dynamics depends crucially on the ratio $\xi_p/\lambda \propto k\xi_p$. Use of a diagrammatic perturbation theory together with a scaling ansatz applied to the spin-wave stiffness correlation function allowed the evaluation of the k and ξ dependence of the spin-wave damping $\Gamma_c(k,\omega,\xi)$ for excitations on the infinite cluster in an appropriate ($k\xi \ll 1$) hydrodynamic regime. We obtain,

$$\Gamma_c(k,\xi) \propto (p-p_c)^{-\nu d+(t-\beta)} k^{d+2} \qquad (7.7.1)$$

The result (7.7.1) is consistent with the dynamic scaling principle of Halperin and Hohenberg (1969). This states that the transverse dynamic structure function χ has the following homogeneous form,

$$\chi(k,\omega,\xi) = k^{-(2-\eta_t+z)} F(k\xi, \omega k^{-z}) \qquad (7.7.2)$$

and implies the following scaling behaviour for the characteristic frequency ω_c and damping Γ_c, at general $k\xi$

$$\omega_c = k^z f(k\xi) \qquad \Gamma_c = k^z g(k\xi)$$

such that $\omega_c \propto k^z \qquad k\xi \gg 1$

and $\omega_c \propto k^z (k\xi)^{2-z} \qquad k\xi \ll 1. \qquad (7.7.3)$

Equating the latter form with $\omega_c = D(p)k^2 = (p-p_c)^{(t-\beta)} k^2$ (Brenig *et al* 1971, Kirkpatrick 1973) yields $z=2+(t-\beta)/\nu$. We infer from our calculation that $g(k\xi) \to (k\xi)^{d+2-z}$ for $k\xi \ll 1$. Further, supposing g(x) to take a power law form in the

critical regime ($k\xi$ large) as well, one obtains

$$\Gamma_c(k,\xi) \propto k^z(k\xi)^\alpha \qquad k\xi \gg 1 \qquad (7.7.4)$$

As indicated in section IV, the calculation of the exponent α will yield important information relating to the existence of localised excitations at p_c.

The perturbation theory also yielded a closed form expression for the transverse dynamic structure factor in this regime; for the scaling function F(x,y) we obtain,

$$F(x,y) = \frac{x^{2+d-z}}{(y-x^{2-z})^2 + (x^{2+d-z})^2} \qquad (7.7.5)$$

from which we were able to identify the critical exponents $\eta_t=2$ and $z=2+(t-\beta)/\nu$.

In section V we used finite size scaling ideas to deduce the exponents $\eta_t'=\eta_t+(\beta/\nu)$ and $z'=z$ for the finite cluster response in terms of those found above for the infinite cluster. Finally, in section VI we used a multicritical scaling assumption for the decay rate Γ_c, such that

$$\Gamma_c(k,\xi) = k^z g(k\xi) \qquad (7.7.6)$$

where now ξ is a function of temperature T as well as $(p-p_c)$ given by the crossover form,

$$\xi \sim (p-p_c)^{-\nu} B\left[\frac{T}{(p-p_c)^{\varphi}}\right] \qquad (7.7.7)$$

and, using the results of section IV were able to determine the following temperature dependent behaviour in the hydrodynamic regime at $p=p_c$, $0<T\ll 1$, $k\xi \ll 1$,

$$\Gamma_c \propto T^{-(2+d-z)\nu/\varphi} k^{d+2} \qquad (7.7.6a)$$

More relevant to a possible experimental situation is the corresponding site diluted system. In the case of random site dilution the Green function solution to the equations of motion is analogous to (K10). However, averaging over site disorder configuration introduces a multiplicative factor P(p) into the Green function. This is easily seen to be the case by considering the response of the infinite cluster to a uniform field (k=0). Therefore, for a site-diluted system with a site-dependent oscillating field, we obtain (cf (K10)),

$$\langle G(\underline{k},\underline{k}';\omega)\rangle = \frac{\delta_{\underline{k},\underline{k}'}\ P(p)}{\omega - (\langle D\rangle k^2+\Sigma(\underline{k},\omega))} \qquad (7.7.8)$$

(7.7.2) in turn implies for the site-diluted infinite cluster response function, the following scaling form,

$$\chi^{site}(k,\omega,\xi) = k^{-(2-\eta_t{}^{site}+z^{site})}\ F(k\xi,\omega k^{-z^{site}})$$

$$\text{where}\quad F(x,y) = \frac{x^{(2+d-z-\beta/\nu)}}{(y-x^{2-z})^2 + (x^{2+d-z})^2} \qquad (7.7.9)$$

and so we identify $\eta_t{}^{site} = 2+\beta/\nu$ and the scaling law (7.3.7) for the dynamical exponent $z^{site} = 2+(t-\beta)/\nu$ still applies. Furthermore, the arguments presented in section V remain valid for the case of site dilution and so,

$$\eta_t{}'^{site} = \eta_t + \beta/\nu = 2\ (1+\beta/\nu) \qquad \text{and}$$

$$z'^{site} = z = 2 + (t-\beta)/\nu \qquad (7.7.10)$$

are the index relations for the site diluted finite cluster response.

The inclusion of finite cluster response is important, in an experimental context, if scattering measurements are being made particularly close to, or below, the percolation threshold p_c. Even then, the dynamics does not appear to be altered significantly: η_t is enhanced only by a small factor β/ν and z is unchanged

In the introduction we asserted that the dilution- induced one dimensional dynamics is distinct in certain crucial respects from that in higher dimensions. The reason for this exceptional d=1 dynamics is that the percolation threshold p_c in one dimension is equal to unity : below p_c=1 the chain breaks up into disjoint, finite segments. This has two main dynamical consequences. Firstly, the critical, 'anomalous', regime is not anomalous at all as there is no fractal infinite cluster such as normally governs the anomalous side of the crossover. In fact as $k\xi\to\infty$ one is approaching the pure chain limit and the response to a transverse field is a Lorentzian centered at ω_c with half-width Γ_c given by (see Appendix N and Stinchcombe and Harris 1983),

$$\omega_c \propto k^2$$

$$\Gamma_c \propto k^2(k\xi)^{-1}$$

$$\text{and therefore}\qquad (\Gamma_c/\omega_c) = (k\xi)^{-1} \xrightarrow[k\xi\to\infty]{} 0 \qquad (7.7.11)$$

The damping vanishes in the critical limit and there exist propagating spin-waves with unrenormalised spin-wave stiffness Ja^2. From (7.4.4) and (7.4.6) we identify the one dimensional dynamic exponent $z=2$ and note that this is merely the pure, spin-wave value. Secondly, in the hydrodynamic regime, the response arises entirely from chain segments very much smaller than the wavelength $\lambda=2\pi/k$ of the forcing field and the scattering is dominated by a broad, smeared response (see Appendix N). The effective medium behaviour observed in higher dimensions for $k\xi \ll 1$ cannot occur in one dimension and the reduced damping Γ_c/ω_c tends to a constant non-zero value (Appendix N).

In contrast, in higher dimensions, the percolation threshold p_c, is strictly less than unity. An infinite cluster exists with fractal dimension $d_f<d$ which controls the anomalous dynamics for $k\xi \gg 1$ and gives rise to a dynamic exponent $z=2+(t-\beta)/\nu=d_w$ (Rammal and Toulouse 1982) strictly greater than two. Here d_w is the random walk dimension for the infinite percolation cluster (Stanley *et al* 1982). Further, in the hydrodynamic limit, the dynamic structure function exhibits not the broad response seen in the one dimensional instance but instead a Lorentzian response (L2) that tends to a delta function as $(k\xi)\to 0$, for $d>1$,

$$\lim_{k\xi\to 0}\left[\frac{\Gamma_c}{\omega_c}\right] = \lim_{k\xi\to 0}\left[\frac{(p-p_c)^{-\nu d+(t-\beta)}\, k^{d+2}}{(p-p_c)^{t-\beta}\, k^2}\right] = 0 \qquad (7.7.12)$$

This disappearance of the damping is the result of the effective medium behaviour alluded to above; the damping vanishes and the spin-wave stiffness is renormalised by a factor $D(p)/D(1)$.

The explicit calculations have been carried out for the hydrodynamic region where perturbation from unattenuated spin-waves was ideal, the self energy being much smaller than the $\langle D\rangle k^2$ term in the Green function denominator. Though this gives scaling statements related to the full crossover, detailed forms for the scaling function in the critical regime are still unknown and are the subject of continuing work.

The analogous calculations to those given in this chapter have been carried out for two sublattice systems, namely the antiferromagnet and ferrimagnet on hypercubic lattices. These calculations are summarised in Appendix P.

Chapter 8

Bloch Walls and Anomalous Longitudinal Glauber Dynamics of Dilute Anisotropic Magnets at the Percolation Threshold.

The relaxational dynamics of the d-dimensional, classical anisotropic Heisenberg (Ising-Heisenberg) model near the percolation bicritical point ($p=p_c, T=0$) is considered. As in the corresponding Ising system, the relevant physical process involves the activation of domain walls over a hierarchy of energy barriers. In this system the domain boundaries are quasi-one-dimensional Bloch walls and we show that a simple scaling theory gives exact results for the Bloch wall energy and length across the whole range of anisotropy. These results are used to derive explicit expressions for the characteristic time τ_c in the various scaling regimes of interest. In particular, it is found that the conventional dynamic scaling hypothesis for τ_c is violated at sufficiently low temperatures in all cases of non-vanishing anisotropy, and the crossover to this new *singular dynamic scaling* behaviour is demonstrated explicitly. This work has been submitted to Phys. Rev. B. (Christou and Stinchcombe 1987).

I. Introduction

In this chapter we investigate the non-linear dynamic critical properties of the bond diluted anisotropic Heisenberg (Ising-Heisenberg) ferromagnet paying particular attention to the activation of non-linear kink excitations (Mikeska 1981) across the percolation cluster nodes (de Gennes 1976, Skal and Shkovskii 1975).

Study of the problem is motivated by various considerations. Firstly, dilute magnets, characterised by relatively simple Hamiltonians, are often amenable to experimental and analytic study and have yielded rich dilution-induced critical behaviour for thermostatic properties (see eg Stinchcombe 1983). Further, in more recent years considerable interest has been focussed on *linear* dynamical phenomena near the percolation transition (Alexander and Orbach 1982, Rammal and Toulouse 1983). Such diverse problems as

random walks, lattice vibrations, Glauber-Ising dynamics (Glauber 1963) and spin-waves (see chapter seven and appendix P of this thesis) are in fact governed by linear equations of motion which are isomorphic under a mapping of the frequency variable and much is now known about these problems on percolation clusters (Alexander and Orbach 1982, Rammal and Toulouse 1983) and other self-similar, non-Euclidean structures (Family 1983 [lattice animals] and chapter three of this thesis [SAWs] and appendix B [DLA]). Non-linear phenomena are inherently more difficult to deal with and much less is known about these.

Now, relaxational dynamics in disordered anisotropic spin systems is a non-linear process (Gefen *et al* 1980). Recently, attention was drawn to this area by the neutron scattering experiment of Aeppli *et al* (1984) on the quasi-two-dimensional layer Ising magnet $Rb_2(Mg_{1-p}Co_p)F_4$ near the percolation threshold of the magnetic cobalt ions (p_c=0.59) and at very low temperatures T. According to the dynamic scaling hypothesis of Hohenberg and Halperin (1977), the frequency moments of the time-delayed density-density correlation function near criticality are homogeneous functions of degree z in the wavevector k and inverse correlation length $1/\xi$,

$$\langle \omega^n \rangle^{1/n} = \xi^{-z} f_n(k\xi) \qquad k, 1/\xi \to 0 \qquad (8.1.1)$$

$f_n(x)$ being universal scaling functions and z the dynamic critical exponent. In particular the characteristic time τ_c (reciprocal of structure function width Γ) is expected to take the following form (Stauffer 1975, Birgeneau *et al* 1976)

$$\tau_c \equiv 1/\Gamma \propto \xi^z \qquad (8.1.2)$$

which for the Ising model at p_c becomes

$$\tau_c(T) = [\ \exp(2J\nu_p/T)\ ]^z \qquad (8.1.3)$$

Using the assumption of conventional dynamic scaling, (8.1.3), Aeppli *et al* found an anomalously high value for z (z=2.4±0.1, cf z(pure,expt.)=1.7) and subsequent analytic treatments which have assumed the form (8.1.3) (Kumar 1984, Achiam 1985) have given values for z in qualitative agreement with the experiment.

Since then however, the validity of the conventional dynamic scaling hypothesis for Ising dynamics at p_c has been questioned by Henley (1985), Harris and Stinchcombe (1986) and Stinchcombe (1985). These authors treated the kinetic Ising model (KIM)

subject to single-spin flip Glauber dynamics with non-conserved order parameter. Provided the percolation correlation length ξ_p is much greater than the thermal correlation length ξ_T (in particular this is true for all $T\neq 0$, exactly at p_c) then it is known that in one dimension the dynamics is controlled by domain wall diffusion (Cordery *et al* 1981). In higher dimensions near the percolation threshold the ramified substrate may be considered to be a random network of one-dimensional links (de Gennes 1976, Skal and Shkovskii 1975) along which one expects similar domain boundary diffusion. On a pure one dimensional chain the domain wall motion is that of a Gaussian random walk (fig.8.1a) and so (8.1.3) is satisfied with z=2 (cf the solution of Glauber dynamics on the Ising chain (Glauber 1963)). On a dilute d>1 network at p_c the Ising wall diffuses until it reaches a node (fig.8.1b). According to the rules of Glauber dynamics the flipping rate of the spin A is here suppressed by a factor

$$\epsilon = e^{-(mE/k_BT)} \qquad (8.1.4)$$

E being the Ising one-dimensional domain wall energy (=2J) and m>0 is the net number of extra walls created after activation onto the branch. In particular m=1 for the branch of fig.8.1b. As pointed out by Henley (1985), the ensemble of percolation cluster junctions form a network which presents a 'collective' energy barrier to the propagation of the domain wall. This is a result of the correlations induced between the newly created walls when a Bloch wall activates onto a branching point. Moreover, it appears that these percolation cluster energy barriers are unbounded (Henley 1985) and scale logarithmically with separation L,

$$E_{max}(L)/2J = Z\log L + \text{const.} \qquad (L\to\infty) \qquad (8.1.5)$$

This activation process over a sequence of percolation cluster barriers provides the physical mechanism for the violation of the conventional dynamic scaling hypothesis for Ising dynamics. Identifying τ_c as being the time taken for a domain wall to diffuse a correlation length (Henley 1985), one finds (Harris and Stinchcombe 1986) that it satisfies a *singular* dynamic scaling form, with leading singularity

$$\tau_c(T) = \xi_T(T)^{A\log\xi_T(T)} \qquad (8.1.6)$$

or

$$\tau_c(T) = \left[\exp(4J^2\nu_p^2/T^2) \right]^A \qquad (8.1.7)$$

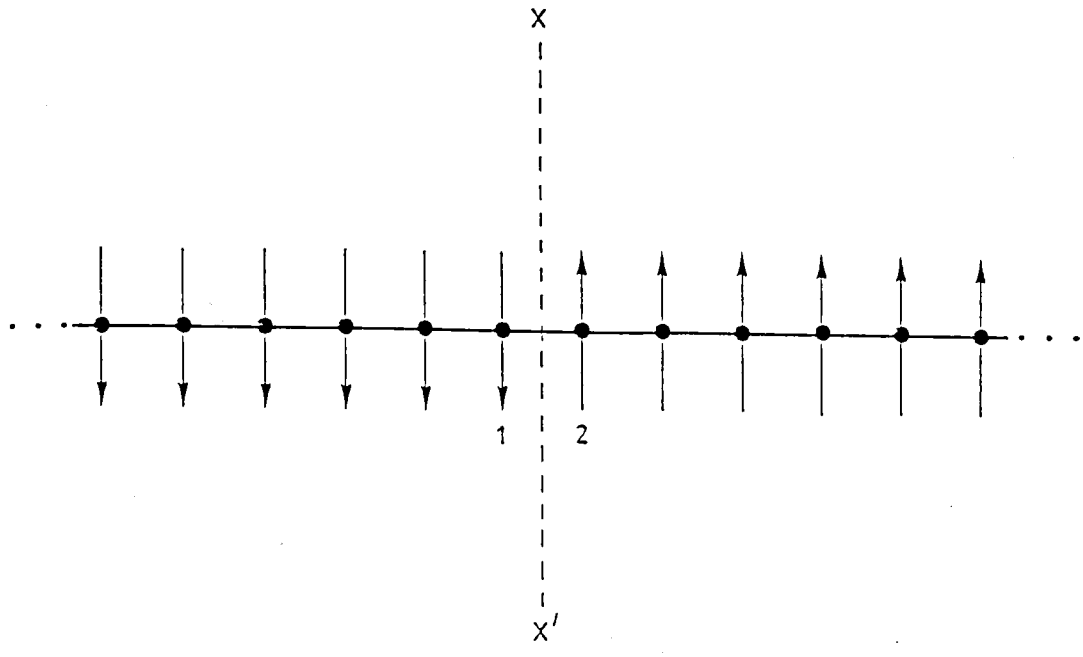

Fig.8.1a: Domain wall in one dimensional Ising magnet. As it costs no energy to flip either spin 1 or 2, the domain boundary XX' performs a Gaussian random walk and so $\tau_c \sim (\xi/a)^2$.

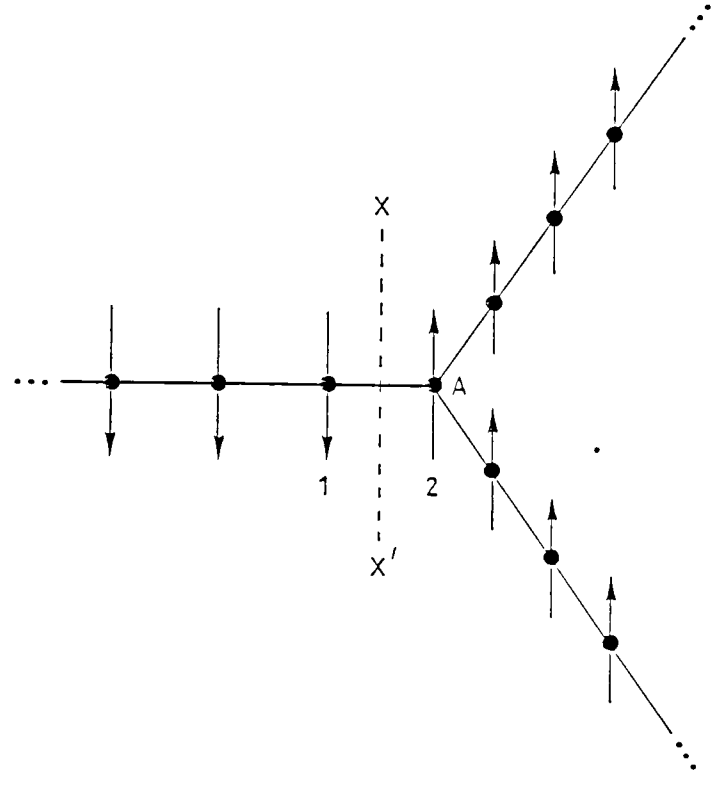

Fig.8.1b: Schematic representation of a percolation cluster node. It costs energy 2J to flip spin 2 and so the rate for activation of the domain wall XX' across A is suppressed by a factor e^{2J/k_bT}. Clearly at T=0 the wall is trapped to the left of A.

and therefore having a *diverging* "effective critical exponent" $z \equiv A\log\xi_T(T) = 2JA\nu_p/T$ $(T \to 0)$, where $A = (2\nu_p \log 2)^{-1}$. Subsequent numerical work for the dynamics of the diluted KIM on both site- and bond-diluted lattices (Rammal and Benoit 1985a,b, Jain 1986a,b, Chowdhury and Stauffer 1986) confirms that $\log\tau_c(T)$ depends quadratically on $\log\xi_T(T)$ and strongly suggests that the exponent A is universal.

In the present work we generalise the above ideas to the *kinetic* anisotropic Heisenberg model (AH). This Hamiltonian provides a more realistic representation of the real magnets which contain competing uniaxial Ising-like and isotropic Heisenberg-like interactions. By varying the anisotropy variable α in the AH Hamiltonian this system allows contact between the Ising model, for which we expect the singular dynamic scaling form (8.1.6) above, the isotropic Heisenberg model, which we expect to satisfy conventional dynamic scaling (see eg chp.7 and Appendix P), and the real systems which lie somewhere in between these two. Evidently, one task is to make explicit the crossover from conventional to singular dynamic scaling for these systems.

The linear, spin-wave dynamics of the AH model on percolation clusters has been considered elsewhere (Christou, unpublished); in the present chapter we treat the relaxational kink dynamics at $p=p_c$. We consider the dynamics, as in the case of the KIM, to be controlled by domain wall diffusion governed by a generalised form of Glauber dynamics. For the AH, the domain boundaries are extended one-dimensional Bloch walls (Bloch 1932) (fig.8.2) and we show that for low enough temperatures the characteristic time τ_c violates the conventional dynamic scaling hypothesis in all situations of non-vanishing anisotropy.

A plan of this chapter is as follows: For completeness we briefly summarise the existing scaling theory results for static properties of the pure 1d chain and for the dilute AH magnet near p_c (Stinchcombe 1980a,b,c). These will be required later. In section III we examine the one-dimensional Bloch wall whose properties turn out to be crucial to the percolative dynamics for the dilute $d>1$ systems. In section IV we present, in the spirit of Harris and Stinchcombe (1983), two complementary approaches to the problem of calculating τ_c: a random cluster renormalisation which treats the real

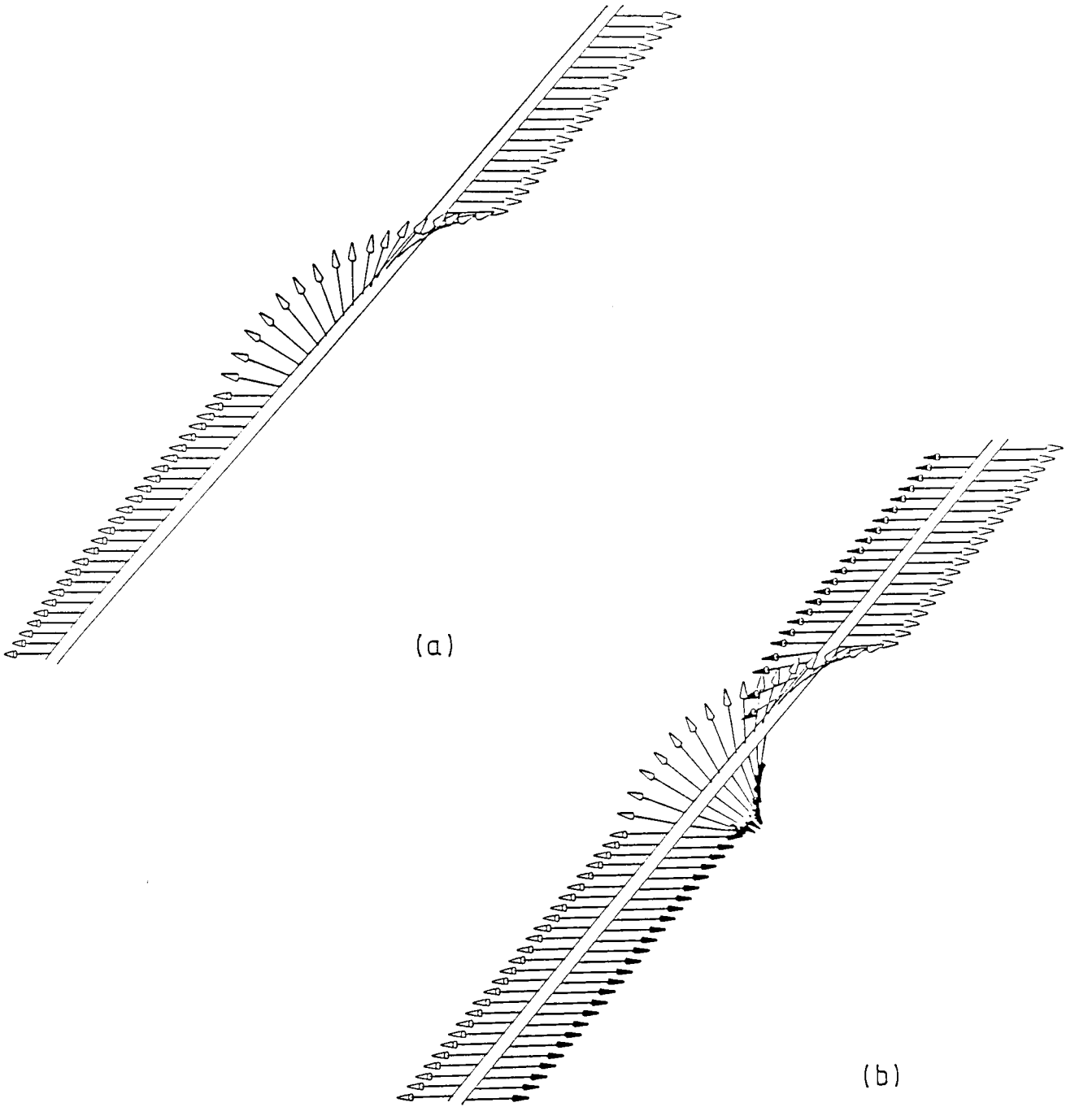

Fig.8.2: The Bloch wall for the one dimensional (a) ferromagnet and (b) antiferromagnet. In the continuum approximation, the anisotropy energy density at any point equals the exchange energy density at the same point.

random system in an approximate manner preserving the essential physical processes (diffusion,activation and geometrical self-similarity) and an exact calculation using a non-random fractal representation of the cluster geometry which again captures the notion of activation of domain walls across a hierarchy of energy barriers. Formal expressions are obtained for the characteristic time τ_c, as a function of the AH correlation length, which are displayed explicitly in the various limiting regimes of interest. A short summary is presented in section V.

II. Scaling Theory for the Static Critical Behaviour of Pure and Dilute Anisotropic Heisenberg Magnets

In this and subsequent sections we consider the classical ($S\to\infty$), bond-dilute uniaxially anisotropic Heisenberg (AH) Hamiltonian,

$$H = - \sum_{<ij>} J_{ij} \{ \alpha \underline{S}_i . \underline{S}_j + (1-\alpha) S_i^z S_j^z \} \qquad (8.2.1)$$

where the coupling constants J_{ij} are randomly and independently $0,J>0$ with respective probabilities $(1-p),p$ and $\eta \equiv 1-\alpha$ is a measure of the anisotropy. For $\alpha=1$ ($\eta=0$) we recover the isotropic Heisenberg Hamiltonian while for $\alpha=0$ ($\eta=1$) we obtain the Ising Hamiltonian. $\alpha\to\infty$ gives the XY model, however we concern ourselves only with $\alpha,\eta \in [0,1]$. The corresponding Hamiltonian with single ion anisotropy does not display this crossover quite so transparently.

For convenience, we use the following two independent combinations, θ and u, of the basic variables α,T as follows,

$$\cosh \theta = 1/\alpha \qquad (8.2.2a)$$

$$u = K \tanh\theta + F(\theta) \qquad (8.2.2b)$$

where $K=J/k_BT$ and

$$F(\theta) \approx \tfrac{1}{2} \log\theta \qquad \theta \gg 1$$

$$\approx 0 \qquad \text{otherwise} \qquad (8.2.3)$$

Consider, firstly, the pure one-dimensional AH chain. Here it may be readily shown (Stinchcombe 1980a) that under a renormalisation of the length scale by a factor

b, θ and u are mapped onto θ' and u' given approximately by

$$\theta' = b\theta, \qquad u' = u \tag{8.2.4}$$

These recursion relations become exact in the low temperature limit $K\to\infty$. θ scales as an inverse length and is therefore a *scaling variable* for the correlation length while u is a marginal, crossover, variable. In the AH chain the critical behaviour is driven by the divergence of the one dimensional longitudinal correlation length ξ_1 (the transverse correlation length remaining finite even at T_c). We may express the inverse longitudinal correlation length (ICL) $\mathbb{Q}_1 \equiv 1/\xi_1$ as

$$\mathbb{Q}_1 = \theta\, \Phi_1(u) \tag{8.2.5}$$

For $u\gg1$, $u\ll1$ the correlations between spins are Ising-like and Heisenberg-like respectively and so $\Phi_1(u)$ assumes the following asymptotic forms (Stinchcombe 1980a):

$$\begin{aligned} \Phi_1(u) &= c/u && u\ll1 \\ &= de^{-2u} && u\gg1 \end{aligned} \tag{8.2.6}$$

c and d are constants. $u^*\simeq1$ represents the so-called *crossover temperature* across which the one dimensional spin-spin correlations change from Ising to Heisenberg form.

The scaling properties of the inverse longitudinal correlation length $\mathbb{Q}$ for dilute *higher* dimensional systems (d>1) may be conveniently expressed in terms of those for the pure 1d chain above (Stinchcombe 1980b,c). For d>1 near the percolation bicritical point we have

$$\mathbb{Q} \equiv 1/\xi = \theta\, B(x,y) \tag{8.2.7}$$

where θ is defined as above and has the same behaviour under renormalisation. The crossover variables (arguments of the scaling function B) are

$$\begin{aligned} x &= \frac{\mathbb{Q}_1}{(\,\theta(\tanh\theta)^{1/\varphi_H-1}\,)} \\ y &= \frac{(\delta p)^{\nu_p}}{\theta} \end{aligned} \tag{8.2.8}$$

where $\delta p \equiv |p-p_c|$, ν_p is the percolation correlation length ξ_p critical exponent, and φ_H is the thermal-percolation crossover exponent related to the Heisenberg thermal exponent ν_t^H for the Heisenberg-percolative fixed point by

$$\varphi_H = \nu_t^H/\nu_p \tag{8.2.9}$$

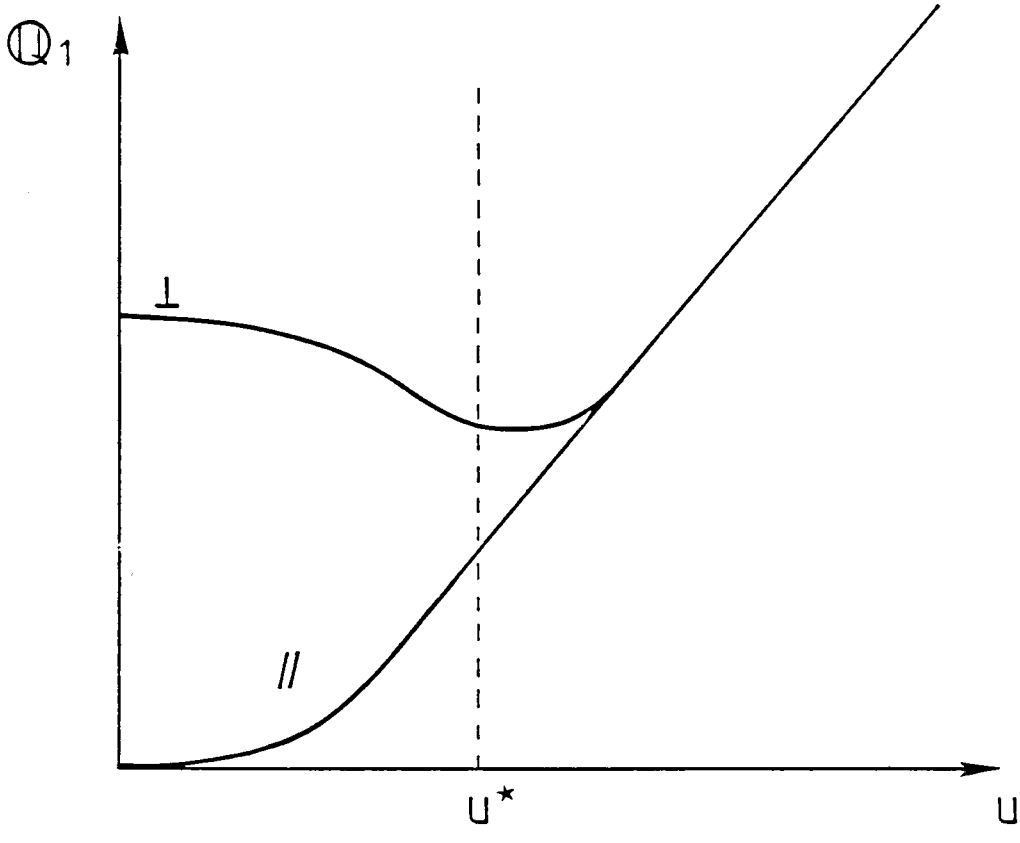

Fig.8.2c.: Inverse longitudinal and transverse correlation lengths vs. reduced temperature u for pure chain. Anisotropy-induced crossover occurs at reduced temperature u^* (from Stinchcombe 1980b).

At the percolation threshold y=0, the d>1 ICL $\mathbb{Q}$ may be related to the pure one-dimensional ICL $\mathbb{Q}_1$ as follows

$$\mathbb{Q}(x,y=0) \propto \begin{cases} \mathbb{Q}_1{}^{\nu}p & x\ll 1 \\ \mathbb{Q}_1{}^{\nu}{}_t{}^H & x\gg 1 \end{cases} \qquad (8.2.10)$$

Here 'x small' is the Ising-like side and 'x large' is the isotropic side of the anisotropy-induced crossover; the crossover temperature is, in this case, given by $x^*\simeq 1$.

It remains now to establish some results for the one-dimensional Bloch wall before proceeding to a consideration of Bloch wall dynamics in section IV.

III. The One Dimensional Bloch Wall

As indicated in the introduction, the energy of the one-dimensional Bloch wall as a function of anisotropy is of central importance in a discussion of domain boundary propagation on percolation clusters. In this section we show how scaling theory gives exact results for the Bloch wall energy and length in one dimension and we examine the validity of continuum approximations for the case of arbitrary anisotropy.

As stressed above we are addressing the *classical* problem. In this large spin regime the spins may be viewed as classical vectors with well defined length (which we normalise to unity) and orientation, specified by polar and azimuthal angles θ and φ. The spin components are then given by

$$\begin{aligned} S^z &= \cos\theta \\ S^x &= \sin\theta\cos\varphi \\ S^y &= \sin\theta\sin\varphi \end{aligned} \qquad (8.3.1)$$

For an infinite chain of spins in a specified configuration $\{\theta_i,\varphi_i\}$, we may easily evaluate the configurational energy relative to the global ground state $\{\theta_i=0\}$ using the Hamiltonian (8.2.1),

$$E/J = \sum_n \left\{ 1 - \alpha\sin\theta_n\sin\theta_{n+1}\cos(\varphi_n-\varphi_{n+1}) - \cos\theta_n\cos\theta_{n+1} \right\} \qquad (8.3.2)$$

For the one-dimensional case (or in general dimension, for a planar wall) it is sufficient to treat φ_i=const. and so without loss of generality we may consider φ_i=0.

We seek the global minimum of the functional $E(\{\theta_i\})$ subject to the boundary condition $\theta_{-\infty}=0$, $\theta_{\infty}=\pi$. This ground state corresponds, of course, to an isolated Bloch wall. The simplest procedure to adopt is to assume that the angular displacement between adjacent spins is small and constant, ie

$$\theta_{n+1}-\theta_n = \pi a/L \qquad (8.3.3)$$

where L/a ($\gg\pi$) is the number of spins in the Bloch wall. Then, from (8.3.2), one obtains for the Bloch wall energy,

$$E/J = \pi(2\alpha(1-\alpha))^{\frac{1}{2}} \qquad (8.3.4)$$

to leading order in $(1-\alpha)$. In deriving (8.3.4) a continuum assumption has been made in which first differences go over into derivatives and summations into integrals.

From the above calculation we also find the Bloch wall length as a function of anisotropy,

$$L/a = \pi\left[2\alpha/(1-\alpha)\right]^{\frac{1}{2}} \qquad (8.3.5)$$

The rather *ad hoc* supposition that the angular displacement between adjacent spins be constant may be dispensed with by carrying out the variational calculation in the continuum limit, valid for small anisotropy ($\eta=(1-\alpha)\ll 1$). Here we set $|\theta_{n+1}-\theta_n|=\delta(n)\ll 1$ and we take first and second differences into their corresponding derivatives as above. In this way we obtain the following functional integral equation to second order in $(d\theta/dx)$ for $E\{\theta(x)\}$:

$$\frac{E\{\theta(x)\}}{J} = \int_{-\infty}^{\infty}\frac{\alpha}{2}\left[\frac{d\theta}{dx}\right]^2 dx + \int_{-\infty}^{\infty}(1-\alpha)\left\{\sin\theta\left[\sin\theta+\left[\frac{d\theta}{dx}\right]\cos\theta\right]+\tfrac{1}{2}\left[\frac{d\theta}{dx}\right]^2\cos^2\theta\right\}dx \qquad (8.3.6)$$

which satisfies the following Euler–Lagrange equation:

$$\frac{d^2\theta}{dx^2} - \frac{(1-\alpha)\sin 2\theta}{(\alpha+(1-\alpha)\cos^2\theta)} = 0 \qquad (8.3.7a)$$

However, as we are concerned at the moment only in the continuum regime $\eta\equiv 1-\alpha\ll 1$, we take (8.3.7a) to first order in $(1-\alpha)$:

$$\frac{d^2\theta}{dx^2} - \left[\frac{1-\alpha}{\alpha}\right]\sin 2\theta = 0 \qquad (8.3.7b)$$

Allowing for explicit time-dependence in $\{\theta_i\}$ converts (8.3.7b)into a Sine–Gordon

equation with propagating soliton solutions (see Mikeska 1981). Solving (8.3.7b) subject to $d\theta/dx=0$ for $\theta=0,\pi$ and substituting into (8.3.6) gives the following results for the Bloch wall energy and length,

$$E/J = 2(2\alpha(1-\alpha))^{\frac{1}{2}} \qquad (8.3.8)$$

$$\begin{aligned} L/a &= \log[\tan((\pi-\epsilon)/2)/\tan(\epsilon/2)].[\alpha/(2(1-\alpha))]^{\frac{1}{2}} \\ &= 2\log[\cot(\epsilon/2)].[\alpha/(2(1-\alpha))]^{\frac{1}{2}} \end{aligned} \qquad (8.3.9)$$

Strictly, here L/a is the distance between spin 0 with $\theta_0=\epsilon$ and spin L with $\theta_L=\pi-\epsilon$, and therefore L/a diverges as $\epsilon\to 0$.

The above derivation is exact in the limit of low anisotropy $\eta=1-\alpha\ll 1$. For general η (eg $\eta\sim 1$), the continuum theory breaks down and similarly we expect the results derived therefrom, in particular eqns. 8.3.4,8.3.5,8.3.8,8.3.9, to be violated. Thus for general η the discrete problem needs to be tackled directly. From (8.3.2) the discrete Euler equation is now, after some algebra,

$$\theta_{n+1} = 2\tan^{-1}[(1/\alpha)\tan\theta_n] - \theta_{n-1} \qquad (8.3.10)$$

or substituting $t_n=\tan\theta_n$,

$$t_{n+1} = \frac{2\alpha t_n - \alpha^2 t_{n-1} + t_{n-1}t_n^2}{\alpha^2 - t_n^2 + 2\alpha t_{n-1}t_n} \qquad (8.3.11)$$

We have performed a numerical investigation of (8.3.11). We take $0<t_1=-t_0=\delta\ll 1$. Subject to these initial values and setting some value to the anisotropy parameter α, (8.3.11) generates a chain configuration comprising a sequence of well defined and well separated Bloch walls (for sufficiently small δ) whose mean energy and length can be easily evaluated. The fractional standard deviation of the energies and lengths of the walls, even for relatively small chains of ten thousand spins, is much less than a percentage point. For $\delta<10^{-5}$ no significant dependence of E/J, L/a on δ is observed for chains up to one million spins long; δ merely alters the gap between the Bloch walls: as $\delta\to 0$, separation of walls $\to\infty$. A sample of our results over the range of anisotropy is shown in fig.(8.3a,b).

Finally, we demonstrate how the scaling theory (section II) for the classical AH chain may be used to derive exact expressions for the wall energy E/J and length L/a which have been arrived at by a different method by Gochev (1983). We firstly address

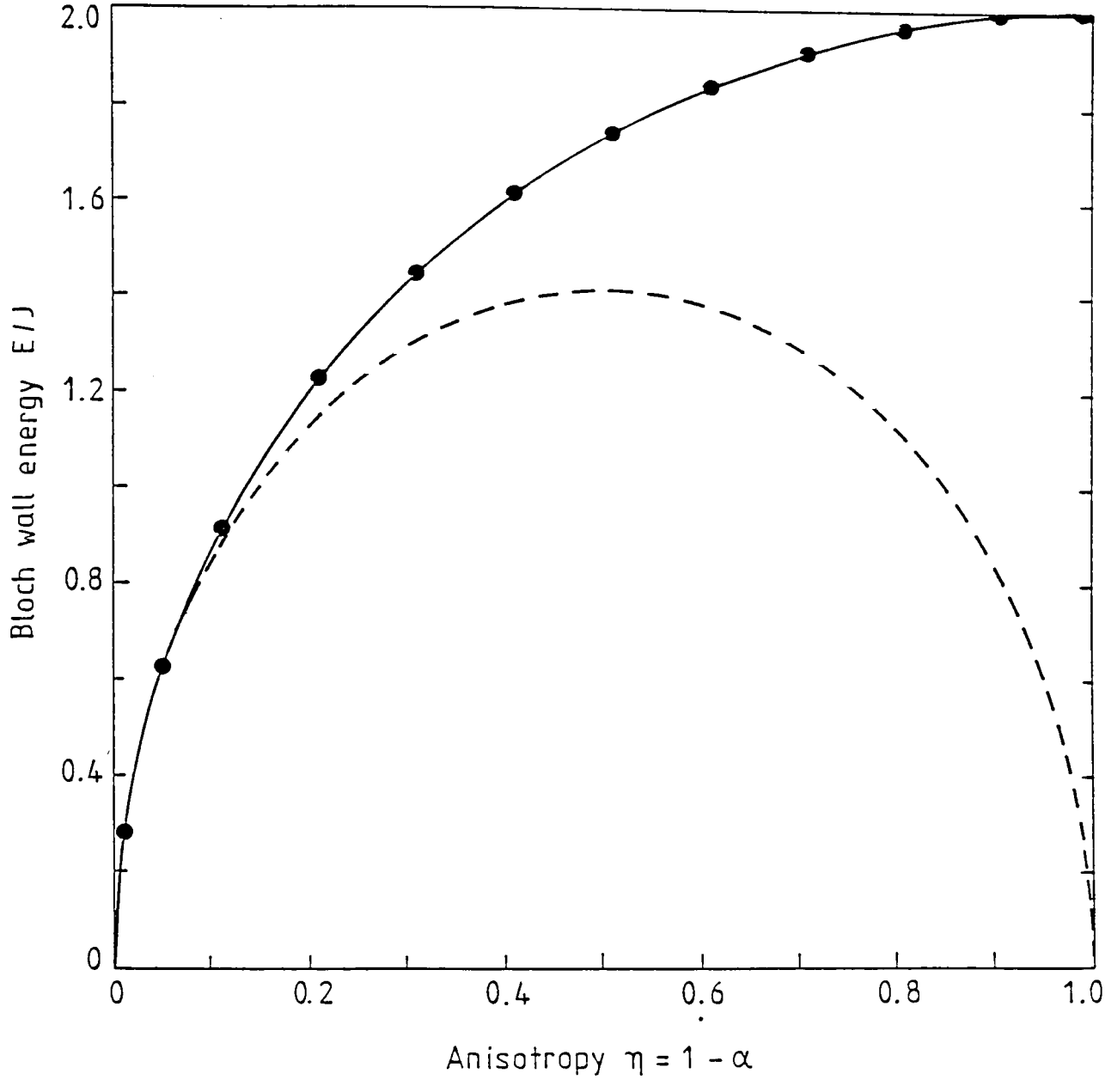

Fig.8.3a: Bloch wall energy E/J vs. anisotropy $\eta=1-\alpha$ for a one dimensional wall. The dotted curve is the approximate continuum result from the variational calculation (8.3.8) valid in the low anisotropy regime $\eta \ll 1$. The points represent a sample of our numerical results obtained by direct iteration of (8.3.11) for a chain of 10^6 spins. The energy variances are much smaller than the size of the circles and are in excellent agreement with the scaling theory result.

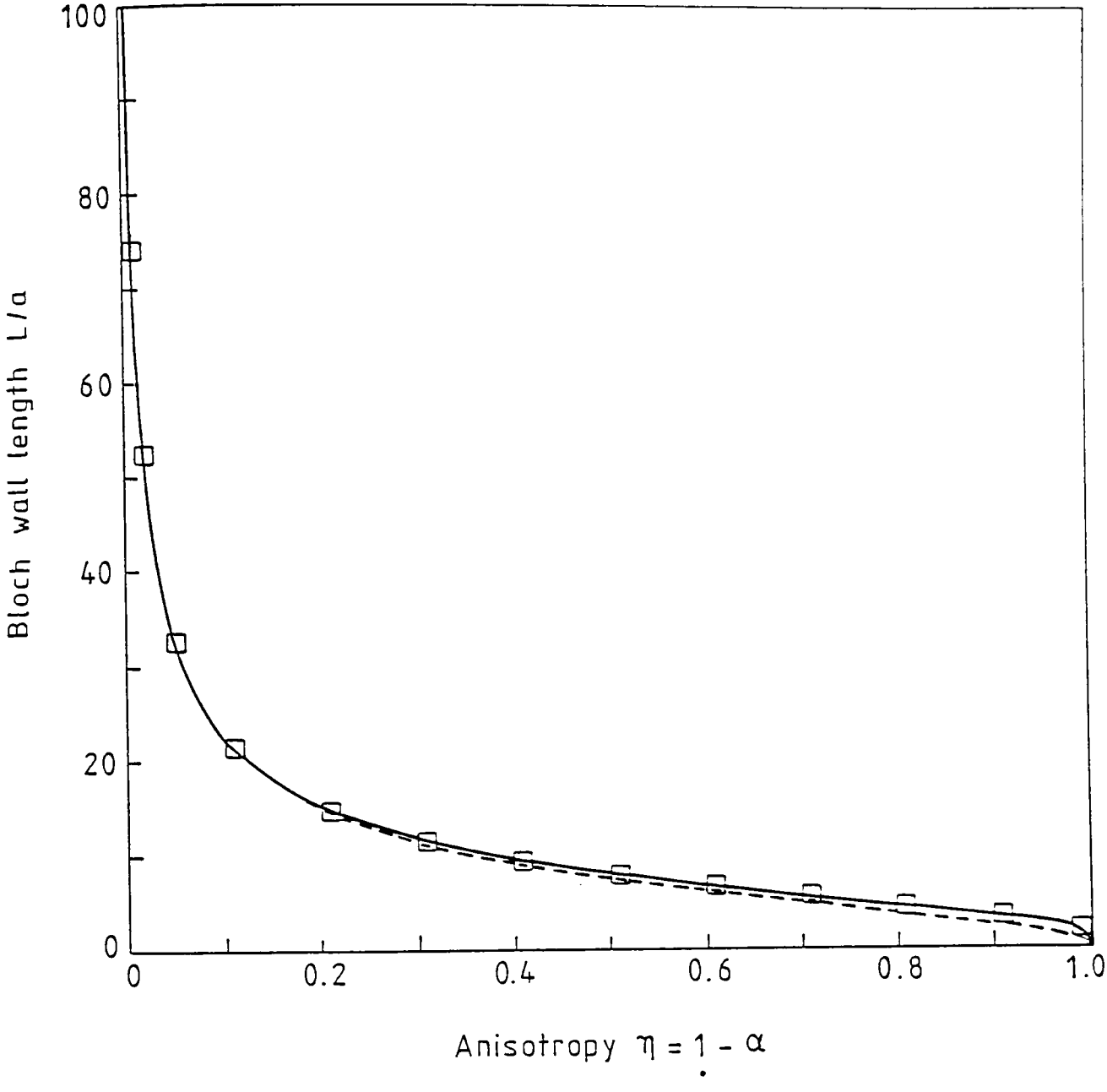

Fig.8.3b: Bloch wall length L/a vs. anisotropy $\eta=1-\alpha$ for a one dimensional wall. Notice that the variational result (dotted line) (8.3.9) does not diverge significantly from the scaling theory result (full line) (8.3.15) even for large anisotropy $\eta\sim1$. Once again the numerical data (squares) agree very well with the exact solution.

the simpler problem of the Bloch wall length.

Without loss of generality we may express L/a as a function of the anisotropy scaling variable thus

$$L/a = \theta^{\gamma} f(\theta) \qquad (8.3.12)$$

for some function $f(\theta)$. We remark that L/a does *not* depend on T. Further, under a renormalisation group length scaling transformation scaling the lattice constant a by a factor b, the wall length L/a transforms as

$$(L/a)' = (L/a)/b \qquad (8.3.13)$$

(8.3.13) together with $\theta'=b\theta$ imply the solution $\gamma=-1$ and $f(\theta)$ invariant under the RG mapping, ie

$$f(\theta) = f(b\theta) \qquad (8.3.14)$$

However as we are treating the 1d chain, the length scaling factor b is arbitrary (in contrast to the situation in some regular fractals, eg Sierpinski gasket) and hence $f(\theta)=C$,const. Matching (8.3.12) with the variational result (8.3.9) in the low anisotropy regime gives C and so we have

$$L/a = \frac{\log[\tan(\pi-\epsilon/2)/\tan(\epsilon/2)]}{\theta} = \frac{2\log[\cot(\epsilon/2)]}{\theta} \qquad (8.3.15)$$

which is valid over the whole range of anisotropy and is precisely the form obtained by Gochev[35]. Furthermore, the scaling theory may be used to derive the Bloch wall energy E/J using the following argument. The RG recursion relation for the anisotropy α and the reduced inverse temperature K are derived by stipulating that the partition function remains invariant under a partial trace over decimated short range degrees of freedom. A corollary is that the reduced energy E/k_BT of the spin configuration is also an invariant.

Now, under repeated length scaling (say, a sequence of b=2 decimations) a general AH one-dimensional chain, characterised by variables θ and u, will flow towards the Ising fixed point. This process is reversed by inverting the recursion relations. Hence,

$$E/k_BT = (2J/k_BT)'$$
$$= 2[(u-F(2^m\theta))/\tanh(2^m\theta)] \qquad (8.3.16)$$

where $(\ldots)'$ denotes the inverse RG transformation referred to above and we have used

$u'=u$. The variables u,θ and function F are as defined in section II, E is the Bloch wall energy and m is an integer ($\to\infty$). The scaling theory is exact at very low temperatures ($K\to\infty$) and so we set $T\to 0$. We therefore obtain the following expression for the Bloch wall energy E,

$$E/J = 2\tanh\theta$$
$$= 2(1-\alpha^2)^{\frac{1}{2}} \qquad (8.3.17)$$

in agreement with the result of Gochev (1983) for the classical chain. In figs.(8.3a,b) we summarise and contrast some of the results of this section. In the remainder of this chapter we will use eqn.3.17 to study Bloch wall motion on percolation clusters.

IV. Non-linear Relaxational Dynamics near the Percolation Bicritical point ($p=p_c, T=0$)

We begin by considering the motion of an extended, non-local Bloch wall on a one-dimensional chain. The motion of the complete wall is governed by Glauber dynamics (Glauber 1963), according to the following prescription:

i) Choose at random a direction in which to move the wall. This may be to the left ($\theta_m(t+\Delta t)=\theta_{m+1}(t)$) or to the right ($\theta_m(t+\Delta t)=\theta_{m-1}(t)$).

ii) Evaluate the change in configurational energy, ΔU, should the wall move to its new position. If $\Delta U\leq 0$ then the wall is moved in the chosen direction with certainty; if $\Delta U>0$ then the wall will move with a probability $e^{-(\Delta U/k_BT)}$.

For the one dimensional case, of course, translational invariance ensures that no net energy is ever lost or gained when the wall takes a step and so it performs a random walk giving z=2, as in the case of the Ising chain.

With obvious modifications the above scheme generalises to provide a description of the motion of Bloch walls on percolation clusters. Whenever a Bloch wall is contained entirely within a link, as may occur for high anisotropy $\eta\ll 1$ or very near p_c ($\xi_p\to\infty$) where the node-node separation diverges, it will diffuse as a random walk until it reaches a node. However, according to the prescription above, whenever a wall straddles such a percolation cluster *branching point*, the rate for moving further onto the branch one step is suppressed by a factor

$$\epsilon(\theta_0{}^i,\theta_0{}^f) \propto \exp[(1/k_BT)\{U(\theta_0{}^f)-U(\theta_0{}^i)\}] \qquad (8.4.1)$$

where the spin 0 at the node has polar angle θ_0^i, θ_0^f respectively before and after the step is made further onto the branch. $U(\theta_0)$ is the configurational energy of the forked Bloch wall when the node spin has polar angle θ_0 relative to the z-axis. Hence for a complete traversal of an *isolated* branch the associated rate suppression factor ϵ_{AH} is given simply as a product of such factors (8.4.1) for each of the constituent steps, ie

$$\epsilon_{AH} = \prod\{\epsilon(\theta_0^i, \theta_0^f)\} \propto \exp\{(1/k_BT)\sum(U(\theta_0^f)-U(\theta_0^i))\} \qquad (8.4.2)$$

The exponential sum collapses telescopically, and, noting that $U(\pi)-U(0)$ is E, the Bloch wall energy, we obtain the rate suppression factor for complete activation onto the branch

$$\epsilon_{AH} = \sigma e^{2w} \qquad (8.4.3)$$

with $w \equiv u-F(\theta) \equiv \frac{1}{2}\{E/k_BT\} = K\tanh\theta$ and σ is a constant dependent only on the detailed choice of flip rate.

We now proceed to derive expressions for the characteristic relaxation time for kink diffusion on percolation clusters. Closed forms for τ_c are exhibited in the limiting Ising-like $u \ll 1$ and Heisenberg-like $u \gg 1$ regimes. We use two complementary approaches: firstly, we treat a random system using an approximate cluster renormalisation. We then treat a regular fractal model of the cluster geometry exactly.

A) Cluster renormalisation for AH critical dynamics.

We present an approximate real-space renormalisation for Bloch wall diffusion on a bond-dilute lattice in $d>1$.

The details of the length scaling procedure that we use here are described by Harris and Stinchcombe (1986). To be specific, we treat a cluster of a bond-dilute hexagonal lattice as shown in fig.8.4. In fact, it turns out that our formalism is rather more general and, for example, it is straightforward to demonstrate that, apart from constant factors, the expressions we obtain for τ_c are identical for, say, a $b=\sqrt{2}$ cluster on the square lattice. Besides, if the critical dynamics is universal, as appears to be the case for the leading term in the Ising case (Jain 1986b), then no generality is lost in treating any specific lattice type. Similarly, in three dimensions, we might treat a $b=\sqrt{3}$

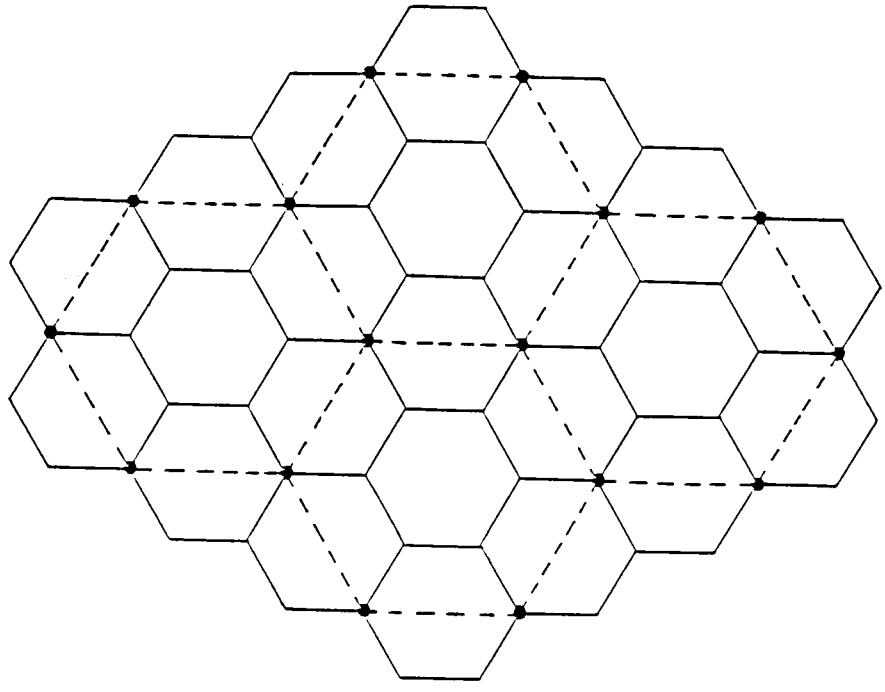

(a)

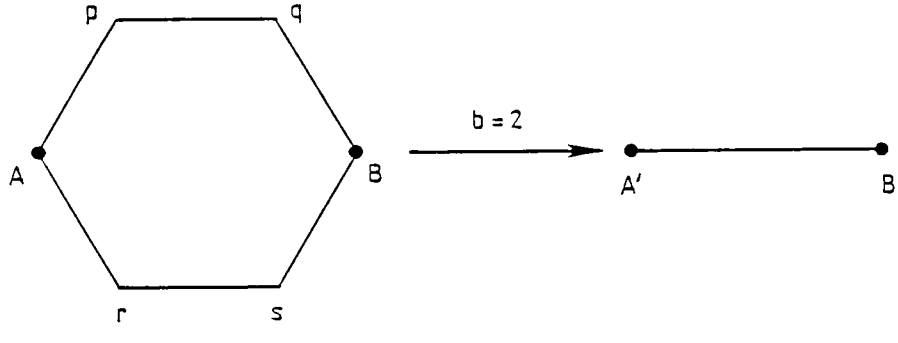

(b)

Fig.8.4:

a) Decimation of the d=2 hexagonal lattice by a scaling factor b=2. original lattice (full bonds) is replaced by an isomorphic but dilated one (dotted bonds).

b) Our real space RG treats the cluster AB which is mapped onto A'B'.

cluster renormalisation on the cubic lattice (see Stanley *et al* (1982) for a general discussion of cluster renormalisation).

Using the standard Cordery-Sarker-Tobochnik (CST) (1981) domain wall diffusion scenario, we argue that, as for the Ising case, the rate limiting step is activation of domain walls over percolation cluster branching points. In contrast to the Ising case however, this activation process is not local to a branching point since initially L/a may be large, and therefore not all such branching points are equivalent. However, in the spirit of CST we identify the slowest process to be activation over *isolated* branching points such that involve the complete activation of the Bloch wall (as opposed to activation, for example across small blobs, which is a faster process). Such percolation cluster points exist even for large L/a owing to the self-similarity of the substrate. We use the Harris-Stinchcombe (1986) renormalisation process together with the result (8.4.3) for the Bloch wall rate suppression factor ϵ_{AH}. Notice that in the Ising limit, $\alpha=0$, $\epsilon_{AH}=\sigma e^{2K}$ as used in Harris and Stichcombe (1986).

Although all the arguments below apply to $\xi_T<\xi_p$, for which domain boundary diffusion arguments are valid, we take $\xi_p\to\infty$ for convenience in the exposition. The recursion relations follow,

$$\begin{aligned} \tau' &= \gamma e^{2W}\tau \\ (\xi/a)' &= (1/b)(\xi/a) \\ \theta' &= b\theta \end{aligned} \qquad (8.4.4)$$

where τ is the time taken to traverse a bond on the original lattice, τ' the corresponding time for the decimated lattice and γ is a constant. In fact γ depends on the detailed renormalisation prescription and lattice type as discussed by Harris and Stinchcombe (1986). This is unavoidable and a typical drawback of real-space RG calculations (Stanley *et al* 1982). For our purposes, this is not important when $\theta\neq0$ (ie $\alpha\neq1$) as e^{2W} provides the most singular terms.

We stress that all the other (faster) processes such as activation across small blobs (relative to the Bloch wall length) etc. and in particular simple diffusion along quasi-one-dimensional paths are neglected since these provide less singular correction terms to (8.4.4) and are irrelevant near the bicritical point.

In d=3, w scales in a very different way to that in d=2 and care must be taken to distinguish these two situations.

For the specific case of the hexagonal lattice under consideration the length scaling factor is b=2. Now, in general w is related to the d>1 dilute AH correlation length (section II),

$$w = u\text{-}F(\theta) = \Phi_1^{-1}\{[\theta(\xi/a)^{1/\tilde{\nu}}]^{-1}\} - F(\theta). \qquad (8.4.5)$$

The notation has already been established in section II. Notice that here Φ_1^{-1} denotes the *inverse* function of Φ_1 and not its reciprocal. $\tilde{\nu}$ is fixed according to the value of the crossover exponent x,

$$\begin{aligned} \tilde{\nu} &= \nu_p && x \ll 1 \\ &= \nu_t^H && x \gg 1 \end{aligned} \qquad (8.4.6)$$

The idea is to construct a function $I(\tau(\xi/a,\theta),\xi/a,\theta)$ which is invariant under the aforementioned length scaling process, where we define $\tau'=\tau((\xi/a)',\theta')$.Through successive length scalings one transforms the parameters ξ,θ to a non-critical region $\xi/a\sim 1$ and hence, using the scale-invariance of I, one solves for $\tau_c=(\tau(1,(\xi/a)\theta)/\tau(\xi/a,\theta))$.

However, we may express $I(\tau(\xi/a,\theta),\xi/a,\theta)$ as follows,

$$I(\tau(\xi/a,\theta),\xi/a,\theta) = \log\tau(\xi/a,\theta) + G(\xi/a,\theta) + \varrho(\theta) \qquad (8.4.7)$$

where $\varrho(\theta)$ satisfies $\varrho(2\theta)=\varrho(\theta)-\log\gamma$ and $G(\xi/a,\theta)$ satisfies,

$$\begin{aligned} G(\xi/a,\theta) &= G(\xi/2a,2\theta) + 2w \\ &= G(\xi/2a,2\theta) + 2\Phi_1^{-1}\{[\theta(\xi/a)^{1/\tilde{\nu}}]^{-1}\} - 2F(\theta) \end{aligned} \qquad (8.4.8)$$

In principle the above functional equation gives $G(\xi/a,\theta)$ and hence we obtain an implicit equation for $\tau(\xi/a,\theta)$ in terms of that in a simple regime as follows:

$$I(\tau(\xi/a,\theta),\xi/a,\theta) = I(\tau(1,(\xi/a)\theta),1,(\xi/a)\theta). \qquad (8.4.9)$$

This yields

$$\log\tau_c = \log\{\tau(1,(\xi/a)\theta)/\tau(\xi/a,\theta)\} = G(\xi/a,\theta)-G(1,(\xi/a)\theta)+\varrho(\theta)-\varrho((\xi/a)\theta). \qquad (8.4.10)$$

For $\theta=0$, the isotropic case, we have w=0 therefore $G(\xi/a,\theta)$=const. and so

$$\tau_c = \tau(1,\theta=0)/\tau(\xi/a,\theta=0) \propto [\xi/a]^z \qquad (8.4.11)$$

which is the conventional dynamic scaling form with $z=(\log\gamma)/(\log 2)$, the usual form for the dynamical critical exponent. This form is in agreement with the corresponding linear dynamical result for spin-waves on percolation clusters in the isotropic Heisenberg magnet (Chp.7 and Appendix P) and arises as a result of the well known correspondence between diffusive relaxational dynamics and spin-wave precessional dynamics.

To find further explicit reductions of (8.4.10) we consider in turn the following important limiting regimes:

i) $u\gg 1, d=2$ *(Ising-like regime)*

In this case we note that (section II),

$$(\xi/a) = \mathbb{Q}_1^{-\tilde{\nu}} = (\theta\Phi_1(u))^{-\tilde{\nu}}$$

or
$$\Phi_1(u) = (\xi/a)^{-1/\tilde{\nu}}/\theta \qquad (8.4.12)$$

and so under a b=2 decimation, say, $\Phi_1(u)$ scales by a factor $2^{(1/\tilde{\nu})-1}$. However in d=2, $2^{(1/\tilde{\nu})-1}<1$ for both ν_p and ν_t^H and, given that $\Phi_1(u)$ is monotone decreasing, we see that u increases under scaling. As $u\gg 1$ in the original, unrenormalised model the correlation length maintains the same form under decimation,

$$(\xi/a) \propto (\theta e^{-2u})^{-\tilde{\nu}}$$

and hence
$$e^{2W} \propto (\xi/a)^{1/\tilde{\nu}}\theta e^{-2F(\theta)} \qquad (8.4.13)$$

and from (8.4.8,8.4.10) we obtain the following invariant

$$I(\tau(\xi/a,\theta),\xi/a,\theta) = \log\tau(\xi/a,\theta)+A(\log(\xi/a))^2+B\log(\xi/a)+h(\theta) \qquad (8.4.14)$$

where $A=(2\tilde{\nu}\log 2)^{-1}$, $B=[(\log\gamma)/(\log 2)-(2\tilde{\nu})^{-1}]$, and $h(2\theta)=h(\theta)-f(\theta)$ such that

$$f(\theta) \sim 0 \qquad \theta\gg 1$$
$$\sim \log\theta \qquad \text{otherwise} \qquad (8.4.14a)$$

Using (8.4.9) we may evaluate the characteristic time $\tau_c\equiv\tau(1,(\xi/a))/\tau(\xi/a,\theta)$,

$$\tau_c=\tau(1,(\xi/a)\theta)/\tau(\xi/a,\theta)=M(\xi/a)^{A\log(\xi/a)} \qquad (8.4.15)$$

where M is a constant at the extreme Ising limit $\theta=\infty$ and a finite polynomial in $(\xi/a)\theta$ otherwise. (8.4.15) is precisely the singular dynamic scaling form obtained for the Ising

system (Harris and Stinchcombe 1986). In particular, in the Ising limit $x \to 0$, the dynamic exponent becomes $(2\nu_p \log 2)^{-1}$ which agrees with the result of Harris and Stinchcombe (1986).

ii) $u \gg 1$, d=3 *(Ising-like regime)*

In this situation $2^{(1/\tilde{\nu})-1} > 1$ and so u decreases under length scaling. This introduces difficulties as this behaviour under scaling drives u, and hence the one-dimensional ICL, through the anisotropy-induced crossover temperature and the argument used above breaks down. In this particular case there are two possibilities. The simplest situation is that during decimation u decreases but does not reach the anisotropy-induced crossover temperature $u^* \sim 1$. Here we construct a scaling invariant $I^{u \gg u^*}$ as above and make the approximation that it is valid for all $u > u^*$. We then use an analogous expression to (8.4.9) to derive τ_c. The other possibility is that the decimation drives u across $u^*=1$. Here, we construct two scaling invariants. The first one, $I^{u \gg u^*}$, valid for $u > u^*$ and the second, $I^{u \ll u^*}$, valid for $u < u^*$. These two invariants are matched across $u^* \sim 1$ at which point $\xi = \tilde{\xi}$, $\theta = \tilde{\theta}$ and $\tau = \tilde{\tau}$

$$\begin{aligned} I^{u \gg u^*}(\tau(\xi/a,\theta),\xi/a,\theta) &= I^{u \gg u^*}(\tilde{\tau}(\tilde{\xi},\tilde{\theta}),\tilde{\xi},\tilde{\theta}) \\ &= I^{u \ll u^*}(\tilde{\tau}(\tilde{\xi},\tilde{\theta}),\tilde{\xi},\tilde{\theta}) \\ &= I^{u \ll u^*}(\tau(1,(\xi/a)\theta),1,(\xi/a)\theta) \end{aligned} \qquad (8.4.16)$$

Now, $I^{u \gg u^*}$ is precisely the function obtained above while, owing to the values of the arguments of $I^{u \ll u^*}$, the RHS of (8.4.16) contains only logarithmic divergences in (ξ/a). We therefore obtain, retaining only the most singular terms, an expression identical to that above for d=2,

$$\tau_c = \tau(1,(\xi/a))/\tau(\xi/a,\theta) \propto (\xi/a)^{A \log(\xi/a)} \qquad (8.4.17)$$

where $A=(2\tilde{\nu}\log 2)^{-1}$ as above. We note the presence of less divergent polynomial corrections arising from the $h(\theta)$ and RHS terms.

iii). u≪1, d=3 *(Heisenberg-like regime)*

Here u decreases under decimation. Hence (ξ/a) maintains the same form under scaling,

$$(\xi/a) \propto (\theta/u)^{-\tilde{\nu}} \qquad (8.4.18)$$

Therefore

$$e^{2W} \propto e^{2\theta(\xi/a)^{1/\tilde{\nu}}-2F(\theta)} \qquad (8.4.19)$$

and from this we construct the corresponding scaling invariant

$$I(\tau(\xi/a,\theta),\xi/a,\theta) = \log\tau+C(\theta(\xi/a)^{1/\tilde{\nu}})+\ell(\theta) \qquad (8.4.20)$$

where $C=2(1-2^{1-(1/\tilde{\nu})})^{-1}$, greater than zero in d=3, and $\ell(2\theta)=\ell(\theta)+2F(\theta)-\log\gamma$. Using the same procedure as above we extract the characteristic time,

$$\tau_c = \tau(1,(\xi/a)\theta)/\tau(\xi/a,\theta) = [\tau(1,0)/\tau(\xi/a,0)]e^{C\theta(\xi/a)^{(1/\tilde{\nu})}} \qquad (8.4.21)$$

This appears to be a novel singular dynamic scaling form. However in the region of validity of (8.4.21) the expression in the exponent is constrained to be very small and so

$$\tau_c = [\tau(1,0)/\tau(\xi/a,0)] \propto (\xi/a)^z \qquad (8.4.22)$$

which is the conventional dynamic scaling form.

We finally consider the equivalent regime in d=2.

iv). u≪1, d=2 *(Heisenberg-like regime)*

As u increases under scaling, similar considerations as outlined for case ii) apply here. A similar argument to that used in that case gives, using (8.4.18),

$$\tau(\xi/a,\theta) \propto (\xi/a)^z\exp(-C\theta(\xi/a)^{1/\tilde{\nu}})$$
$$\sim (\xi/a)^z \qquad (8.4.23)$$

in agreement with the conventional dynamic scaling hypothesis (8.1.2) although we note that this time $C<0$.

We conclude this section with a brief presentation of the results of the corresponding calculations on an exact fractal representation of the cluster geometry.

B). AH Critical Dynamics on Non-random Fractal.

The explicit fractal we consider is described in fig.(8.5). For simplicity we suppose that the anisotropy is sufficiently high that the Bloch wall length L is less than s. It is straightforward to extend the argument to the general case and no change in the leading order singularity for τ_c occurs, and so we derive expressions for the simpler situation.

The percolation network between a pair of sites separated by a distance ξ_p is modelled by the n^{th} iterate of the fractal of fig.(8.5). In order to satisfy hyperscaling and convexity conditions (Kaufman and Griffiths 1983) we choose the length scale dilatation factor $b=(r+2s)^{1/d}$ and therefore $\xi_p=(r+2s)^{n/d}$.

Let $\Gamma(n)$ be the rate (ie inverse time) for traversal of an n^{th} stage bond by a domain wall incident on it. $\Gamma(n)$ satisfies the following recurrence relation (Harris and Stinchcombe 1986),

$$\Gamma^{-1}(i) = r^2\Gamma^{-1}(i-1)+\epsilon_{AH}(i-1)s^2\Gamma^{-1}(i-1) \qquad i\geq 2$$

and $$\Gamma^{-1}(1) = (r-(L/a))^2\Gamma^{-1}(0)+\epsilon_{AH}(1)s^2\Gamma^{-1}(0) \qquad (8.4.24)$$

where $\epsilon_{AH}(i)\propto\exp(2w_i)$, and $w_i=w(\xi(i),\theta(i))$. Hence, taking logs and applying (8.4.22) recursively gives

$$\log\tau_c = \log\Gamma^{-1}(n) \approx \sum_{m=2}^{n} w_m \propto \sum_{m=2}^{n} \Phi_1^{-1}\{\theta(r+2s)^{n/(\tilde{\nu}d)}\} \qquad (8.4.25)$$

and we have ignored the less divergent $F(\theta)$ terms and assumed that $\xi\propto\xi_p$ for fixed $\lambda=(\xi_p/\xi_T)$.

We list the explicit forms for τ_c in the regimes defined in the text for the cluster renormalisation, the details of the calculations being similar to those for that case:

i). $u\gg 1$, $d=2$ *(Ising-like regime)*

Here (8.4.25) yields,

$$\tau_c \propto (\xi/a)^{A\log(\xi/a)} \qquad (8.4.26)$$

where $A=\{(2\tilde{\nu}/d)\log(r+2s)\}^{-1}$ in exact correspondence with the equivalent calculation for the Ising magnet (Harris and Stinchcombe 1986).

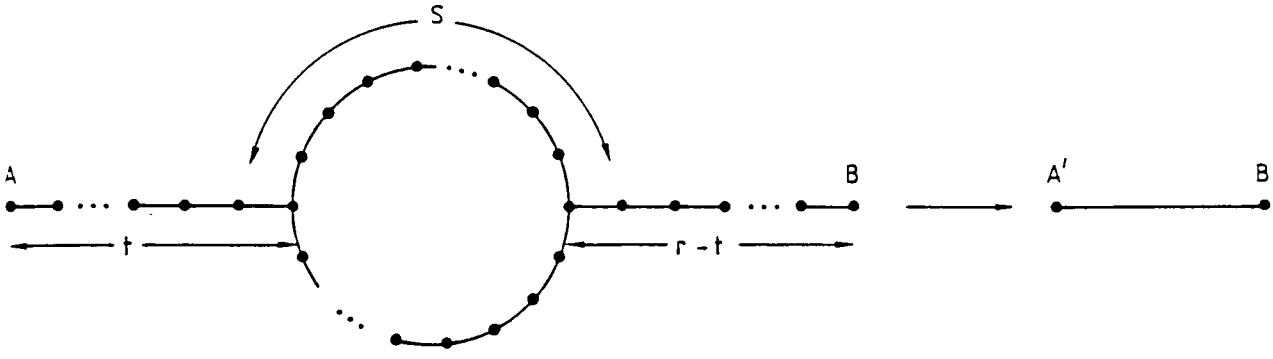

Fig.8.5: Regular fractal representation of the percolation cluster. The scaling factor $b=(r+2s)^{1/d}$ is chosen to satisfy convexity relations and hyperscaling.

ii). u≫1, d=3 *(Ising-like regime)*

As in the corresponding random calculation, (8.4.17), we obtain for the regular fractal,

$$\tau_c \propto (\xi/a)^{A\log(\xi/a)} \qquad (8.4.27)$$

where we have used (8.4.25) and (8.2.6).

iii). u≪1, d=3 *(Heisenberg-like regime)*

In this situation,

$$w(m) \propto \theta(r+2s)^{(m/\tilde{\nu}d)}$$

and consequently

$$\tau_c \propto \tau(1,0)/\tau(\xi/a,0)e^{C\theta\xi^{(1/\tilde{\nu}d)}}$$
$$\propto (\xi/a)^z \qquad (8.4.28)$$

the conventional scaling form. C is defined in section A. above and we recall that the exponent is constrained to be small in this regime despite the divergence of ξ/a. Finally,

iv). u≪1, d=2 *(Heisenberg-like regime)*

$$\tau_c \propto \tau(1,0)/\tau(\xi/a,0)e^{C\theta\xi^{(1/\tilde{\nu}d)}}$$
$$\propto (\xi/a)^z \qquad (8.4.29)$$

as above since $\theta\xi^{(1/\tilde{\nu}d)} \ll 1$ in this regime.

V.Summary and Discussion

To summarise, we have investigated Bloch wall dynamics on percolation clusters in the bond-diluted classical anisotropic Heisenberg model using cluster renormalisation and a regular fractal representation. In order to derive expressions for the characteristic domain boundary diffusion times one required knowledge of the Bloch wall energy for arbitrary anisotropy. In section III we used straightforward scaling arguments to derive the wall energy and length which turn out to be expressible in terms of natural scaling

variables for the statics of the pure one dimensional AH model,

$$E/J = 2\tanh\theta$$

$$L/a = \frac{2\log(\cot(\epsilon/2))}{\theta} \qquad (8.5.1)$$

In all cases of non-vanishing anisotropy we observe that for low enough temperatures conventional dynamic scaling is violated.

The parameter $u=K\tanh\theta+F(\theta)$, the scaling variable for the one-dimensional correlation length, is shown to control the d>1 dynamics at the percolation threshold. In the high temperature regime $u \ll u^*$, where the one-dimensional correlations are Heisenberg-like, we find that conventional dynamic scaling applies:

$$\tau_c = \tau(1,(\xi/a)\theta)/\tau(\xi/a,\theta) \propto (\xi/a)^z \qquad (8.5.2)$$

This is consistent with studies of spin-waves in the isotropic system at $p=p_c$ (Chp.7 and Appendix P) and arises in this case from the isomorphism existing between diffusion and linearised spin-wave theory.

As one passes the crossover temperature $u^* \sim 1$ and enters $u \gg u^*$, the low temperature or *Ising-like* regime, we have shown that the Glauber Bloch wall dynamics crosses over to an anomalous form obeying a *singular dynamic scaling* form:

$$\tau_c \propto (\xi/a)^{A\log\xi} \qquad (8.5.3)$$

where ξ/a is the d>1, $p=p_c$ AH system correlation length (8.2.10) and $A=(2\tilde{\nu}\log 2)^{-1}$. In particular we recover $\tilde{\nu}=\nu_p$ and $\xi=\xi_{Ising} \propto \exp(2J\nu_p/T)$ in the Ising limit ($\theta=\infty$), and thence (8.5.5) yields (8.1.7) in agreement with the earlier studies of Henley (1985) and Harris and Stinchcombe (1986).

Conclusions.

We conclude this thesis with a brief survey of the new results obtained and some suggestions for further research.

We have used both real space and momentum space renormalisation group techniques to study dynamical problems on a range of both regularly and statistically scale-invariant structures. The main results of this thesis may be summarised as follows:

(i) Using Niemeyer-van Leeuwen blocking ideas we were able to obtain a sequence of approximations to the quantity β_s/β in good broad agreement with the corresponding numerical investigations (Watson 1985) in two dimensions. We were further able to exhibit a relation between the crossover exponent and certain system fractal dimensions.

(ii) For DLA, we have shown that the conjecture of Aharony and Stauffer (1984) regarding anomalous diffusion is more appropriate than the Alexander-Orbach (1983) conjecture. We have obtained values for the walk dimension d_w and the spectral dimension d_s in good agreement with related Monte Carlo work (Meakin and Stanley 1983).

(iii) Using similar RSRG techniques to those in (ii) above we investigated diffusion on the model for proteins of Helman *et al* (1984). This work was conclusive in that the suggestion of Helman *et al* that $d_w=2$ seemed ruled out. However, owing to inherent uncontrolled approximations (eg cell interfacing, recursion relation truncation) the finer issue of the splitting of dynamical universality classes was left somewhat unclear. An attempt to gain further understanding of this point using exact enumerations and series analysis still appeared to leave the question of the relevance of the crosslinks to dynamics open.

(iv) We were able to construct a method to evaluate spin and field theoretic Hamiltonians for a variety of walk models and in particular for SAWs with crosslinks (the model in (iii) above). Further, we were able to introduce resistances into the Hamiltonians using the usual Potts model in the limit when the number of states q tends to zero. The relation between SAWs and GRWs was exhibited in terms of flow through an extended parameter space allowing for arbitrary bare values for the two sets

of distinct symmetry quartic potentials. One key result of this work was the $O(\epsilon^2)$ determination for the non-trivial resistive crossover exponent φ for GRWs. We were also able to establish that the potentials due to crosslinks in the SAW field theory were in fact irrelevant (to $O(\epsilon)$) thereby resolving the problems in (iii) above.

(v) Using scaling ideas together with perturbative methods we presented an investigation of the damping of spin waves in Heisenberg ferromagnets near the percolation threshold. It was evident that the perturbation theory was convergent only for $k\xi \ll 1$, the hydrodynamic regime. It was shown, in this regime, that the spin wave damping and transverse response functions obeyed the usual dynamic scaling hypothesis of Halperin and Hohenberg (1967) and we developed relationships between infinite cluster and finite cluster ensemble exponents. The results were extended with similar conclusions to the more realistic two-sublattice systems.

(vi) In the dilute anisotropic Heisenberg case, however, we have demonstrated a crossover from relaxational behaviour arising from the conventional dynamic scaling principle to new singular dynamic scaling forms. Thus, the anisotropy α represents a relevant perturbation. This behaviour is much in line with intuitive ideas on these matters in the theory of critical phenomena.

As far as further work is concerned, there seem to be many opportunities. One clear immediate task is to extend the exact enumerations for "protein structure" and analyse the resulting series using Padé techniques. This is currently being done by the author. Further information like probability distribution functions are also being extracted.

The procedure for developing Hamiltonian formulations of Chps.5,6 seems fairly general and one may be able to apply it to the conformational and also to the resistive properties of further interesting problems. One such problem is that of spiral SAWs (Fisher *et al* 1984) for which numerical experiments indicate that the winding number has curious scaling properties. To gain theoretical insight into this problem would be worthwhile. This method may, of course, also be applied to non-walk problems and one speculates whether it might be able to shed any light on the elusive field theory for

DLA.

In chapter 7 the perturbation theory diverged when $k\xi$ was not very much less than unity. More interesting and anomalous behaviour is expected to occur in the critical regime $k\xi \gg 1$. A reformulation or extension of our method to gain access to this regime is highly desirable as it relates to the question of localisation and fractons (see Alexander and Orbach 1983).

Finally, early in the Introduction we stated the isomorphism between spin waves, diffusion, phonons and the like, yet in the literature no clear and explicit understanding of the equivalence of measurable quantities has emerged. Thus, rederiving results for, say, spin waves and random walks in a unified manner would be a useful longer term research objective.

Note Added:

Bray and Moore (1977) have used scaling arguments for semi-infinite systems to determine β_1 (in the notation of our chapter two this is β_s) in terms of certain other percolation exponents. In particular they derive the following relation:

$$\beta_1 = \tfrac{1}{2}\,\nu\,(d-2+\eta_{\parallel}) \qquad (I)$$

where ν is the (bulk) correlation length exponent and $\eta_{\parallel}$ measures the decay of correlations at T_c (or p_c) between sites at the surface – including correlations mediated by the (semi-infinite) bulk. In d=2, ν is believed to be exactly $4/3$ (den Nijs 1979) for percolation. Subsequent to the work in chapter two, Cardy (1985) has given an exact calculation for the exponent $\eta_{\parallel}$ for the q-state Potts and n-vector models using conformal mapping techniques. In particular, for percolation ($q \to 1$ limit of the Potts model) he obtains $\eta_{\parallel} = 2/3$. Thus, using (I) above, it follows that $\beta_1 = 4/9$ in two dimensions. Further, (2.6.4) of chapter two allows one to express D_f in terms of $\eta_{\parallel}$:

$$D_f = \tfrac{1}{2}\,(d-\eta_{\parallel}) \qquad (II)$$

$$= 2/3 \qquad \text{in two dimensions.}$$

This (exact) result compares favourably with our RSRG result $D_f \sim 0.7$. (II) may also be derived using the relation $D_f = \Delta_1/\nu$ (Stinchcombe, Essam, private communication), where Δ_1, the surface gap exponent, is given by $\Delta_1 = \frac{1}{2}\nu(d-\eta_{\parallel})$ (Bray and Moore 1977).

Appendix A

Finite Size Scaling for β_s.

Let $P(\xi,L)$ be the probability that a site, in a specified (d−1)-dimensional plane, is in the bulk (ie d-dimensional) infinite cluster. Then the usual finite size scaling ansatz is written as

$$P(\xi,L) \propto L^{\epsilon} f(\xi/L) \qquad \text{(A1)}$$

where ξ is the system (ie bulk) correlation length and f is a scaling function with the following properties

$$\begin{aligned} f(x) &\to \text{const.} && x\to\infty \\ &\to x^{\epsilon} && x\to 0 \end{aligned} \qquad \text{(A2)}$$

where $\epsilon=-\beta/\nu$.

We wish to consider the set S where

S={x:site x is in (d−1)-dimensional hyperplane and connected to an infinite number of sites <u>below</u> the slice}

Then, denoting the probability of $x\epsilon S$ as $P(x\epsilon S)$, it follows that

$$P(x\epsilon S) = P(\xi,L).H \qquad \text{(A3)}$$

where H is the (conditional) probability that a site in the infinite cluster will remain so when a slice has been made. But, we may write H without loss of generality in terms of ξ and L:

$$H(\xi,L) = (p-p_c)^{\beta_s-\beta}\, G(\xi,L) \qquad \text{(A4)}$$

such that

$$\begin{aligned} G(\xi,L) &\to \text{const} && L\gg\xi \\ &\to \xi^{(\beta_s-\beta)/\nu}\, g(L) && L\ll\xi. \end{aligned} \qquad \text{(A5)}$$

Notice that we have made no assumptions concerning the scaling behaviour of H yet —— we have simply asserted that *very* near the percolation threshold (ie $\xi/L\to\infty$) we

expect it to be independent of $(p-p_c)$ and that for a *nearly* infinite system (ie $L/\xi \to \infty$) we should not expect it to depend on L. Then using (A3), we obtain

$$P(x \epsilon S) \propto L^{\epsilon} (p-p_c)^{(\beta_s-\beta)} f(\xi/L) G(\xi,L) \qquad (A6)$$

However, by definition, the (generalised) surface percolation probability $P_s(\xi_s,L) = P(x \epsilon S)$ and we postulate a scaling form for this function analogous to (A1) for the bulk function. Thus

$$P_s(\xi_s,L) \propto L^{\alpha'} r(\xi_s/L) \qquad (A7)$$

with

$$r(x) \to \text{const.} \qquad x \gg 1$$
$$\to x^{\epsilon'} \qquad x \ll 1.$$

Here ξ_s is the *surface* correlation length, which relates to the surface clusters of sites that are elements of S. It diverges according to the surface exponent ν_s:

$$\xi_s \sim |p-p_c|^{-\nu_s}. \qquad (A8)$$

By the standard arguments $\epsilon' = -\beta_s/\nu_s \equiv D_f-(d-1)$, where D_f is the fractal dimensionality of S and β_s is as discussed in Chp.2.

Therefore we obtain

$$L^{\epsilon'} r(\xi_s/L) \propto L^{\epsilon} (p-p_c)^{(\beta_s-\beta)} f(\xi/L) G(\xi,L) \qquad (A9)$$

In the regime $L \gg \xi, \xi_s$, (A9) is obeyed identically. However for $L \ll \xi, \xi_s$ we obtain the g(L) as

$$g(L) \propto L^{\epsilon-\epsilon'} \propto L^{[\beta/\nu - \beta_s/\nu_s]}. \qquad (A10)$$

Finally, we use assumption that there are only the two controlloing length scales ξ and ξ_s together with the *ansatz*

$$G(\xi,L) = \ell(\xi_s/L) \qquad (A11)$$

with the consequence that $\nu=\nu_s$. Choosing ξ in (A11) gives the same result.

Hence we obtain the result

$$D_f = (d-1) - \beta_s/\nu. \qquad (A12)$$

The result (2.6.5) follows.

Appendix B.

B1. Random walks on the Sierpinsky Gasket.

We test the legitimacy of (3.4.8) by applying it to a related system, percolation. In the spirit of section 3 of Chapter 3 we have used fugacity transformation methods to determine d_s for Sierpinsky gasket models of the Infinite Incipient Cluster in two dimensions. Strictly speaking, Sierpinsky gaskets model the IIC backbone but we here use them as simple models for the full infinite cluster. Explicitly, we have performed b=2,4,8 renormalisations as in fig.3.6 and obtained $d_w(2)=1.82$, $d_w(4)=2.01$, $d_w(8)=2.08$ using the mid-point rule as above. We then apply the extrapolation rule $d_w(b)=d_w+C_1/(\log b)+C_2/(\log b)^2$ to obtain $d_w=2.22$ and hence $d_s=1.43$. Gefen *et al* (1981) have performed the resistance rescaling calculation for the Sierpinsky gasket and obtain $d_s=2\log 3/\log 5$ and therefore,for percolation in d=2, the RHS of (3.3.13) becomes

$$\frac{d_s(\text{exact, regular})}{d_s(\text{R.G., regular})} \approx 0.954. \qquad \text{(B1)}$$

Now, for the random system we use the accurate numerical results of Zabolitzky (1984) (d_s("exact",random)=1.322), and the RG results of Reynolds *et al* (1980), $d_f=1.898$ and of Sahimi and Jerauld (1983), $d_w=2.810$ (yielding the estimate d_s(R.G.,random)=1.351). The LHS of (3.4.8) thus becomes

$$\frac{d_s(\text{exact, random})}{d_s(\text{R.G., random})} \approx 0.979. \qquad \text{(B2)}$$

The error involved in using the relation (3.4.8) for percolation is therefore less than 2½%. This result therefore supports the argument given at the end of section 4, for the use of (3.4.8).

B2. Dynamic Universality Classes for Diffusion-Limited Aggregation and Lattice Animals.

We generalise the method of Chapter 3 and demonstrate that Witten-Sander clusters lie in a distinct dynamic universality class to random lattice animals. This work has been published in J.Phys. A (Christou and Stinchcombe 1986d).

A feature arising from the renormalisation group (RG) theory (Wilson and Kogut 1974) is that diverse systems undergoing continuous phase transitions, characterised by a diverging controlling length, partition themselves into universality classes. Within a universality class, systems which seem, in a superficial sense at least, very different to each other have critical behaviour which is essentially the same: the apparent differences becoming irrelevant as one approaches criticality.

The critical behaviour for a particular system is governed by a set of critical exponents and a subset of these are the same for all the constituent systems of a particular universality class. It is convenient to divide the set of universality classes into two groups: static and dynamic. Systems within the same static universality class will have the same exponents characterising the singularities in the static properties and equivalently for dynamic universality classes. We recall that two systems may be in the same static universality class but in distinct dynamic ones and *vice versa*.

In RG theory one may represent the set of universality classes by an isomorphic set of critical surfaces embedded in a parameter space. Systems with the same critical behaviour will flow toward the same critical point.

In this appendix we generalise the real space renormalisation group (RSRG) method presented in chapter 2 in order to investigate two related models, diffusion limited aggregation (DLA) (Witten and Sander 1981) and random lattice animals (Family 1983). It has been shown that DLA, a kinetic growth process, and lattice animals, which are equilibrium random clusters, are in distinct *static* universality classes in both the isotropic (Gould *et al* 1983) and directed (Green 1984) cases. In the following we extend the parameter space used by these authors to show that these respective systems also lie in distinct dynamic universality classes.

We consider the model of generalised DLA in two dimensions described by Gould *et al* (1983) in which the role of the seed site in the growth process of DLA is replaced by a general random cluster. It has been shown using Monte Carlo methods (Sander and Witten 1982) that the critical properties of the aggregate are unchanged in the limit of large cluster growth relative to seed size. Gould *et al* (1983) used a two-parameter b=2 single cell RSRG method to show that these models had different static fixed points in a two dimensional parameter space implying, for example, distinct fractal dimensions d_f (Mandelbrot 1982). A procedure analogous to this was developed by Green (1984), however she constrained the cluster to grow only eastwards or northwards favouring growth along the (1,1) axis. Green also observed distinct static fixed points using a b=2 renormalisation.

Now, the dynamic exponent for these systems is the *random walk dimensionality* d_w (see chapter 2) for random walks on the fractal space. In order to determine the structure of the parameter space from which one extracts d_w, three parameters, or fugacities are used. A fugacity K is associated with each occupied site of the fractal cluster, another fugacity W is associated with each step of the incoming particles and a third fugacity V is associated with each step of a 'myopic ant' (de Gennes 1976) confined to walk on the cluster.

Within the RSRG procedure the square lattice is mapped onto one isomorphic to it together with an accompanied length scale dilatation of factor b. The parameters K,W,V are mapped onto K',W',V' on the new lattice. This may be represented as a flow in parameter space as pointed out above. A cluster approximation (see Stanley *et al* 1982 and refs. therein) is used to determine the explicit RG transformation. We seek qualitative information relating to the RG flow in parameter space, and not accurate numerical values of the dynamic exponent d_w, and we accordingly confine our attention to the simplest, b=2, renormalisation. To obtain reliable values for the exponents at the various fixed points one must use larger cells in order to diminish cell interfacing problems (Stanley *et al* 1982). We work on the premise that these interfacing problems do not affect the qualitative structure of the flow through parameter space, and in particular that the universality classes remain unaffected.

We evaluate the RG transformations in a manner described in chapter 2 except that one must now consider all possible lattice animal configurations (both spanning and non-spanning) as seed sites in the b=2 cell. For the static parameters K,W, Gould *et al* (1983) obtain the following recursion relations,

$$K' = 3K^3 + K^4 + 6K^3W(1+W+2W^2) + 4K^4W(1+2W+2W^2+4W^3) \qquad (B3)$$

$$W' = W^2 + 2W^3 + 5W^4 + 14W^5 + 2KW^2(1+W+3W^2+5W^3) + K^2W^2(1+2W^2) \qquad (B4)$$

(B4) contains all possible spanning random walks in a cell with some sites (non-spanning) already occupied.

Similarly for V we obtain the following transformation:

$$\begin{aligned}\tfrac{1}{2}K'V' = {} & ((1/3)V^2+(1/9)V^3+(7/27)V^4+(13/81)V^5)(\alpha K^3+2K^3W+K^3) \\ & + ((1/9)V^3+(13/81)V^5)(\alpha K^3+2K^3W+K^3) \\ & + ((1/4)V^2+(1/4)V^4)(\alpha K^3+2K^3W+K^3) \\ & + ((1/6)V^2+(1/12)V^3+(5/36)V^4+(1/9)V^5)(\beta K^4+8K^4W^2+4K^4W+K^4)\end{aligned} \qquad (B5)$$

where $\alpha=2W^2(1+2W)K^3$ and $\beta=8W^3(1+2W)K^4$.

Equations (B3),(B4) and (B5) have the flow pattern in parameter space shown in fig.B.1. This demonstrates that DLA and lattice animals are indeed in distinct dynamic universality classes The triply unstable critical fixed point E is the dynamic fixed point for DLA where one evaluates the eigenvalue $\lambda_{W=}(\partial V'/\partial V)_{K^*,W^*,V^*}$ from which one determines $d_w = \log\lambda_w/\log b$. The significance of the other fixed points is indicated in Table B.1. We note that the behaviour of the flow lines in the (K,W) plane is identical to that found by Gould *et al* since K'=f(K,W) and W'=g(K,W).

We now perform the analogous calculation for the problem of directed generalised DLA-lattice animals. The recursion relations for K and W for a b=2 transformation are given by Green:

$$K' = 2K^3 + K^4 + 4K^3W^2(1+2W) + 8K^4W^3(1+2W) + 4K^3W + 4K^4W(1+2W) \qquad (B6)$$

$$W' = W^2 + 2W^3 + W^2K^2 + 2KW^2(1+W) \qquad \text{(B7)}$$

and for the generalised directed problem we obtain the following transformation for V',

$$\begin{aligned}\tfrac{1}{2}K'V' = {} & ((1/3)V^2+(1/9)V^3+(7/27)V^4+(13/81)V^5)(\alpha K^3+2K^3W+K^3) \\ & + ((1/9)V^3+(13/81)V^5)(\alpha K^3+2K^3W+K^3) \\ & + ((1/4)V^2+(1/4)V^4)(\ 0\ ) \\ & + ((1/6)V^2+(1/12)V^3+(5/36)V^4+(1/9)V^5)(\beta K^4+8K^4W^2+4K^4W+K^4)\end{aligned} \qquad \text{(B8)}$$

α and β being defined as above.

These equations yield a flow diagram qualitatively equivalent to that obtained in the isotropic problem. We therefore conclude that directed DLA and directed lattice animals are also in distinct dynamic universality classes.

As a final remark we note that the fixed points F and G of fig.B.1 are artifacts of the method in both the isotropic and directed calculations. This is so since when K=0 there is no cluster available on which anomalous diffusion (characterised by the parameter V) can occur. However on examining the behaviour of the recursion relations as $K\to 0$ one observes that only quasi-one-dimensional spanning clusters contribute weight to the RHS of equations (B5) and (B8). One may therefore identify F as the fixed point for random walks on a 1d substrate . However random walks in one dimension have identical critical behaviour to those in two dimensions ($d_w=2$), and static and dynamic random walk fixed points are equivalent ($d_f=d_w$). We therefore interpret F as the dynamic fixed point for random walks in two dimensions. Similarly, G is to be identified as the static fixed point for random walks on a one dimensional substrate where the kinetic growth interpretation for the walks (Nakanishi and Family 1984) has been used in generating the recursion relations.The above view is consistent with the distribution of the fixed points for the other two systems.

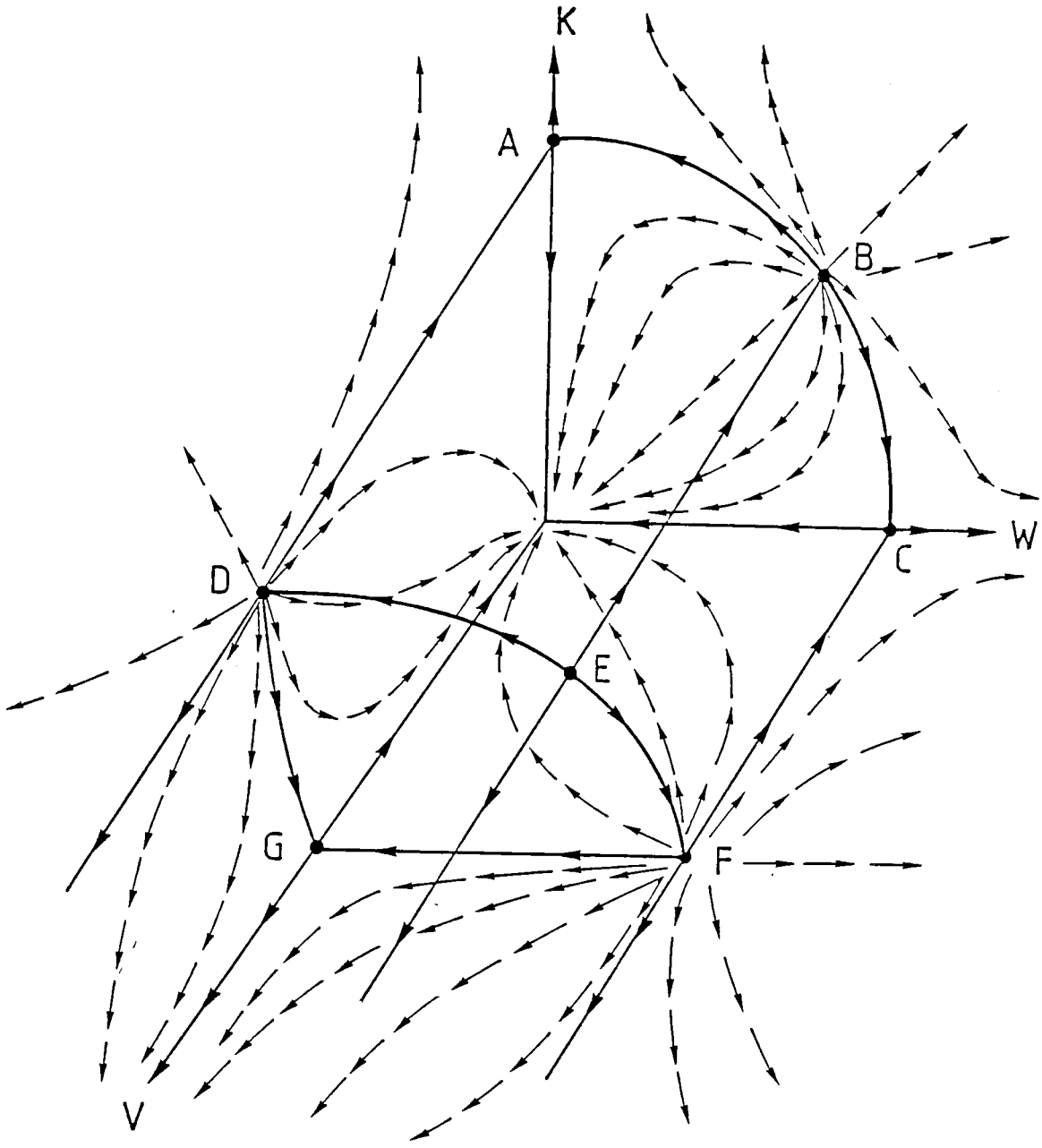

Fig.B1.: Renormalisation Group flow diagram for transformations (B3),(B4),(B5) and (B6),(B7),(B8). The arrows indicate the local flow direction. The significance of the fixed points A,B,C,D,E,F,G is indicated in Tables B.1 and B.2.

Table B.1. Fixed points for *isotropic* (upper of two numbers in each pair) generalised DLA and the corresponding *directed* problem (lower number in each pair), (refer to fig.B.1).

Nature of Fixed Point.	K^*	W^*	V^*
A. Lattice Animals, Static	0.532 0.618	0 0	0 0
B. DLA, Static	0.392 0.420	0.274 0.337	0 0
C. Random Walk, Static	0 0	0.347 $\frac{1}{2}$	0 0
D. Lattice Animals, Dynamic	0.532 0.618	0 0	1.033 1.058
E. DLA, Dynamic	0.392 0.420	0.274 0.337	1.048 1.080
F. Random Walk, Dynamic	0 0	0.347 $\frac{1}{2}$	0.963 0.950
G. Random Walk, Static (Kinetic interpretation)	0 0	0 0	0.963 0.950

Table B.2. Fixed points for *directed* generalised DLA (refer to fig.B.1).

Nature of Fixed Point.	K^*	W^*	V^*
A. Lattice Animals, Static	0.618	0	0
B. DLA, Static	0.420	0.337	0
C. Random Walk, Static	0	$\frac{1}{2}$	0
D. Lattice Animals, Dynamic	0.618	0	1.058
E. DLA, Dynamic	0.420	0.337	1.080
F. Random Walk, Dynamic	0	$\frac{1}{2}$	0.950
G. Random Walk, Static (Kinetic interpretation)	0	0	0.950

Appendix C

Why are Replicated Gaussian Variables needed for Random Walks ?

To illustrate the need for the replication of the Gaussian variables in the spin Hamiltonian (5.40) for GRWs, we now calculate $\langle u(x)\underline{v}(x).\underline{v}(x')u(x')\rangle$ for a (trivial) two site problem. We denote the respective Gaussian variables u and w with corresponding Potts variables $\underline{a}$ and $\underline{b}$. Firstly, we carry out a calculation of the correlation function without replicating the Gaussian variables. Thus we write the correlation function

$$\langle uw\underline{a}^1.\underline{b}^1\rangle = \frac{\int e^{-\frac{1}{2}u^2}du\ e^{-\frac{1}{2}w^2}dw\ \underset{\underline{a},\underline{b}}{Tr}\ e^{-H}(\underline{a}^1.\underline{b}^1\ uw)}{\int e^{-\frac{1}{2}u^2}du\ e^{-\frac{1}{2}w^2}dw\ \underset{\underline{a},\underline{b}}{Tr}\ e^{-H}} \qquad (C1)$$

where

$$e^{-H} = \exp\Big\{ -\tfrac{1}{2}K\ uw \prod_{\beta}\Big\{1+\frac{q-1}{1+t}\ \underline{a}^{\beta}.\underline{b}^{\beta}\Big\}\Big\}$$

$$= \exp\{ -\tfrac{1}{2}K\ uw\ \mathbb{U}\} \qquad (C2)$$

which defines $\mathbb{U}$. Performing the integration over the Gaussian variables by the usual methods gives:

$$\langle uw\underline{a}^1.\underline{b}^1\rangle = \frac{\underset{\underline{a},\underline{b}}{Tr}\left[\ \underline{a}^1.\underline{b}^1\ (Det\ A)^{-3/2}\ K\mathbb{U}\ \right]}{\underset{\underline{a},\underline{b}}{Tr}\left[(Det\ A)^{-\frac{1}{2}}\right]}\ . \qquad (C3)$$

where $\mathbb{U}$ is defined in (C2) and the matrix A is given by:

$$A = \begin{bmatrix} 1 & K\mathbb{U} \\ K\mathbb{U} & 1 \end{bmatrix}. \qquad (C4)$$

It is straightforward to show (but tedious in algebra) that the denominator in (C3) is in fact unity when the appropriate limits ($m\to 0, q\to 0, t\to 0$) are taken. Thus we may expand the numerator of (C3) and we obtain:

$$\langle uw\underline{a}^1.\underline{b}^1\rangle = \sum_{r=0}^{\infty} \underset{\underline{a},\underline{b}}{\mathrm{Tr}}\ \underline{a}^1.\underline{b}^1\ K^{2r+1}\ U^{2r+1}\ \frac{(\frac{1}{2}+r)!}{r!\ (\frac{1}{2})!}$$

$$= \sum_{r=0}^{\infty} q^{2m}\ \frac{(\frac{1}{2}+r)!}{r!\ (\frac{1}{2})!}\ K^{2r+1}\ \langle \underline{a}^1.\underline{b}^1\ U^{2r+1}\rangle . \left\{\langle U^{2r+1}\rangle\right\}^{m-1}$$

$$= \sum_{r=0}^{\infty} q^{2m}\ \frac{(\frac{1}{2}+r)!}{r!\ (\frac{1}{2})!}\ K^{2r+1}\ \langle \underline{a}^1.\underline{b}^1\ U^{2r+1}\rangle \ \Big/ \langle U^{2r+1}\rangle$$

$$= \sum_{r=0}^{\infty} q^{2m}\ \frac{(\frac{1}{2}+r)!}{r!\ (\frac{1}{2})!}\ K^{2r+1}\ \frac{(t+q)^{2r+1} - t^{2r+1}}{(t+q)^{2r+1} + (q-1)t^{2r+1}} \qquad \text{(C5)}$$

and so we obtain ($q \to 0$) the incorrect result:

$$\langle uw\underline{a}^1.\underline{b}^1\rangle = \sum_{r=0}^{\infty} \frac{(\frac{1}{2}+r)!}{r!\ (\frac{1}{2})!}\ K^{2r+1}\ (1 - \frac{t}{2r+1}) \qquad \text{(C6)}$$

since the numerical weight factor is wrong: it should be unity. Now, replicating the Gaussian variable $u \to u^{\alpha}$, where $\alpha=1,\ldots,n$ and similarly for w, such that

$$e^{-H} = \exp\Big\{ -\tfrac{1}{2} K \sum_{\alpha} u^{\alpha} w^{\alpha} \prod_{\beta} \{1 + \frac{q-1}{1+t}\ \underline{a}^{\beta}.\underline{b}^{\beta}\} \Big\} . \qquad \text{(C7)}$$

After a little work one obtains, in this case,

$$\langle u^1 w^1\ \underline{a}^1.\underline{b}^1\rangle = \underset{\underline{a},\underline{b}}{\mathrm{Tr}}\ \underline{a}^1.\underline{b}^1 (KU/(1-KU^2))$$

$$= \underset{\underline{a},\underline{b}}{\mathrm{Tr}} \sum_{r=0}^{\infty} K^{2r+1}\ \underline{a}^1.\underline{b}^1\ U^{2r+1}$$

$$= \sum_{r=0}^{\infty} K^{2r+1}\ q^{2m}\ \frac{\langle \underline{a}^1.\underline{b}^1\ U^{2r+1}\rangle}{\langle U^{2r+1}\rangle}$$

$$= \sum_{r=0}^{\infty} K^{2r+1} (1 - \frac{t}{(2r+1)}) \qquad \text{(C8)}$$

which is the required result.

Appendix D

Walk Susceptibilities as Correlation Functions.

In this appendix we derive (5.41) first for GRWs and then for SAWs. We start by noting that H_{uv} in (5.40) can be written as a sum of Hamiltonians for different replicas:

$$H_{uv} = \sum_{\alpha} h(u_\alpha, v), \tag{D1}$$

where

$$h(u,v) = \tfrac{1}{2} \sum_{x,x'} M_{x,x'}(\{\underline{v}\}) u(x)\ u(x'), \tag{D2}$$

where

$$M_{x,x'}(\{\underline{v}\}) = -K\gamma_{x,x'} \left[\prod_{\beta=1}^{m} \left[1 + \frac{q-1}{1+t}\, \underline{v}_\beta(x).\underline{v}_\beta(x') \right] \right] \tag{D3a}$$

$$\equiv -K\gamma_{x,x'}\ \Omega_{x,x'}\ . \tag{D3b}$$

Thus

$$\langle u_1(x)\underline{v}_1(x).\underline{v}_1(x')u_1(x')\rangle =$$

$$\frac{\operatorname{Tr}_{\underline{v}} \left\{ \underline{v}_1(x)\cdot\underline{v}_1(x') \operatorname{Tr}_{u}\ u_1(x)\ u_1(x') \prod_{\alpha=1}^{n} e^{-h(u_\alpha, v)} \right\}}{\operatorname{Tr}_{v} \left\{ \operatorname{Tr}_{u} \prod_{\alpha=1}^{n} e^{-h(u_\alpha, v)} \right\}} \ . \tag{D4}$$

We set $z(v) = \operatorname{Tr}_{u_\alpha} e^{-h(u_\alpha, v)}$, and since u_α is a dummy variable z is independent of α, but does, of course, depend on the $\underline{v}$'s. Thus

$$\langle u_1(x)\underline{v}(x)\cdot\underline{v}_1(x')u_1(x')\rangle =$$

$$\frac{\underset{\underline{v}}{\mathrm{Tr}}\left\{\underline{v}_1(x)\cdot\underline{v}_1(x')\ \underset{u_1}{\mathrm{Tr}}\ u_1(x)\ u_1(x')\ e^{-h(u_1,v)}\ z(v)^{n-1}\right\}}{\underset{v}{\mathrm{Tr}}\ z(v)^n} . \qquad \text{(D5)}$$

Now let $n \to 0$ so that $z(v)^n = 1$ and use (5.4) to express the trace over u as matrix inverse. Then

$$\langle u_1(x)\underline{v}_1(x)\cdot\underline{v}_1(x')u_1(x')\rangle = \underset{\underline{v}}{\mathrm{Tr}}\ \underline{v}_1(x)\cdot\underline{v}_1(x')\ [A^{-1}(\{\underline{v}\})_{x,x'}]. \qquad \text{(D6)}$$

where $A_{x,x'}\equiv\delta_{x,x'}+M_{x,x'}$. Next we expand the matrix inverse A^{-1} in powers of K:

$$[A^{-1}(\{\bar{v}\})]_{x,x'} = \delta_{x,x'} + K\gamma_{x,x'}\,\Omega_{x,x'}$$

$$+ K^2 \sum_{x_2} \gamma_{x,x_2}\,\gamma_{x_2,x'}\,\Omega_{x,x_2}\,\Omega_{x_2,x'} \ \ldots \qquad \text{(D7)}$$

and the term of order K^N is

$$K^N \sum_{x_2}\cdots\sum_{x_N}\ \prod_{i=1}^{n}\left[\ \gamma_{x_i,x_{i+1}}\ \Omega_{x_i,x_{i+1}}\ \right], \qquad \text{(D8)}$$

where $x_1 = x$ and $x_{N+1}=x'$. According to (D3)

$$\Omega_{x,x'} = \prod_{\beta=1}^{m}\left[1+\frac{q-1}{1+t}\ \underline{v}_\beta(x)\cdot\underline{v}_\beta(x')\right]. \qquad \text{(D9)}$$

We describe (D7) as an expansion over all random walks γ_N of N steps and associated with each walk there is the factor

$$W(\gamma_N,\{\underline{v}\}) = \prod_{\beta=1}^{m} w(\gamma_N,\underline{v}_\beta), \qquad \text{(D10)}$$

where

$$w(\gamma_N,\underline{v}) = \prod_{<x,x'>\subseteq\gamma_N}\left[1+\frac{q-1}{1+t}\,\underline{v}(x)\cdot\underline{v}(x')\right]. \qquad (D11)$$

Here $<\ldots> \subseteq \gamma_N$ indicates a product over bonds with one factor for each step.

If a given bond is traversed by ℓ steps it carries a factor

$$C_\ell = \prod_{\beta=1}^{m}\left[1+\frac{q-1}{1+t}\,\underline{v}_\beta(x).\underline{v}_\beta(x')\right]^\ell. \qquad (D12)$$

Note that $\underline{v}_\beta(x)\cdot\underline{v}_\beta(x')$ only assumes the two values 1 and $-(q-1)^{-1}$. This fact allows us to write C_ℓ as

$$C_\ell = \left[1+\frac{(1+q/t)^\ell-1}{q}\right]^m\left[\frac{t}{1+t}\right]^{m\ell}$$

$$\times\prod_{\beta=1}^{m}\left\{1+\frac{(q-1)[(1+q/t)^\ell-1]}{q+[(1+q/t)^\ell-1]}\,\underline{v}_\beta(x)\cdot\underline{v}_\beta(x')\right\}. \qquad (D13)$$

The order of limits is important here. Of the four variables which are to be set to zero, the first limit to take is $m\to 0$, so that q^m and t^m are both unity. (We will see this is the right order of limits in a moment.) From Harris and Lubensky (1987) it is clear that we must set $q \to 0$ before t, so that $q/t = 0$. These considerations lead to the result,

$$\lim_{q\to 0}\left[\lim_{m\to 0} C_\ell\right] = \prod_{\beta=1}^{m}\left[1+\frac{q-1}{1+\frac{t}{\ell}}\,\underline{v}_\beta(x)\cdot\underline{v}_\beta(x')\right]. \qquad (D14)$$

Thus for a bond traversed ℓ times t is replaced by t/ℓ. This is expected, of course, because t^{-1} is proportional to the conductance of the bond. From this analysis we see that w in (D11) can be written as

$$w(\gamma_N,\underline{v}_\beta) = \prod'_{<x,x'>\subseteq\gamma_N}\left[1+\frac{q-1}{1+\frac{t}{\ell}}\,\underline{v}_\beta(x)\cdot\underline{v}_\beta(x')\right], \qquad A(15)$$

where Π' indicates a product over bonds covered by the random walk taking each bond once in the product. The replacement $t \to t/\ell$ takes account of multiple coverings. Thus we have

$$\langle u_1(x)\underline{v}_1(x)\cdot\underline{v}_1(x')u_1(x')\rangle =$$

$$\sum_N K^N \sum_{\{\gamma_N\}} \mathrm{Tr}_{v_1}\left[\underline{v}_1(x)\cdot\underline{v}_1(x')w(\gamma_N,\underline{v}_1)\prod_{\beta=2}^{m} z(\gamma_N)\right], \qquad \text{(D16)}$$

where we set $z(\gamma_N) = \mathrm{Tr}_{v_\beta} w(\gamma_N,\underline{v}_\beta)$, and since $\underline{v}_\beta$ is a dummy variable, z does not depend on β. In the limit $t\to 0$, $q\to 0$, with $q/t\to 0$, the partition function $z(\gamma_N)$ is the generating function for spanning trees, and we have that $z(\gamma_N) \sim q^{n_\gamma}$, where n_γ is the number of sites covered by γ. If we were to set q to zero before m, we would get no information from (D16). To get the desired result, we set m to zero before q, so that $q^m \to 1$. This quantity occurs in the renormalization group recursion relations, so the order of limits are important. Thus we have

$$\lim_{q\to 0}\left[\lim_{n,m\to 0}\langle u_1(x)\underline{v}_1(x)\cdot\underline{v}_1(x')u_1(x')\rangle\right] =$$

$$\sum_N K^N \sum_{\{\gamma_N\}} \frac{\mathrm{Tr}_{\underline{v}}\, \underline{v}(x)\cdot\underline{v}(x')\, w(\gamma_N,\underline{v})}{\mathrm{Tr}_{\underline{v}}\, w(\gamma_N,\underline{v})} \qquad \text{(D17a)}$$

$$= \sum_N K^N \sum_{\{\gamma_N\}} (1 - tR_{x,x'}) + 0(t^2) \qquad \text{(D17b)}$$

$$= \chi_0(x,x') - t\chi_1(x,x') + 0(t^2), \qquad \text{(D17c)}$$

where we used (5.36) to pass from (D17a) to (D17b). The result, (D17c), is equivalent to (5.41), Q.E.D.

We now outline the analogous proof for SAWs. We begin with the Hamiltonian H_{sv} in (5.42), and note that it may be written as a sum over 'bond Hamiltonians' $H_b(x,x')$,

$$H_{sv} = \sum_{<x,x'>} H_b(x,x') , \qquad \text{(D18)}$$

where

$$H_b(x,x') = -K\left\{\sum_\alpha s_\alpha(x)s_\alpha(x')\exp\left[J(\sigma_0-\sigma_b)(q-1)\sum \underline{v}_\beta(x).\underline{v}_\beta(x')\right]\right\}$$

$$- T(x)T(x')J\sigma_b(q-1)\sum_\beta \underline{v}_\beta(x).\underline{v}_\beta(x') \quad , \quad (D19)$$

where σ_0 is the conductance of a step along the SAW and σ_b that of a bridge bond. We define the density matrix ρ,

$$\rho = e^{-H_{sv}} = e^{-\sum_{<x,x'>} H_b(x,x')} = \prod_{<x,x'>} \rho(x,x') \quad , \quad (D20)$$

where, because of the trace laws in (5.12) and (5.43), it effectively takes the following form,

$$\rho(x,x') = e^{-H_b(x,x')}$$

$$= \left\{1 + K\sum_\alpha s_\alpha(x)s_\alpha(x')\exp\left[J(\sigma_0-\sigma_b)(q-1)\sum_\beta \underline{v}_\beta(x).\underline{v}_\beta(x')\right]\right\}$$

$$\times \exp\left[T(x)T(x')J\sigma_b(q-1)\sum_\beta \underline{v}_\beta(x).\underline{v}_\beta(x')\right] . \quad (D21)$$

In writing this result we used the fact that T(x)T(x') is effectively 0 if either x or x' is not on the SAW inasmuch as T(x) has a non-zero trace only if accompanied by two s_α's. If sites x and x' are both on the SAW, then T(x)T(x') can be replaced by unity.

We first evaluate $<s_\alpha(x_1)s_\alpha(x_2)>$,

$$<s_\alpha(x_1)s_\alpha(x_2)> = \underset{sv}{Tr}\,[s_\alpha(x_1)s_\alpha(x_2)\,\rho] \,/\, \underset{sv}{Tr}\,\rho$$

$$= \underset{s_\alpha,\underline{v}_\beta}{Tr}\,(s_\alpha(x_1)s_\alpha(x_2)\prod_{<x,x'>}\rho(x,x')) \quad , \quad (D22)$$

where $\rho(x,x')$ is given in (D21) and we explicitly indicate that the trace is over all n replicas of s_α and over all m replicas of v_β. We have used the result Tr ρ = 1 which applies in the limit n→0. This is easily seen to be the case since Tr ρ generates loops each with an associated multiplicative factor n. When (D22) is expanded in powers of

K, each term in the trace may be associated with a unique SAW with end-points at x_1 and x_2. There is therefore a one-to-one correspondence between terms in (D22) which give non-zero contributions to $<s_\alpha(x_1)s_\alpha(x_2)>$ and SAWs.

$$<s_\alpha(x_1)s_\alpha(x_2)> = \sum_{\ell} K^{\ell} \sum_{\gamma \subseteq \Gamma_\ell(x_1,x_2)} \mathrm{Tr}_{\underline{v}_\beta} \cdot$$

$$\exp\left[J(\sigma_0-\sigma_b)(q-1) \sum_{\beta,i} \underline{v}_\beta(y_i).\underline{v}_\beta(y_{i+1}) + \sum_{nn} \sigma_b(q-1) \sum_{\beta} \underline{v}_\beta(z).\underline{v}_\beta(z') \right] \qquad \text{(D23)}$$

Note that the factor in brackets in (D23) is the replicated Hamiltonian for a Potts model of the walk γ, where γ is a SAW from x_1 to x_2 of length ℓ covering the sites $y_1, y_2, \ldots, y_{\ell+1}$ such that $y_1 = x_1$ and $y_{\ell+1} = x_2$. Also z and z' are nearest neighbours in the set $\{y_i\}$. This Hamiltonian represents the associated network (with bridges): for bonds of the SAW the coupling constant is $J(\sigma_0-\sigma_b)+J\sigma_b = J\sigma_0$ whereas for bridge bonds (i. e. bonds connecting nearest neighboring sites which are <u>not</u> adjacent sites along the SAW) the coupling constant is $J\sigma_b$. The resistor network associated with γ is denoted $\Omega(\gamma)$ and the Potts Hamiltonian for $\Omega(\gamma)$ <u>for a single replica</u> is denoted $H[\Omega(\gamma),\underline{v}]$. With these notations we evaluate the factor in brackets in (D23) as

$$\mathrm{Tr}_{\underline{v}^\beta} \exp\left[\sum_{\beta=1}^{m} H[(\Omega(\gamma),\underline{v}_\beta] \right] = \left\{ \mathrm{Tr}_{\underline{v}} \exp\left[H[\Omega(\gamma),\underline{v}] \right] \right\}^m \to 1. \qquad \text{(D24)}$$

Hence we obtain

$$<s_\alpha(x_1)s_\alpha(x_2)> = \sum_{\ell} K^{\ell} \sum_{\gamma \subseteq \Gamma_\ell(x_1,x_2)} 1$$

$$= \sum_{\ell} K^{\ell} C_\ell(x_1,x_2) = \chi_0^{saw}(x_1,x_2;K). \qquad \text{(D25)}$$

This verifies the result (5.41a) written for SAWs.

Next, we consider the correlation function as in (5.41b):

$$\langle s_\alpha(x_1)\underline{v}_\beta(x_1).\underline{v}_\beta(x_2)s_\alpha(x_2)\rangle$$

$$= \frac{\underset{s_\alpha,v_\beta}{Tr}\ (\rho s_\alpha(x_1)\underline{v}_\beta(x_1).\underline{v}_\beta(x_2)s_\alpha(x_2))}{\underset{s_\alpha,\underline{v}_\beta}{Tr}\ \rho} \quad . \tag{D26}$$

As before we perform the spin traces to obtain the analog of (D24):

$$\langle s_\alpha(x_1)\underline{v}_\beta(x_1).\underline{v}_\beta(x_2)s_\alpha(x_2)\rangle =$$

$$\sum_\ell K^\ell \sum_{\gamma\subseteq\Gamma_\ell(x_1,x_2)} \left\{ \underset{\underline{v}}{Tr}\ \underline{v}_\beta(x_1).\underline{v}_\beta(x_2)e^{-H[\Omega(\gamma)]} \right\} \left\{ \underset{\underline{v}}{Tr}\ e^{-H[\Omega(\gamma)]} \right\}^{m-1} \tag{D27a}$$

$$= \sum_\ell K^\ell \sum_{\gamma\subseteq\Gamma_\ell(x_1,x_2)} \langle \underline{v}_\beta(x_1).\underline{v}_\beta(x_2)\rangle_{\Omega(\gamma)} \ , \tag{D27b}$$

where $\langle \ldots \rangle_{\Omega(\gamma)}$ denotes an expectation defined with respect to the Hamiltonian of the network, $H[\Omega(\gamma)]$. However, the network theorem then gives the required result (analogous to that found above for the case of GRWs),

$$\langle s_\alpha(x_1)\underline{v}_\beta(x_1).\underline{v}_\beta(x_2)s_\alpha(x_2)\rangle = \sum_\ell K^\ell \sum_{\gamma\subseteq\Gamma_\ell(x_1,x_2)} [\,1-tR(x,x')\,]$$

$$= \chi_0{}^{saw}(x_1,x_2) - t\chi_1{}^{saw}(x_1,x_2) . \tag{D28}$$

where we have used the property that all sites on SAWs are connected and so $\nu(x,x')=1$; t, as usual, is 1/J. The result (D29) is the analogue for SAWs of (5.41) and is what we wanted to verify.

Appendix E

Field Theoretic Formulation for Valence Walks.

To illustrate the procedure for obtaining a field theoretic representation from the bilinear Hamiltonians we have developed, we here construct the field theory for valence walks. For the resistive properties the field theories are much more complicated and their renormalization group analysis considerably more involved as we shall see in chapter six.

To obtain a field theory we invoke the Hubbard-Stratanovich transformation, which in matrix notation is

$$\exp\Big[\ 1/2 \sum_{x,x'} A_{x,x'}\ u_x\ u_{x'}\ \Big]$$

$$= C \int DY\ \exp\Big[\ -1/2 \sum_{x,x'} A_{x,x'}\ y_x\ y_{x'} + \sum_x u_x\ y_x\ \Big]\ , \qquad \text{(E1)}$$

where C is a constant and DY indicates integration over all y variables from $-\infty$ to $+\infty$. We drop the factors of C since in the zero replica limit they become unity. Here (E1) yields

$$\rho \equiv \exp\Big[-\frac{1}{2} \sum_{x,\alpha} u_\alpha(x)^2 + \frac{K}{2} \sum_{x,x',\alpha} \gamma^{-1}_{x,x'} u_\alpha(x) s_\alpha(x) u_\alpha(x') s_\alpha(x')\Big]$$

$$= \exp\ [\ -\frac{1}{2} \sum_{x,\alpha} u_\alpha(x)^2] \int DY_\alpha \Big\{ \exp\Big[-\frac{1}{2K} \sum_{x,x',\alpha} \gamma^{-1}_{x,x'} y_\alpha(x)^2\Big]$$

$$X \prod_x \exp\ [\ \sum_\alpha y_\alpha(x)\ u_\alpha(x)\ s_\alpha(x)\ ]\ \Big\}\ . \qquad \text{(E2)}$$

To get a field theory in terms of the y's, we trace over the u's and s's. The trace over the u's gives a free energy functional of Y as

$$\operatorname*{Tr}_u\ \rho(\{Y\}) = \exp[-\frac{1}{2} \sum \gamma^{-1}_{x,x'}\ y_\alpha(x)\ y_\alpha(x')]$$

$$x,x',\alpha$$

$$\times \prod_{x,\alpha} \mathrm{Tr}_{s} \exp\left[\tfrac{1}{2}\, y_{\alpha}(x)^{2}\, s_{\alpha}(x)^{2} \right]. \qquad \text{(E3)}$$

Evaluating the traces over s_α using the trace reules of (15), we get a free energy functional of Y as

$$-H(\{y\}) = -\frac{1}{2K} \sum_{x,x',\alpha} y_{\alpha}(x)\, \gamma^{-1}_{x,x'}\, y_{\alpha}(x')$$

$$+ \sum_{x,\alpha} \ln\left[1 + \sum_{r} \left[\tfrac{1}{2}\, y_{\alpha}(x)^{2} \right]^{r} \frac{1}{r!}\, 1_{r} \right]. \qquad \text{(E4)}$$

Note that we have obtained the explicit dependence of H({y}) on the valence fugacities. For a renormalization group analysis one need keep only terms in the expansion in powers of Y up to order y^4.

Appendix F

Derivation of Field Theory for SAW.

In this Appendix we derive the field theoretic Hamiltonian for the SAW walk model with nearest-neighbour crosslinks. We may write the SAW Hamiltonian as a sum of bond terms

$$H_{sv} = \sum_{<x,x'>} H_b(x,x') \qquad \text{(F1)}$$

where

$$H_b(x,x') = -K \sum_{\alpha=1}^{n} s_\alpha(x) s_\alpha(x') \prod_{\beta=1}^{m} \left[1 + \frac{q-1}{1+t} \underline{v}_\beta(x) . \underline{v}_\beta(x') \right] .$$

$$- \lambda T(x) T(x') J(q-1) \sum_{\beta=1}^{m} \underline{v}_\beta(x) . \underline{v}_\beta(x') \qquad \text{(F2)}$$

As in the case of GRWs the first term may be expanded and is readily seen to consist of a sum of bilinear terms in single-site operators. We introduce fields $\{\Phi\}$ conjugate to these terms such that

$$\underset{sv}{\mathrm{Tr}}\, e^{-H_{sv}} = \int D\Phi \underset{sv}{\mathrm{Tr}}\, e^{-L^{saw}(\Phi,s,v)} \qquad \text{(F3)}$$

We obtain $L^{saw}(\Phi,s,v)$ using the usual Hubbard-Stratanovich transformation. As in the case of GRWs, we may decompose $L^{saw}(\Phi,s,v)$ as a sum of two terms

$$L^{saw}(\Phi,s,v) = L_0^{saw}(\Phi) + V^{saw}(\Phi,s,v) \qquad \text{(F4)}$$

where

$$L_0^{saw}(\Phi)=\tfrac{1}{2}\sum_{x,x'}\gamma^{-1}_{x,x'}\sum_{\ell}\frac{(1+1/J)^{\ell}}{K}\sum_{S_1}\varphi_{\alpha,\beta_1,\beta_2,\ldots,\beta_\ell}^{\mu_1,\mu_2,\ldots,\mu_\ell}(x)\varphi_{\alpha,\beta_1,\ldots,\beta_\ell}^{\mu_1,\ldots,\mu_\ell}(x')$$

$$-\tfrac{1}{2}\sum_{S_2}\varphi_{\alpha,\beta_1,\beta_2,\ldots,\beta_\ell}^{\mu_1,\mu_2,\ldots,\mu_\ell\ 2} \qquad \text{(F5)}$$

and

$$V^{saw}(\varphi,s,v)=\sum_x\sum_{\ell=0}\sum_{\substack{\{\beta_i\}\\{\mu_i}\}}}(q-1)^{\frac{1}{2}}\varphi_{\alpha,\beta_1,\beta_2,\ldots,\beta_\ell}^{\mu_1,\mu_2,\ldots,\mu_\ell}(x)\ s^{\alpha}(x)\prod_{i=1}^{\ell}v_{\beta_i}^{\mu_i}(x)$$

$$\cdot\prod_{<x,x'>}e^{\left[\lambda J(q-1)T(x)T(x')\sum_{\beta=1}^{m}\underline{v}_\beta(x).\underline{v}_\beta(x')\right]}$$

$$+\tfrac{1}{2}\sum_{S_2}\varphi_{\alpha,\beta_1,\ldots,\beta_\ell}^{\mu_1,\ldots,\mu_\ell}(x) \qquad \text{(F6)}$$

We now perform the trace over the s_α:

$$e^{-L^{saw}(\Phi)}=e^{-\{L_0{}^{saw}(\Phi)+V^{saw}(\Phi)\}}=\operatorname*{Tr}_s\operatorname*{Tr}_v\left[e^{-L^{saw}(\Phi,s,v)}\right] \qquad \text{(F7)}$$

so that

$$V^{saw}(\Phi)=-\log\left[\operatorname*{Tr}_s\operatorname*{Tr}_v e^{-V^{saw}(\Phi,s,v)}\right] \qquad \text{(F8)}$$

Then, using the relation,

$$e^{\{\lambda J(q-1)T(x)T(x')\sum_{\beta=1}^{m}\underline{v}_\beta(x).\underline{v}_\beta(x')\}}=\prod_{\beta=1}^{m}\left[\frac{1}{J\lambda}+q\,\delta_{\sigma_\beta(x),\sigma_\beta(x')}\right] \qquad \text{(F9)}$$

which is valic subject to the trace rules (6.3). We have neglected contant multiplicative factors which become unity in the limit of zero replicas (in the correctly chosen order). We therefore obtain

$$V^{saw}(\Phi) = \frac{1}{8} \sum_{\substack{<x,x'>, x=x' \\ \{\beta\},\{\mu\},\alpha,\alpha'}} \varphi_{\alpha,\{\beta\}}^{\{\mu\}}(x)^2 \, \varphi_{\alpha',\{\beta\}}^{\{\mu\}}(x')^2$$

$$- \frac{1}{8} \sum_{\substack{<x,x'> \\ \{\beta_{1,2,3,4}\},\{\mu_{1,2,3,4}\} \\ \alpha,\alpha'}} \varphi_{\alpha,\{\beta_1\}}^{\{\mu_1\}}(x)\varphi_{\alpha,\{\beta_2\}}^{\{\mu_2\}}(x)\varphi_{\alpha',\{\beta_3\}}^{\{\mu_3\}}(x')\varphi_{\alpha',\{\beta_4\}}^{\{\mu_4\}}(x').$$

$$\cdot \; Tr \; Tr \; q^{2m} \left[\prod_i v^{\mu_1 i} \prod_j v^{\mu_2 j} \prod_k v^{\mu_3 k} \prod_\ell v^{\mu_4 \ell} \prod_{\beta=1}^{m} \left\{ \frac{1}{J\lambda} + q \, \delta_{\sigma_\beta(x),\sigma_\beta(x')} \right\} \right] \tag{F10}$$

which yields (6.33).

Appendix G

Tests of the Spin and Field Theoretic Hamiltonian Descriptions of SAWs.

We show in this appendix that the spin Hamiltonian for SAWs, (5.42), and the corresponding field theory, (6.32,6.33), do indeed give the expected results for small circuits. This may be regarded as a test that our Hamiltonians are indeed sensible.

a) 'Spin' Hamiltonian.

We use (5.42) to calculate the resistance of the circuit shown in fig.G1. Using the rules for addition of resistances the result we seek is

$$\langle p^1 r^1 \underline{a}.\underline{c} \rangle = K^2 \left(1 - \frac{R(1,3)}{J}\right) \qquad \text{(G1a)}$$

$$= K^2 \left(1 - \frac{1}{J}\,\frac{2}{(3\lambda+1)}\right) \qquad \text{(G1b)}$$

However, we may write the correlation function as follows:

$$\langle p^1 r^1 \underline{a}.\underline{c} \rangle = \frac{K^2 \; Tr_{\underline{a},\underline{b},\underline{c}} \left[\underline{a}.\underline{c} \, \exp\{J(1+\lambda)(q-1)(\underline{a}.\underline{b}+\underline{b}.\underline{c})+J\lambda(q-1)\underline{a}.\underline{c}\} \right]}{Tr_{\underline{a},\underline{b},\underline{c}} \left[\exp\{J(1+\lambda)(q-1)(\underline{a}.\underline{b}+\underline{b}.\underline{c})+J\lambda(q-1)\underline{a}.\underline{c}\} \right]} \qquad \text{(G2)}$$

However, we may rewrite the exponential as in Chps.5.6 in the more useful form:

$$\exp\{J\underline{a}.\underline{b}\} = \left[1 + \frac{(q-1)}{(1+t)}\,\underline{a}.\underline{b}\right] \qquad \text{(G3)}$$

which is valid within the trace in the limit of zero replicas that we consider. Thus our correlation function becomes

$$Z\langle p'r'\underline{a}.\underline{c}\rangle = K^2 \underset{\underline{a},\underline{b},\underline{c}}{\mathrm{Tr}} \left\{ \left[\frac{(q-1)}{(1+\frac{1}{J\lambda})} \right] (\underline{a}.\underline{c})^2 + \left[\frac{(q-1)}{(1+\frac{1}{J(1+\lambda)})} \right] (\underline{a}.\underline{b})(\underline{b}.\underline{c})(\underline{c}.\underline{a}) \right.$$

$$\left. + \left[\frac{(q-1)}{(1+\frac{1}{J(1+\lambda)})} \right]^2 \left[\frac{(q-1)}{(1+\frac{1}{J\lambda})} \right] (\underline{a}.\underline{b})(\underline{b}.\underline{c})(\underline{c}.\underline{a})^2 \right\} \qquad (G4)$$

Where the partition function Z is the same as the RHS except for the leading $\underline{a}.\underline{c}$ term. Expressing the numerator trace as a sum of three expectations and using the following results:

$$\langle \underline{a}.\underline{c} \rangle = (q-1)^{-1} \rightarrow -1 \quad q\rightarrow 0 \qquad (G5a)$$

$$\langle (\underline{a}.\underline{b})(\underline{b}.\underline{c})(\underline{c}.\underline{a}) \rangle = (q-1)^{-2} \rightarrow 1 \quad q\rightarrow 0 \qquad (G5b)$$

$$\langle (\underline{a}.\underline{b})(\underline{b}.\underline{c})(\underline{c}.\underline{a})^2 \rangle = (q-2)/(q-1)^3 \rightarrow 2 \quad q\rightarrow 0 \qquad (G5c)$$

A little algebra then yields the required result (G1). An analogous calculation applies to the evaluation of the resistance of the circuit shown in fig.G2. Rather more involved expectation values (four different Potts vectors) need to evaluated and we quote our new results here for reference:

$$\langle (\underline{a}.\underline{b})(\underline{b}.\underline{c})(\underline{c}.\underline{d})(\underline{d}.\underline{a}) \rangle = (q-1)^{-3} \rightarrow -1 \quad q\rightarrow 0 \qquad (G6a)$$

$$\langle (\underline{a}.\underline{b})(\underline{b}.\underline{c})(\underline{c}.\underline{d})(\underline{d}.\underline{a})^2 \rangle = (q-2)/(q-1)^4 \rightarrow -2 \quad q\rightarrow 0. \qquad (G6b)$$

Using the method described above, one obtains again the required result for the resistance. This method can obviously be generalised to calculate the resistance of, in principle, arbitrary circuits; however, it is extremely tedious.

b) Field Theoretic Hamiltonian.

The method described above is direct compared to the check we now perform. Owing to the algebraic complexities involved we shall limit ourselves to a check of the resistance of the simplest possible circuit, namely a *single* bond! Recall however that even a single bond in our formalism in fact comprises two parallel bonds of conductance

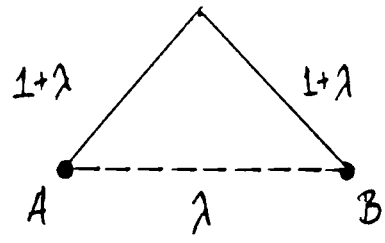

Fig.G1.: We calculate the resistance between A and B in this triangular circuit using the Spin Hamiltonian formulation for SAWs. The *backbone* bonds have a conductance $1+\lambda$ while the crosslink bond only has conductance λ.

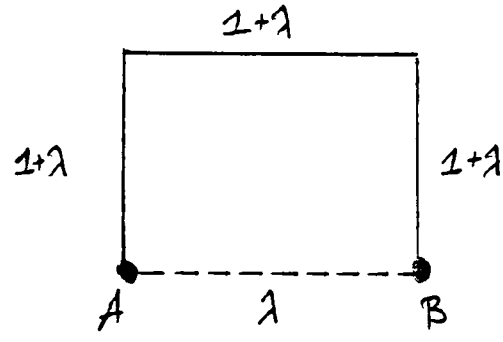

Fig.G2.: We calculate the resistance between A and B in this square circuit using the Spin Hamiltonian formulation for SAWs.

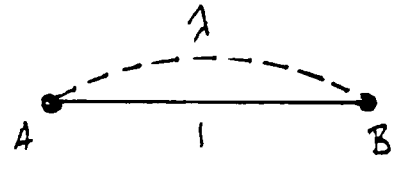

Fig.G3.: We calculate the resistance of the simplest possible circuit (A→B) using the Field-Theoretic Hamiltonian for SAWs.

1,λ respectively.

We wish to evaluate the correlation function $<s_\alpha(x)s_\alpha(x')\underline{v}^\beta(x).\underline{v}^\beta(x')>$ for the two site circuit shown in fig.G3. This *spin-Potts* correlation function for SAWs may be expressed in terms of one relative to the field theory (6.32,6.33) in an analogous manner to that shown for GRWs in (6.39):

$$<s_\alpha(x)s_\alpha(x')\underline{v}^\beta(x).\underline{v}^\beta(x')> = -\frac{(1+t)}{K}\gamma_{x,x'}^{-1}$$

$$+\left[\frac{1+t}{K}\right]^2 \sum_{y,y'}\gamma_{xy}^{-1}<\varphi_{\alpha,\beta}^{\mu}(y)\varphi_{\alpha,\beta}^{\mu}(y')>\gamma_{y'x'}^{-1} \qquad (G7)$$

Consider first the bare field theoretic propagator $G_o(x,x')=<\varphi_{\alpha,\beta}{}^{\mu}(x)\varphi_{\alpha,\beta}{}^{\mu}(x')>_o$:

$$<\varphi_{\alpha,\beta}{}^{\mu}(x)\varphi_{\alpha,\beta}{}^{\mu}(x')>_o = \left\{\frac{1+t}{\gamma K} - 1\right\}^{-1}_{xx'}$$

$$= \Lambda\gamma_{xx'} + \Lambda^2\sum_z \gamma_{xz}\gamma_{zx'} + \Lambda^3\sum_{z,z'}\gamma_{xz}\gamma_{zz'}\gamma_{z'x'} \qquad (G8)$$

where $\Lambda = \{K/(1+t)\}$. Hence a zeroth approximation to the spin correlation function, and hence resistance, is

$$<s_\alpha(x)s_\alpha(x')\underline{v}^\beta(x).\underline{v}^\beta(x')> \sim -\frac{(1+t)}{K}\gamma_{x,x'}^{-1} + \frac{(1+t)}{K}\gamma_{x,x'}^{-1} + \delta_{x,x'} + \frac{K}{(1+t)}\gamma_{x,x'}$$

$$\sim \delta_{x,x'} + [K/(1+t)]\gamma_{x,x'} \qquad (G9)$$

Now, we treat the corrections to first order in the potential $V(\varphi)$, ie we consider the expectation $<\varphi\varphi V>$. Neglecting the *anomalous* term in V arising from the crosslinks, it may be shown that the 'u' and 'v' potentials give the following contributions to the correlation function

$$<s_\alpha(x)s_\alpha(x')\underline{v}^\beta(x).\underline{v}^\beta(x')> \sim \delta_{x,x'} + [K/(1+t)]\gamma_{x,x'} - [K/(1+t)]\gamma_{x,x'} + K\gamma_{x,x'}$$

$$\sim \delta_{x,x'} + K\gamma_{x,x} \qquad (G10)$$

where the first two terms in the first line arise from the unperturbed propagator as

described above. The third term arises from the v potential and the last from the u potential.

All that remains to do is to calculate the effect of the (m−1) *direct product* potentials w(i). We remark that when $\lambda=0$, the v potential only connects x with itself (and not to nearest neighbours), and further, there are no other terms contributing to $\langle ssvv\rangle$ to O(K) thus $\langle ssvv\rangle = K(1-t)\gamma_{x,x'}$ as required for the single bond with conductance unity. To calculate the contribution of the w(p), it is necessary to consider the possible scenarios for the presence of the external replica β on the internal propagators in the v and u vertices. We do not report the details of this arduous combinatoric problem. The resulting contribution if β is one of the p v−replicas is

$$\binom{m-1}{p-1} K \sum_{\ell=0}^{m-p} \frac{1}{(1+t)^{\ell+1}} (q-1)^{\ell} \left\{ \frac{(m-p)!}{(m-p-\ell)!\ell!} \right\} \qquad \text{(G11)}$$

while if β is one of the (m−p) u−replicas the corresponding contribution to $\langle ssvv\rangle$ is

$$\binom{m-1}{p} \left\{ K \sum_{\ell=0}^{m-p-1} \frac{1}{(1+t)^{\ell+1}} (q-1)^{\ell+1} \left\{ \frac{(m-p-1)!}{(m-p-1-\ell)!\ell!} \right\} + K \sum_{\ell=0}^{m-p-1} \frac{(q-1)^{\ell}}{(1+t)^{\ell}} \left\{ \frac{(m-p-1)!}{(m-p-1-\ell)!\ell!} \right\} \right\}. \qquad \text{(G12)}$$

where the two terms result from having or not having β in the external legs respectively.

Taking the appropriate limits yields the total contribution from w(p) as:

$$(-1)^p Kt/\lambda^p \qquad \text{(G13)}$$

Hence the total contribution from the anomalous potentials is $-Kt/(1+\lambda)$. This then gives the required result for the correlation function to O(K):

$$\langle s_\alpha(x) s_\alpha(x') \underline{v}^\beta(x) . \underline{v}^\beta(x') \rangle \sim \delta_{x,x'} + K \left[1 - \frac{t}{1+\lambda} \right] \gamma_{x,x'} . \qquad \text{(G14)}$$

QED.

Appendix H

Cross-over Calculations to order ϵ^2.

For the cross-over calculation needed to discuss the effect of infinitesimal t, we must evaluate the contributions from the diagrams of Fig. 6.4 when each line has a propagator $g_j^{-1}=r_j+q^2$, where j is the number of replica indices assigned to the line in question. Let there be k replicas on the external line: i.e. we are evaluating r_k'. In diagram 6.4c we see that each line must have the same replica indices as the external line. Accordingly, each internal line is a g_k and from this diagram we thus have

$$\omega' = -64b^2 v^2 B'(0)\omega \qquad \text{(H1)}$$

In diagram 6.4b we see that one internal line is constrained to have the same indices as the external line. The other two lines can either have a given replica index or not. Thus from this diagram we have

$$r_k' = -128b^2 uv \sum_p \frac{m!(q-1)^p}{(m-p)!p!} \left[B(0) + \frac{k+2p}{3} \omega B(0)' \right]. \qquad \text{(H2)}$$

Note that since there are three internal lines, changing r on one of them leads to a factor 1/3B(0)'. Thus from diagram 6.4b we obtain

$$\omega' = -\frac{128}{3} b^2 uvB(0)' \omega \qquad \text{(H3)}$$

Next, consider diagram 6.4a. For each of the k replicas on the external lines there are seven types of coverings of the internal lines with replica indices as follows: type 1: all lines covered; type 2: all but the bottom line covered; type 3: all but the middle line covered; type 4: all but the top line covered; type 5: only the top line covered; type 6: only the middle line covered; and type 7: only the bottom line covered. We let $p_1,p_2,\ldots,p_6$ be the number of replicas having coverings of types 1,2,...6, respectively. For the m-k replicas not on the external lines there are five types of coverings. Types 1-4 are the same for replicas which do occur on the external line. Type 5 corresponds to covering no lines. For these replicas we let

ℓ_1, ℓ_2, ℓ_3 and ℓ_4 be the number of replicas having coverings of types 1,2,3, and 4, respectively. It is easily seen that the top line is covered $p_1+p_2+p_3+p_5+\ell_1+\ell_2+\ell_3 \equiv N$ times and thus represents the propagator $g(r_N)$. To the order we consider, all three lines are equivalent and we write

$$r_k' \sim u^2 \sum_{\{p\}} \sum_{\{\ell\}} B(r_N)(q^2-3q+3)^{p_1} (q-2)^{p_2+p_3+p_4} (q^2-3q+2)^{\ell_1} \cdot (q-1)^{\ell_2+\ell_3+\ell_4}$$

$$\times k!\,(m-k)! \prod_{j=1}^{6} (p_j!)^{-1} \prod_{j=1}^{4} (\ell_j!)^{-1} \left[\left(k-\sum_{j=1}^{6} p_j\right)!\left(m-k-\sum_{j=1}^{4} \ell_j\right)!\right]^{-1} \qquad \text{(H4)}$$

where the q-dependent form factors are essentially thoe of Fig. 6.5, and the factorials gives the number of ways of choosing the replicas. Now we substitute $p_5 = K - p_1 - p_2 - p_3$ and $\ell_3 = L - \ell_1 - \ell_2$ and sum over the p's and ℓ's to find

$$r_k' = -64\, u^2 \sum_{K,L} B(r_{K+L}) \frac{k!\,(m-k)!\,q^m (q-1)^{K+L}}{(k-K)!\,K!\,L!\,(m-k-L)!} \qquad \text{(H5a)}$$

$$= -64\, u^2 \sum_{N} B(r_N) \frac{m}{(m-N)!\,N!} (s-1)^N s^m \qquad \text{(H5b)}$$

$$= -64\, u^2 B(r_0), \qquad \text{(H5c)}$$

where we let $m \to 0$ in the last step. This diagram therefore gives $\omega' = 0$. Collecting the results for all diagrams of Fig.6.4 we find

$$\omega' = -64 b^2 B'(0) \omega [v^2 + \tfrac{2}{3} uv]. \qquad \text{(H6)}$$

Finally we turn to the calculations for Fig. 6.6. Inspection of Eq. (18) in Bruce *et al* (1974) indicates that we only need to consider the r dependence of the propagator which does not intersect the external vertex. This corresponds to the term of order $C(r)^2$ in Eq.(18) of Bruce *et al* (1974). The other term from this type of diagram is cancelled in a way discussed in detail in Bruce *et al* (1974). Thus we focus our attention on the factor A'(0) due to the derivative of this propagator which occurs when

we consider its dependence on r. Diagram 6.6c is the simplest one. Here, by the nature of the v vertices (actually they must be v_b vertices in the sense of Table 6.2) all propagators have the same replica indices. Thus in the recursion relation for r_k', this diagram gives a contribution of order

$$r_k' = -64b^2 v^2 C(0) A(r_k) \qquad \text{(H7)}$$

For all other diagrams of Fig. 6.6 the propagator in question can be covered by 0,1,...m replicas, so that a sum like that in (6.50) occurs. From these other diagrams we find

$$r_k' = -64b^2 (u^2+2uv)C(0) \sum_p \frac{m!}{m-p!-p!} (s-1)^p A(r_p) \qquad \text{(H8a)}$$

$$= -64b^2 (u^2+2uv)C(0)A(r_0) \qquad \text{(H8b)}$$

These results are included in the full results to order ϵ^2 written in (6.56) and (6.63), (6.64).

Appendix J

Logarithmic Corrections.

In this appendix we obtain the form for the logarithmic corrections to scaling for d near 4. We use the Rudnick–Nelson approach via differential recursion relations (Rudnick and Nelson 1976), whereby the differential recursion relation analogous to (6.63) is, to order ϵ,

$$\frac{dr_k(\ell)}{d\ell} = 2r_k(\ell) + A\left[\frac{v(\ell)}{1+r_k(\ell)} + \frac{u(\ell)}{1+r_0(\ell)}\right], \qquad (J1)$$

We will initially confine our attention to the case $u(\ell)=-v(\ell)$ (ie the GRW problem) and then the analogue of (6.56) is of the form

$$\frac{dv(\ell)}{d\ell} = \epsilon v(\ell) - \frac{Bv(\ell)^2}{[1+r_0(\ell)]^2} \qquad (J2)$$

Now substitute $r_k(\ell) = r_0(\ell) + k\omega(\ell)$, into (J1), so that

$$\frac{d\omega(\ell)}{d\ell} = 2\omega(\ell) - \frac{Av(\ell)}{[1+r_0(\ell)]^2}\omega(\ell) \qquad (J3)$$

The solution to this equation is

$$\ln\left[\frac{\omega(\ell)}{\omega(0)}\right] = 2\ell - \int_0^\ell \frac{Av(\ell')}{[1+r_0(\ell')]^2}\, d\ell \qquad (J4a)$$

$$= (2 - \frac{A}{B}\epsilon)\ell + \frac{A}{B}\ln\left[\frac{v(\ell)}{v(0)}\right], \qquad (J4b)$$

where we have used (J2) to carry out the integration. We use the solution to (J2), viz. (Rudnick and Nelson 1976):

$$v(1) = v(0)e^{\epsilon\ell}\left[1 + \frac{B}{\epsilon}v(0)(e^{\epsilon\ell}-1)\right]^{-1} \qquad (J5)$$

and set $1 = r(\ell) = r(0)e^{z\ell} \equiv re^{z\ell}$. Then (J4) becomes

$$\omega(\ell) = \omega(0)r^{-(1-\frac{A}{2B}\epsilon)H-A/B}, \qquad (J6)$$

where A/B = 1/2, H is given by (6.81) with C = Bv(0), and $\omega(0) = t$. Since χ_1 is $-r^{-1}\partial\omega/\partial t$, we have

$$\chi_1 \sim \omega(\ell)/[r\omega(0)], \qquad (J7)$$

from which (6.80) follows.

We now generalise this prescription to the case $v(\ell)+u(\ell)\neq 0$ and calculate the effect of the w(i) potentials on the recursion relation for $r(\ell)$ and hence $\omega(\ell)$. The resulting recursion relation is as follows:

$$r_k' = b^{2-\eta}\{r_k+8vA(r_k)+8\sum_{\substack{a=0,\ldots,k\\ b=0,\ldots,m-k\\ c=0,\ldots,a+b}}\binom{k}{a}\binom{m-k}{c}(A(r_{k-a+c}))(q-1)^c w(m-a-b) \qquad (J8)$$

as in (6.84). In the Rudnick–Nelson formulation (Rudnick and Nelson 1976) (J8) becomes to first order in ϵ:)

$$\frac{dr_k}{d\ell} = 2r_k(\ell) + A.\sum_{p,q,x}\binom{k}{p}\binom{m-k}{q}\binom{p+q}{x}\frac{(q-1)^x}{1+r_{k+x-p}(\ell)}w(m-p-q) \qquad (J9)$$

where the bare value of w(i) is $(J\lambda)^{-1}$. In order to emphasise that the w are also functions of the length scaling factor ℓ we now denote them $w(i,\ell)$. Putting $r_k(\ell)=r_0(\ell)+k\omega(\ell)$ into (J9) yields:

$$\frac{d\omega(\ell)}{d\ell} = 2\omega(\ell) - B.\sum_{p,q,x}\binom{k}{p}\binom{m-k}{q}\binom{p+q}{x}\frac{(q-1)^x}{(1+r_0(\ell))^2}w(m-p-q,\ell)\omega(\ell)\binom{k+x-p}{k} \qquad (J9)$$

where $w(m-p-q,\ell)$ is given by $w_0(\ell)(J\lambda)^{(p+q)}$, where $w(\ell)$ tranforms, to first order in ϵ, as in (6.83) and $w_0(0)=1$. B is a constant. The summation may be completed straightforwardly to yield $\omega(\ell)$ and hence, using (J7), χ_1. The result (6.85) for the corrections to scaling follows using the method shown in the first part of this appendix.

Appendix K

Green Function Calculation in Hydrodynamic Limit.

In the following we perform the Green function calculation of section IV of Chapter 7 in rather more detail than presented in the text. In particular we derive equations (7.4.3),(7.4.8) and (7.4.12) and perform a perturbation expansion for the self energy $\Sigma(\underline{k},\xi)$. We begin with the continuum equation of motion (7.4.2)

$$-i\frac{\partial \underline{u}(\underline{r},t)}{\partial t} = h(\underline{r},t) + \underline{\nabla}.((D(\underline{r})-\langle D\rangle)\nabla u(\underline{r},t)) + \langle D\rangle\nabla^2 u(\underline{r},t) \tag{K1}$$

Fourier transformation of (K1) with respect to space and time yields,

$$\omega\varphi(\underline{k},\omega) = \frac{1}{(2\pi)^d}\int\{\Delta(\underline{k}'-\underline{k})\underline{k}.\underline{k}'\}\varphi(\underline{k}',\omega)d^d\underline{k}' + k^2\langle D\rangle\varphi(\underline{k},\omega) + H(\underline{k},\omega) \tag{K2}$$

where

$$\varphi(\underline{k},\omega) = \iint e^{i(\underline{k}.\underline{r}-\omega t)}u(\underline{r},t)\, d^d\underline{r}dt$$

$$H(\underline{k},\omega) = -\iint e^{i(\underline{k}.\underline{r}-\omega t)}h(\underline{r},t)\, d^d\underline{r}dt$$

$$\Delta(\underline{k}) = \int e^{i\underline{k}.\underline{r}}(D(\underline{r})-\langle D\rangle)\, d^d\underline{r} \tag{K3}$$

and we have used the d-dimensional Fourier convolution theorem,

$$\frac{1}{(2\pi)^d}\int F(\underline{k}-\underline{u})G(\underline{u})\, d^d\underline{u} = \int e^{i\underline{k}.\underline{r}} f(\underline{r})g(\underline{r})\, d^d\underline{r} \tag{K4}$$

where F and G are the spatial Fourier transforms of f and g respectively. We have used the standard results concerning Fourier transforms of derivatives.

Now, define $G(\underline{k},\underline{k}';\omega)$ through the integral equation,

$$\varphi(\underline{k},\omega) = \int H(\underline{k}',\omega)G(\underline{k},\underline{k}';\omega)d^d\underline{k}' \tag{K5}$$

using (K4) we obtain the Green function equation of motion (7.4.3),

$$(\omega-\langle D\rangle k^2)\; G(\underline{k},\underline{k}";\omega) = \int\{\Delta(\underline{k}'-\underline{k})\underline{k}.\underline{k}'\}G(\underline{k}',\underline{k}";\omega)\frac{d^d\underline{k}'}{(2\pi)^d} + \delta(\underline{k}-\underline{k}") \tag{K6}$$

Now, define the unperturbed, virtual crystal propagator $G^0(\underline{k},\underline{k}';\omega)$,

$$G^0(\underline{k},\underline{k}';\omega) = \frac{\delta(\underline{k}-\underline{k}')}{(\omega-\langle D\rangle k^2)} \equiv \delta(\underline{k}-\underline{k}')\; g^0(\underline{k};\omega) \tag{K7}$$

Then (K6) into (K5) yields,

$$G(\underline{k},\underline{k}";\omega) = G^0(\underline{k},\underline{k}";\omega) + \iint G^0(\underline{k},\underline{\lambda}';\omega)\; V(\underline{\lambda}',\underline{\lambda}")\; G(\underline{\lambda}",\underline{k}";\omega)d^d\lambda'\frac{d^d\lambda"}{(2\pi)^d} \tag{K8}$$

where $$V(\underline{\lambda}',\underline{\lambda}") = \{\Delta(\underline{\lambda}'-\underline{\lambda}")\}(\underline{\lambda}'.\underline{\lambda}") \tag{K8a}$$

is the vertex interaction. We may represent (K8) formally by the Dyson form,

$$\underline{\underline{G}} = \underline{\underline{G}}^0 + \underline{\underline{G}}^0\underline{\underline{V}}\underline{\underline{G}} \tag{K9}$$

We are therefore now in a position to proceed with the perturbation expansion.

Now, for the purpose of the perturbation theory, and so that the analogy with related calculations (Edwards 1958, Edwards and Jones 1971) be made transparent, we take a discrete viewpoint with the understanding that the summations over $\underline{k}$-space resulting from the calculation will finally 'go over' to integrals.

Define the Self Energy $\Sigma(\underline{k},\omega)$ as in (7.4.7) which (in discrete notation) implies that,

$$\langle G(\underline{k},\underline{k}';\omega)\rangle = \frac{\delta_{k,k'}}{(\omega-(\langle D\rangle k^2-\Sigma(\underline{k},\omega))} \equiv \delta_{\underline{k},\underline{k}'}\langle G(\underline{k};\omega)\rangle \tag{K10}$$

Note that now δ is a Kronecker delta. The configurational average ensures that $\langle G(\underline{k},\underline{k}';\omega)\rangle$ is diagonal in momentum space.

We represent the vertex $V(\underline{k},\underline{k}')$ diagrammatically as shown in fig.7.1a and the unperturbed propagator (not dependent on configuration of disorder) as shown in fig.7.1b We then obtain a perturbation series for the self energy $\Sigma(\underline{k},\omega)$ by the usual methods

(see Edwards and Jones 1971), and this has the representation as a sum of all possible diagrams of the type shown in fig.7.2. In the last line of fig.7.2 we have arranged the perturbation series such that $\Sigma^{(1)}(\underline{k},\omega)$ is the leading order term in a regime where the series is convergent.

The diagram rules are (note analogy with the work of Edwards and Jones 1971):

i) Form product of vertex interactions and take configurational average. Associating a factor $<(D(\underline{r})-<D>)^N>$ to each vertex joining N interactions.

ii) Multiply expression i) by the internal unperturbed propagators.

iii) Integrate (or sum) over independent internal wave-vectors.

Implicit in the calculation is a dependence on the percolative correlation length (characterising the configurationally averaged disorder) of both unperturbed propagator and interaction vertex.

To illustrate the dependence of the graphs on $k\xi$ and $(D(\underline{r})-<D>)$, we consider first the contribution to $\Sigma^{(1)}(\underline{k},\omega)$ of the diagram of second order in V. It will be shown later that this is, in fact the dominant term in the continuum approximation.

Using the above rules we derive the following leading order expression for the self-energy,

$$\Sigma(\underline{k},\omega,\xi) = \int g^0(\underline{k}',\omega) < |V(\underline{k},\underline{k}')|^2 > \frac{d^d\underline{k}'}{(2\pi)^d} \qquad (K11)$$

where, as usual, $<\ldots>$ denotes configurational averaging. Thus we obtain (7.4.8),

$$\Sigma(\underline{k},\omega,\xi) = \int \frac{< |\Delta(\underline{k}-\underline{k}')|^2 > (\underline{k}.\underline{k}')^2}{(\omega-<D>k'^2)} \frac{d^d\underline{k}'}{(2\pi)^d} \qquad (K12)$$

The poles of the Green function $<G(\underline{k},\underline{k}';\omega)>$ yield the excitation spectrum and so the spin-wave damping $\Gamma_c(\underline{k},\omega)$ is given by the imaginary part of the pole. We therefore obtain the following leading order approximation to $\Gamma_c(\underline{k},\omega)$,

$$\Gamma_c(\underline{k},\xi) = \int < |\Delta(\underline{k}-\underline{k}')|^2 > (\underline{k}.\underline{k}')^2 \, \delta(\omega-<D>k'^2) \, \frac{d^d\underline{k}'}{(2\pi)^d}$$

(K13)

In order to perform the integration in (K13) one must evaluate the configurational average involved. However, by definition

$$<|\Delta(\underline{q})|^2> = \iint e^{i\underline{q}.(\underline{r}_1-\underline{r}_2)} <(D(\underline{r}_1)-<D>)(D(\underline{r}_2)-<D>)> \, d^d\underline{r}_1 d^d\underline{r}_2$$

(K14)

Further, ξ_p is the controlling length scale in the problem and so we assign the following translationally invariant scaling form to the spin-wave stiffness correlation function $<(D(\underline{r}_1)-<D>)(D(\underline{r}_2)-<D>)>$,

$$<(D(\underline{r}_1)-<D>)(D(\underline{r}_2)-<D>)> = <(D(\underline{r})-<D>)^2> \, F\left[\frac{\underline{r}_1-\underline{r}_2}{\xi_p}\right]$$

$$\propto (p-p_c)^{2(t-\beta)} \, F\left[\frac{\underline{r}_1-\underline{r}_2}{\xi_p}\right]$$

(K15)

In general F(x) is a monotone decreasing function of x and has the following limiting behaviour

$$\lim_{x\to 0} F(x) = A \qquad \lim_{x\to\infty} F(x) = 0. \qquad \text{(K16)}$$

The form for the general n-point correlation function is given by (7.4.11). According to the discussion in section IV the correlation function (K15) becomes vanishingly small for $|\underline{r}_1-\underline{r}_2|/\xi_p < 1$.

Therefore (K15) implies that (K14) becomes,

$$<|\Delta(\underline{q})|^2> = \xi^d <(D(\underline{r})-<D>)^2> \, G(\underline{q}\xi)$$

$$\propto (p-p_c)^{2(t-\beta)-\nu d} \, G(\underline{q}\xi) \qquad \text{(K17)}$$

$$\propto <(D(\underline{r})-<D>)^2> \, \xi^d$$

to leading order in $q\xi$ since $G(0)\neq 0$ exists. G(x) is the Fourier transform of F(x) and is

bounded. The second real-space integration establishes overall conservation of momentum during the scattering process. Finally using the approximation $\omega(\underline{k}) \approx <D> k^2$ in (K13) we obtain,

$$\Gamma_c(\underline{k},\xi) \propto \frac{<(D(\underline{r})-<D>)^2> \xi^d k^{d+2}}{<D>}$$

$$\propto (p-p_c)^{-\nu d+(t-\beta)} k^{d+2} \qquad \text{(K18)}$$

which is the result (7.4.12) required.

Finally, by giving a general formula for evaluating the k,ξ and $(D(\underline{r})-<D>)$ dependence of a general graph, we show that, in the limit $k\xi \ll 1$, the graph $\Sigma^{(1)}(\underline{k},\omega)$ is indeed the leading order term in the perturbation expansion . We illustrate the procedure for calculating the contribution due to a given graph using the examples from fig.7.2. Firstly we evaluate the graph labelled $\Sigma^{(2)}$ in fig.7.2:

$$\Sigma^{(2)}(\underline{k},\omega) = <\int\int V(\underline{k},\underline{k}') g^0(\underline{k}',\omega) V(\underline{k}',\underline{k}'') g^0(\underline{k}'',\omega) V(\underline{k}'',\underline{k}) \frac{d^d\underline{k}' d^d\underline{k}''}{(2\pi)^{2d}}>$$

(K19)

The integrals and unperturbed propagators factorise from the configurational average and so using the definition (K8a) for the interaction vertex and that for the unperturbed propagator (K7), we must evaluate the following expression,

$<\Delta(\underline{k}-\underline{k}')\Delta(\underline{k}'-\underline{k}'')\Delta(\underline{k}''-\underline{k})> =$

$$\iiint e^{i(\underline{k}-\underline{k}').\underline{r}_1 + i(\underline{k}'-\underline{k}'').\underline{r}_2 + i(\underline{k}''-\underline{k}).\underline{r}_3} .<(D(\underline{r}_1)-<D>)\ldots(D(\underline{r}_3)-<D>)> d^d\underline{r}_1 d^d\underline{r}_2 d^d\underline{r}_3$$

(K20)

Therefore, using the geometric scaling ansatz (7.4.11) for the 3-point correlation function we find

$$<\Delta(\underline{k}-\underline{k}')\Delta(\underline{k}'-\underline{k}'')\Delta(\underline{k}''-\underline{k})> = <(D(\underline{r})-<D>)^3>\xi^{-2d}$$

$$.G((\underline{k}''-\underline{k}')\xi,(\underline{k}'-\underline{k}'')\xi)$$

$$\propto (p-p_c)^{3(t-\beta)-2\nu d}\, G((\underline{k}''-\underline{k}')\xi,(\underline{k}'-\underline{k}'')\xi) \qquad (K21)$$

where G arises from the $\underline{r}$-space integrations of the spin-wave stiffness correlation function in (K20) and is bounded at the origin.

Substituting (K21) into (K19) and making the approximation $\omega \approx \omega_c = <D>k^2$ applicable in the hydrodynamic regime, yields the contribution $\Gamma^{(2)}=\mathrm{Im}\Sigma^{(2)}$ to the damping, with the following k,ξ dependence

$$\Gamma^{(2)}(k,\xi) \propto \frac{<(D(\underline{r})-<D>)^3>((p-p_c)^{-\nu d}\, k^{2d+2}}{<D>}$$

$$\propto k^z(k\xi)^{d+2-z} \qquad (K22)$$

In the continuum approximation ($k\xi$ small) $\Gamma^2 \ll \Gamma^1$, as $<(D(\underline{r})/<D>)-1)> \ll 1$.

Similarly for the graph $\Sigma^{(3)}$ we must now evaluate

$$\Sigma^3(\underline{k},\omega) = <\iint V(\underline{k},\underline{k}')g^0(\underline{k}',\omega)V(\underline{k}',\underline{k}'').$$

$$.g^0(\underline{k}'',\omega)V(\underline{k}'',\underline{k}''')g^0(\underline{k}''',\omega)V(\underline{k}''',\underline{k})\frac{d^d\underline{k}'\,d^d\underline{k}''\,d^d\underline{k}'''}{(2\pi)^{3d}}>$$

(K23)

Performing the analogous calculation to that for $\Sigma^{(2)}(\underline{k},\omega)$, the k and ξ dependence of the corresponding contribution, $\Gamma^{(3)}$, to the damping is

$$\Gamma^{(3)}(\underline{k},\xi) \propto \frac{<(D(\underline{r})-<D>)^2>^2\ (p-p_c)^{-\nu d}\ k^{d+2}}{<D>^3}$$

$$= k^z(k\xi)^{d+2-z} \qquad (K24)$$

as before. However $\Gamma^{(3)} \ll \Gamma^{(1)}$ since it is of higher order in the fluctuation variable.

For $\Sigma^{(4)}$, we find

$$\Sigma^{(4)}(\underline{k},\omega) = \langle \iint V(\underline{k},\underline{k}')g^0(\underline{k}',\omega)V(\underline{k}',\underline{k}'') \cdot$$

$$\cdot g^0(\underline{k}'',\omega)V(\underline{k}'',\underline{k}-\underline{k}'+\underline{k}'')g^0(\underline{k}-\underline{k}'+\underline{k}'',\omega)V(\underline{k}-\underline{k}'+\underline{k}'',\underline{k})\frac{d^d\underline{k}'\,d^d\underline{k}''}{(2\pi)^{2d}}\rangle$$

(K25)

This yields a dependence of $\Gamma^{(4)}$ on k and ξ as in (K22), however associated with the diagram is a factor $\langle(D(\underline{r})-\langle D\rangle)^2\rangle^2/\langle D\rangle^3$ and so $\Gamma^{(4)} \ll \Gamma^{(1)}$ once again. In fact, as Langer (1960) points out, we need not consider graphs with insertions such as $\Sigma^{(4)}$ but only the so-called *skeleton diagrams*. The insertions may be treated by using the full propagator $g(\underline{k},\omega)$ in the skeleton diagrams and solving self-consistently, a procedure analogous to mass renormalisation in field theory.

Consider now a general graphical contribution to the self-energy $\Sigma^{\ell,m,n}(\underline{k},\omega)$ composed of

i) ℓ vertices,

ii) m 'independent' unperturbed propagators,

iii) n interactions, such that n_i interactions meet at vertex ℓ_i, $n=\sum n_i$.

Notice in fact that $m=n-\ell$. It is easy to see that the corresponding contribution to the damping $\Gamma^{\ell,n}$ has the following form,

$$\Gamma^{\ell,n}(k,\xi) \propto \frac{\{\prod_{\ell_i} \langle(D(\underline{r})-\langle D\rangle)^{n_i}\rangle\}\, k^{d+2}\, \xi^{-d}}{\langle D\rangle^{n-1}} .$$

$$\propto k^z\,(k\xi)^{d+2-z} \qquad \text{(K26)}$$

where we have used (7.3.7). It is now transparent from (K26) that for $k\xi \ll 1$ the leading order contributions to the damping are obtained from the diagrams with the minimum number of interactions, n=2 : $\Sigma^{(1)}$ is the only such diagram.

In order to evaluate $\Gamma_c(k,\xi)$ for larger $k\xi$ one must take into account the higher

order contribution contribution in $k\xi$ from the Fourier transformed correlation functions and so in principle a sum over all diagrams to all orders is required. From the above discussion it follows that here $\Gamma_c(k,\xi)/k^z$ is a power series in $k\xi$ and so, within the radius of convergence of the expansion,

$$\Gamma_c(k,\xi) = k^z g(k\xi) \qquad \text{(K27)}$$

For even larger values of $k\xi$ and in particular in the critical regime ($k\xi \gg 1$) the perturbation expansion is divergent as the perturbation terms are larger than $<D>k^2$. The fluctuations completely dominate the dynamics. Infinite resummation of the series would however still lead to a form (K27). The dynamic scaling principle for the spin-wave damping provides the justification for the extension of (K27) beyond the radius of convergence of the perturbation expansion.

Appendix L

Transverse Dynamic Structure Function in the limit $k\xi \ll 1$.

We evaluate the form of the transverse dynamic structure function in the hydrodynamic regime ($k\xi \ll 1$). Firstly, note that $\chi(k,\omega,\xi)$ is merely the imaginary part of the configurationally averaged Green function $\langle G(\underline{k};\omega)\rangle$. However, by definition,

$$\langle G(\underline{k};\omega)\rangle \equiv \frac{1}{\omega - (\langle D\rangle k^2 + \Sigma(\underline{k},\omega))}$$

$$\approx \frac{1}{\omega - (\langle D\rangle k^2 + i\Gamma_c(\underline{k},\xi))}$$

$$= \frac{1}{\omega k^{-z} - \{(k\xi)^{2-z} + i(k\xi)^{2+d+z}\}} \qquad \text{(L1)}$$

where we have used the forms $\langle D\rangle = (k\xi)^{2-z}k^z$ and $\Gamma_c = (k\xi)^{2+d-z}$, applicable in the hydrodynamic regime. It then follows,

$$\chi(k,\omega,\xi) = \lim_{\epsilon\to\infty} \{ \operatorname{Im} \langle G(\underline{k};\omega+i\epsilon)\rangle \}$$

$$\approx \frac{k^{-z}(k\xi)^{2+d-z}}{(\omega k^{-z} - (k\xi)^{2-z}) + (k\xi)^{2(2+d-z)}} \qquad \text{(L2)}$$

(L2) is a Lorentzian of width $(k\xi)^{2+d-z}$ centered about $(k\xi)^{2-z}$. It satisfies the dynamic scaling principle $\chi(k,\omega,\xi) = k^{-(2-\eta_t+z)}\, F(k\xi, \omega k^{-z})$ from which we deduce that,

$$\eta_t = 2$$

and from (7.3.7) $$z = 2+(t-\beta)/\nu \qquad \text{(L3)}$$

Appendix M

Finite Cluster Response.

In this appendix we evaluate the static and dynamic critical exponents η_t' and z' respectively by considering the collective response of the ensemble of finite clusters near p_c, when a transverse field is applied.

Consider a finite cluster comprised of s bonds. One may argue that, on length scales small compared to the dimensions of the cluster, its static and dynamical properties will be identical to those of the infinite cluster. One often encounters this type of reasoning in the theory of finite size scaling and, as we shall see below, a consequence of this premise is that finite size effects manifest themselves solely in the form of low-energy cut-off dependent only on cluster size s. The problem associated with cluster shape is avoided by implicitly taking an average over all clusters with equal number of bonds

If we denote {F}, the set of finite clusters and $N_{\{F\}}(\omega_0)$, the number of eigenfrequencies on this set with frequency less than or equal to ω_0, then one may write (Maggs and Stinchcombe 1986),

$$N_{\{F\}}(\omega_0) = \sum_s N_s(\omega_0) n_s \qquad \text{(M1)}$$

Here $N_s(\omega_0)$ is the number of eigenfrequencies less than or equal to ω_0 (ie integrated density of states) on a cluster of s sites; n_s is the number of clusters containing s bonds and s_0 is a frequency dependent cut-off size.

If we now introduce $\chi_f(k,\omega,\xi)$, the response function for excitations on the ensemble of finite clusters and use the following relationships,

$$N_{\{F\}}(\omega_0) = \int^{\omega_0} \rho(\omega_0)\, d\omega = \int_{-\infty}^{\infty}\int^{\omega_0} \chi(k,\omega,\xi)\, d\omega\, d^d\underline{k} \qquad \text{(M2)}$$

and $N_s(\omega_0) = sN(\omega_0)$. $\rho(\omega)$ is the infinite cluster density of states. We obtain, using (M1) and (M2) the following relation between finite cluster response χ_f and infinite cluster response χ,

$$\int_{-\infty}^{\infty}\int^{\omega_0} \chi_f(k,\omega,\xi)\ d\omega\ d^d\underline{k} \quad = \quad \sum_{s>s_0} \int_{-\infty}^{\infty}\int^{\omega_0} \chi(k,\omega,\xi)\ d\omega\ d^d\underline{k}\ (sn_s) \tag{M3}$$

At $p=p_c$, the distribution of the number of clusters n_s containing s bonds is given (Essam 1980) by the following power law,

$$n_s \propto s^{-2-1/\delta} \tag{M4}$$

As we may choose p arbitrarily close to p_c we use (M4) in (M2).

Relating the cut-off size s_0 to ω_0 via a diffusion argument, Maggs and Stinchcombe (1986) obtained

$$s_0 \sim \omega_0^{-d_f/d_w} \tag{M5}$$

where d_w is the infinite cluster anomalous diffusion exponent and d_f is the fractal dimension (Mandelbrot 1982) of the infinite cluster.

Allowing the sum (M2) to tend to an integral and assuming a dynamic scaling scaling form for the infinite cluster response one therefore obtains,

$$\int_{-\infty}^{\infty}\int^{\omega_0} \chi_f(k,\omega,\xi)\ d\omega\ d^d\underline{k} \quad \propto \quad \int_{-\infty}^{\infty}\int^{\omega_0} \chi(k,\omega,\xi)\ \omega_0^{d_f/\delta d_w}\ d\omega\ d^d\underline{k}$$

$$\propto \int_{-\infty}^{\infty}\int^{\omega_0} k^{-(2-\eta_t+z)} F(k\xi, \omega\xi^z)\ \omega_0^{d_f/\delta d_w}\ d\omega d^d\underline{k}$$

$$\propto \int^{\omega_0} \xi^{(2-\eta_t+z)-d} F_1(\omega\xi^z)\ \omega_0^{d_f/\delta d_w}\ d\omega$$

$$\propto \xi^{\{2-\eta_t-d-(zd_f/\delta d_w)\}} F_2(\omega_0\xi^z) \tag{M6}$$

and so, differentiating with respect to ω_0,

$$\int_{-\infty}^{\infty} \chi_f(k,\omega,\xi)\ d\omega \quad \propto \quad \xi^{\{2-\eta_t-d-(zd_f/d_w)+z\}} F_3(\omega_0\xi^z) \tag{M7}$$

Now assign a dynamic scaling form as in (7.5.2) for χ_f with critical indices η_t' and z'. Using the relations $z=d_w$, applicable to the isotropic Heisenberg ferromagnet (Rammal and Toulouse 1982), and $d/d_f=1+(1/\delta)$ (Essam 1980) it follows that

$$\eta_t' = \eta_t + \beta/\nu \qquad \text{and} \quad z' = z = 2+(t-\beta)/\nu$$
$$= 2 + \beta/\nu. \tag{M8}$$

Appendix N

Spin Waves on the Disordered One-Dimensional Chain.

In one dimension, the zero temperature linearised equation of motion (7.2.3) is exactly soluble (Stinchcombe and Harris 1983) and one may obtain a closed form expression for the transverse dynamic structure factor satisfying the dynamic scaling hypothesis,

$$\chi(k,\omega,\xi) = k^{-(2-\eta_t+z)}\, M(k\xi,\omega k^{-z}) \qquad \text{(N1)}$$

with $\eta_t=2$ and $z=2$ and

$$M(a,b) = \frac{\pi\coth[(\pi/2a)\sqrt{(J/b)}]\{1+\cos[\pi\sqrt{(J/b)}]\}}{a^2b(b/J-1)^2\{\cosh[(\pi/a)\sqrt{(J/b)}]+\cos[\pi\sqrt{(J/b)}]\}}. \qquad \text{(N2)}$$

M(a,b) has the following asymptotic properties,

i) Hydrodynamic limit $k\xi \ll 1$

$$M(a,b) \xrightarrow[a\to 0]{} \frac{2\pi\{1+\cos[\pi\sqrt{(J/b)}]\}}{a^2b(b/J-1)^2} \exp\left[-\frac{\pi}{a}\left[\frac{J}{b}\right]^{\frac{1}{2}}\right] \qquad \text{(N3)}$$

from which we obtain

$$\omega_c = \frac{J\pi^2}{6\xi^2} \quad \text{and} \quad \Gamma_c = \frac{J\pi^2}{\xi^2}. \qquad \text{(N4)}$$

ii) Critical limit $k\xi \gg 1$

$$M(a,b) \xrightarrow[a\to\infty]{} \frac{1}{2J} \frac{1/a}{(1/a)^2+[\sqrt{(J/b)}-1]^2} \qquad \text{(N5)}$$

Hence $$\omega_c = Jk^2 \quad \text{and} \quad \Gamma_c = \frac{2Jk}{\xi} \qquad \text{(N6)}$$

Appendix P

Spin Waves in Antiferromagnets near the Percolation Threshold.

The damping of spin-waves in bond-diluted Heisenberg antiferromagnets in d dimensions is considered using a method developed for the ferromagnetic case by the authors. We treat the hydrodynamic limit $q\xi \equiv (k-\pi)\xi \ll 1$ and derive an expression for the damping $\Gamma_c(q,\xi) \propto (p-p_c)^{-\mu}\, q^{d+1}$, where $\mu = \nu d - \frac{1}{2}\{2t-\beta-(d-2)\nu\}$ which is consistent with the dynamic scaling principle. We also obtain a closed form expression for the response function and consider finite cluster response. The critical dynamic properties of the corresponding site-diluted system are then examined. Finally, we contrast d=1 and d>1 and then generalise our results to the ferrimagnet. This work has been published in J.Phys. C (Christou and Stinchcombe 1986f).

1. Introduction.

In this appendix we investigate the damping of transverse spin-wave excitations in bond-diluted d-dimensional Heisenberg antiferromagnets near the percolation threshold p_c where, in d>1, the dynamics is controlled by a ramified infinite cluster of connected sites. The corresponding ferromagnetic situation has been studied in detail in chapter seven (see also Christou and Stinchcombe (1986e)) and we draw heavily from that chapter illustrating the analogies between the two problems.

Non-critical effects in dilute antiferromagnets have been investigated using Green function techniques by Jones and Edwards (1971) who derive an expression for the non-critical damping in a low frequency, long wavelength regime for low disorder and obtain an estimate for the critical vacancy concentration below which long range order is unstable against spin-waves. CPA calculations of increasing sophistication have been performed for the disordered antiferromagnet by Tahir-Kheli (1972), Buyers *et al* (1972), Elliott and Pepper (1973) and Holcomb (1974,1976) in both site- and bond-diluted cases and these authors obtained expressions for response functions and

single particle density of states. However these effective-medium calculations were seen to fail in the critical region where the dynamics becomes anomalous as a result of the divergence of the correlation length $\xi \to \infty$.

In the present work the critical dynamic effects are treated. We take a continuum viewpoint, valid in the hydrodynamic regime near the percolation threshold ($q \equiv (k-\pi) \to 0, 1/\xi \to 0, q\xi \ll 1$) at zero temperature and we derive an appropriate differential equation describing the dynamics. This equation is treated using a diagrammatic perturbation theory in a manner similar to that in the case of the ferromagnet (Chapter 7). We obtain an expression for the transverse dynamic structure function ('response function') in this regime and generalise the method to deal with the effects of the finite clusters on the response and also to non-zero temperature. We contrast the d>1 dynamics to that in d=1 and finally we remark on the ferrimagnet.

We consider the dynamics of a bond-diluted, isotropic Heisenberg antiferromagnet on a d-dimensional hypercubic lattice at zero temperature. The ground state is taken to consist of two interpenetrating sublattices of up (A) and down (B) spins respectively. The Hamiltonian for this system is

$$H = \sum_{<ij>} J_{ij}\, \underline{S}_i \cdot \underline{S}_j - \sum_i \underline{h}_i \cdot \underline{S}_i \qquad \text{(P1)}$$

and we work in the classical limit of large spin magnitude, S, normalised to unity. The field $\underline{h}_i$ is transverse ($h^z=0$). The summation is over nearest neighbours and the coupling constant J_{ij} is equal to 0,J (>0) with probabilities (1-p) and p respectively for a given pair i,j. Here p is the bond occupation density.

The equation of motion for the site-representation operator $S_k^+(t)$ ($\equiv S_k^x + iS_k^y$) in the linearised spin-wave approximation is straightforwardly obtained from (P1),

$$-i(-1)^{\alpha_k} \frac{d}{dt} S_k^+ = \sum_{<jk>} J_{jk}(S_j^+ + S_k^+) - h_k^+ \qquad \text{(P2)}$$

where $\alpha_k = 1,0$ on the up and down sublattices respectively.

2. Decimation and Continuum Approximation.

In order to proceed with the continuum limit valid in $q\xi \ll 1$ we require an

equation which displays the Goldstone symmetry of the antiferromagnet explicitly. We obtain such an equation by expressing the time-dependent behaviour of S_k^+ in terms of spins on the same sublattice. This procedure suppresses the two-sublattice structure of the ground state and loses information on the relative phases and amplitudes of the excitation on the respective sublattices. However such a mapping onto a quasi-ferromagnetic system turns out to be very useful in the continuum limit as we demonstrate below. Firstly we obtain, for the A,B sublattices respectively, the following time-Fourier-transformed equations from (P2),

$$\omega S_i^+ = \sum_{<ik>} J_{ik}(S_k^+ + S_i^+) \quad - \quad h_i^+(\omega) \qquad \text{(P3a)}$$

$$-\omega S_j^+ = \sum_{<jl>} J_{jl}(S_l^+ + S_j^+) \quad - \quad h_j^+(\omega) \qquad \text{(P3b)}$$

where i,l denote spins on sublattice A and j,k are on sublattice B. Eliminating (or *decimating*) S_k^+ from (P3a) yields,

$$\omega S_i^+ = \sum_{<ik>} J_{ik} \left\{ S_i^+ - \left\{ \frac{\sum_{<lk>} J_{lk} S_l^+ - h_k^+}{\left[\omega + \sum_{<lk>} J_{lk} \right]} \right\} \right\} \quad - \quad h_i^+(\omega) \qquad \text{(P4)}$$

An analogous expression is obtained for the B sublattice with ω replaced by $-\omega$. Near criticality we require $\omega/J \ll 1$; moreover, we note that $h/\omega \ll 1$ is a necessary condition for the validity of the linear response theory as h/ω is a measure of the field-induced spin deviation. We therefore expand (P4) in Taylor series to second order in ω/J, h and (original) lattice parameter a and this yields the following partial differential equation,

$$-\omega^2 u(\underline{r},\omega) = \tfrac{1}{2} \underline{\nabla} C^2(\underline{r}) . \underline{\nabla} u(\underline{r},\omega) + C^2(\underline{r}) \nabla^2 u(\underline{r},\omega) + H(\underline{r},\omega) \qquad \text{(P5)}$$

Here $S_i^+(\omega) \rightarrow u(\underline{r},\omega)$, $(2aJ_{ij})^2 \rightarrow C^2(\underline{r})$ and $\omega h_i^+(\omega) \rightarrow H(\underline{r},\omega)$ in the continuum approximation. $C^2(\underline{r})$ is the local antiferromagnetic spin-wave dispersion coefficient which fluctuates about its mean value $<C^2>$ over length scales determined by the correlation length ξ. Clearly we may write (P5) in terms of fluctuations $(C^2 - <C^2>)$

as

$$-\omega^2 u = \underline{\nabla}.\left[\tfrac{1}{2}(C^2-\langle C^2\rangle)\underline{\nabla}u\right] + \tfrac{1}{2}\left[C^2-\langle C^2\rangle\right]\nabla^2 u + \langle C^2\rangle\nabla^2 u + H \qquad \text{(P6)}$$

3. Green Function Method for Antiferromagnetic Spin-Waves

Now, taking the spatial Fourier transform of (P6) yields the following Green function equation of motion,

$$(\omega^2-\langle C^2\rangle k^2)\ G(\underline{k},\underline{k}";\omega) = \int \tfrac{1}{2}\Delta(\underline{k}-\underline{k}')\{\underline{k}.\underline{k}'+k'^2\}G(\underline{k}',\underline{k}";\omega)\ d^d\underline{k}' + \delta(\underline{k}-\underline{k}") \qquad \text{(P7)}$$

where $G(\underline{k},\underline{k}';\omega)$ is defined by

$$\varphi(\underline{k},\omega) = \int H(\underline{k}',\omega)G(\underline{k},\underline{k}';\omega)\ d^d\underline{k}' \qquad \text{(P8)}$$

and $\varphi(\underline{k},\omega)$, $\Delta(\underline{k})$ and $H(\underline{k},\omega)$ are the spatial Fourier transforms of $u(\underline{r},\omega)$, $(C^2(\underline{r})-\langle C^2\rangle)$ and $-H(\underline{r},\omega)$ respectively. We note that the wave-vector $\underline{k}$ refers to a spin-wave on the decimated lattice and we require $k\to 0$ and $k\xi \ll 1$.

We now introduce the unperturbed, virtual crystal, Green function $G^0(\underline{k},\underline{k}';\omega)$, defined by

$$G^0(\underline{k},\underline{k}';\omega) = \frac{\delta(\underline{k}-\underline{k}')}{(\omega^2 - \langle C^2\rangle k^2)} = \delta(\underline{k}-\underline{k}')\ g^0(\underline{k},\omega) \qquad \text{(P9)}$$

(P9) allows us to write (P7) in the form

$$G(\underline{k},\underline{k}";\omega)=G^0(\underline{k},\underline{k}";\omega)+\int G^0(\underline{k},\underline{\lambda}';\omega)V(\underline{\lambda}',\underline{\lambda}")G(\underline{\lambda}",\underline{k}";\omega)\frac{d^d\underline{\lambda}'\,d^d\underline{\lambda}"}{(2\pi)^d} \qquad \text{(P10)}$$

where the interaction is

$$V(\underline{\lambda}',\underline{\lambda}") = \tfrac{1}{2}\Delta(\underline{\lambda}'-\underline{\lambda}")\{\underline{\lambda}'.\underline{\lambda}" + \lambda"^2\} \qquad \text{(P11)}$$

Now (P10) may be formally expressed by the Dyson form,

$$\underline{\underline{G}} = \underline{\underline{G^0}} + \underline{\underline{G^0}}\,\underline{\underline{V}}\,\underline{\underline{G}}. \qquad \text{(P12)}$$

The self-energy is defined as usual by

$$\langle G \rangle = G^0 + G^0 \sum \langle G \rangle \qquad \text{(P13)}$$

where $\langle \ldots \rangle$ denotes a configurational average over disorder. Using (P9), it follows that (P13) has the solution

$$\langle G(\underline{k},\underline{k}';\omega) \rangle = \frac{\delta(\underline{k}-\underline{k}')}{\omega^2 - \{\langle C^2 \rangle k^2 + \sum(\underline{k},\omega)\}} = \delta(\underline{k}-\underline{k}')\langle G(\underline{k};\omega) \rangle \qquad \text{(P14)}$$

The configurational average ensures that $\langle G(\underline{k},\underline{k}';\omega) \rangle$ is diagonal in momentum space.

The transverse response function $\chi(q,\omega,\xi)$ may be defined as the imaginary part of the total antiferromagnetic Green function $\langle G^{(T)}(\underline{q},\omega) \rangle, q \equiv k-\pi$, which we discuss below, and the dynamic scaling principle of Halperin and Hohenberg (1967,1969) indicates that $\chi(q,\omega,\xi)$ takes the following homogeneous form near criticality $(q \equiv k-\pi \to 0, \omega \to 0, 1/\xi \to 0)$,

$$\chi(q,\omega,\xi) = q^{-(2-\eta_t+z)} F(q\xi, \omega q^{-z}) \qquad \text{(P15)}$$

k is here the wave-vector of the spin-wave on the antiferromagnetic system and the limit $q \equiv k-\pi \to 0$ gives the staggered response. (P15) has implications for the characteristic frequency ω_c and width Γ_c,

$$\omega_c = q^z f(q\xi) \qquad \Gamma_c = q^z g(q\xi) \qquad \text{(P16)}$$

In the hydrodynamic regime of the critical region we recover the linear antiferromagnetic dispersion law

$$\omega_c = C(p)\, q. \qquad \text{(P16a)}$$

(P16) together with (P16a) thus imply that $C(p) \propto \xi^{1-z}$. Harris and Kirkpatrick (1977) have related the hydrodynamic antiferromagnetic dispersion relation coefficient $C^2(p) \equiv \langle C^2 \rangle$ to the ratio of the bulk DC conductivity $\sigma(p) \sim (p-p_c)^t$ and the transverse susceptibility $\chi^{\perp} \sim (p-p_c)^{-\tau}$,

$$C^2(p) \propto \sigma(p)/\chi^{\perp}(p)$$

$$\propto (p-p_c)^{t+\tau}. \qquad \text{(P16b)}$$

Further, scaling arguments (see eg Harris and Kirkpatrick 1977) indicate that τ may be related to static percolative exponents:

$$\tau = t-\beta-(d-2)\nu, \qquad \text{(P16c)}$$

Hence using (P16a,b,c) one obtains the following relation between the dynamic

exponent z and static percolation exponents

$$z = 1+(1/2\nu)(2t-\beta-(d-2)\nu) \qquad \text{(P17)}$$

Supposing now that in the hydrodynamic region at criticality ($q\xi \ll 1, 1/\xi \to 0$) Γ_c takes the following form

$$\Gamma_c \propto (p-p_c)^{-\lambda}\, q^b \qquad \text{(P18)}$$

it therefore follows from the dynamic scaling principle (P15) that

$$\lambda = (b-1)\nu - \tfrac{1}{2}(2t-\beta-(d-2)\nu). \qquad \text{(P19)}$$

A diagrammatic technique based on the method of Edwards (1958) may be used to evaluate the self-energy $\sum(\underline{k},\omega)$ and hence through (P14) to obtain the damping (together with λ and b), given by the imaginary part of the pole of $<G>$, and an expression for $<G>$ itself. The details are similar to the corresponding calculation for the ferromagnetic case.

Define

$$\gamma_c(\underline{k},\xi) = \lim_{\epsilon\to 0} \{ \mathrm{Im}\sum(\underline{k},\omega+i\epsilon) \}. \qquad \text{(P20)}$$

then following the calculation in Chapter 7 we obtain for $k\xi \ll 1$,

$$\gamma_c(\underline{k},\xi) \approx \frac{<(C^2(r)-<C^2>)^2>}{<C^2>}\, \xi^d\, k^{d+2}$$

$$\propto (p-p_c)^{-\theta} k^{d+2} \qquad \text{(P21)}$$

with $\theta = \nu d-[2t-\beta-(d-2)\nu]$. To obtain the damping we must return to (P14), from which, for weak damping (hydrodynamic regime)

$$<G(\underline{k};\omega)> \approx \frac{1}{\omega^2 - \{<C^2>k^2+i\gamma_c(\underline{k},\xi)\}}$$

$$\approx \frac{1}{\omega - <C^2>^{\frac{1}{2}}k - i\Gamma_c(\underline{k},\xi)} \cdot \frac{1}{(2<C^2>^{\frac{1}{2}}k)} \qquad \text{(P22)}$$

where the damping is $\Gamma_c=\gamma_c/(2<C^2>^{\frac{1}{2}}k)$ and is given for $k\xi \ll 1$ by

$$\Gamma_c(k,\xi) \propto (p-p_c)^{-\mu}\, k^{d+1} \qquad \text{(P23a)}$$

Hence, for the original, undecimated lattice this becomes for $q\equiv k-\pi \to 0, 1/\xi \to 0$ and $q\xi \ll 1$

$$\Gamma_c(q\equiv k-\pi\to 0,\xi) \propto (p-p_c)^{-\mu}\, q^{d+1} \qquad \text{(P23b)}$$

with $\mu=\nu d-\frac{1}{2}\{2t-\beta-(d-2)\nu\}$ which is consistent with the dynamic scaling principle

(P16). Using arguments analogous to Chapter 7, (P23) becomes for larger $q\xi$ ($q\to 0, 1/\xi\to 0$) within the radius of convergence of the perturbation expansion,

$$\Gamma_c(q,\xi) = q^z\, g(q\xi) \qquad \text{(P24)}$$

with $z=1+\{2t-\beta-(d-2)\nu\}/2\nu$, which is precisely the dynamic scaling prediction. (P16) extends (P24) to general $q\xi$.

Proceeding along the lines of Chapter 7 we now derive a form for the total Green function $<G^{(T)}(\underline{q},\omega)>$, with $q\equiv k-\pi$. Note that

$$<G^{(T)}(\underline{q},\omega)> = G^{AA}+G^{AB}+G^{BA}+G^{BB}$$

$$= 2(G^{AA}+G^{AB}). \qquad \text{(P25)}$$

Here we denote by $G^{XY}(q\equiv k-\pi,\omega)\equiv\ll S_k{}^{+X}, S_{-k}{}^{-Y}\gg$ the Fourier transformed retarded thermal Green function describing interactions between spins on sublattices X,Y. The last line follows since in the continuum limit the sublattice symmetry is not broken by the disorder, to a good approximation. However using (P3), for vanishing field, it follows that

$$S_k{}^{\pm B} = \frac{J(\pm k)S_k{}^{\pm A}}{(\omega-J(\underline{0}))} \qquad \text{(P26)}$$

and so for small $q\equiv k-\pi$, using the Goldstone symmetry of the antiferromagnet, we obtain

$$<G^{(T)}(\underline{q},\omega)> \approx 4G^{AA}(\underline{q},\omega). \qquad \text{(P27)}$$

$G^{AA}(\underline{q},\omega)$ is given by (P22). Hence using the expressions $\gamma_c=q^z(q\xi)^{d+1-z}$ and $\omega_c=<C^2>^{\frac{1}{2}}q$ and $<C^2>^{\frac{1}{2}}=\xi^{1-z}$, appropriate for the undecimated lattice as $q\equiv(k-\pi)\to 0$, we have

$$<G^{(T)}(\underline{q};\omega)> \approx \frac{q^{-2z}}{[\omega q^{-z} - \{(q\xi)^{1-z}+i(q\xi)^{1+d-z}\}]}\ \frac{1}{(q\xi)^{1-z}} \qquad \text{(P28)}$$

and so the transverse response function $\chi(q,\omega,\xi)$ takes the form

$$\chi(\underline{q},\omega,\xi) = \lim_{\epsilon\to 0}\{\mathrm{Im}\,<G^{(T)}(\underline{q};\omega+i\epsilon)>\}$$

$$\approx \frac{q^{-2z}(q\xi)^d}{[(\omega q^{-z}-(q\xi)^{1-z})^2 + (q\xi)^{2(1+d-z)}]} \qquad \text{(P29)}$$

For fixed $q\xi$, (P29) is a Lorentzian function of the variable ωq^{-z}, with width $(q\xi)^{1+d-z}$, centered about $(q\xi)^{1-z}$. It satisfies the requirements of the dynamic scaling principle and so we see that

$$z = 1+\{2t-\beta-(d-2)\nu\}/2\nu$$

$$\eta_t = 2-z. \qquad \text{(P30)}$$

4. Finite Cluster Response, Site-dilution and Multicritical Behaviour.

In order to evaluate the effect of response from the ensemble of finite clusters we use a finite size scaling argument introduced by Chapter 7 for the ferromagnetic case. We find that if it is assumed that the finite cluster response function satisfies dynamic scaling characterised by the corresponding critical exponents η_t' and z', then

$$z' = z = 1+\{2t-\beta-(d-2)\nu\}/2\nu$$

$$\eta_t' = \eta_t + (zd_f/\delta d_w) \qquad \text{(P31)}$$

where d_f is the fractal dimension of the infinite cluster (Mandelbrot 1982) governing the length scaling of mass $M \sim L^{d_f}$; d_w is the random walk dimensionality (Stanley *et al* 1982) governing the asymptotic time dependence $\langle R \rangle \sim t^{1/d_w}$ of the displacement of a particle diffusing on the fractal infinite cluster; and δ governs the distribution of cluster number with size: $n_s \sim s^{-2-1/\delta}$ (Essam 1980). Now the master equation for diffusion and that for ferromagnetic spin-waves (in the linearised approximation) are isomorphic and so $d_w=z^F$, where z^F the dynamic exponent for the Heisenberg ferromagnet. Further, a simple crossover argument for the ferromagnetic dispersion shows that

$$z^F = d_w = 2+(t-\beta)/\nu \qquad \text{(P32)}$$

and therefore using the corresponding antiferromagnetic result (P17) we identify

$$z^{AF} = z^F - (d_f/2)$$

or

$$z^{AF} = z^F(1-d_s/4) \qquad \text{(P33)}$$

where we have used the relation $d_f=d-\beta/\nu$. (33) relates the ferromagnetic and antiferromagnetic dynamic exponents and $d_s=2d_f/d_w$ is the ferromagnetic/diffusive

spectral dimension (Alexander and Orbach 1982). Assuming the validity of the Alexander–Orbach (1982) conjecture (which at worst is a very good approximation) then

$$z^{AF} \approx {}^{2}/_{3}\, z^{F} \qquad \text{(P34)}$$

Using the relation $d/d_f = 1+1/\delta$ (Essam 1980) we therefore find that

$$\begin{aligned} \eta_t' &= \eta_t + \frac{z^{AF}}{z^F}.\frac{\beta}{\nu} \\ &= \eta_t + (1-d_s/4)\beta/\nu \\ &\approx \eta_t + {}^{2}/_{3}(\beta/\nu) \end{aligned} \qquad \text{(P35)}$$

We now consider the related problem of site–diluted Heisenberg antiferromagnets. Following an argument in Chapter 7 we obtain a form for the site–diluted transverse response function analogous to (P29),

$$\chi(q,\omega,\xi) = q^{-(2-\eta_t^{site}+z^{site})}\, F(q\xi, \omega q^{-z^{site}})$$

$$\text{with } F(x,y) = \frac{x^{(1+d-z-\beta/\nu)}}{(y-x^{1-z})^2 + (x^{1+d-z})^2} \qquad \text{(P36)}$$

where $\eta_t^{site} = \eta_t + \beta/\nu$ and $z^{site} = z$ are the critical exponents for the site–diluted infinite cluster. Moreover, we find that finite cluster response in the site–diluted case is governed by critical indices $\eta_t'^{site}$ and z'^{site} given by

$$\eta_t'^{site} = \eta_t' + (1-d_s)\beta/\nu \approx \eta_t + (5/3)(\beta/\nu) \qquad \text{(P37)}$$

$$z'^{site} = z = 1 + (1/2\nu)(2t-\beta-(d-2)\nu).$$

Thus far we have been considering dynamics at T=0. In order to generalise our results to non–zero temperature we use the following multicritical scaling ansatz for the total correlation length (now allowing for thermal as well as percolation effects),

$$\xi \sim (p-p_c)^{-\nu}\, B(T/(p-p_c)^{\varphi}) \qquad \text{(P38)}$$

in which the scaling function B(x) has the following asymptotic behaviour,

$$\begin{aligned} B(x) &\to B_0 && x \to 0 \\ &\to B_\infty x^{-\nu/\varphi} && x \to \infty. \end{aligned} \qquad \text{(P39)}$$

φ is the antiferromagnetic Heisenberg thermal–percolation crossover exponent. In the novel hydrodynamic regime $p-p_c=0, 0<T\ll 1, q\xi \ll 1$ we obtain the following expression for

the damping in d>2,

$$\Gamma_c(q,\xi) \propto T^{-(1+d-z)\nu/\varphi} q^{d+1} . \qquad \text{(P40)}$$

However we remark that, as for the zero temperature hydrodynamic regime, the rescaled damping vanishes with $q\xi$

$$(\Gamma_c/\omega_c) \propto (q\xi)^d \to 0 \qquad \text{as} \quad q\xi \to 0 . \qquad \text{(P41)}$$

5. The One Dimensional Case.

As indicated above, the case of d=1 is exceptional in that the divergence of the (percolative) correlation length $\xi \to \infty$ occurs at the pure limit, since here $p_c=1$. Also, as the dilution breaks the one-dimensional chain into finite segments, no infinite cluster exists such as normally governs anomalous dispersion. From these two observations we expect that the rescaled damping should vanish in d=1 in the critical regime $q\xi \gg 1$ and in this regime the dispersion relation should be that of the pure system. In fact the linearised equations of motion may be solved exactly in 1d (Maggs and Stinchcombe 1984) giving the following solution for the response function,

$$\chi(q,\omega,\xi) = q^{-(2-\eta_t+z)} F(q\xi, \omega q^{-z}) \qquad \text{(P42)}$$

where $\eta_t=1$ and z=1 and

$$F(a,b) = \frac{\pi}{2a^2b^2J} \coth\{\pi J/2ab\} \left\{ \frac{1-\sin(\pi J/b)}{\{b/2J-1\}^2[\cosh(\pi J/ab)-\sin(\pi J/b)]} + \frac{1+\sin(\pi J/b)}{\{b/2J+1\}^2[\cosh(\pi J/ab)+\sin(\pi J/b)]} \right\} \qquad \text{(P43)}$$

However in the hydrodynamic limit $q\xi \ll 1$,

$$F(a,b) \xrightarrow[a\to 0]{} \frac{\pi}{a^2b^2J} \exp\left[-\frac{\pi J}{ab}\right] \left\{ \frac{(1-\sin(\pi J/b)}{(b/2J-1)^2} + \frac{(1+\sin(\pi J/b))}{(b/2J+1)^2} \right\} \qquad \text{(P44)}$$

and so $\omega_c \sim J/\xi$ and $\Gamma_c \sim J/\xi$. In the critical regime $q\xi \gg 1$,

$$F(a,b) \underset{a\to\infty}{\longrightarrow} \frac{\pi}{8J^3} \frac{1/a}{1/a^2 + (2J/b-1)^2} \qquad \text{(P45)}$$

and hence we recover the pure system dispersion law $\omega_c \sim 2Jq$, and $\Gamma_c \sim 2J/\xi$. We note then that in the critical regime $q\xi \gg 1$ the rescaled damping indeed vanishes as expected,

$$(\Gamma_c/\omega_c) = (q\xi)^{-1} \to 0 \qquad \text{as} \qquad q\xi \to \infty \qquad \text{(P46)}$$

6. Application to the Ferrimagnet.

Finally, we discuss the generalisation of the above arguments to the two-sublattice *ferrimagnet*. Here the spins on the A sublattice, say, have unit magnitude while those on the other sublattice have magnitude $\sigma<1$. In this case (P3a) and (P3b) become for the A and B sublattices respectively,

$$\omega S_j^+ = \sum_{<jl>} J_{jl}(S_l^+ + \sigma S_j^+) - h_j^+(\omega) \qquad \text{(P47a)}$$

$$-\omega S_i^+ = \sum_{<ik>} J_{ik}(\sigma S_k^+ + S_i^+) - \sigma h_i^+(\omega) \qquad \text{(P47b)}$$

Decimating S_l^+ from (P47a) thus yields:

$$\omega S_j^+ = \sum_{<jl>} J_{jl} \left\{ \sigma S_j^+ - \left[\frac{\sum_{<lk>} J_{lk}\, \sigma S_k^+ - \sigma h_l^+}{\left[\omega + \sum_{<lk>} J_{lk} \right]} \right] \right\} - h_j^+(\omega) \qquad \text{(P47c)}$$

The continuum equation that one obtains from (P47c), say, is, after some algebra,

$$(1-\sigma)\omega u + \tfrac{1}{2}(\sigma/J)u\omega^2 = -2\sigma(J\nabla^2 u + \underline{\nabla} J . \underline{\nabla} u)a^2 - \tfrac{1}{2}(\sigma/J)h\omega - (1-\sigma)h \qquad \text{(P48)}$$

An analogous equation is obtained for (P47b). For $\sigma=1$ we recover the antiferromagnetic equation of motion (P5), as required.

It follows that, for $\sigma \neq 1$, in the hydrodynamic limit $q\xi \ll 1$, with corresponding low frequency ω, we retrieve the acoustic (Goldstone) mode given by,

$$-\omega u(\underline{r},\omega) = D(\underline{r})\nabla^2 u(\underline{r},\omega) + \underline{\nabla}D(\underline{r}).\underline{\nabla}u(\underline{r},\omega) + h(\underline{r},\omega) \qquad \text{(P49)}$$

The term $D(\underline{r})$ is simply the *ferromagnetic* spin-wave stiffness coefficient (see Harris and Kirkpatrick 1977) renormalised by a factor $(\sigma/_1-\sigma)$. However (P49) is then of the same form as the corresponding continuum equation for the ferromagnet and the consequences follow in the same manner. To obtain the full ferrimagnetic Green function $<G^{(T)}(\underline{q};\omega)>$ however, a procedure similar to that above for the antiferromagnet is required and we find

$$<G^{(T)}(q\equiv k-\pi;\omega)> \propto \langle\langle S_k^{+A}, S_{-k}^{-A}\rangle\rangle \qquad \text{(P50)}$$

as in the case of the antiferromagnet. The full transverse ferrimagnetic response function is therefore ($q\xi \ll 1$)

$$\chi(q,\omega,\xi) = \frac{q^{-z}(q\xi)^{d+2-z}}{\left[(\omega q^{-z}-(q\xi)^{2-z})^2 + (q\xi)^{2(2+d-z)}\right]} \qquad \text{(P51)}$$

from the corresponding result for the ferromagnet (see Appendix L) with k replaced by $(k-\pi)\equiv q$. $z=2+(t-\beta)/\nu$ is the ferromagnetic dynamic exponent.

7. Summary.

In summary, we have applied the theory, developed elsewhere for the damping of ferromagnetic spin-waves near p_c, to the case of the antiferromagnet and also to the ferrimagnet. Expressions obtained for the damping and response functions are consistent with the dynamic scaling principle. The response from finite clusters was considered and the corresponding critical exponents derived using a relation between the ferromagnetic and antiferromagnetic dynamic exponents z^F, z^{AF}. The phenomenological distinction between bond and site dilution was investigated and the consequences for the critical behaviour established. The one-dimensional case was also examined and it was demonstrated that the critical behaviour was analogous to that in the corresponding ferromagnetic one-dimensional model (Chapter 7).

References

Achiam Y. (1985) Phys. Rev. B 31 4732.

Aeppli G.,Guggenheim H. and Uemura Y.J. (1984) Phys. Rev. Lett. 52 942.

Aharony A. (1976) *Dependence of Universal Critical Behaviour on Symmetry and Range of Interactions* in 'Phase Transitions and Critical Phenomena', vol. 6, eds. C.Domb and M.S.Green (Academic Press: London).

Aharony A. and Stauffer D. (1984) Phys. Rev. Lett. 52 2368.

Aizenmann M. (1982) Commun. Math. Phys. 86 1.

Alexander S. and Orbach R. (1982) J. Phys. Lett. (Paris) 43 L625.

Allen J.P., Colvin J.T., Stinson D.G., Flynn C.P. and Stapleton H.J. (1982) Biophys. J. 38 299.

Anderson P.W. (1952) Phys. Rev. 86 694.

Ashcroft N.W. and Mermin N.D. (1976) *Solid State Physics*, p.704 (Holt Saunders: Philadelphia).

Ball R.C. and Cates M.E. (1984) J.Phys. A.: Math. and Gen. 17 L531.

Banavar J.R., Harris A.B. and Koplik J. (1983) Phys. Rev. Lett. 51 1115.

Barber M.N. (1975) J.Phys.C.:Solid. St. Phys. 8 L203.

Berlin T.H. and Kac M. (1952) Phys. Rev. 86 821.

Bhattacharya S. and Chakrabarti B.K. (1984) Z.Phys.B. 57 151.

Birgeneau R.J., Cowley R.A., Shirane G. and Guggenheim H.J. (1976) Phys. Rev. Lett. 37 940.

Blease J., Essam J.W. and Place C.M. (1978) J.Phys.C.:Solid St. Phys. 11 4009.

Bloch F. (1932) Z.Phys. 74 295.

Bray A.J. and Moore M.A. (1977) J.Phys. A: Math. and Gen. 10 1927.

Brenig W., Wolfle P. and Dohler G. (1971) Z.Phys. 246 1.

Brézin E., Le Guillou J.C. and Zinn-Justin J. (1976) in *Phase Transitions and Critical Phenomena*, eds. C. Domb and M.S. Green, vol.6 (Academic).

Broadbent S.R. and Hammersley J.M. (1957) Proc. Camb. Phil. Soc. 53 629.

Bruce A.D., Droz M. and Aharony A. (1974) J.Phys.C.:Solid St. Phys. 7 3673.

Buyers W.J.L., Pepper D.E. and Elliott R.J. (1972) J.Phys.C.:Solid St. Phys. 5 2611.
Cardy J.L. (1985) Nucl. Phys. B 240 514.
Chowdhury D. (1976) submitted to J.Phys.A.:Math. and Gen.

Chowdhury D. and Chakrabarti B.K. (1985) J.Phys.A.:Math. and Gen. 18 L377.

Chowdhury D. and Stauffer D. (1986) J.Phys.A.:Math. and Gen. 19 L19.

Christou A. and Stinchcombe R.B. (1986a) J.Phys.A.:Math. and Gen. 19 757.

Christou A. and Stinchcombe R.B. (1986b) J.Phys.A.:Math. and Gen. 19 2625.

Christou A. and Stinchcombe R.B. (1986c) J.Phys.A.:Math. and Gen. 19 L357.

Christou A. and Stinchcombe R.B. (1986d) J.Phys.A.:Math. and Gen. 19 L451.

Christou A. and Stinchcombe R.B. (1986e) J.Phys.C.:Solid St. Phys. 19 5895.

Christou A. and Stinchcombe R.B. (1986f) J.Phys.C.:Solid St. Phys. 19 5917.

Christou A. and Stinchcombe R.B. (1987) *submitted to Phys. Rev. B.*

Coniglio A. (1981) Phys. Rev. Lett. 46 250.

Cordery R., Sarker S. and Tobochnik J. (1981) Phys. Rev. B. 24 5402.

Dasgupta C., Harris A.B. and Lubensky T.C. (1976) Phys. Rev. B. 17 1375.

DeBell K. (1979) J.Phys.C.:Solid St. Phys. 12 L605.

de Gennes P.–G. (1972) Phys. Lett. A. 38 339.

de Gennes P.–G. (1975) J.Phys. (Paris) 36 281.

de Gennes P.–G. (1976) La Reserche 7 919.

de Gennes P.–G. (1979) *Scaling Concepts in Polymer Physics* (Cornell University Press: New York).

de Queiroz S.L.A. and Chaves C.M. (1980) Z.Phys. B. 40 99.
den Nijs (1979) J.Phys.A: Math. and Gen. 12 1857.
des Cloiseaux (1980) J.Phys. Lett. 41 L151.

des Cloiseaux (1981) J.Phys. 42 635.

Dickerson R.E. and Geis I (1983) *Hemoglobin* (Benjamin–Cummings, Menlo Park, California).

Domb C. and Joyce G.S. (1972) J.Phys.C.:Solid St. Phys. 5 956.

Dunfield L.G. and Noolandi J. (1980) Phys. Rev. B. 22 2586.

Edwards S.F. (1958) Phil. Mag. 3 1020.

Edwards S.F. and Jones R.C. (1971) J.Phys.C.:Solid St. Phys. 4 2109.

Elliott R.J. and Pepper D.E. (1973) Phys. Rev. B. 8 2374.

Emery V.J. (1975) Phys. Rev. B. 11 239.

Entin-Wohlman O., Alexander S., Orbach R. and Kin-Wah Yu (1984) Phys. Rev. B. 29 4588.

Essam J.W. (1980) Rep. Prog. Phys. 43 835.

Essam J.W. and Garelick H. (1967) Proc. Phys. Soc. 92 136.

Falconer K.J. (1986) *The Geometry of Fractal Sets* (CUP).

Family F. (1983) J.Phys.A.:Math. and Gen. 16 L97.

Family F. and Coniglio A. (1984) J.Phys.A.:Math. and Gen. 17 L285.

Ferrell R.A., Menyhard N., Schmidt H., Schwabl F. and Szepfalusy P. (1967) Phys. Rev. Lett. 18 891.

Fisher M.E. (1968) Phys. Rev. 176 257.

Fisher M.E. (1969) J. Phys. Soc. Jpn. 26 suppl. 44.

Fisher M.E. (1974) *The Renormalisation Group in the Theory of Critical Behaviour*, Rev. Mod. Phys. 46 597.

Fisher M.E. (1982) *Scaling, Universality and Renormalisation Group Theory* in Critical Phenomena (Springer-Verlag).

Fisher M.E. (1984) J. Stat. Phys. 34 667.

Fisher M.E., Privman V. and Redner S. (1984) J.Phys.A.:Math. and Gen. 17 L569.

Flory P.J. (1953) *Principles of Polymer Chemistry* (Cornell University Press: New York).

Forrest S.R. and Witten T.A. (1979) J.Phys.A.:Math. and Gen. 12 L109.

Fortuin C.M. and Kasteleyn P.W. (1972) Physica (Utrecht) 57 536.

Gefen Y., Aharony A. and Alexander S. (1983) Phys. Rev. Lett. 50 77.

Gefen Y., Aharony A., Mandelbrot B.B. and Kirkpatrick S. (1981) Phys. Rev. Lett. 47 1771.

Gefen Y., Mandelbrot B.B. and Aharony A. (1980) Phys. Rev. Lett. 45 855.

Given J.A. and Mandelbrot B.B. (1983) J.Phys.B. 16 L565.

Glauber R.J. (1963) J. Math. Phys. 4 294.

Gochev I.G. (1983) Sov. Phys. JETP 58 115.

Gould H., Family F. and Stanley H.E. (1983) Phys. Rev. Lett. 50 686.

Gould H. and Kohin R.P. (1984) J.Phys.A.:Math. and Gen. 17 L159.

Green J.E. (1984) J.Phys.A.:Math. and Gen. 17 L437.

Griffiths R.B. (1965) J. Chem. Phys. 43 1958.

Guttmann A.J. and Wormald N.C. (1984) J.Phys.A.:Math. and Gen. 17 L271.

Guyer R.A. (1984) Phys. Rev. A. 30 1112.

Halperin B.I. and Hohenberg P.C. (1967) Phys. Rev. Lett. 19 700.

Halperin B.I. and Hohenberg P.C. (1969) Phys. Rev. 117 952.

Harris A.B. (1974) J.Phys.C.:Solid St. Phys. 7 1671.

Harris A.B. (1987) *to be published.*

Harris A.B. and Christou A. (1987a) *submitted to J.Phys.A.:Math. and Gen.*

Harris A.B. and Christou A. (1987b) *submitted to J.Phys.A.:Math. and Gen.*

Harris A.B., Leath P.L., Nickel B.G. and Elliott R.J. (1974) J.Phys.C.:Solid St. Phys. 7 1693.

Harris A.B. and Kirkpatrick S. (1977) Phys. Rev. B. 16 542.

Harris A.B. and Lubensky T.C. (1974) Phys. Rev. Lett. 33 1540.

Harris A.B. and Lubensky T.C. (1987) Phys. Rev. B., *to appear.*

Harris C.K. and Stinchcombe R.B. (1983) Phys. Rev. Lett. 50 1399.

Harris C.K. and Stinchcombe R.B. (1985) Phys. Rev. Lett. 56 869.

Hausdorff F. (1919) Mathematische Annalen 79 157.

Havlin S. (1984) Phys. Rev. Lett. 53 1705.

Helman J.S., Coniglio A. and Tsallis C. (1984) Phys. Rev. Lett. 53 1195.

Henley C.L. (1985) Phys. Rev. Lett. 54 2030.

Hentschel H.G.E. and Procaccia I. (1977) Phys. Rev. Lett. 49 1158.

Hohenberg P.C. and Halperin B.I. (1977) Rev. Mod. Phys. 49 435.

Holcomb W.K. (1974) J.Phys.C.:Solid St. Phys. 7 4299.

Holcomb W.K. (1976) J.Phys.C.:Solid St. Phys. 9 1771.

Hoshen J. and Kopelmann R. (1976) Phys. Rev. B. 14 3438.

Ising E. (1925) PhD thesis, unpublished.

Izyumov Y. (1966) Proc. Phys. Soc. 87 505.

Jain S. (1986) J.Phys.A.:Math. and Gen. 19 L57.

Jain S. (1986) J.Phys.A.:Math. and Gen., *to appear*.

Jones R.C. and Edwards S.F. (1971) J.Phys.C.:Solid St. Phys. 6 L194.

Kadanoff L.P. (1966) Physics 2 263.

Kadanoff L.P. (1976) Ann. Phys. (NY) 100 559.

Kaneyoshi T. (1969) Prog. Theor. Phys. 42 477.

Kasteleyn P.W. and Fortuin C.M. (1969) J. Phys. Soc. Jpn. Suppl. 53 1195.

Kaufman M. and Griffiths R.B. (1983) Phys. Rev. B. 28 2109.

Kim Y. (1983) J.Phys.C.:Solid St. Phys. 16 1345.

Kirchoff G. (1847) Ann. Physik 72 497.

Kirkpatrick S. (1973) Solid St. Commun. 12 2109.

Kirkpatrick S. (1979) Les Houches, eds. R. Balian, R. Maynard and G. Toulouse (North-Holland).

Korenblit I. Ya. and Shender E.F. (1978) Usp. Fiz. Nauk. 126 233.

Kumar D. (1984) Phys. Rev. B. 30 2961.

Lage E. (1987) *to appear*.

Langer J.S. (1960) Phys. Rev. 120 714.

Langer J.S. (1980) Rev. Mod. Phys. 52 1.

Last B.J. (1972) M.Sc. Thesis, University of Birmingham (Unpublished).

Lax M., Barrett A.J. and Domb C. (1978) J.Phys.A.:Math. and Gen. 11 361.

Leyvraz F. and Stanley H.E. (1983) Phys. Rev. Lett. 51 2048.

Lewis S.J. and Stinchcombe R.B. (1984) Phys. Rev. Lett. 52 1021.

Ma S-K. (1973) Rev. Mod. Phys. 45 589.

Maggs A.C. and Stinchcombe R.B. (1984) J.Phys.A.:Math. and Gen. 17 1555.

Maggs A.C. and Stinchcombe R.B. (1986) J.Phys.A.:Math. and Gen. 19 L63.

Mandelbrot B.B. (1977) *Fractals: Form, Chance and Dimension* (Freeman: San Francisco).

Mandelbrot B.B. (1982) *The Fractal Geometry of Nature* (Freeman: San Francisco).

McKenzie D.S. (1976) Phys. Rep. 27c 35.

Meakin P. (1983) Phys. Rev. A. 27 1495.

Meakin P. (1984) Phys. Rev. B. 29 3722.

Meakin P. and Stanley H.E. (1983) Phys. Rev. Lett. 51 1457.

Migdal A.A. (1976) Sov. Phys. JETP 42 743.

Mikeska H.J. (1981) J. Appl. Phys. 52 1950.

Montroll E.W. and West B.J. (1979) in *Fluctuation Phenomena*, eds. E.W. Montroll and J.L. Lebowitz (Amsterdam: North-Holland)

Murray G.A. (1966) Proc. Phys. Soc. 89 87.

Nakanishi H. and Family F. (1984) J.Phys.A.:Math. and Gen. 17 427.

Nickel B.G. (1974) J.Phys.C.:Solid St. Phys. 7 1719.

Niemeyer Th., Pietronero L.and Weismann H.J. (1984) Phys. Rev. Lett. 52 1033.

Niemeyer Th. and van Leeuwen J.M.J. (1974) Physica 71 17.

Nightingale M.P. (1977) Phys. Lett. 59A 486.

Nittmann J., Daccord G. and Stanley H.E. (1985) Nature 314 141.

Onsager L. (1944) Phys. REv. 65 117.

Osborne C.F. (1971) J.Phys.C.:Solid St. Phys. 4 2929.

Poincaré H. (1916) *Oeuvres de Henri Poincaré* (Paris: Gauthier Villars).

Priest R.G. and Lubensky T.C. (1976) Phys. Rev. B. 13 4159; B. 14 5125(E).

Privman V. (1983) J.Phys.A.:Math. and Gen. 16 L571.
Rammal R. and Toulouse G. (1983) J.Phys.Lett. 44 L13.
Rammal R. and Benoit A. (1985) J. Phys. Lett (Paris) 46 L667.

Rammal R. and Benoit A. (1985) Phys. Rev. Lett. 55 649.

Redner S. and Reynolds P.J. (1981) J.Phys.A.:Math. and Gen. 14 2679.

Reynolds P.J., Klein W. and Stanley H.E. (1977) J.Phys.C.:Solid St. Phys. 10 L167.

Reynolds P.J., Klein W. and Stanley H.E. (1978) J.Phys.A.:Math. and Gen. 11 L199.

Reynolds P.J., Klein W. and Stanley H.E. (1980) Phys. Rev. B. 21 1223.

Rudnick J. and Nelson D.R. (1976) Phys. Rev. B. 12 2208.

Sahimi M. and Jerauld G.R. (1983) J.Phys.C.:Solid St. Phys. 16 L1043.

Sahimi M. and Jerauld G.R. (1984) J.Phys.A.:Math. and Gen. 17 L165.

Sander L.M. and Witten T.A. (1982) Bull. Am. Phys. Soc. 27 305.

Sen P.N. (1981) Geophysics (USA) 46 1417.

Skal A.S. and Shklovskii B.I. (1975) Sov. Phys. Semicond. 8 1029.

Sneddon L. (1978) D.Phil thesis, unpublished (Oxford).

Stanley H.E. (1968) Phys. Rev. 176 718.

Stanley H.E. (1971) *Introduction to Phase Transitions and Critical Phenomena* (OUP).

Stanley H.E., Reynolds P.J., Redner S. and Family F. (1982) in *Real Space Renormalisation,* eds. T. Burkhardt and J.M.J. van Leeuwen (Springer: New York), p.169.

Stanley H.E. and Coniglio A. (1984) Phys. Rev. B. 29 522.

Stapleton H.J., Allen J.P., Flynn C.P., Stinson D.G. and Kurtz S.R. (1980) Phys. Rev. Lett. 45 1456.

Stauffer D. (1975) Z. Phys. B. 22 161.

Stauffer D. (1979) Phys. Rep. 54 1.

Stephen M.J. and Grest G.S. (1977) Phys. Rev. Lett. 38 567.

Stinchcombe R.B. (1979) J.Phys.C.:Solid St. Phys. 12 2656.

Stinchcombe R.B. (1980a) J.Phys.C.:Solid St. Phys. 13 L133.

Stinchcombe R.B. (1980b) J.Phys.C.:Solid St. Phys. 13 3713.

Stinchcombe R.B. (1980c) J.Phys.C.:Solid St. Phys. 13 3723.

Stinchcombe R.B. (1983) *Dilute Magnetism* in 'Phase Transitions and Critical Phenomena', vol. 7, eds. C.Domb and J.L.Lebowitz (Academic Press: London).

Stinchcombe R.B. (1985) in *Scaling Phenomena in Disordered Systems,* eds. R. Pynn and A. Skjeltorp (Plenum: New York).

Stinchcombe R.B. (1985) J.Phys.A.:Math. and Gen. 18 L1169.

Stinchcombe R.B. (1986) in *Scaling Phenomena in Disordered Systems*, eds R. Pynn and A. Skjeltorp (Plenum).

Stinchcombe R.B. and Harris C.K. (1983) J.Phys.A.:Math. and Gen. 16 4083.

Stinchcombe R.B. and Watson B.P. (1976) J.Phys.C.:Solis. St. Phys. 9 3221.

Swendsen R.H. (1982) J. Appl. Phys. 53 1920.

Tahir-Kheli R.A. (1971) Phys. Rev. B. 6 2826.

Thouless D.J. (1978) Les Houches (North Holland Press) eds. Balian, Maynard and Toulouse, 1.

Toulouse G. (1974) Nuovo Cimento B23 234.

Toulouse G. and Pfeuty P. (1975) *Introduction au Groupe de Renormalisation* (PUG).

Vicsek T. (1983) J.Phys.A.:Math. and Gen. 16 L647.

Watson B.P. (1985) Private communication.

Widom B. (1965) J. Chem. Phys. 43 3892, 3898.

Witten T.A. and Sander L.M. (1981) Phys. Rev. Lett. 47 1400.

Witten T.A. and Sander L.M. (1983) Phys. Rev. B. 27 5686.

Williams T. and Bjerknes R. (1972) Nature 236 19.

Wilson K.G. (1972) Phys. Rev. Lett. 28 584.

Wilson K.G. and Fisher M.E. (1972) Phys. Rev. Lett. 28 240.

Wilson K.G. and Kogut J. (1974) Phys. Rep. 12 75.

Wilson K.G. (1975) Rev. Mod. Phys. 47 773.

Yang Y.S., Liu Y. and Lam P.M. (1985) Z.Phys. B. 59 445.

Young A.P. and Stinchcombe R.B. (1975) J.Phys.C.:Solid St. Phys. 8 L535.

Zabolitzky J.G. (1984) Phys. Rev. B. 30 4077.

Zia R.K.P. and Wallace D.J. (1975) J.Phys.A.:Math. and Gen. 8 1495.